ABSTRACT

Title of Dissertation: **SPONGE MUTUALISM IN THE FACE OF CLIMATE CHANGE**

Jan Vicente, Doctor of Philosophy, 2016

Directed By: Dr. Russell T. Hill, Professor,
Institute of Marine and Environmental Technology, University of Maryland Center for Environmental Science

Three epizoic symbioses between new sponge species of the genera *Plakortis*, *Haliclona*, and *Xestospongia deweerdtae* are reported here. Barcoding of the cytochrome oxidase subunit 1, 28S rRNA and 18S rRNA genes allowed me to formally describe the *Plakortis* spp. as *P. deweerdtaephila* and *P. symbiotica*. Both *Plakortis* spp. are obligate hosts of the sponge *X. deweerdtae*. Unlike *Plakortis* spp., *X. deweerdtae* can have a free-living lifestyle. This discovery motivated me to: 1) Use next-generation sequencing to ask whether microbial symbionts are playing a role in shaping these sponge associations; 2) Evaluate how top-down factors influence these associations by analyzing crude extracts of each species by LCMS and determine their palatability to fish to test if chemical defenses from *Plakortis* spp. translocate into the *Xestospongia* tissue,

and protect it from predation, and 3) Test whether the *X. deweerdtae* and *P. deweerdtaephila* sponge pairs in Panama are more resilient than free-living *X. deweerdtae* in the face of climate change. My results on bacterial and sponge cell counts revealed that *Plakortis* spp. are high microbial abundance sponges and that *X. deweerdtae* and *H. plakophila* are low microbial abundance sponges. Diversity indices showed no differences in microbial richness but a higher Simpson's index (*D*) for *Plakortis* spp. than both epibionts. Microbial community shifts in *X. deweerdtae* epibionts not observed in the free-living lifestyle were a consequence of the presence of microbial phyla found in the *Plakortis* spp. basibiont, suggesting the possibility of horizontal transfer of symbionts from the basibiont to the epibiont. Crude extracts from tissues of both free-living and associated lifestyles of *X. deweerdtae* confer chemical defense. These results suggest that top-down predation pressures from reef fish do not influence the associated life-style of *X. deweerdtae*. Exposure to high pCO_2 and warmer temperature revealed that acidification had an ameliorating effect against necrosis caused by high temperatures in free-living and associated individuals of *X. deweerdtae* as well as their *P. deweerdtaephila* basibiont. The *X. deweerdtae* epibiont was more resistant to temperature increments than *P. deweerdtaephila*. I performed a similar experiment on an invasive Hawaiian sponge *Mycale grandis* and discovered that neither acidification nor temperature affect skeleton synthesis. Taken together these findings suggest that these symbioses are mutualistic in nature and that sponges are likely to survive the predicted temperature and pCO_2 conditions for the end of the century.

SPONGE MUTUALISM IN THE FACE OF CLIMATE CHANGE

By

Jan Vicente

Dissertation submitted to the Faculty of the Graduate School of the
University of Maryland, College Park, in partial fulfillment
of the requirements for the degree of
Doctor of Philosophy
2016

Advisory Committee:
Professor Russell T. Hill, Chair
Professor Feng Chen
Associate Professor J. Sook Chung
Associate Professor Rosemary Jagus
Fishery Biologist Jose A. Rivera
Professor Robert W. Thacker
Professor Daniel E. Terlizzi, Dean's Representative

Dedication

I dedicate this dissertation to my father Dr. Vance P. Vicente who introduced me to the magnificent world of sponges at the age of five. I also dedicate this dissertation to previous mentors at the University of Puerto Rico, the University of North Carolina Wilmington, the University of Maryland as well as friends and family who gave me their unconditional love and support during the past six years.

Acknowledgements

There are a number of people who were instrumental to the completion of each chapter of this dissertation. I would like to first thank Dr. Russell T. Hill for giving me the opportunity to work independently throughout my PhD research and for fostering an environment of camaraderie and support among fellow graduate students and postdocs in the laboratory. I would like to thank Ryan Powell and Leah Blasiak, as well as other previous and present members of the Hill laboratory who have helped me trouble-shoot many challenges in the molecular aspects of this dissertation.

I am indebted to Dr. Joseph Pawlik for allowing me the opportunity to participate in four scientific research cruises that provided field access to the most remote dive sites of the Caribbean and revealed the discovery of these cryptic, novel sponge associations. These cruises also gave me the opportunity to meet and collaborate with a number of excellent scientists including Dr. Sven Zea who throughout the years has significantly contributed to the taxonomic study of *Plakortis* spp. and *Xestospongia* spp. I thank Lucas Moitinho-Silva for help writing scripts and for assistance during the processing of the microbial community analysis of this project. I am indebted to Rachel Collin and Plinio Gondola for hosting me at the Smithsonian Tropical Research Institute (STRI) at the Bocas del Toro research station. Arcadio Castillo, Micah J. Marty, Steve E. McMurray, Jaaziel García Hernández and Milton Carlo are thanked for SCUBA diving assistance. Micah is also thanked for his assistance during an entire summer running experiments with me at STRI. We thank Cristina Diaz for

providing help with the discussion of the taxonomy of *Xestospongia deweerdtae* and Robert W. Thacker for providing key discussion points on the nature of these novel sponge-sponge interactions. Cristina and Robert are also thanked for hosting the 2010 NSF-AToL: Taxonomy, Systematics, and Ecology of Caribbean course that provided me with fundamental taxonomic training. We thank Torsten Thomas, Nicole Webster and Joe Lopez for coordinating the submission of samples to the Earth Microbiome Project. We also thank Lucas and Cole G. Easson for teaching a bioinformatics workshop for processing next-generation sequencing data of sponge microbial communities.

I thank NOAA's Dr. Nancy Foster Scholarship program, not only for funding my dissertation but for also allowing me to do an internship at the Hawaiian Island Humpback Whale National Marine Sanctuary. This opportunity also allowed me to collaborate with fellow former scholar Dr. Nyssa Silbiger whose help was invaluable in the completion of a 27-day ocean acidification experiment at the Hawaiian Institute of Marine Biology. We thank Hollie Putnam for her logistical support and Megan Donahue for advice on experimental design of the ocean acidification experiment on *Mycale grandis*. I thank Dr. Rosemary Jagus for giving me the opportunity to be a NOAA LMRCSC scholar during the first two years of my PhD studies and for providing professional development opportunities throughout my doctoral studies. Other funding for this dissertation was provided by the American Museum of National History Lerner-Gray Fund for Marine Research, the Smithsonian Tropical Research Institute short-term fellowship program, and the NSF BIO/IOS Program (IOS-0919728).

Statement of Contribution

Micah J. Marty conducted fish feeding assays to determine the palatability of *Xestospongia deweerdtae* and *Plakortis species*. Micah also collected the $\delta^{13}C/\delta^{15}N$ data. Lucas Moitinho-Silva wrote multiple scripts for the microbial community analysis of *Plakortis* spp. *X. deweerdtae*, *H. plakophila*, and seawater samples.

Table of Contents

List of Tables

List of Figures

Chapter 1: Introduction

1.1. Mutualistic sponge-sponge symbioses

Sessile invertebrates in benthic habitats face a variety of environmental challenges that affect their morphology, growth, distribution and survival. One of the most dominant and versatile groups of invertebrates to cope with these challenges is sponges (phylum Porifera). In order to dominate in space limited habitats, sponges may produce antifouling secondary metabolites, have fast growth rates, or may reproduce by fragmentation to outcompete other sessile invertebrates (Kubanek *et al.* 2002; Blanquer *et al.* 2008; Leong & Pawlik 2010b). One of the most interesting but understudied adaptation strategies that sponges have evolved is their ability to develop specialized associations with other sponge species detailed below.

Cases of sponge-sponge epizoic interactions have long been reported in the literature. The first reports by Sollas (1888b) described *Triptolemma cladosus* overgrowing and penetrating the tissue of *Corallistes thomasi* in samples collected by the Challenger expedition in the Indian Ocean. Subsequently, a number of *Triptolemma* spp. were observed to grow on several sponge species from the Mediterranean, the northeastern Atlantic and South Africa (Maldonado 2002). The first reports highlighting sponge-sponge interactions as a facilitation strategy to counteract pressures of competition were of sponges observed in reef caves of the Adriatic Sea (Fig. 1.1a) (Rützler 1970; Sarà 1970). Reef caves can be crowded environments where sponges cope with space limitation by forming epizoic interactions as is the case of *Aplysilla sulfurea* which fully overgrows the basibiont *Haliclona* (*Gellius*) *fibulatus*. Interestingly *A. sulfurea* overgrowth does

not interfere with pumping rates in *H. fibulatus*' or lead to any sign of necrosis (Rützler 1970). In open coral reef communities, sponge epizoic interactions have been described as a facilitation strategy for surviving abiotic threats such as strong storm surges, but the cost of the interaction can also result in overgrowth and death of the host sponge (Wulff 1997, 2008b). The ability of opportunistic sponges to overgrow other sponge species may result from faster growth rates because of photosynthetic symbionts or by their ability to invest more energy in growing quickly rather than in producing chemical defenses (Walters & Pawlik 2005; Pawlik *et al.* 2008a; Wulff 2008b).

There have been several studies highlighting facilitative interactions between coral reef and sea grass bed sponges, where epizoism does not result in the host being smothered (Wilcox *et al.* 2002; Ávila *et al.* 2007; Wulff 2008a). For example, to avoid predation, the coral reef sponge *Lissodendoryx colombiensis* forms assemblages with several sea grass sponge species (*Cliona caribbaea*, *Amphimedon erina*, *Clathria schoenus*, and *Tedania klausi*) that deter the sponge-eating seastar, *Oreaster reticulatus* (Wulff 2008b) (Fig. 1.1b). In turn, the sea grass species use *L. colombiensis* as a substrate for stable settlement. Other relationships that have persisted for longer periods of time have resulted in more specialized associations as observed between the sponge pairs *A. erina* and *Geodia vosmaeri* (Fig. 1.1c) (Engel & Pawlik 2000; Wilcox *et al.* 2002; Ramsby *et al.* 2012). Intriguingly, *A. erina* that associates with *L. colombiensis* commonly overgrows the palatable sponge *G. vosmaeri* protecting it from *O. reticulatus* (Ramsby *et al.* 2012). Similar to the epi/basibiont interaction between

A. erina and *G. vosmaeri*, the Arctic sponge *Stryphnus fortis* is commonly overgrown by the epibiont *Hexadella dedritifera*. In this case the compound ianthelline is thought to be produced by the epibiont and is translocated and bioaccumulated by the basibiont *S. fortis* (Fig. 1.1d) (Cárdenas 2016). The compound ianthelline has micro and macrofouling properties, which could potentially protect the sponge pair from infectious bacteria or fouling by other smothering marine invertebrates.

Specialized sponge associations are an interesting evolutionary process as sponges have very specific allorecognition mechanisms. The specificity of the recognition process can be so precise that an individual of the same species is able to reject contact by an allogeneic individual (Saito 2013). Self to non-self recognition is, therefore, an important process for sponges to avoid getting overgrown by a different sponge species or other colonial invertebrates. However, in specialized sponge-to-sponge symbioses involving different species, sponge tissues accept overgrowth from other species. The benefit of associating with one another is apparently great enough to override the rejection response and enable the coexistence of different sponge species in contact with one another.In this dissertation, I investigate the ecological benefits driving the persistence of these relationships that have previously been little studied. I further investigate microbial ecological aspects that could be driving some of the possible benefits gained by sponges associating with other heterospecifics.

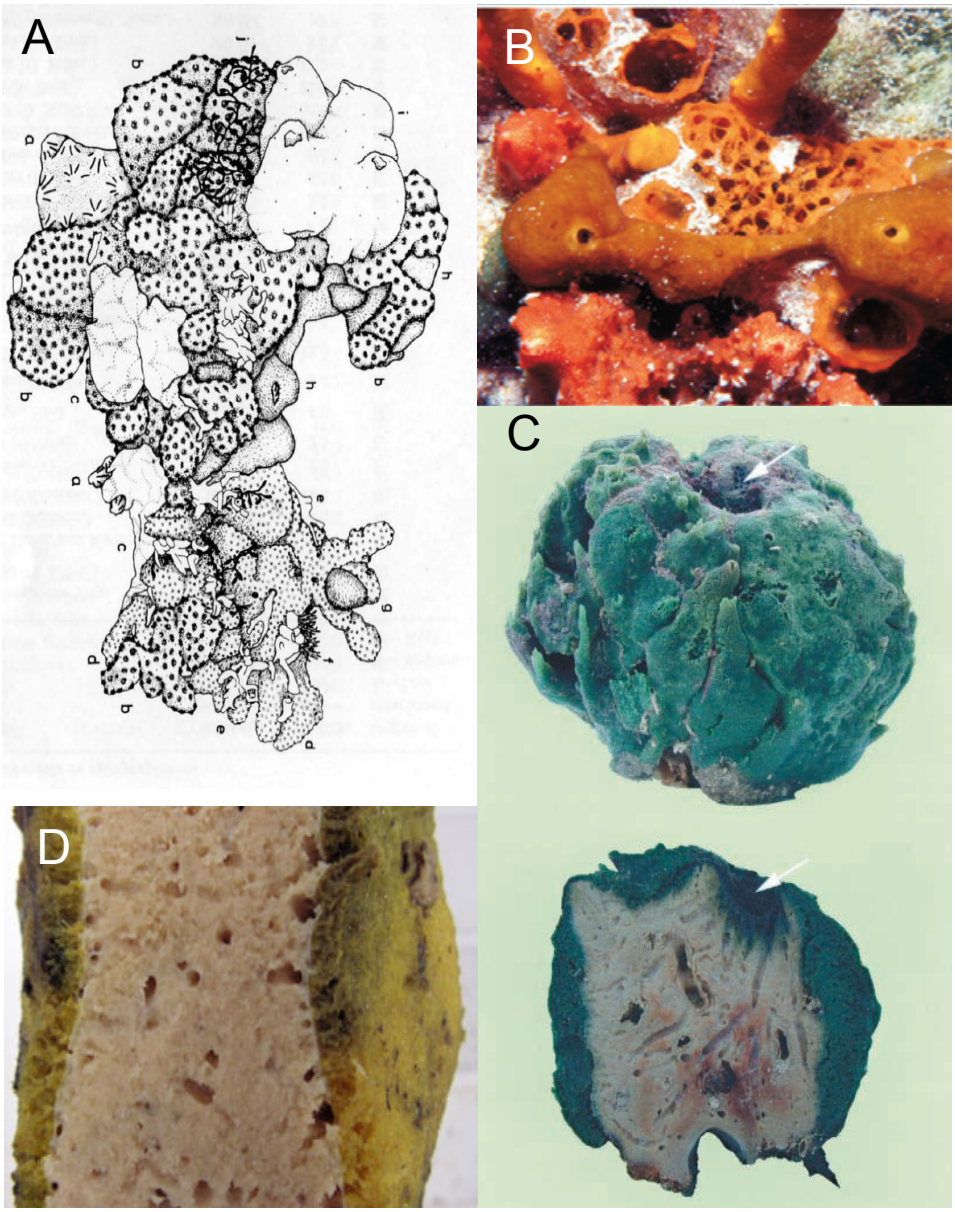

Figure 1.1. Examples of sponge-sponge epizootic interactions. Sponge assemblages of heterospecifics in (A) sea caves of the Adriatic Sea where nine species are mostly supported by the basibiont sponge *Fasciospongia cavernosa* (adapted from Rützler (1970)). (B) In seagrass habitats of the Caribbean the basibiont sponge *Lissodendoyx colombiensis* (*Lc*) is overgrown and protected from predation by the unpalatable epibiont sponges *Chondrilla caribensis* (*Cc*),

Clathria schoenus, and *Tedania klausi* (adapted from (Wulff (2012)). (C) The specialized association between *Amphimedon erina* (*Ae*) overgrowing *Geodia vosmaeri* (*Gv*) also protects the sponge pair from starfish predation in seagrass beds of the Caribbean (adapted from Rambsy and colleages (2012)). (D) *Hexadella dedritifera* produces the antifouling compound Ianthelline and fully overgrows *Stryphnus fortis* (*Sf*) in Northern Norway (adapted from Cardenas (2016)).

1.2. Microbial sponge symbionts: the advantages of having a diverse microbiome.

Sponges have been co-evolving with microbial symbionts for more than 500 million years and host the highest microbial diversity of any invertebrate (Webster *et al.* 2010). Recent advances in next-generation sequencing methods along with greater sampling efforts have revealed the presence of 41 microbial phyla and 40,000 operational taxonomic units (OTUs) at 97% sequence similarity in only 81 sponge species (Thomas *et al.* 2016). The interactions between these diverse microbiomes and the sponge hosts can be very important for the overall health and survival of the sponge as observed in phototrophic sponges harboring cyanobacterial symbionts that produce organic carbon and fix nitrogen for the sponge host to assimilate as food (Freeman & Thacker 2011). In some cases, cyanobacterial sponge symbionts can supply the sponge with antifungal secondary metabolites that the sponge could use to prevent diseases (Bewley *et al.* 1996). Furthermore, sponge microbial symbionts carry out important roles in

the cycling of nitrogen, sulfur, and phosphate (Hoffmann *et al.* 2005; Mohamed *et al.* 2008; Mohamed *et al.* 2010; Zhang, Blasiak*, et al.* 2015). This cycling of nutrients has been shown to play important roles beyond the sponge body and into benthic-pelagic coupling processes where dissolved carbon and nitrogen are made bioavailable to benthic food webs around coral reef ecosystems (Lesser 2006; Southwell *et al.* 2008; De Goeij *et al.* 2013).

The microbial diversity in a single sponge species can exceed 9,000 OTUs spanning more than 20 phyla at 97% sequence similarity as observed in the sponge *Carteriospongia foliascens* or can be as low as 1,000 OTUs spanning only three phyla at 95% sequence similarity as observed in *Ianthella basta* (Luter *et al.* 2010; Webster *et al.* 2010; Luter *et al.* 2015). These striking microbial diversity differences in sponge microbiomes were first observed under transmission electron microscopy (TEM) (Levi & Porte 1962; Vacelet & Donadey 1977) in which where some sponge species, termed “bacteriosponges”, exhibited a densely packed bacterial community, while others, termed “normal” sponges show a mesohyl completely lacking bacteria (Reiswig 1981). These sponges are currently classified as high microbial abundannce (HMA) sponges and low microbial abundance sponges (LMA) respectively (Fig. 1.2). HMA sponges are defined as sponges having a microbial community distinct from that in the surrounding seawater with a concentration exceeding that of seawater by 2 to 4 orders of magnitude while LMA sponges have bacterial concentrations and a community structure similar to those found in seawater (Hentschel *et al.* 2003; Giles *et al.* 2013). More than 58 species have been surveyed and classified as

HMA or LMA based on cell counts by epifluorescence and TEM (Gloeckner *et al.* 2014).

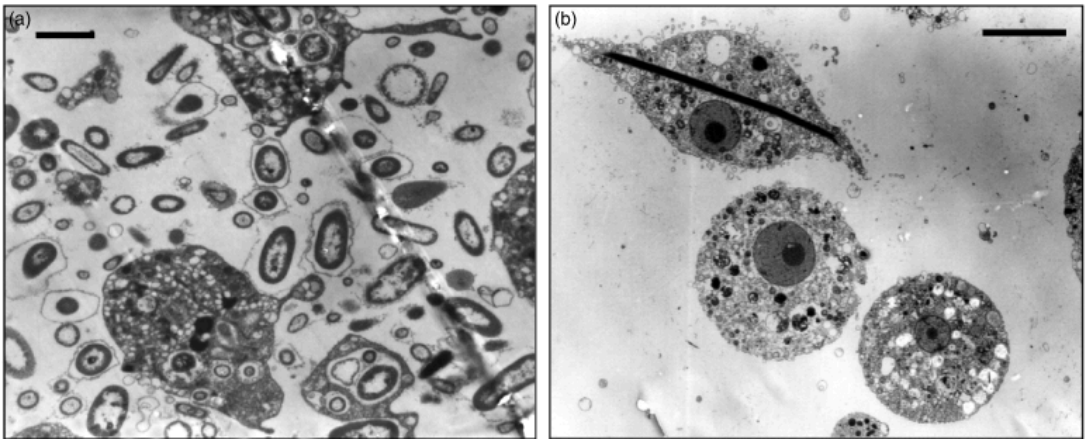

Figure 1.2. Transmission electron microscopy sections of high microbial abundance and low microbial abundance sponges. Micrograph sections of (a) *Xestospongia muta* (HMA) and (b) *Callyspongia vaginalis* (LMA) sponges (adapted from (Hentschel *et al.* 2006). More than 8,000 OTUs have been reported from *X. muta* (Thomas *et al.* 2016) while *C. vaginalis* has a rather simple bacterial community (Giles *et al.* 2013). Scale bars are (a) 1.5 and (b) 5 μm.

A lifestyle depauperate of microbial symbionts prevents LMA sponges from acquiring nutrients derived from its microbiota and therefore these sponges appear to invest more energy in heterotrophic feeding on particulate organic matter (POC) with faster pumping rates (Weisz *et al.* 2008; Schläppy *et al.* 2010). Conversely, HMA sponges have a densely packed mesohyl and pump water slowly relying less on heterotrophic feeding of filtered POC (Weisz *et al.* 2007). In

many cases HMA sponges host photosynthetic symbionts, which could be a source of nitrogen from nitrogen fixing bacteria and dissolved organic carbon from photosynthetic symbionts (Freeman & Thacker 2011). Nitrification is also a common process in HMA sponges where ammonia is converted to either nitrate or nitrite subsequently, which could be a nutrient source for either the host sponge or organisms in the oligotrophic conditions of the surrounding reef (Corredor *et al.* 1988; Diaz & Ward 1997; Southwell *et al.* 2008).

Such lifestyle disparities between HMA and LMA sponges are interesting to consider when questioning the nature of specialized sponge-sponge symbioses. For example, are these specialized associations influenced by bottom-up processes in which metabolic products from microbial symbionts of one sponge are used as a food source by its sponge pair? If we take for example the specialized *A. erina*/*G. vosmaeri* sponge pair, it is possible that *A. erina* is a LMA sponge and *G. vosmaeri* a HMA sponge. Based on previous HMA and LMA surveys of sponges, the common Caribbean reef sponge *Amphimedon compressa* and the Red Sea sponge *Amphimedon ochracea* are both LMA sponges (Angermeier *et al.* 2012; Gloeckner *et al.* 2014). *Amphimedon compressa* and *A. erina* also have closely related bacterial communities with low Simpson's diversity indices (*D'*) (Easson & Thacker 2015; Rodríguez-Marconi *et al.* 2015). On the other hand, four different *Geodia* species from cold-water coral reefs in Norway were found to be HMA sponges suggesting that this characteristic is a common phylogenetic feature for the *Geodia* genus (Schöttner *et al.* 2013). Therefore, it is likely that *A. erina* and *G. vosmaeri* are indeed LMA

and HMA sponges respectively. Perhaps *G. vosmaeri* has a similar microbial community to *Geodia barretti*, which creates anoxic environments within it's tissue and switches its metabolism to fermentation. This in turn could allow sulfur reducing bacteria to use these fermentation products as substrate that can be consumed by the sponge (bacterial farming) (Hoffmann 2003). These metabolic products could also be transferred to the epibiont *A. erina*. How bottom-up factors shape the *A. erina*/*G. vosmaeri* sponge pair has yet to be investigated. Top-down predation pressures from the spongivorous seastar *O. reticulatus* help explain how the chemically defended *A. erina* protects *G. vosmaeri* from predation. The chemical ecology of sponges is also very important to consider when describing the nature of sponge-sponge symbioses.

1.3. Chemical ecology of Caribbean sponges

Like many invertebrates, sponges are benthic, sessile organisms that use a variety of strategies to outcompete other sessile organisms (i.e. reef building corals, seaweed, octocorals, bryozoans and ascidians). Among the strategies that help solve the problem of space limitation, the ability to produce secondary metabolites that exhibit antifouling, distasteful, antibiotic and/or cytotoxic properties is a key advantage that sponges have over other benthic invertebrates. Overall, sponges have a remarkable ability to produce natural products and are the leading phylum in producing new natural products, accounting for 30% of all marine natural products characterized since the discovery of nucleoside derivatives isolated from *Tethya crypta* in the 1950s

(Mehbub *et al.* 2014). However, not all compounds exhibit antibiotic properties and as strategy to improve the discovery of antibiotic compounds, scientists often look at the ecological roles of these metabolites to guide their efforts to identify those that exhibit antibiotic properties.

One of the most important ecological roles of secondary metabolites in Caribbean sponges is predator deterrence against spongivorous fish (Pawlik 2011). Spongivory by fishes was first thought to be nonselective because a number of fish species were observed to feed on a wide variety of sponge species (Randall & Hartman 1968). For example, angelfish were observed to feed on over 20 sponge species. By feeding on small amounts of a variety of sponge species, reef fish might avoid being exposed to any specific secondary metabolite (Wulff 1994). Spongivory was therefore thought to have little effect on the distribution of sponge species in coral reef environments. These initial observations motivated a series of sponge palatability assays on over 70 sponge species using the generalist bluehead wrasse to determine if there was a preference for angelfishes to feed on some sponge species over others (Pawlik *et al.* 1995). These assays revealed that while most sponge species were chemically defended, some species were undefended species. Intriguingly, undefended sponge species correlated with the majority of the sponge species found in the gut contents of spongivorous reef fishes categorized by Randall and Hartman (1968) (Pawlik 1997).

This hypothesis was later applied at the ecosystem level where surveys revealed that chemically defended sponges were more commonly found on the

reef whereas palatable sponge species were frequently found living on mangrove roots where spongivorous fishes are not present (Pawlik *et al.* 1995). Interestingly, mangrove sponges were also found living under coral rocks on the reef, potentially hiding from spongivorous reef fishes. When these rocks were exposed on the reef, several species like *Tedania ignis* and *Chondrosia collectix* were consumed within 24 hrs (Dunlap & Pawlik 1996). It was evident that spongivory by fish species plays important role in shaping the distribution between chemically defended and palatable sponges in coral reef and mangrove habitats.

Ecological tradeoffs between chemically defended and palatable sponges were tested to determine if palatable sponges grew faster than defended sponges in order to withstand predation pressures. Sponge growth rates and survival were correlated for several sponges found on coral reefs and compared to those found in mangrove habitats (Wulff 2005). A clear correlation between growth rate and survival was observed for mangrove sponge species but not for coral reef sponges; meaning that palatable mangrove sponge species relied more on growth for survival than chemically defended coral reef sponges. Further studies using healing experiments tested this hypothesis on chemically defended and palatable sponges in coral reef sponges (Walters & Pawlik 2005). The study compared healing rates of three chemically defended sponge species vs. four palatable sponges species, all exhibiting a vase shaped morphology. The four palatable sponges healed wounds two to three times faster than chemically defended species. The study confirmed that not only do palatable sponge

species in mangrove habitats exhibit a faster growth rate than coral reef sponges, but that palatable sponge species common to coral reef habitats also exhibit the same evolutionary adaptation (Walters & Pawlik 2005). Additional studies using predator exclusion experiments on coral reef sponges by comparing growth rates of chemically defended and palatable sponges inside and outside of cages confirmed that un-caged palatable sponges grew more slowly than palatable caged sponges. Conversely, growth rates of chemically defended sponges did not change between caged and un-caged sponges (Leong & Pawlik 2010a; Pawlik *et al.* 2013).

Understanding how important chemical defenses are in influencing sponge species distribution in mangrove and coral reef habitats is important when answering the question “why do sponges interact with other sponges?”. It is apparent that chemical defenses play a key role in the survival of species in habitats exhibiting strong predation pressures as observed in seagrass beds and coral reefs. Therefore, sponges that lack chemical defenses but that allocate their resources into growing and dispersing quickly might associate with sponges that are chemically defended to offset this need. Although all of the previously discussed seagrass bed sponge pairs consist of palatable sponge species associating with a chemically defended sponge, it is not clear whether these sponges allocate their resources according to the association status with their counterparts. It is also important to consider that sponges are found in a variety of habitats that might not exhibit the same predation pressures as those observed in reef cave habitats.

1.4. Impact of ocean acidification and thermal stress on symbiotic relationships in coral reefs

Temperature and pCO_2 have increased at alarming rates from industrial emissions derived from fossil fuels in addition to the elimination of natural buffers through deforestation and land use (Doney *et al.* 2012). These emissions consist of an abundance of gases (CO_2, N_2O, CH_4, chlorofluorocarbons, tropospheric ozone, aerosols) that trap heat (Doney *et al.* 2012). In addition, increased atmospheric pCO_2 has increased the absorption of oceanic pCO_2, which results in ocean acidification. The increase in oceanic pCO_2 causes an increase in inorganic carbon (HCO_3^-) and protons that consequently reduce the pH, carbonate ion and calcium carbonate saturation states (Doney *et al.* 2009). These processes have caused extreme climate change scenarios where ocean temperatures and pCO_2 have coupling effects and are expected to increase 3°C and 1100 µatm respectively by the end of the century (Riahi *et al.* 2011). These conditions are predicted to be an imminent threat to a variety of organisms in the marine environment starting from primary producers and cascading to higher trophic levels in the food chain (Huesemann *et al.* 2002).

Ocean acidification and thermal stress in the marine environment affect a variety of physiological processes in many organisms (Fabry *et al.* 2008). Calcifying organisms are at a greater disadvantage than others because increasing carbonate solubility increases the cost of calcification (Wood *et al.* 2008). Among the most valuable of such susceptible organisms are reef building

corals which sustain the highest productivity of any ecosystem (McClanahan & Obura 1996). In addition to the increased energy costs of calcification, corals have to withstand thermal stresses which destabilize the mutualistic relationship between corals and dinoflagellates and resulting in bleaching (Brown 1997). The coupling effect of both acidification and thermal stress also increases their susceptiblity to diseases (Hoegh-Guldberg *et al.* 2007). Despite the enormous attention drawn to studying the physiological response of coral reefs to climate change, it is also important to consider the impact of climate change on other competitors of the reef that are potentially more resilient.

Organisms such as sponges that do not biomineralize a calcium carbonate skeleton seem to be more resilient under future climate change scenarios (Bell *et al.* 2013). Although a small proportion of sponges have a calcareous skeleton (3% of sponges) that are sensitive to dissolution from ocean acidification (Smith *et al.* 2013), over 90% of sponges have a skeleton made of either silica or collagen fibers (Hooper & Van Soest 2002). In some coral reefs of the Caribbean, sponges make up to 80% of the biomass and are important components of coral reefs (Diaz & Rützler 2001; McMurray *et al.* 2015). Sponges are involved in essential benthic-pelagic processes that allow for the transportation of pelagic carbon to benthic trophic levels. This is thought to explain why coral reefs in the Caribbean are able to maintain such a high biodiversity while living in oligotrophic conditions (De Goeij *et al.* 2013). However, sponges as resilient competitors also play a parasitic role in coral reefs.

Some sponges are able to penetrate the tissue of coral with etching cells and produce acid to detach $CaCO_3$ chips from the substrate in a process known as bioerosion (Bergquist 1978; Pomponi 1980). This parasitic relationship is enhanced under ocean acidification since the pH needed to detach $CaCO_3$ chips from the substrate is already lowered and might slightly compensate the cost of metabolic requirements for acid production and mechanical boring by the sponge (Wisshak *et al.* 2012). Similar trends of increased bioerosion from ocean acidification have been observed in boring sponges in the Caribbean and the Great Barrier Reef (Wisshak *et al.* 2013; Stubler *et al.* 2014). However it is hard to predict how a combined increase in pCO_2 and temperature will affect boring since bioerosion rates decreased under hotter and colder temperatures (Wisshak *et al.* 2013).

Resilience to thermal tolerance varies across species with some being more resilient to warmer temperatures than others. Like corals, sponges that host *Symbiodinium* and Cyanobacteria bleach and loose their photosymbionts due to rising temperatures (Vicente 1989; Hill *et al.* 2016). In the Caribbean and in the Mediterranean Sea, the impact of warmer seawater temperatures has caused local extinction events in keratose (aspiculated) sponges (Vicente 1989; Cebrian *et al.* 2011). In mesocosm studies, thermal stress caused necrosis and eliminated key bacterial symbionts from the Australian sponge *Rhopaloeides odorabile* at 33°C (Webster *et al.* 2008). While several species of keratose sponges are sensitive to warmer temperatures, six spiculated Caribbean sponges survived higher temperatures and high pCO_2 treatments. Temperature

increases without the pCO_2 enrichment actually accelerated attachment rates to substrates (Duckworth *et al.* 2012).

Measuring resilience at the individual sponge level and monitoring the parasitic relationship between sponges and corals in the face of climate change is important to predict how the benthic community of coral reefs in the Caribbean will respond to a changing climate. Studying transitions from coral to sponge dominated reefs is important as these benthic transitions could play a role in structuring higher trophic levels (Silveira *et al.* 2015). Despite the number of studies emphasizing how sponges are outcompeting corals, little attention has been paid to how mutualistic relationships between sponges will be affected by both of these abiotic factors in the future. These are important concepts to consider, as coral reefs in the Caribbean are already more accurately described as sponge reefs. By studying the interaction of mutualistic sponge associations we might have a better idea of which sponge species will persist. Sponges in association with other heterospecifics can grow more quickly and exhibit higher survivorship than those growing alone (Wulff 1997). Will sponge pairs between heterospecific sponge species enhance resilience or will sponges continue evolving independently from one another in future acidification and thermal stress scenarios?

1.5. Purpose and objectives for describing three new cases of sponge-sponge symbioses

In the present study, we report and describe three novel specialized sponge associations between species of *Plakortis* and *Xestospongia* and *Haliclona* found living in reef caves and cryptic habitats of the Bahamas, Puerto Rico and Panama (Fig. 1.3). Photographic images of the association from these sponges have been documented by Pomponi (Twilight Zone Expedition Team 2007, NOAA-OER www.photolib.noaa.gov/htmls/reef3932.htm) at a depth of 60 m in the Cayman Islands and by Zea *et al.* (2009). These are the first apparent obligate symbiosis for *Plakortis* spp. as these sponges have never been found in a free-living form.

1.5.1. Objective 1: Taxonomic evaluation of sponge pairs

My aim in this dissertation was to conduct morphological assessments and sequenced the cytochrome oxidase I (*cox1*), 28S rRNA and 18S rRNA genes to complete the proper taxonomic identification and classification of all species involved in the association. I hypothesized that *X. deweerdtae* is highly polymorphic as a result of its free-living and associated lifestyles with both *Plakortis* spp. and that the epibiont with oxeas is a new *Haliclona* sp.

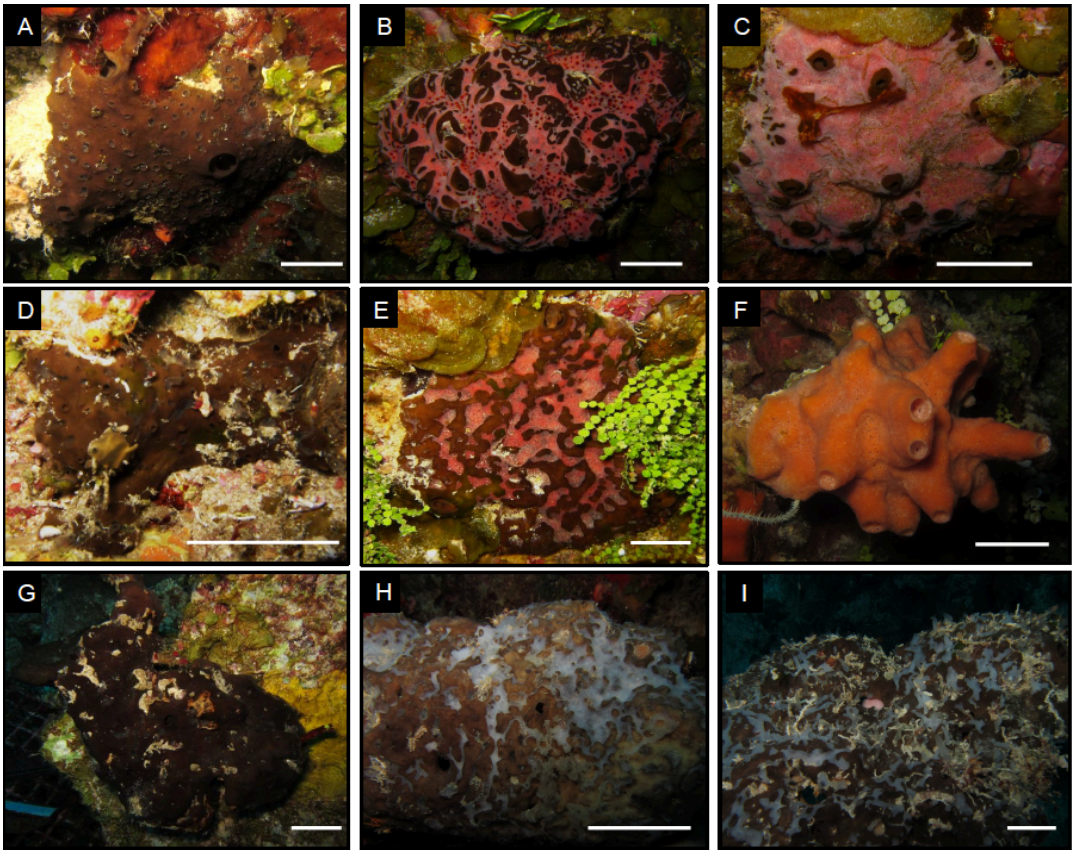

Figure 1.3. Sponge pair growth stages between *Plakortis*, *Xestospongia* and *Haliclona* species. Sponge pairs of (A) *Plakortis deweerdtaephila* sp. nov. (brown) associated with *Xestospongia deweerdtae* (translucent spots) at a recruit stage. (B, C) *P. deweerdtaephila* adult growing massively with *X. deweerdtae* (pink). (D) *Plakortis symbiotica* sp. nov. recruit associated with *X. deweerdtae* (translucent spots). (E) *P. symbiotica* adult associated with *X. deweerdtae*. (F) Free-living morphotype of *X. deweerdtae*. (G-I) *P. symbiotica* associated with *Haliclona plakophila* sp. nov. (blue) growing with encrusting and papillate morphology. Scale bar (A) 1 cm, (B–D), (G–I) 5 cm, (E–I) 2 cm.

Frequent field observations of these interactions motivated the following objectives and hypotheses for this study.

1.5.2. Objective 2: Microbial abundance, diversity of microbial symbionts and stable isotopes ($\delta^{15}N$, $\delta^{13}C$) of sponge pairs.

To determine how bacterial symbionts are involved in shaping the nature of the different sponge pairs I counted the abundance of bacteria per μm^2 of sponge tissue for each species. I used next-generation sequencing to partially sequence the 16S rRNA gene and characterize the bacterial communities of each pair and used stable isotopes to determine if free-living individuals of *X. deweerdtae* have a similar diet to associated individuals. Analysis of stable isotopes ($\delta^{15}N$, $\delta^{13}C$) allowed me to determine whether the *X. deweerdtae* epibiont competes with either *Plakortis* spp. basibiont for a similar isotopic niche space. I hypothesized that both *Plakortis* spp. are HMA sponges with a different microbial community from epibionts that span a different isotopic niche space. From the brittle consistency of the epibionts, I hypothesized that these are LMA sponges (Gloeckner *et. al* 2014) with a rather simple bacterial community.

1.5.3. Objective 3: Chemical ecology of sponge-pairs: testing the chemical defense hypothesis

To test the chemical defense hypothesis I prepared squid pellets with sponge extracts from both sponge pairs separately and fed them to the spongivore, sharpnose puffer *Canthigaster rostrata* and the generalist, bluehead

wrasse *Thalassoma bifasciatum* to determine the palatability of both species. We hypothesized that *Plakortis* spp. are chemically defended (unpalatable) sponges and that epibionts are palatable sponges.

1.5.4. Objective 4: Resilience of sponge pairs to climate change

I explored how increasing acidity and thermal stress affect the mutualistic interaction between *Plakortis symbiotica* sp. nov. and *Xestospongia deweerdtae*. Equally distributed individuals from both lifestyles were collected and placed in experimental tanks where pCO_2 and temperature are manipulated as individual and combined factors that simulated conditions to be expected by the end of the century (+3°C, 1100 µatm. A balanced experimental design using both free-living and associated individuals of *X. deweerdtae* allowed me to determine whether the associated lifestyle was less prone to the progress of necrotic tissue over free-living sponges. I hypothesized that sponge pairs are more resilient than free-living forms based on previous studies that suggest that associated heterospecific sponges demonstrate increased growth rates and survival rates compared to those living freely (Wulff 1997).

1.5.5. Objective 5: How does climate change impact spicule biomineralization

I conducted experiments to simulate ocean acidification and thermal stress on the Hawaiian invasive sponge *Mycale grandis* and monitored silica uptake in a closed incubation system. Sponges were also exposed to a 26-day

flow through experiment to test how spicule morphology was affected by acidification or thermal stress. Based on previous uptake models proposed for other siliceous sponges, like *S. domuncula* I hypothesized that: treatments with pCO_2 enrichment would accelerate silica uptake rates of *M. grandis* resulting in enhanced spicule production and denser skeletons (more silicification) and that temperature increments of 3°C would increase silica uptake rates through increased metabolism.

1.5.6. Objective 5: Discussion points on the nature of the *Plakortis*, *Xestospongia* and *Haliclona* sponge-sponge symbioses and their fate in a changing climate

I consolidated the results of the associated microbial communities, chemical ecology and resilience to climate change of the sponge pairs to predict the response of the Caribbean sponge community to climate change. Will sponge species live in cooperation to survive in a changing climate?

Chapter 2. Sponge epizoism in the Caribbean and the discovery of new *Plakortis* and *Haliclona* species, and polymorphism of *Xestospongia deweerdtae* (Porifera)

2.1. Abstract

The discovery by Vicente *et al.* (2014) of specialized epizoic symbioses between sponges of the genera *Plakortis* and *Xestospongia* revealed the obligate interaction of two new *Plakortis* spp. associating with *Xestospongia deweerdtae* and a new *Xestospongia* sp. In this study I formally describe the two new *Plakortis* spp. as *Plakortis deweerdtaephila* sp. nov. (previously reported as *Plakortis* sp. 1), *Plakortis symbiotica* sp. nov. (previously reported as *Plakortis* sp. 2) and describe the new *Xestospongia* sp. epibiont as *Haliclona* (*Halichoclona*) *plakophila* sp. nov. *Plakortis deweerdtaephila* only associates with *X. deweerdtae*, and has very small to large straight diods (24.2–233.7 μm long) and triods (26.4–102.6 μm long) that form large ectosomal circular meshes (114–329 μm diameter). *P. symbiotica* associates with both *X. deweerdtae* and *H. plakophila,* has larger curved diods (71.9–141.8 μm long) and triods (20.4–70.6 μm long) that form smaller ectosomal circular meshes (43–121 μm diameter) than *P. deweerdtaephila*. Phylogenetic analysis of *cox1* and *cob* gene fragments revealed a strongly supported clade that grouped both *Plakortis* spp. nov. distantly from any other known *Plakortis* spp. *H. plakophila* is described as a thin encrusting veneer of tissue with occasional papillae, so far only found associated with *P. symbiotica* in La Parguera, Puerto Rico. Phylogenetic analysis of 18S rRNA and *cox1* gene fragments place it distantly from any known clade of Haplosclerida. We found a new associated morphotype of *X. deweerdtae* from Bocas del Toro Panama, which completely overgrew *P. deweerdtaephila*. In addition, free-living morphotypes from Panama produce larger S-shaped and

round bracket shaped strongyles never before observed for this species, leading me to redescribe *X. deweerdtae*. All *X. deweerdtae* morphotypes shared >99% sequence homology of *cox1*, 18S rRNA and 28S rRNA genes with the holotype of *X. deweerdtae*. This study highlights the highly variable morphological characters of *X. deweerdtae* influenced by lifestyle and environmental factors. This study is also the first time that an obligate symbiosis with a heterospecific sponge is used as a key taxonomic character, in the description of the three new sponge species described here.

2.2. Introduction

In the last two decades, more than 55 new species of sponges of the Class Homoscleromorpha have been described, increasing the species number by 50% (Ereskovsky *et al.* 2009; Muricy 2011; Domingos *et al.* 2013; Cruz‐Barraza *et al.* 2014). Homoscleromorpha is the smallest class with a total of 103 described species (Van Soest *et al.* 2016), partly explaining the rapid discovery rate. The application of molecular phylogeny and cytological approaches have also helped discriminate cryptic species with limited diagnostic characters (Boury-Esnault *et al.* 1995; Muricy *et al.* 1996; Muricy *et al.* 1998; Vishnyakov & Ereskovsky 2009). In addition, expeditions with submersibles to access deep mesophotic and disphotic habitats have revealed new homoscleromorph species and genera in these environments (Ereskovsky *et al.* 2009; Rützler *et al.* 2014; Van Soest *et al.* 2014).

After many years of reclassifying Homoscleromorpha, it was officially accepted as the fourth class of Porifera (Gazave *et al.* 2012). This small class consists of one order (Homosclerophorida (Dendy 1905)) with two families distinguished by the absence Oscarellidae (Lendenfeld 1887) or presence Plakinidae (Schulze 1880) of a mineral skeleton. The Plakinidae include *Plakinastrella* (Schulze 1880), *Plakina* (Schulze 1880), *Plakortis* (Schulze 1880), *Corticium* (Schmidt 1862), *Placinolopha* (Topsent 1928) and the recently discovered genus *Tetralophophora* (Rützler *et al.* 2014).

Species belonging to the genus *Plakortis* are a valuable source of novel cyclic peroxides with biologically active properties (Gochfeld & Hamann 2001;

Rudi *et al.* 2003; Berrué *et al.* 2005; Jiménez-Romero *et al.* 2010; Dalisay *et al.* 2011). *Plakortis* spp. are cosmopolitan and have the highest diversity in the Tropical Western Atlantic (TWA) with 12 species (Domingos *et al.* 2015) and an additional two species proposed by Vicente *et al.* (2014) that are formally described in this study. Of particular interest is the obligate symbiotic lifestyle that the new species have in association with *Xestospongia deweerdtae* (Lehnert & Van Soest 1999) and a new *Haliclona* (subgenus *Halichoclona*) described here. Sponge pairs are found in cryptic habitats of the Bahamas, Puerto Rico (Vicente et al. 2014; Zea *et al.* 2014), Belize (Rützler *et al.* 2014) and Panama (this study) encompassing three ecoregions of the Caribbean (Spalding *et al.* 2007). These are the only known *Plakortis* spp. in the world that associate with other sponges and this is a key taxonomic character in the description of these new species. Interestingly, both epibionts of *Plakortis* spp. belong to the marine Haplosclerida. Like many homoscleromorph species, haplosclerids can be very difficult to classify, owing to the lack of useful morphological characters, paradoxically being one of the most specious orders of the class Demospongiae (De Weerdt 2002). The genus *Haliclona* in the family Chalinidae Grant, 1836 has the highest diversity in the order with more than 420 species (Van Soest *et al.* 2016). There are 35 species of *Haliclona* in the TWA of which seven belong to the subgenus *Halichoclona* (De Laubenfels 1932) (Bispo *et al.* 2014; Muricy *et al.* 2015). This study adds a new species from the Caribbean to this subgenus. In addition, the study highlights the remarkable polymorphic nature of *X. deweerdtae*, presumably influenced by lifestyle and environmental factors. The conspecificity

of all morphotypes of *X. deweerdtae* as well as the description of the new species were confirmed by phylogenetic analysis using partial sequences of the cytochrome oxidase (b and c), 18S rRNA and 28S rRNA genes.

2.3. Methods

2.3.1. Specimen collection

Sponge specimens were collected from the Bahamas in July 2011, Puerto Rico in August 2012 and October 2015, and Panama in May 2015 in depths of 4-36 m by SCUBA diving (Fig. 2.1). Pieces (100 g) of the entire sponge pair were removed from the base attached to the bedrock. Specimens were brought to the surface and carefully dissected to avoid DNA cross-contamination between species. Underwater photographs were taken for each specimen collected. Paratype and holotype specimens for all sponges were deposited in the Smithsonian Institution National Museum of Natural History in Washington, DC. Voucher samples of sponge pairs and free-living morphotypes of *X. deweerdtae* collected in Panama were also deposited in the “Museo de Biología Marina y Limnología” at the University of Panama as required by the collection permit of fauna No. 5 issued by the “Autoridad Nacional del Ambiente (ANAM)”. Samples collected in Puerto Rico were authorized by permit number 2010-IC-043 (R-VS-PVS15-SJ-00190-08062010) and samples collected in the Bahamas were authorized by unnumbered scientific permits. Catalogue numbers and acronyms for sponge collections are: USNM1254645 (holotype) and USNM1254647 for *Plakortis deweerdtaephila* sp. nov.; USNM1254650 (holotype) and USNM1254649 for *Plakortis symbiotica* sp. nov.; USNM1254650 (holotype) for

Haliclona plakophila sp. nov.; USN1254644, USNM1254645, USNM1254646, USNM1254647, USNM1254648, and USNM1254649 for *Xestospongia deweerdtae*.

2.3.2. Sectioning and spicule preparation

Sponge pieces (1-cm^3) containing both ectosome and choanomal tissue were preserved in 4% paraformaldehyde for 24 h and then transferred to 70% ethanol. Sponge pieces were dehydrated in an ascending alcohol series of 35%, 50% and 70%, and embedded in paraffin; 7–60 µm thick sections were cut perpendicular to the surface through the ectosome and choanosome by using a LKB 3128 Ultratome IV. Tangential sections of the ectosome were done directly by hand on frozen sponge material using a scalpel. Small sponge pieces (25 mg) were boiled in nitric acid until the solution turned clear, then centrifuged and washed with distilled water two times to remove the acid; water was then changed to 95% ethanol for storage. A few drops of the spicule suspension were placed on a slide and observed under the light microscope (LM) for measurements and photography. Thirty to fifty spicules per species and per spicule type were measured [lengths and widths, expressed herein as minimum–*mean* [±1 standard deviation (SD)]-maximum length / width in µm (n)] using ImageJ® (Abràmoff *et al.* 2004) (http://imagej.nih.gov/ij/) by Light Microscopy (LM). A few drops of the spicule suspension were added to a stub, air dried, and imaged under high vacuum a JEOL 5600 SEM Scanning Electron Microscope (SEM) at the Nano Imaging Facility, University of Maryland Baltimore County.

2.3.3. DNA extraction, sequencing and phylogenetic analysis

Sponge pieces (30-50 mg) were kept in RNAlater and frozen at −80°C. DNA was extracted by using the Qiagen AllPrep DNA/RNA Mini Kit, following the manufacturer's instructions. Previously designed specific internal and pair-end primers (Vicente *et al.* 2014) were used to amplify *cox1* (Folmer *et al.* 1994), 18S rRNA and 28S rRNA genes. Diplo-cob primers (Lavrov *et al.* 2008) were used to amplify a fragment of the cytochrome b (*cob*) gene for the new *Plakortis* spp. Polymerase chain reactions and sequencing reactions were carried out as described in Vicente *et al.* (2014). Sequences were assembled and edited using Sequencher® version 5.4.1 sequence analysis software, Gene Codes Corporation, Ann Arbor, MI USA http://www.genecodes.com. Double coverage reads allowed for accurate editing of sequences. Edited consensus sequences for each gene were exported into a single fasta file and uploaded with MEGA 5 (Tamura *et al.* 2011). Sequences were then aligned using the ClustalW function with default parameters. The closest relatives to these sequences were found by searching in GenBank using the BLAST function and were used as reference sequences for alignment and tree generating purposes. The Tamura Nei model with uniform rates among sites was used to run the Maximum Likelihood analysis (Tamura & Nei 1993). The nearest-neighbor interchange ML heuristic method with data resampled using 1,000 bootstrap replicates was used. Sequences of all holotype and paratype specimens for this study were deposited in GenBank under accession numbers KX668497-KX668531.

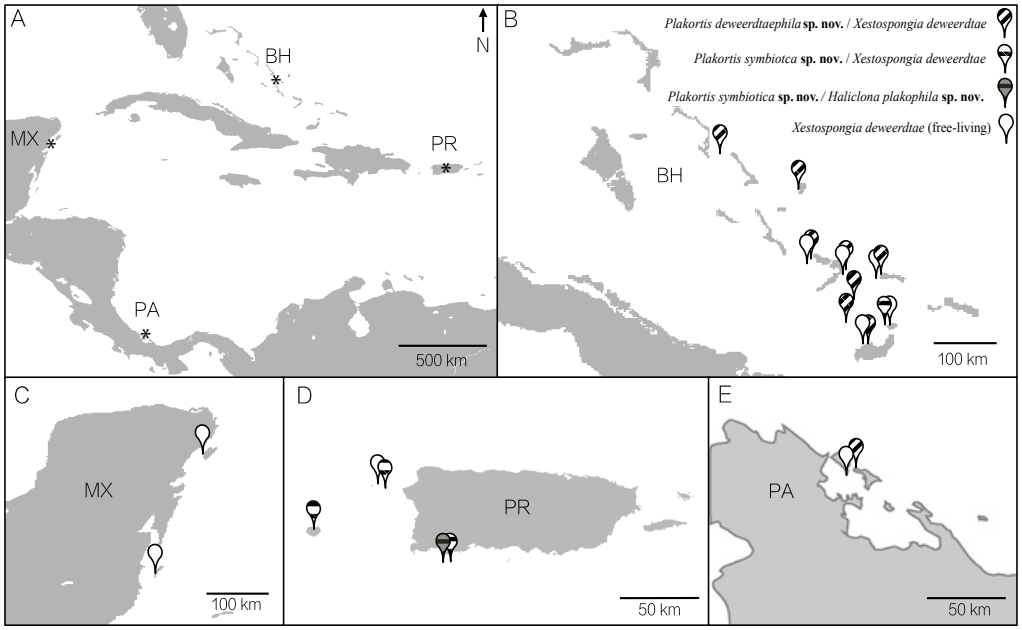

Figure 2.1 Map of collection sites. Map represents collection sites of *Plakortis deweerdtaephila* sp. nov., *Plakortis symbiotica* sp. nov., *Haliclona plakophila* sp. nov. and *Xestospongia deweerdtae* in the Caribbean (A). Detailed map of sponge species and sponge pair locations for the Bahamas (Little San Salvador, San Salvador, Hogsty Reef, Acklins, Mayaguana, Mira Por Voz, Plana Cays, Little Inagua, Great Inagua) (B), Mexico (Cozumel, Banco Chinchorro) (C), Puerto Rico (Mona, Desecheo, La Parguera) (D), and Panama (Bocas del Toro Province) (E). A list of sponge species and their life-style are indicated in the legend on panel B. The *P. symbiotica* and *H. plakophila* pair has been found only on the south coast of Puerto Rico.

2.3. Results

Systematics

2.3.1. Class Homoscleromorpha (Bergquist 1978)

Order Homosclerophorida (Dendy 1905)

Family Plakinidae (Schulze 1880)

Genus *Plakortis* (Schulze 1880)

Definition. Plakinidae with the skeleton formed by diods, with a variable abundance or absence of triods. Diactine derived microscleres (microrhabds), quasiamphiasters, spined diods and spheres may be present in some species; calthrops are absent (Muricy 2011).

2.3.1.1. *Plakortis deweerdtaephila* sp. nov.

(Fig. 2.2; Table 2.1)

Plakortis halichondrioides; Zea *et al.* 2009 (photographic guide).

Non: *Plakortis halichondrioides* (Wilson 1902), a valid species.

Plakortis sp. 1; Vicente *et al.* 2014 (ecology and symbiosis).

Plakortis sp. 1-"under *Xestospongia deweerdtae* associated"; Zea *et al.* 2014 (photographic guide).

Type material. Holotype and type locality: Dolphin Rock, Bocas del Toro, Panama (9.35076° N, -82.1863° W), 14 m depth, coll. Jan Vicente, May 20, 2015. Paratype: San Salvador, Bahamas (24.0406° N, -74.5314° W), 32 m depth, coll. Jan Vicente, July 19, 2011.

Specimens examined for comparison (other than those described here)**.** *Plakortis halichondrioides*: PHBH, San Salvador (24.0406° N, -74.5314° W), Bahamas, 32 m coll. Jan Vicente, July 19, 2011; PHPR, La Parguera, Puerto Rico (17.8883° N, -66.9981° W), 32 m depth coll. Jan Vicente, June 12, 2012.

Diagnosis. Thinly and thickly encrusting to massive cushions with a soft surface and compressible body. Found always associated as basibiont of *X. deweerdtae*. The latter may partially cover (Bahamas) or may completely overgrow *P. deweerdtaephila* sp. nov. (Panama). Oscules can be large and slightly elevated (Bahamas) or can be small and even with the surface when growing underneath *X. deweerdtae* (Panama). Color is dark brown with occasional olive green patches *in vivo* and exudes a light brown pigment when preserved in ethanol. Reticulated tangential ectosomal skeleton and a vaguely reticulated choanosomal skeleton with lacunae. Spicules are triods, diods and very small diods.

Description. External morphology is influenced by the growth progression of *X. deweerdtae* on the body of *Plakortis deweerdtaephila* sp. nov. For example, in Panama it can be thinly encrusting (Fig. 2.2A) growing underneath a thick (1 cm) mat of *X. deweerdtae*; very small oscules (1-3 mm). In the Bahamas, sponge pairs form 3 × 30 cm by 1-8 cm thick compressible cushions. *X. deweerdtae* may overgrow the entire colony of *Plakortis deweerdtaephila* sp. nov. except around the elevated oscules, which are 0.2-0.9 cm in diameter (Fig. 2.2B). Oscules in

preserved specimens are contracted. External color is dark brown and internal color is light brown. Surface is smooth, soft and irregular. Consistency is compressible, and easily torn.

Skeleton. Ectosome is composed of a disorganized tangential reticulation of diods and triods. Multispicular tracts are not well defined but form circular meshes, 114–*205*–329 µm diameter (n=20; Fig. 2.2C). Spicules never break the surface of the ectosome. When *X. deweerdtae* forms inner channels within the choanosome of *P. deweerdtaephila* sp. nov. the ectosome forms a barrier between the two sponge species (Vicente *et al.* 2014). The ectosome (30-50 µm thick) can be easily distinguished from the choanosome with an abundance of subectosomal lacunae and by having a denser aggregation of pigmented cells (Fig. 2.2D). The choanosome is dense with a confused reticulation of diods and triods that form circular meshes of varying diameters (Fig. 2.2E).

Spicules. Diods can be very small to large. Large diods are slightly bent but mostly straight, slightly sinuous, with a thick center. Ends of large diods are sharp and sometimes bent (Fig. 2.2F-G): Small diods are rare, also thicker in the center and mostly straight. Small diods in Panama (Fig. 2.2F) can be as small as 50 µm and in the Bahamas (Fig. 2.2H) can be as small as 24 µm. Size (length × width) for Panama, 50–*173.2* (±37.1)–234 µm × 4.3–*7.9* (±1.7)–11.0 µm; Bahamas, 24–*107.6* (±43.4)–172 µm x 2.4–*3.7* (±0.7)–4.8 µm (Table 1). Triods are not abundant, being Y-shaped, smooth, and with sharp endings that are sometimes

bent (Fig. 2.2I) Size for Panama, 40–*64.2* (±15.8)–103 µm × 1.8–*5.9* (±2.2)–10.9 µm; Bahamas, 26–*45.1* (±11.3)–67 µm × 2.4–*3.3* (±0.5)–4.8 (Table 1). Microrhabds, quasiamphiasters and spheres are absent.

Habitat and ecology. Extensive surveys performed in the Caribbean suggest that this sponge is obligately associated with *X. deweerdtae* as free-living forms of *P. deweerdtaephila* sp. nov. have not been observed in more than 25 surveys that spanned 4 countries in the Caribbean: Mexico, Bahamas, Puerto Rico (Vicente *et al.* 2014) and Panama in this study. *P. deweerdtaephila* /*X.deweerdtae* sponge pairs have been documented from small sponge recruits to massive adults (Fig. 1.3A-C). These sponge pairs are found on the upper level (30-36 m) of mesophotic reef habitats, on vertical walls, shaded sides of pinnacles, as well as cryptic habitats (roof of overhangs and reef caves) of the Caribbean. In Panama the new species was found in a depth of 14 m, on the shaded sides of spur and groove hard bottom habitats exposed to high wave energy; individuals are completely overgrown by *X. deweerdtae* to the point where the new species is not visible unless the sponge pair is broken.

Distribution. Bahamas (Little San Salvador, San Salvador, Acklins, Mayaguana, Mira Por Voz, Plana Keys, Hogsty Reef; see also Vicente *et al.* 2014, Zea *et al.* 2014) and Panama (Dolphin Rock, Bocas del Toro) (Fig. 2.1B, E).

Etymology. The name *deweerdtaephila* denotes the close association with *Xestospongia deweerdtae*, from *phila* meaning “living or growing by preference”.

Taxonomic remarks. There are currently 12 *Plakortis* species known for the TWA of which seven occur in the Caribbean: *P. angulospiculatus* (Carter 1883), *P. zyggompha* (De Laubenfels 1934), *P. halichondrioides* (Wilson 1902), *P. simplex* Schulze, 1880, *P. myrae* (Ereskovsky *et al.* 2014), *P. edwardsi* (Ereskovsky *et al.*, 2014), and *P. dariae* (Ereskovsky *et al.* 2014). *P. deweerdtaephila* sp. nov. does not have any microrhabds or quasiamphiasters which places it among the *P. simplex* species group according to Muricy (2011). This species complex includes *P. galapagensis* (Desqeyroux-Faundez & Van Soest 1997), *P. insularis* (Moraes & Muricy 2003), *P. communis* (Muricy *et al.* 2015), *P. albicans* (D’Croz *et al.* 2005), *P. Copiosa* (Pulitzer-Finali 1993), *P. Erythraena* (Lévi 1958), *P. Japonica* (Hoshino 1981), *P. simplex* (Schulze 1880), *P. zyggompha*, *P. nigra* (Lévi 1953) *P. edwardsi*, and *P. dariae*. By having two size classes of diods the new species is more similar to *P. edwardsi* and *P. dariae* that inhabit vertical shaded sides of reef boulders in Martinique and were collected along depths of 22-26 m.

The external morphology of the new species differs from *P. edwardsi* by being more massive (3 × 30 cm by 1-8 cm thick) and having an irregular surface. Oscules of the new species can be elevated with large openings, while in *P. edwardsi* oscules are flush with the surface (Ereskovsky *et al.* 2014). The ectosome of the new species has more organized circular meshes than *P.*

edwardsi, without spicules cluttering open circular spaces. There is also an abundance of subectosomal lacunae that separates the ectosome from the choanosome in the new species that is not mentioned in the description of *P. edwardsi*. The choanosome also has more abundant circular meshes than in *P. edwardsi*. Spicules of specimens from the Bahamas, however, are similar in size and shape to *P. edwardsi*.

Despite having similar spicule sizes to *P. dariae*, the new species differs in external morphology and in the skeleton arrangement of the ectosome and choanosome. Also, the color of *P. dariae* is green, contrasting with the brown of the new species. Sponge individuals of the new species are larger and thicker than *P. dariae*. The new species also has larger oscules and an irregular surface. The ectosome of *P. dariae* is poorly differentiated without subectosomal lacunae. Spicules of *P. dariae* cross the surface of the ectosome while spicules in the ectosome of the new species never cross the surface. The shape of the small diods of *P. dariae* is also irregular with one end blunt which does not coincide with the shape of small diods in the new species that are always symmetrical.

The thick massive shape, brown color and dark color exudate, plus having some spicules reaching sizes >150 µm, led Zea *et a*l. (2009) to erroneously identify *P. deweerdtaephila* as *P. halichondrioides*. This fact was later corrected (Zea *et al*. 2014) after the molecular and spicular comparisons of Vicente *et al.* (2014) demonstrated their distinctiveness. To understand their differences, we made direct comparisons of specimens of *P. deweerdtaephila* sp. nov. with specimens of *P. halichondrioides* from the Bahamas and Puerto Rico.

Morphologically, the ectosomal skeleton of *P. halichondrioides* can be distinguished from *P. deweerdtaephila* in that spicules break the surface of the ectosome. Spicules also protrude inside circular meshes of the ectosome of *P. halichondrioides* and in *P. deweerdtaephila* circular meshes are free of spicules. Spicule sizes are also significantly smaller in *P. deweerdtaephila* than in *P. halichondrioides* (Vicente *et al.* 2014). Differences between *P. deweerdtaephila* and *Plakortis symbiotica* sp. nov. are given below in the taxonomic remarks of the latter species.

Recently, *P. angulospiculatus* was reported from Carrie Bow Cay, Belize, completely overgrown by *X. deweerdtae* (Rützler *et al.* 2014). Spicule size and shape of the *P. angulospiculatus* identified by Rützler *et al.* (2014) are in agreement with *P. dewerdtaephila*. Thus, its identity needs to be confirmed through molecular analysis, as the sequences of *P. angulospiculatus* we used herein (see below) turned out to be distantly related to those of *P. deweerdtaephila*. or *P. symbiotica*. *P. angulospiculatus* is a widespread Caribbean species, and its many reports may encompass several of the species newly described in the last decade (e.g. Domingos *et al*. 2013 and Ereskovsky *et al.* 2014) it needs to be reassessed, preferably from holotype material. The *cob* and *cox1* gene sequences we used from *P. angulospiculatus* individuals were determined by Erpenbeck *et al.* (2007) and Ereskovsky *et al.* (2014), respectively. The only character that apparently may distinguish *P. angulospiculatus* from the two new species of *Plakortis* is its lack of dark brown exudate (Ereskovski *et al.* 2014), but even this needs to be confirmed.

The most important morphological character that differentiates *P. deweerdtaephila* from any *Plakortis* species is that individuals have only been found associated with *X. deweerdtae*. No other sponge associations between *Plakortis* and a *Xestospongia* have been reported other than the *P. symbiotica*/*X. deweerdtae* sponge pair (described below). This is the first time that an obligate symbiosis with a heterospecific sponge species is a taxonomic character of any sponge species.

The larger size of spicules in specimens from Panama in comparison to those from the Bahamas (Table 2.1), reflect a Caribbean wide geographical pattern present in many groups of sponges, attributed to the apparent enrichment of silicon that continental locations experience, in comparison to oceanic ones (Zea 1987).

2.3.1.2. *Plakortis symbiotica* sp. nov.

(Fig. 2.3; Table 2.2)

Plakortis sp. 2; Vicente *et al.* 2014 (ecology and symbiosis).

Type material. Holotype and type locality: basibiont of *Haliclona plakophila* sp. nov., Old Buoy, La Parguera, Puerto Rico (17.9552° N, -67.0532° W), 32 m depth, coll. Jaaziel García-Hernández, October 15, 2015. Paratype, basibiont of *X. deweerdtae*, Old Buoy, La Parguera, Puerto Rico, (17.9552° N, -67.0532° W), 32 m depth, coll. Jan Vicente, August 13, 2012.

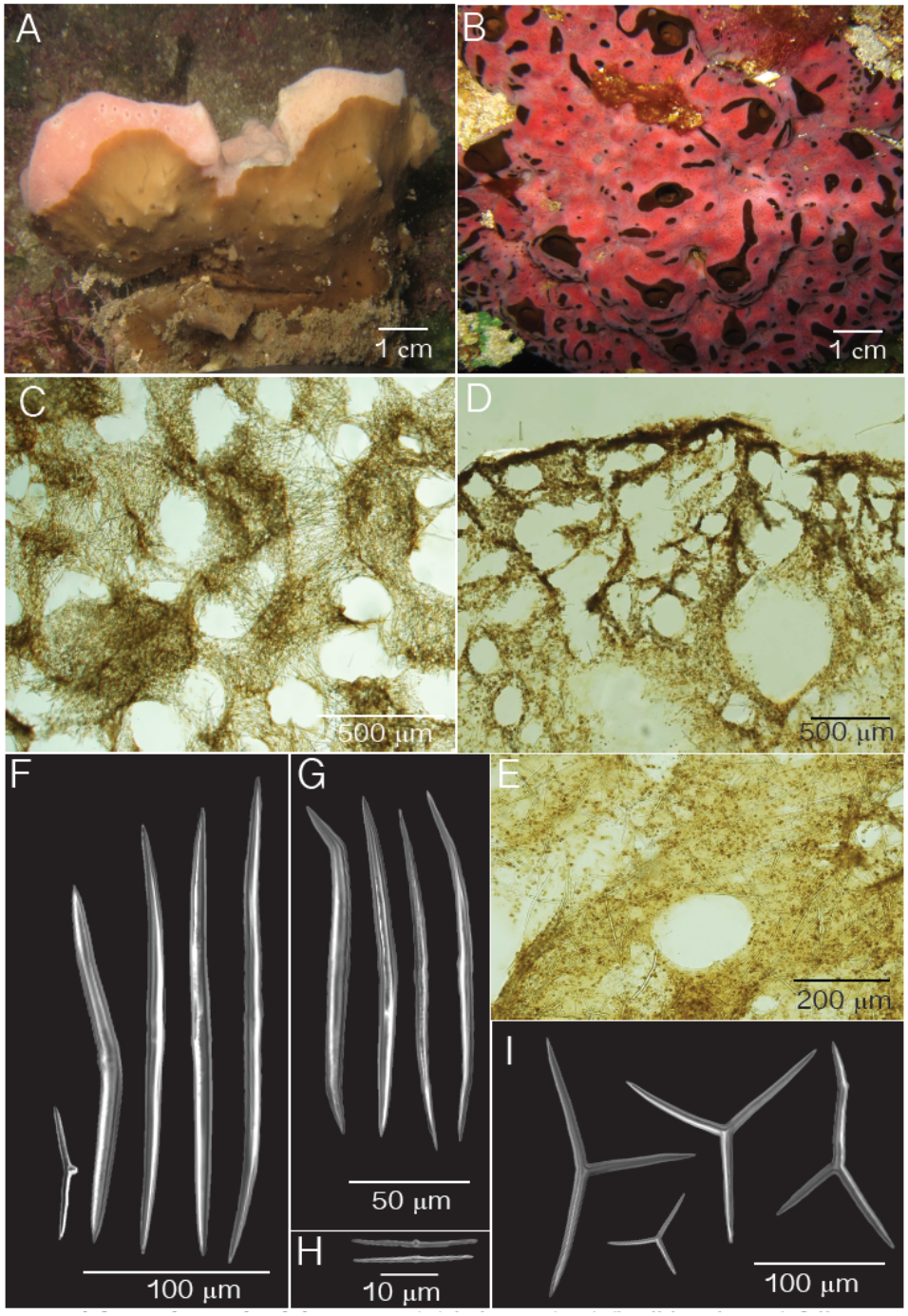

Figure 2.2 Plates of *Plakortis deweerdtaephila* sp. nov. *Plakortis deweerdtaephila* sp. nov**.** (A) holotype (USNM1254645) (basibiont-brown) fully overgrown by *Xestospongia deweerdtae* (epibiont-pink) in Panama; the specimen has been uplifted from the bottom to show the basibiont; oscules

directed downwards are visible; (B) Bahamas USNM1254647 (brown) partially overgrown by *X. deweerdtae* (pink) ; (C) tangential section of the ectosome (LM); (D) perpendicular section through the ectosome and choanosome (LM); (E) close-up of a perpendicular section through the choanosome (LM); (F) diods from specimens from Panama (SEM); (G-H) diods from specimens collected in the Bahamas (SEM); (I) triods from specimens from Panama (SEM).

Specimens examined for comparison (other than those described here)**.** *Plakortis halichondrioides*: PHBH, Little San Salvador, Bahamas, PHPR, La Parguera, Puerto Rico.

Diagnosis. Thickly encrusting cushions with a soft irregular surface and compressible body. Found as basibiont of *X. deweerdtae* but also of *Haliclona plakophila* sp. nov. In Puerto Rico, both *X. deweerdtae* and *H. plakophila* can be found on the same individual of *P. symbiotica* sp. nov. Both sponge epibionts grow as patches on the *P. symbiotica* body, never fully covering the basibiont as observed in *P. deweerdtaephila* sp. nov., but can penetrate the basibiont body forming inner channels. Oscules are slightly elevated from the surface. Color can be dark green and dark brown *in vivo* and exudes a brown pigment when preserved in ethanol. Reticulated tangential ectosomal skeleton and reticulated choanosomal skeleton with lacunae present. Spicules consist of triods and diods one size class.

Table 2.1 Spicule measurements for *Plakortis deweerdtaephila* sp. nov. and *Plakortis symbiotica* sp. nov. Spicule measurements of diods and triods (length and width) of holotypes (h) and paratypes (p) of *Plakortis deweerdtaephila* and *Plakortis symbiotica*. Triod measurements are actine length and width. Measurements are expressed as minimum–*mean* (±1 standard deviation)–maximum. N=30.

Spicule	Specimen	Location*	Length (µm)	Width (µm)
Diod	*Plakortis deweerdtaephila* USNM1254645 (h)	BDT, Panama	50–*173.2* (±37.1)–234	4–*7.9* (±1.7)–11
	Plakortis deweerdtaephila USNM1254647 (p)	SS, Bahamas	24–*107.6* (±43.4)–172	2–*3.7* (±0.7)–5
	Plakortis symbiotica USNM1254650 (h)	LP, Puerto Rico	72–*113.1* (±16.7)–142	2–*3.6* (±0.8)–5
Triods	*Plakortis deweerdtaephila* USNM1254645 (h)	BDT, Panama	40–*64.2* (±15.8)–103	1–*5.9* (±2.2)–11
(actine)	*Plakortis deweerdtaephila* USNM1254647 (p)	SS, Bahamas	26–*45.1* (±11.3)–68	2–*3.3* (±0.5)–5
	Plakortis symbiotica USNM1254650 (h)	LP, Puerto Rico	20–*40.4* (±12.8)–71	2–*3.3* (±0.7)–5

*Location BDT refers to Bocas del Toro, SS refers to San Salvador and LP to La Parguera.

Description. Thick cushions 3×30 cm by 1–3 cm in thickness (Fig. 2.3A). Oscules are slightly elevated measuring 0.3–1.7 cm in diameter. Oscules in preserved specimens are contracted. External and internal color is dark brown; a dark brown pigment is exuded when preserved. Surface is smooth, soft and irregular where *X. deweerdtaephila* or *H. plakophila* grow. Consistency is compressible, and easily torn.

Skeleton. Ectosome is a disorganized tangential reticulation of diods and triods. Multispicular tracts are not well defined but form circular meshes, 43–*73*–121 µm diameter (N=20; Fig. 2.3B). Spicules barely break the surface of the ectosome. When *X. deweerdtae* or *X. plakophila* form inner channels within the choanosome of *P. symbiotica* sp. nov., the ectosome forms a barrier between the two sponge species as observed by Vicente *et al.* (2014, their Fig. 7E and F). The ectosome (60–70 µm thick) is dense and sometimes hard to distinguish from the choanosome. Subectosomal lacunae are present (Fig. 2.3C). The choanosomal skeleton is dense but has an abundance of irregular circular meshes of varying diameters formed by a confused reticulation of diods and triods (Fig. 2.3D).

Spicules. One size class of diods and triods. Diods are significantly sinuously bent, with a thick center. Ends are sharp and significantly bent (Fig. 2.3E-F). Size (length x width): 72–*113.1* (±16.7)–142 µm x 2.2–*3.6* (±0.8)–5.0 µm (Table 2.1). Triods are rare, Y-shaped, smooth, with sharp endings that are sometimes bent

(Fig. 2.3I): 20-*40.4* (±12.8)–71 µm long by 2.0–*3.3*(±0.7)–4.7 µm in width (Table 2.1). Microrhabds, quasiamphiasters and spheres are absent.

Habitat and ecology. Sponge pairs are found on vertical walls (>30 m), shaded side of pinnacles, and reef cave habitats. Like *Plakortis deweerdtaephila* sp. nov., the new species has only been found either associated with *X. deweerdtae* or *H. plakophila*, never free-living (Vicente *et al.* 2014). Sponge pairs have been documented from small recruits (Fig. 1.3) and growth morphologies of sponge pairs remain stable for long periods of time (Fig. 2.4).

Distribution. Bahamas (Little Inagua) and Puerto Rico (Mona Island, La Parguera, Desecheo) (Figure 2.1B, D).

Taxonomic remarks. As in *P. deweerdtaephila* sp. nov., the lack of microrhabds or quasiamphiasters in *P. symbiotica* sp. nov**.** places it outside of the *P. simplex* species group (see above, cf. Muricy 2011). *P. symbiotica* can be distinguished from all species of this complex by its association status with either haploscleromorph, color, shape, size consistency or spicule composition.

Other than *P. deweerdtaephila*, the only other species to associate with *X. deweerdtae* is *P. symbiotica* (but see remarks above regarding *P. angulospiculatus* as basibiont of *X. deweerdtae* from Belize, cf. Rützler et al. 2014). In Puerto Rico, *H. plakophila* sp. nov**.** is also an epibiont of *P. symbiotica*. There are several morphological differences between *P. deweerdtaephila* and *P.*

symbiotica. For example, *P. symbiotica* only has large diods and small diods are absent. The large diods are significantly more bent than in *P. deweerdtaephila* (Fig. 2.2E, F). The ectosome has circular meshes with smaller diameters (43–*73*–121 µm; Fig. 2.3B) than ectosomal circular meshes of *P. deweerdtaephila* **(**114–*205*–329 µm; Fig. 2.2C). The ectosome is denser and harder to differentiate from cross-sections in *P. symbiotica* than in *P. deweerdtaephila* Subectosomal lacunae are present but many fewer than in *P. symbiotica*; the choanosome also appears to have more circular meshes than *P. symbiotica*

As for *P. deweerdtaephila*, *P. symbiotica* spicules were compared with those of *P. halichondrioides* by Vicente *et al*. (2014), and shown to be larger in the latter. Direct comparisons with a specimen of *P. halichondrioides* from Puerto Rico show that *P. symbiotica* can be distinguished by having smaller spicules and like *P. deweerdtaephila* spicules never cross the surface of the ectosome or the open spaces of the circular meshes. Circular meshes are therefore better organized in *P. deweerdtaephila* than in *P. halichondrioides*.

2.3.1.3. Phylogenetic analysis

The phylogenetic analysis used maximum likelihood to compare partial sequences of the *cob* and *cox1* genes of new *Plakortis* spp. to other homoscleromorph sponge sequences deposited in GenBank. The analysis confirmed that *P. deweerdtaephila* sp. nov**.** and *P. symbiotica* sp. nov**.** are more closely related to one another than to any other homoscleromorph or *Plakortis* species (Fig. 3.5). Sequence homology between both species was 93% for *cob*

and 94% for *cox1* and formed a clade that was supported with bootstrap values (85 and 78% respectively). On the other hand, these differences are enough to support their status as separate species, which is further supported by the morphological differences outlined above. The closest relatives to the new species were *P. simplex* and *P. dariae* with a 92% sequence homology for both genes. Despite having similar morphological features to *P. edwardsi*, this species turned out to be more closely related to *P. halichondrioides* and *P. angulospiculatus* in the phylogenetic analysis of both genes (Ereskovsky *et al.* 2014). Strong support values in the phylogenetic analysis for the *P. symbiotica* and *P. deweerdtaephila* clade suggests that the symbiotic association of these sponges with other sponges is perhaps an ancestral and even synapomorphic character.

Etymology. The name *symbiotica* denotes the tendency of the new species to associate with *X. deweerdtae* and *H. plakophila* sp. nov.

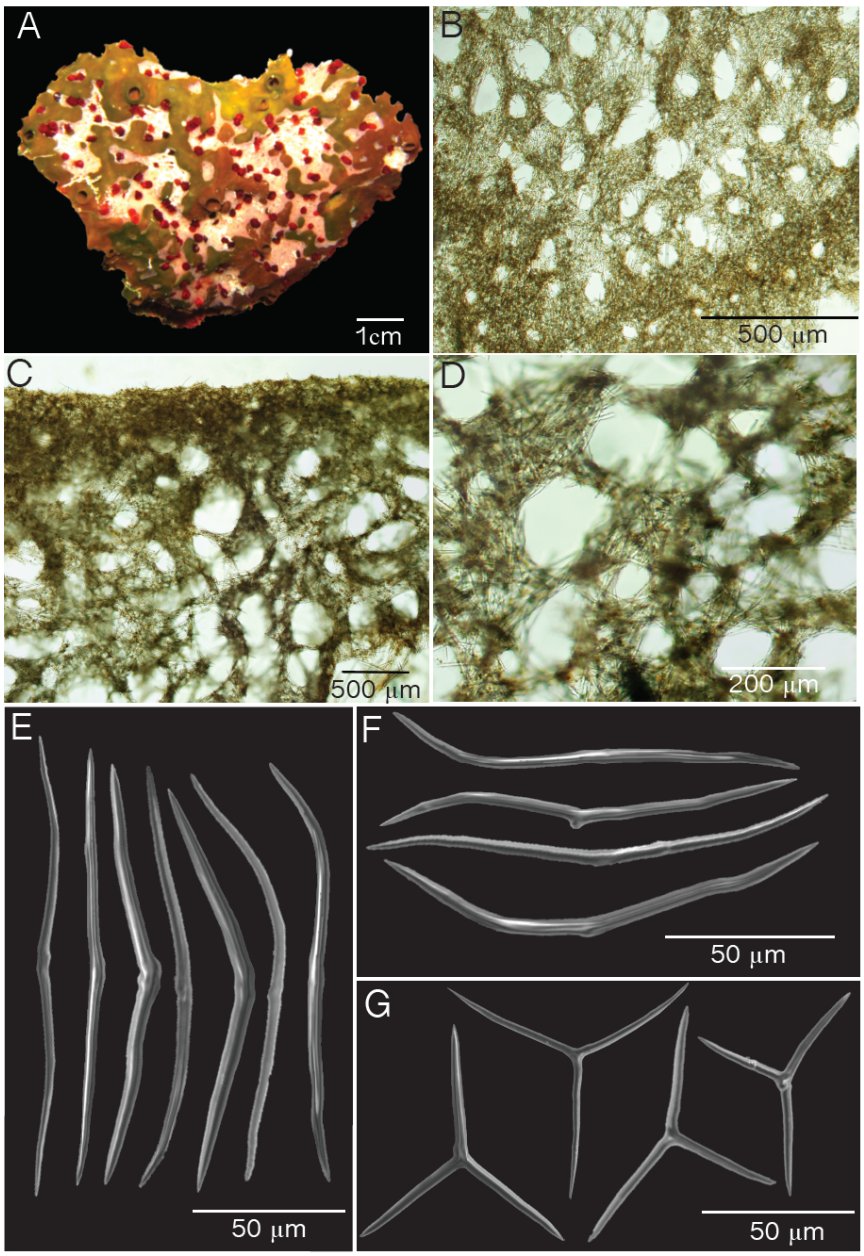

Figure 2.3 Plates of *Plakortis symbiotica* sp. nov. *Plakortis symbiotica* sp. nov. (A) holotype (USNM1254650) (brown) being overgrown by *Xestospongia deweerdtae* (pink) with zoanthids (red) in situ; (B) tangential section of the ectosome (LM); (C) perpendicular section through the ectosome and choanosome (LM); (D) close-up of a perpendicular section through the choanosome (LM); (E-F) diods (SEM); (G) triods (SEM).

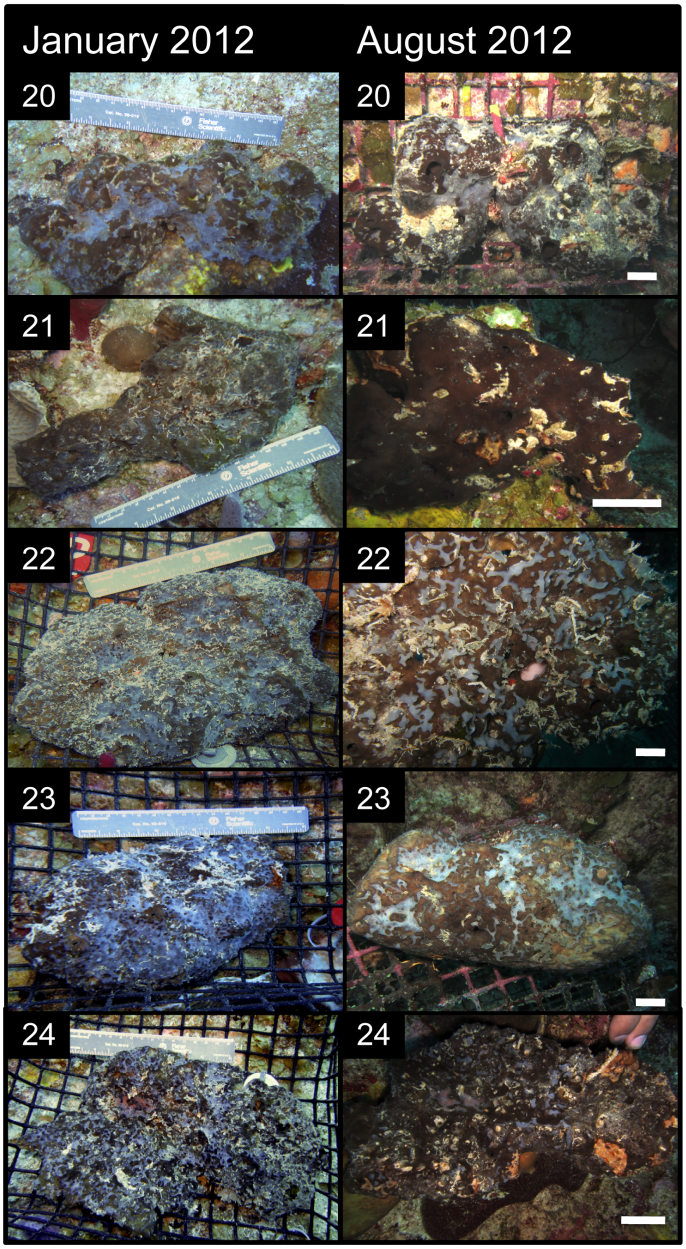

Figure 2.4 Monitored sponge transplants of *Plakortis symbiotica* sp. nov./*Haliclona plakophila* sp. nov. Monitoring growth of *Plakortis symbiotica*/*Haliclona plakophila* transplants during a 7-month period. Numbers indicate the identification for each individual.

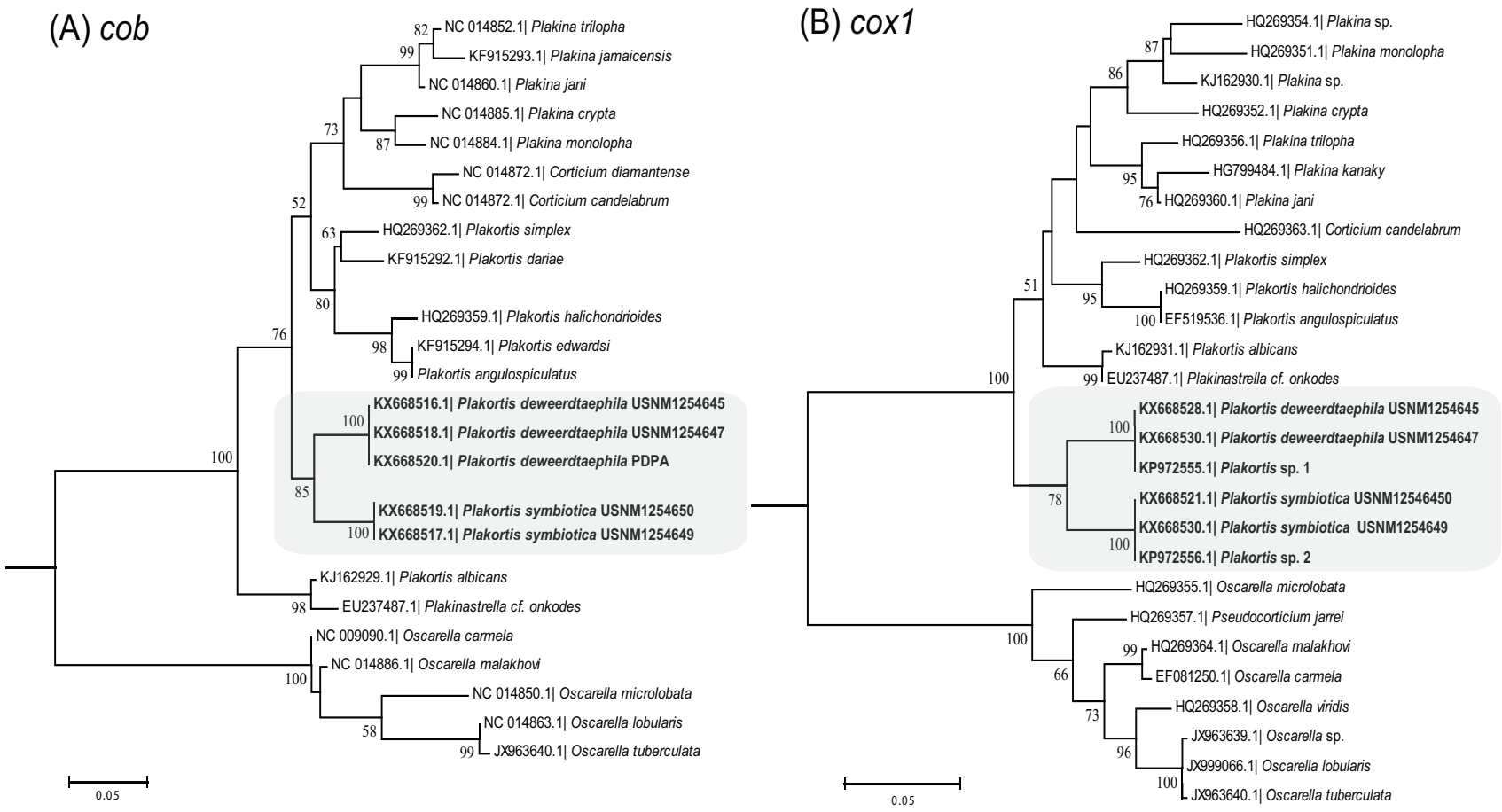

Figure 2.5 Molecular phylogeny of *Plakortis* species using cytochrome b oxidase (*cob*) and cytochrome c oxidase subunit 1 (*cox1*) gene sequence analysis.

Maximum likelihood topology generated from partial sequences of cytochrome b oxidase (*cob*) (A) and cytochrome c oxidase subunit I (*cox1*) (B) of the Homoscleromorpha of this study and from sequences downloaded from GenBank. Topology for both trees is rooted on the sponge *Ectyoplasia ferox* (Duchassaing & Michelloti, 1864) EU23748.1 (Class Demospongiae, Order Axinellida). Bootstrap values less than 50% were omitted from the trees. Coding following the species names refers to the museum catalogue number or collection location (PA-Panama, PR- Puerto Rico, BH-Bahamas) followed by lifestyle (AS-associated, FL-free-living). Species highlighted in bold represented sequences provided by this study.

2.3.2. Class Demospongiae (Sollas 1885)

Order Haplosclerida (Topsent 1928)

2.3.2.1. Family Chalinidae (Gray 1867)

Definition. Haplosclerina with a delicate reticulate choanosomal skeleton of uni-, pausi- or multispicular primary lines, which are regularly connected by unispicular secondary lines. Ectosomal skeleton, if present, a regularly hexagonal, unispicular, tangential reticulation (De Weerdt 2002).

Genus *Haliclona* (Grant 1836)

Definition. Chalinidae with unispicular secondary lines (De Weerdt 2002). Type species: *Spongia oculata* (Pallas 1766).

Subgenus *Halichoclona* (Schmidt 1862)

Definition. Chalinidae with a choanosomal skeleton consisting of a subisotropic, somewhat confused reticulation, commonly intercepted by many choanosomal spaces. Ectosomal skeleton of the same structure as the choanosome, usually very loosely overlaying the choanosome, from which it may be separated by extensive subectosomal spaces. Spongin absent or very scarce, at the nodes of the spicules. Megascleres usually acerate or hastate oxeas. Microscleres, if present, microxeas or sigmas. Sponges commonly relatively crisp and brittle, only slightly compressible (De Weerdt 2002). Type species: *Halichoclona gellindra* (Laubenfels 1932).

2.3.2.1.1. *Haliclona (Halichoclona) plakophila* sp. nov.

(Fig. 2.6; Table 2.2)

Xestospongia sp.; Vicente *et al.* 2014 (ecology and simbiosis).

Diagnosis. *Haliclona* (*Halichoclona*) bluish-white to translucent in color, thinly encrusting with occasional papillate morphology, so far exclusively found in epibiotic association with *P. symbiotica* sp. nov. Ectosome and choanosome consist of a subisotropic skeleton of oxeas.

Holotype and type locality: Old Buoy, La Parguera, Puerto Rico (17.9552° N, -67.0532° W), 32 m depth, coll. Jaaziel García Hernandez, October 15, 2015.

Paratype: PRAS12, and PRAS22, Old Buoy, La Parguera, Puerto Rico, (17.9552° N, -67.0532° W), 32 m depth, coll. Jan Vicente, August 13, 2012. Paratypes.

Description. Shape small, thinly (1-2 mm thick) encrusting veneer of tissue growing in separate patches on the surface of *P. symbiotica* sp. nov. (Fig. 2.6A). Some individuals presented papillated projections from the encrusting body (Fig. 2.6B). Irregular patches of *H. plakophila* sp. nov. occasionally form channels that burrow into *P. symbiotica* sp. nov. Consistency compressible, slightly brittle, delicate, fragile and inelastic. Individuals are bluish-white *in vivo* becoming white or translucent after fixation. Ectosome and choanosome are of the same color. Surface is smooth and very thin unless it burrows into the *Plakortis symbiotica* sp. nov. body. Oscules were not visible.

Skeleton. Ectosomal skeleton with an isotropic, paucispicular, tangential reticulation of oxeas, where 7-10 spicules meet at the nodes, forming 200 μm meshes. Subectosomal lacunae are present (Fig. 2.6C-D). The choanosomal skeleton is formed by a slightly disorganized isotropic reticulation of unispicular oxeas, where 7 spicules meet at each node, forming 100-200 μm meshes (Fig. 2.6D-E). The amount of spongin is very low throughout the ectosomal skeleton but more abundant in the choanosome (Fig. 2.6C-E). Spicules are not bound by spongin at the nodes.

Spicules. Oxeas, smooth, slightly curved at the center, fusiform, with hastate ends: 199–*229.5* (±11.5)–277 µm long by 3.5–*5.9* (±1.1)–8.7 µm in width (Table 2.2, Fig. 2.6F).

Habitat and ecology. Individuals were always found always associated with *P. symbiotica* sp. nov. Free-living individuals of *H. plakophila* sp. nov. have not been found after extensive surveys throughout cryptic habitats of the Caribbean. Sponge pairs are found below 30 m in cryptic habitats growing on vertical walls, on the roof of overhangs and on the bottom of reef cave habitats. We are investigating multiple factors to determine why these sponges are found associated with each other.

Distribution. Only observed at Old buoy, La Parguera, Puerto Rico. Likely to occur in other locations below 30 m along the southern continental shelf of Puerto Rico that offer similar cryptic habitats.

Etymology. The name *plakophila* describes the associated lifestyle with *Plakortis symbiotica* sp. nov., from *phila* meaning “living or growing by preference”.

Taxonomic remarks. Because of its relatively large oxea spicules (most above 200 µm), and like *Xestospongia deweerdtae* being epibiotic to *Plakortis*, this species was initially and preliminarily considered to belong to the genus

Xestospongia (Vicente *et al.* 2014). But after molecular analyses (see below) and detailed examination of skeleton, we concluded that this species belongs to the genus *Haliclona*. Species within *Haliclona* can have a very simple as well as a more complex variety of morphological characteristics, making the classification of species in this genus very challenging. The genus encompasses over 420 species from which approximately 200 have been assigned to six subgenera [*Gellius* (Gray 1867), *Halichoclona*, *Haliclona* (Grant 1836), *Reniera*, *Rhizoniera* (Griessinger 1971), and *Soestella* (De Weerdt 2000)] (De Weerdt 2002; Van Soest *et al.* 2012). In addition, sequences of ribosomal internal transcribed spacer regions of marine haplosclerids show no diversity across species (Redmond & McCormack 2009) and phylogenetic studies using several barcoding genes (cytochrome c oxidase subunit I, 18S and 28S rRNA) indicate that all subgenera of *Haliclona* are polyphyletic (McCormack *et al.* 2002; Redmond *et al.* 2011; Redmond *et al.* 2013).

Despite the taxonomic challenges, a number of morphological characters from these new species are in agreement with the subgenus *Halichoclona*. The new species has a disorganized choanosomal skeleton without clearly distinguishable primary or paucispicular secondary lines. These skeletal properties distinguish it from the subgenera *Gellius*, *Haliclona*, *Rhizoneria*, which have ascending primary lines and a unispicular skeleton connecting secondary lines (De Weerdt 2000, 2002). The absence of ascending primary lines conforms more to the subgenera *Reniera* and *Soestella*. However, the ectosomal skeleton of the new species does not form rounded meshes as observed in *Soestella*. The

ectosomal properties of the new species also do not fit within *Reniera*, since it is irregular, not unispicular with isotropic reticulation and does not have spongin at the nodes. The ectosomal skeleton of the new species is subisotropic and paucispicular which conforms more to *Halichoclona*. It also has subectosomal spaces that allow it to be easily detachable from the choanosome. However, the low abundance of spongin in the new species makes it difficult to unquestionably classify it as *Halichoclona*, as most members of this subgenus only have spongin present at the nodes where spicules meet.

There are 35 species of *Haliclona* sponges throughout the TWA of which seven belong to the subgenus *Halichoclona* (Bispo et al. 2014; Muricy et al. 2015). There are two species described from mangrove habitats in La Parguera, Puerto Rico: *H.* (*H.*) *magnifica* (De Weerdt *et al.* 1991) and *H.* (*H.*) *perforata* (Pulitzer-Finali 1986). *H.* (*H.*) *magnifica* is a massive sponge with thick walled tubes, a dense subisotropic reticulation of the ectosome that loosely overlays the choanosome composed of a subisotropic reticulation of oxeas (De Weerdt et al. 1991). *H*. (*H.*) *perforata* is also massive but with friable consistency; the choanosomal and ectosomal skeletons are a network of single spicules connected by spongin at the nodes. The new species is not massive, has a subisotropic reticulation of spicules, but also a paucispicular reticulation at the ectosome without spongin at the nodes; these characters are not found in either of the two halichoclonids from Puerto Rico.

The other five *H*. (*Halichoclona*) species from the TWA are *H*. (*H.*) *albifragilis* (Hechtel 1965), *H*. (*H.*) *dura* (Sandes *et al.* 2014), *H*. (*H.*) *lernerae*

(Campos *et al.* 2005), *H*. (*H.*) *stoneae* (De Weerdt 2000), and *H*. (*H.*) *vansoesti* (De Weerdt 2000). *H*. (*H.*) *vansoesti* is also blue but forms thick cushions with large elliptical oscules, and has an easily detachable subisotropic ectosomal skeleton (Weerdt *et al.* 1999). *H*. (*H.*) *stoneae* also forms thick cushions with large oscules and large oxeas (De Weerdt 2000). *H*. (*H.*) *lernerae* is found in deep habitats off the coast of northern Brazil and exhibits a massive tube-like morphology (Campos *et al.* 2005). *H*. (*H.*) *dura* is a thickly encrusting sponge with hard incompressible consistency (Sandes *et al.* 2014). The massive, large oscule morphology of these sponges does not fit the new species. However, *H*. (*H.*) *albifragilis* shares the closest morphological characteristics to them. This sponge is small, thinly encrusting, without visible oscula and grows under coral rubble below 74 m in depth, with a subisotropic choanosomal and ectosomal skeleton (De Weerdt 2000). This sponge however, lacks large subectosomal spaces and the new species exhibits large spaces underlying the ectosome. The new species also forms a thin veneer of tissue that exceeds 1 cm patches along the *P. symbiotica* sp. nov. body. There are also inconsistencies with the description of its color and there is no mention of *H*. (*H.*) *albifragilis* with papillated morphology. Phylogenetic analysis of partial sequences for 18S rRNA and *cox* genes from *Haliclona* spp. in GenBank confirmed that *H. plakophila* sp. nov. is a new species (results described below).

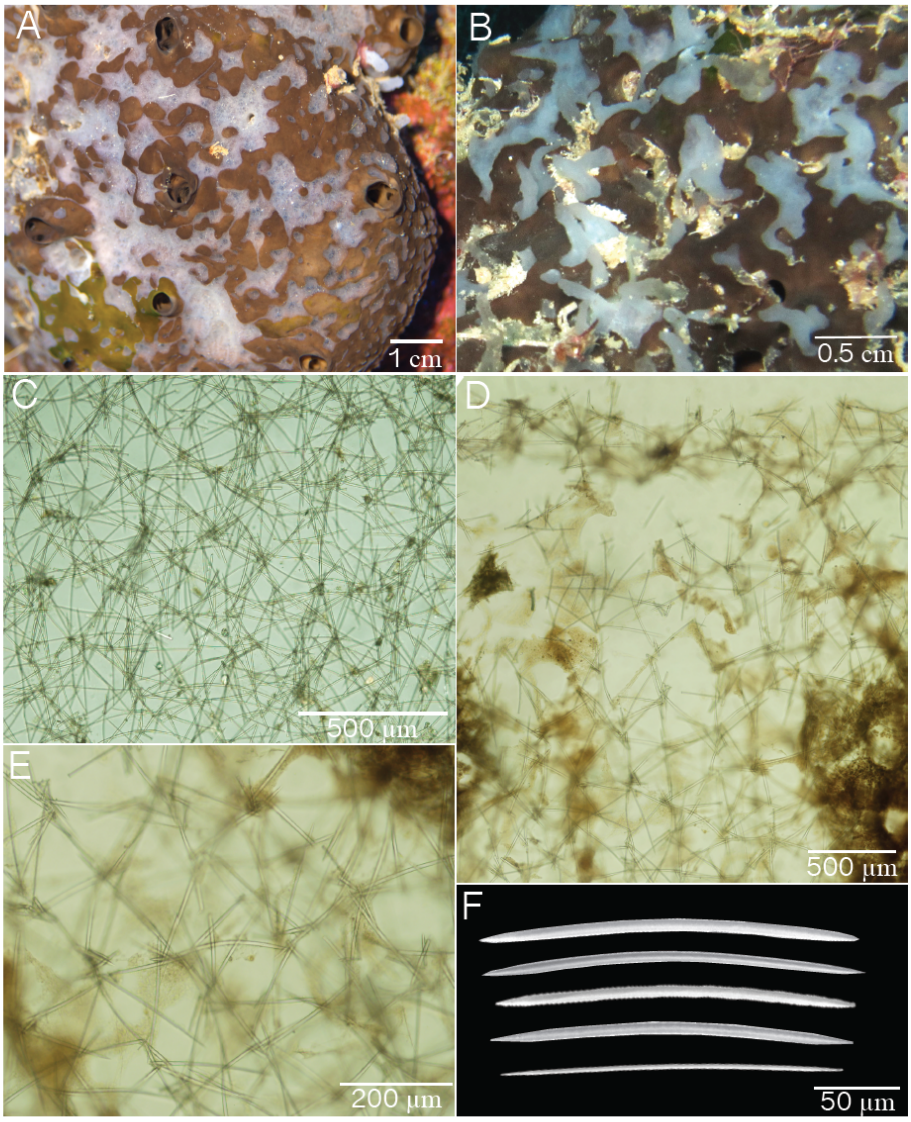

Figure 2.6 Plates of *Haliclona plakophila* sp. nov. *Haliclona plakophila* sp. nov. (A-B) holotype (USNM1254650) growing on *Plakortis symbiotica* sp. nov. (brown), encrusting (A) and papillated (B); (C) tangential section of the ectosome (LM); (D) perpendicular section through the ectosome and choanosome (LM); (E) close-up of a perpendicular section of the choanosome (LM); (F) oxeas (SEM)

Table 2.2 Spicule measurements of Haliclona plakophila sp. nov. Spicule measurements of oxeas (length and width) of *Haliclona plakophila* sp. nov. holotype and paratypes. Measurements are expressed as minimum–*mean* (±1 standard deviation)–maximum. N=50.

Specimen	**Length (µm)**	**Width (µm)**
Haliclona plakophila USNM1254650 (h)	199–*229.4* (±11.6)–256	3.6–*5.5* (±1.1)–8.7
Haliclona plakophila PRAS12 (p)	207–*230.0* (±10.1)–256	3.5–*6.4* (±1.1)–8.7
Haliclona plakophila PRAS22 (p)	207–*229.2* (±12.9)–277	3.6–6.4 (±1.0)–7.6

2.3.2.2. Family Petrosiidae (Van Soest *et al.* 1980)

Definition. Haplosclerida with an ectosomal skeleton consisting of an isotropic reticulation of single spicules or spicule tracts and a choanosomal skeleton verging towards an isotropic reticulation of spicule tracts, in which primary and secondary tracts are indistinct (Van Soest *et al.* 1980).

Genus *Xestospongia* (De Laubenfels 1932)

Definition. Petrosiidae with an ectosomal skeleton consisting only of an isotropic reticulation of single spicules or spicule tracts (Desqueyroux-Faúndez & Valentine 2002).

2.3.2.2.1. *Xestospongia deweerdtae* (Lehnert & Van Soest 1999)

(Figs. 2.7, 2.8; Table 2.3)

Xestospongia deweerdtae [Lehnert & Van Soest 1999: 163, Figs. 44-47; Van Soest & De Weerdt 2001: 114, Fig. 4C-D, 5C-D; Rützler *et al.* 2014: 91; Zea *et al.* 2014 ("-associated" and "-free living" forms); Vicente *et al.* 2014, Figs. 3a-f, 5, 6, 7a-d ecology and symbiosis with *Plakortis* spp.]

Xestospongia sp. 2; Zea 2001: Table 1 (appendix).

Xestospongia sp.-thin pink sheet over *Plakortis*; Zea *et al.* 2009.

Diagnosis. Thinly to thickly encrusting, pink, red and white mottled sponge. Surface smooth. Consistency crispy and only slightly compressible. Ectosome is

a dense tangential reticulation of strongyles bound by spongin. Choanosome is an isotropic reticulation of single spicules with some paucispicular tracts (Lehnert & Van Soest 1999).

Material examined. Holotype: ZMAPOR13584, Discovery Bay, Jamaica, 82 m depth, coll. Helmut Lehnert, June 26, 1996; Punta Caracol, Bocas del Toro, Panama (9.3777° N, 82.1265° W) 8 m, coll. Jan Vicente and Micah J. Marty, June 13, 2015; Dolphin Rock, Bocas del Toro, Panama (9.35076° N, -82.1863° W), 14 m coll. Jan Vicente and Arcadio Castillo May 20, 2015; Yellow Reef, Desecheo Island, Puerto Rico (18.3918° N -67.4760° W) 23 m coll. Jan Vicente October 7, 2011; Old Bouy, La Parguera, Puerto Rico (17.8883° N, -66.9981° W) 31 m, coll. Jan Vicente and Milton Carlo August 8, 2012;, San Salvador, Bahamas, (24.0406° N, -74.5314° W) 33 m coll. Jan Vicente and Steven E. McMurray July 19, 201;, Plana Cays, Bahamas (22.6045° N, -73.5465° W), 32 m coll. Jan Vicente and Steven E. McMurray, July 21, 2011.

Description (Figs. 2.7A–B, Fig 2.8A–B). External morphology is influenced by lifestyle (associated with *P. deweerdtaephila* sp. nov. or *P. symbiotica* sp. nov. or free-living) and by environmental factors. Free-living forms of *X. deweerdtae* in the Bahamas (Fig. 2.7A) and Panama (Fig. 2.8A) fit the original description of Lehnert & Van Soest (1999) and Van Soest & De Weerdt (2001). They form volcano shaped elevations that can measure up to 5 cm in length and with oscules on top, up to 0.7 cm in diameter. Individuals are light to dark pink, purple

(Panama), orange (Bahamas) and turn white when preserved in ethanol; color in the choanosome is the same. Surface smooth; consistency hard, slightly compressible. Although not mentioned in the original description, we noticed that free-living sponges always exude a viscous slime when cut.

The external morphology of associated lifestyles does not fit the original description of *X. deweerdtae*. In the Bahamas, associated individuals can be a thin encrusting veneer of patchy tissue that overlays and burrows into the *Plakortis* spp. body (Fig. 2.7B) with no visible oscula. In Panama, associated individuals are thickly encrusting (1 cm) and completely overgrow the *P. deweerdtaephila* sp. nov. body, forming 6-15 cm diameter plates (Fig. 2.8B; small oscules (1-3 mm) are aligned probably due to the high wave energy environment of Dolphin Rock). Associated individuals are softer, slightly compressible and more brittle than free-living individuals. Color is a light pink and even though we did not find free-living individuals with zoanthids, associated individuals in Puerto Rico were densely covered with red zoanthids (Fig. 2.3A).

Skeleton. Despite the differences in external morphology from the different lifestyles, the ectosome of both associated and free-living morphologies regardless of location consist of a unispicular regular skeleton of strongyles with 6–7 spicules meeting at each node (Fig. 2.7C–D; Fig. 2.8C–D). Meshes of the ectosome are somewhat triangular. The choanosome for all lifestyles and regardless of location consist of an isotropic reticulation of strongyles with

occasional paucispicular tracts, which conform to *X. deweerdtae* (Lehnert & Van Soest 1999) (Fig. 2.7E–H; Fig. 2.8E–H).

Spicules: Thick and sometimes thin strongyles, 151–423 μm long by 6.5–28.2 μm in width. Size and morphology of strongyles depends on the associated status of *X. deweerdtae* and geographical location. Across all geographical areas sampled (Bahamas, Puerto Rico, Panama), associated individuals have smaller and thinner spicules than free-living ones [see also discussion in Vicente *et al.* (2014)]; and between geographical areas, across lifestyles, individuals from island locations such as Bahamas, Puerto Rico and Jamaica have smaller and thinner spicules than those from Panama (Table 2.3).

Habitat and ecology. *X. deweerdtae* was originally described from deep (82 m) fore reef habitats and reef caves of Jamaica (Lehnert & Van Soest 1999) and then later found in reef caves (10–12 m) of Curaçao (Van Soest & De Weerdt 2001). In my study, I found *X. deweerdtae* growing beneath scleractinean corals and on the shaded side of *Agaricia* reefs in Panama at depths as shallow as 2 m. *X. deweerdtae* and *Plakortis* spp. nov. sponge pairs can be found on the shaded side of spur and groove reef formations (14 m) exposed to high wave energy environments in Panama. In the Bahamas and Puerto Rico sponge pairs are found deeper, below 30 m in cryptic habitats growing on vertical walls, on the roof of overhangs and on the bottom of reef caves. Associated individuals of *X.*

deweerdtae are more frequently observed than free-living one when both lifestyles are present in a given area (Vicente *et al.*, 2014).

Distribution. (FL=free-living, AS=associated) Jamaica (Discovery Bay-FL) (Lehnert & Van Soest, 1999) Curaçao-FL (Van Soest & De Weerdt, 2001), Mexico (Cozumel-FL, Banco Chinchorro-FL) (Vicente *et al.*, 2014), Bahamas (Plana Cays-FL-AS, Mayaguana-FL, San Salvador-AS, Little San Salvador-AS, Little Inagua-FL-AS, Acklins-FL, Great Inagua-AS, Mira Por Voz-AS) (Vicente *et al.* 2014; Zea *et al.* 2014), Puerto Rico (Mona-AS, Desecheo-FL-AS, La Parguera-AS) (Vicente *et al.* 2014), Panama, Bocas del Toro (Figure 2.8A-FL, Punta Caracol, Figure 2.8B-AS, Dolphin Rock), Colombia (Serrana Bank-AS) (Zea 2001).

Taxonomic remarks. The polymorphic nature of *X. deweerdtae* is revealed by lifestyle (associated and free-living) and by environmental factors (high wave energy and high silica environments, the latter associated to geographical location). Associated individuals do not exhibit a massive morphology and long volcano shaped oscules mentioned in the original description are absent. Instead, associated sponges are thinly to thickly encrusting. In Panama oscules for associated cases are small but visible (1-3 mm) and colonies are more thickly (0.5-1 cm) encrusting than associated individuals from Puerto Rico and the Bahamas (1 mm). Oscules for associated individuals from Puerto Rico and the Bahamas were not visible. Significantly smaller strongyles are observed in

associated (250 × 12.2 μm) sponges than free-living sponges (346 × 15.5 μm) in three different geographic areas resembling high and low silica concentrations. This was interpreted as a possible benefit for *X. deweerdtae* in terms of a lower investment in skeleton synthesis for support [see discussion in Vicente *et al.* (2014)]. Another possible explanation is that nutrients may be limiting for both sponges and one species might be depriving the other of silica. On the other hand, in the high silica environments in Panama [see D'Croz *et al*. (2005)] longer and thicker spicules were present in both free-living and associated sponges when compared with both associated and free-living individuals of Puerto Rico and the Bahamas (Table 2.3). Free-living individuals from Panama also produced not only thicker and longer strongyles, but also had bent ends that twisted in S-shaped or round brackets (Fig. 2.8I) probably due to hypersilicification (Zea 1987; Zea *et al.* 2014). One other important character from free-living sponges, missing in the original description, is the release of viscous mucus by sponges when cut. Associated sponges however, produce very little mucous when cut. The conspecificity of associated and free-living individuals was confirmed with phylogenetic analysis from partial sequences of the 18S, 28S rRNA and *cox1* genes (see below and Vicente *et al.* 2014).

2.3.2.3. Phylogenetic analysis. To confirm the identity of *Haliclona plakophila* **sp. nov.** as a new species and reconfirm the conspecificity of associated and free-living morphotypes of *Xestospongia deweerdtae* we partially sequenced the 18S, 28S rRNA and *cox1* genes of holotypes and paratype specimens. We

conducted a maximum likelihood analysis from sequences of species belonging to Haplosclerida that were closely related to *Haliclona* spp. and *Xestospongia* spp. deposited in GenBank. The maximum likelihood analysis of the 18S rRNA revealed that the closest relative to *H. plakophila* sp. nov. was *Oceanapia* sp. (GenBank accession no. DQ927317.1) with 91% sequence homology, placing *H. plakophila* sp. nov. distant from any of the monophyletic clades (A-E) previously reported by Redmond *et al.* (2013) (Fig. 2.9A). Members of clade C (Redmond *et al.*, 2013) were not included in the phylogenetic analysis, because sequences from *H. plakophila* sp. nov. were highly dissimilar to species in this clade. Sequences from associated and free-living individuals of *X. deweerdtae* were all >99% homologous to each other and to the holotype of *X. deweerdtae* (ZMAPOR13584), confirming that all specimens of both life styles are conspecific. The closest sequence homologous with *X. deweerdtae* was that of *Dasychalina fragilis* (GenBank accession no. DQ927316.1) with 99% sequence homology belonging to Clade D (Fig. 2.9A). Conspecificity of all *X. deweerdtae* lifestyles, including the holotype specimen, had a >99% sequence homology for the 28S rRNA and *cox1* genes (Fig. 2.9B-C).

I was unable to retrieve enough sequence data from the holotype specimen of *X. deweerdtae* to produce a phylogenetic tree of the *cox1* with strong bootstrap values, encompassing all closely related Haplosclerida species. However, there was enough sequence data to proceed with a maximum likelihood analysis of the *cox1* including members of the Haplosclerida that form monophyletic clades A and B from Redmond *et al.* (2011) (Fig. 2.10). The clade

of all *X. deweerdtae* conspecifics did not fall into either monophyletic clade and the closest relative was *Cribrochalina vasculum* (GenBank accession no. EF519664.1) with 93% sequence homology. Like *X. deweerdtae*, *H. plakophila* sp. nov. also did not fall into either clade A or B and its closest relative was *Petrosia* sp. C (GenBank accession no. JN242216.1) (Fig. 2.10).

2.4. Discussion

Cases of sponge-sponge epizoic interactions have long been reported in the literature. The first reports (Sollas 1888a) described *Triptolemma cladosus* overgrowing and penetrating the tissue of *Corallistes thomasi* in the Indian Ocean. Subsequently, a number of *Triptolemma* spp. were observed to grow on several sponge species from the Mediterranean, the northeastern Atlantic and South Africa (Maldonado 2002). Epizoic interactions have also been found in caves of the Adriatic Sea where *Aplysilla sulfurea* (Schulze 1877) was fully overgrowing the basibiont *Haliclona* (*Gellius*) *fibulatus* (Schmidt 1862) and hypothesized to be an adaptation strategy that offsets competition pressures (Rützler 1970). In Caribbean seagrass beds, chemically defended sponges may overgrow palatable sponges without smothering them and protect them from spongivorous predators (Wulff 1997; Ramsby *et al.* 2012).

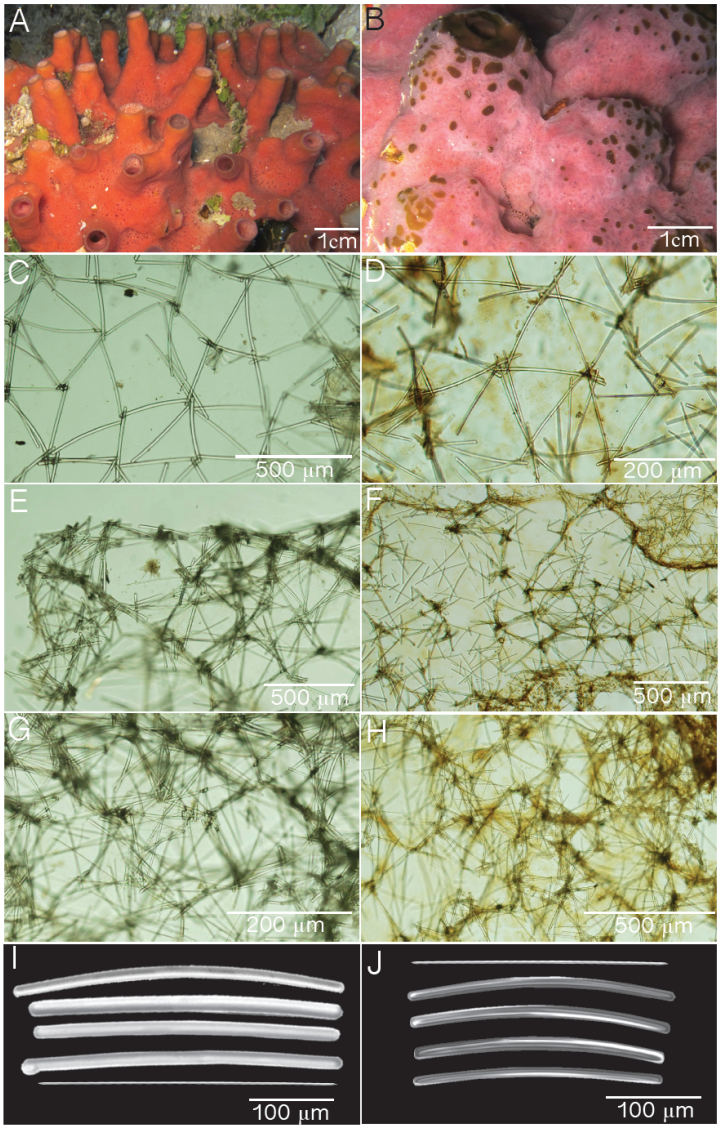

Figure 2.7 Plates of *Xestospongia deweerdtae* from the Bahamas.

Xestospongia deweerdtae from the Bahamas, comparing free living (A, C, E, G, I) and associated (B, D, F, J) life styles. (A, B) in situ underwater images (A, USNM1254646; B, USNM1254647 (pink) with *Plakortis symbiotica* sp. nov. (brown); (C, D) tangential section of the ectosome (LM); (E, F) perpendicular section through the ectosome and choanosome (LM); (G, H) close-up of a perpendicular section through the choanosome (LM); (I, J) strongyles (SEM).

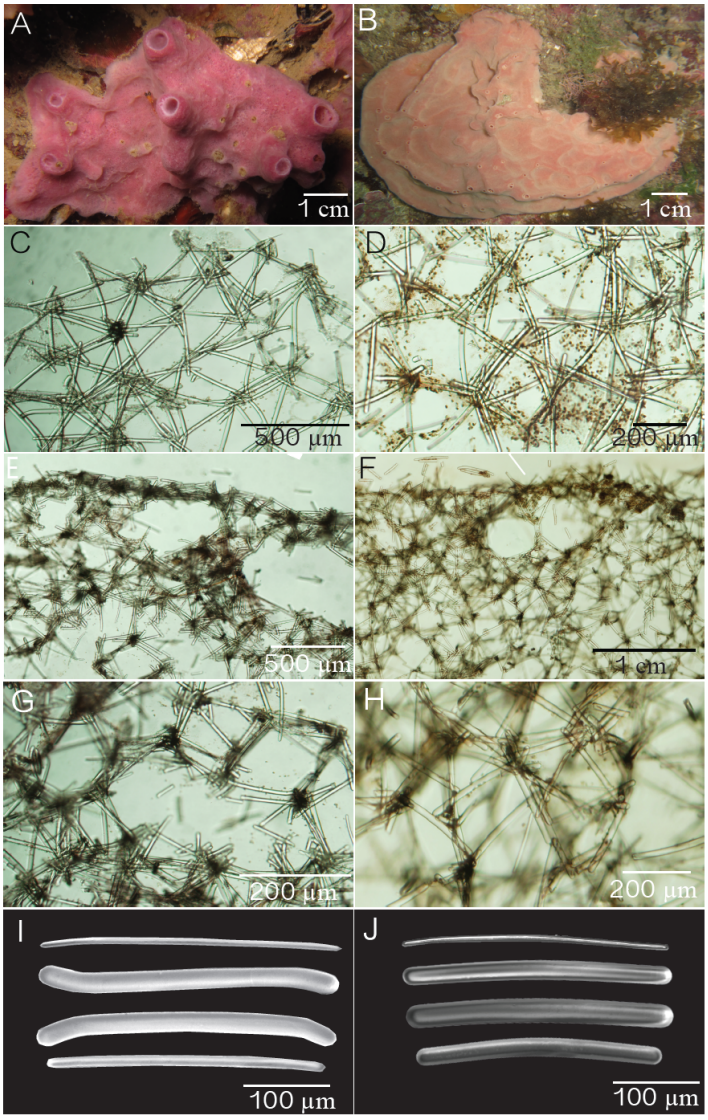

Figure 2.8 Plates of *Xestospongia deweerdtae* from Bocas del Toro Province in Panama. *Xestospongia deweerdtae* from Bocas del Toro Province in Panama, comparing free living (A, C, E, G, I) and associated (B, D, F, J) life styles. (A, B) In situ underwater images (A, USNM1254644; B, USNM1254645 completely overgrowing *Plakortis deweerdtaephila*; (C, D) tangential section of the ectosome (LM); (E, F) perpendicular section through the ectosome and choanosome (LM); (G, H) close-up of a section through the choanosome (LM); (I, J) Strongyles (SEM)

Table 2.3. Spicule measurements for *Xestospongia deweerdtae*. Spicule measurements of strongyles (length and width) of *Xestospongia deweerdtae* associated and free living. Measurements are expressed as minimum–*mean* (±1 standard deviation)–maximum. N=30.

Specimen	Location	Life style	Length (µm)	Width (µm)
ZMAPOR13584*	DB, Jamaica	Free-living	288—*340.9* (± 16.9)—373	6.5—*12.1* (± 2.2)—17.5
USNM1254646	SS, Bahamas	Free-living	305—*336.6* (± 14.8)—362	6.7—*11.8* (± 2.3)—17.2
USNM1254647	SS, Bahamas	Associated	151—*203.0* (± 18.8)—243	6.3—*7.9* (± 1.1)—11.2
USNM1254644	BDT, Panama	Free-living	340—*376.8* (± 19.7)—424	15.5—*21.8* (± 3.6)—28.2
USNM1254645	BDT, Panama	Associated	229—*323.8* (± 22.0)—379	12.8—*18.6* (± 2.8)—23.9
USNM1254648	LP, Puerto Rico	Free-living	296—*324.3* (± 15.2)—355	9.3—*13.0* (± 2.1)—17.7
USNM1254649	LP, Puerto Rico	Associated	159—*223.8* (± 23.5)—274	7.3—*10.2* (± 1.7)—13.8

*Specimen ZMAPOR13584 is the holotype (Lehnert & Van Soest 1999)

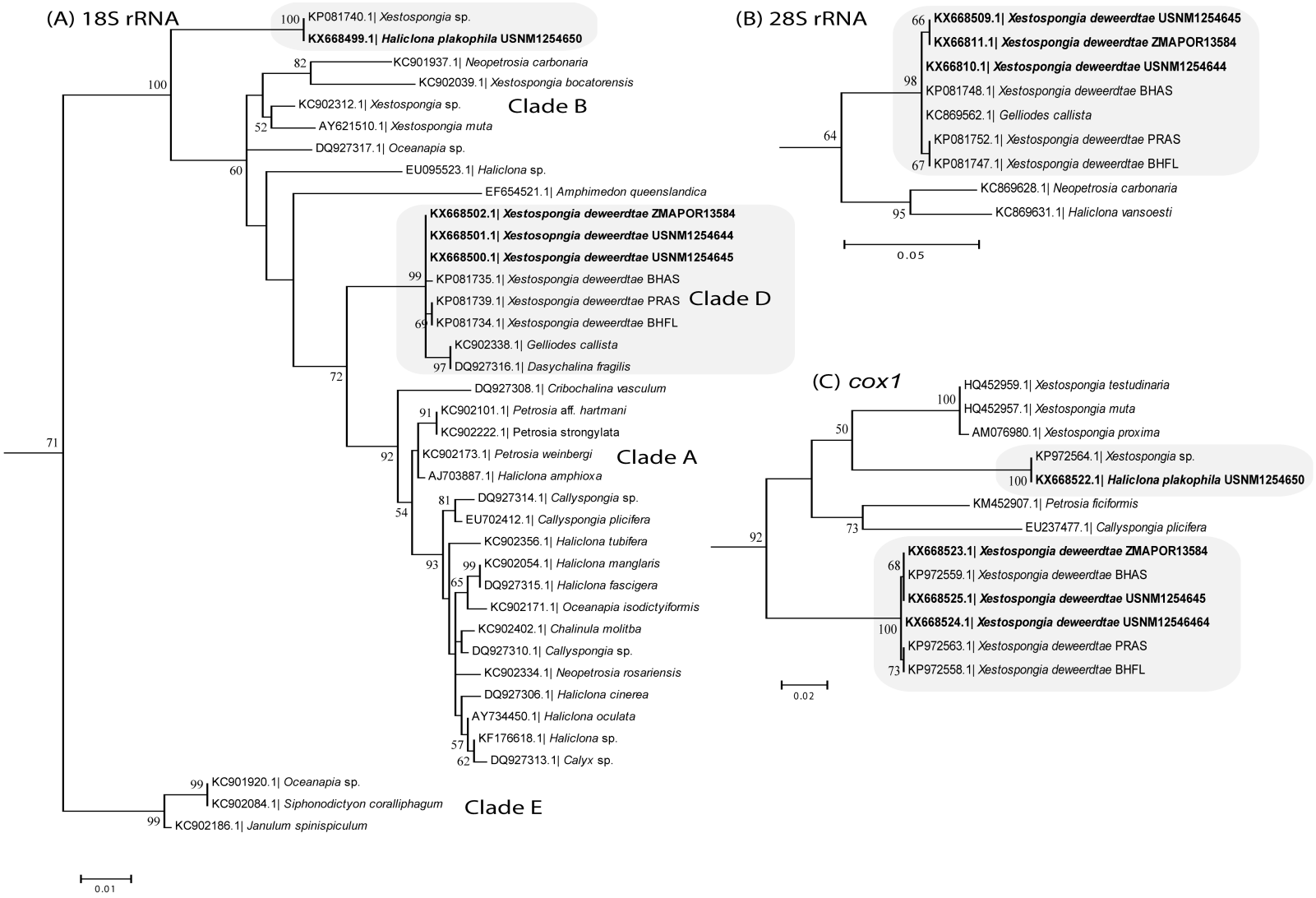
(A) 18S rRNA
KP081740.1| Xestospongia sp.
KX668499.1| Haliclona plakophila USNM1254650
KC901937.1| Neopetrosia carbonaria
KC902039.1| Xestospongia bocatorensis
KC902312.1| Xestospongia sp.
Clade B
AY621510.1| Xestospongia muta
DQ927317.1| Oceanapia sp.
EU095523.1| Haliclona sp.
EF654521.1| Amphimedon queenslandica
KX668502.1| Xestospongia deweerdtae ZMAPOR13584
KX668501.1| Xestosopngia deweerdtae USNM1254644
KX668500.1| Xestospongia deweerdtae USNM1254645
KP081735.1| Xestospongia deweerdtae BHAS
KP081739.1| Xestospongia deweerdtae PRAS
Clade D
KP081734.1| Xestospongia deweerdtae BHFL
KC902338.1| Gelliodes callista
DQ927316.1| Dasychalina fragilis
DQ927308.1| Cribochalina vasculum
KC902101.1| Petrosia aff. hartmani
KC902222.1| Petrosia strongylata
KC902173.1| Petrosia weinbergi
Clade A
AJ703887.1| Haliclona amphioxa
DQ927314.1| Callyspongia sp.
EU702412.1| Callyspongia plicifera
KC902356.1| Haliclona tubifera
KC902054.1| Haliclona manglaris
DQ927315.1| Haliclona fascigera
KC902171.1| Oceanapia isodictyiformis
KC902402.1| Chalinula molitba
DQ927310.1| Callyspongia sp.
KC902334.1| Neopetrosia rosariensis
DQ927306.1| Haliclona cinerea
AY734450.1| Haliclona oculata
KF176618.1| Haliclona sp.
DQ927313.1| Calyx sp.
KC901920.1| Oceanapia sp.
KC902084.1| Siphonodictyon coralliphagum
Clade E
KC902186.1| Janulum spinispiculum
0.01
(B) 28S rRNA
KX668509.1| Xestospongia deweerdtae USNM1254645
KX66811.1| Xestospongia deweerdtae ZMAPOR13584
KX66810.1| Xestospongia deweerdtae USNM1254644
KP081748.1| Xestospongia deweerdtae BHAS
KC869562.1| Gelliodes callista
KP081752.1| Xestospongia deweerdtae PRAS
KP081747.1| Xestospongia deweerdtae BHFL
KC869628.1| Neopetrosia carbonaria
KC869631.1| Haliclona vansoesti
0.05
(C) cox1
HQ452959.1| Xestospongia testudinaria
HQ452957.1| Xestospongia muta
AM076980.1| Xestospongia proxima
KP972564.1| Xestospongia sp.
KX668522.1| Haliclona plakophila USNM1254650
KM452907.1| Petrosia ficiformis
EU237477.1| Callyspongia plicifera
KX668523.1| Xestospongia deweerdtae ZMAPOR13584
KP972559.1| Xestospongia deweerdtae BHAS
KX668525.1| Xestospongia deweerdtae USNM1254645
KX668524.1| Xestospongia deweerdtae USNM12546464
KP972563.1| Xestospongia deweerdtae PRAS
KP972558.1| Xestospongia deweerdtae BHFL
0.02

Figure 2.9 Molecular phylogeny of Haplosclerida using 18S rRNA genes, 28S rRNA genes and *cox1* gene sequence analysis. Maximum likelihood topology generated from partial sequences of (A) 18S rRNA genes, (B) 28S rRNA genes and (C) cytochrome c oxidase subunit I (*cox1*) of the Haplosclerida generated in this study (bold) and sequences downloaded from GenBank. Topology is rooted on *Amphimedon compressa* (Duchassaing & Michelotti 1864) (EU702409.1) for 18S rRNA genes, *Axinella corrugata* (George & Wilson 1919) (DQ915619.1) for 28S rRNA genes and *Amphimedon queenslandica* (Hooper & Van Soest 2006) (DQ915619.1) for *cox1*. Bootstrap values less than 50% have been omitted from the trees. Clades A, B, D and E refer to Fig.4 in Redmond *et al.* (2013). Coding following the species names refers to the museum catalogue number or collection location (PA–Panama, PR–Puerto Rico, BH–Bahamas) followed by lifestyle (AS–associated, FL–free-living). Associated samples from Puerto Rico involve *Plakotis symbiotica* and associated samples from the Bahamas and Panama involve *Plakortis deweerdtaephila*. Species highlighted in bold represented sequences provided by this study.

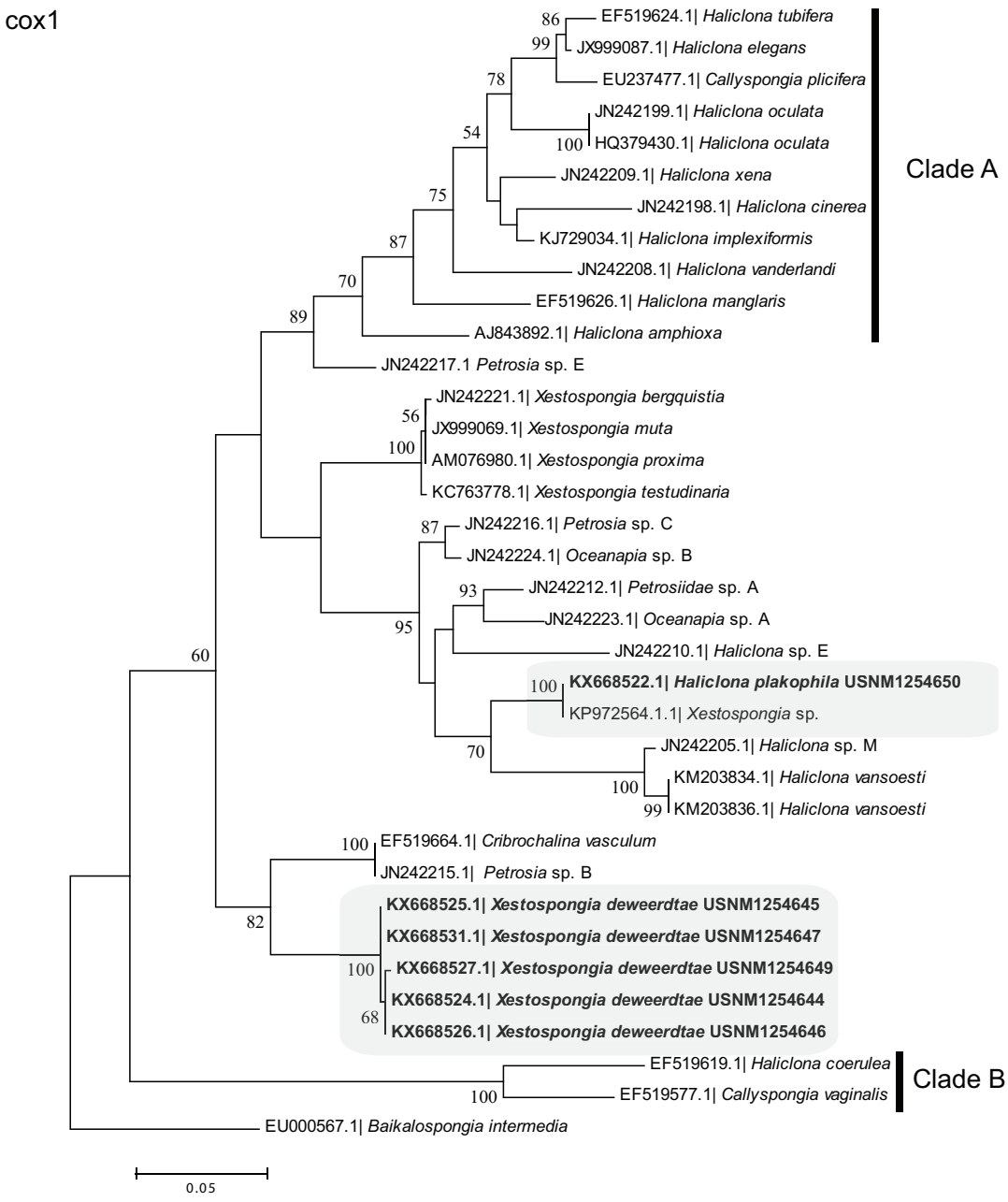

Figure 2.10 Molecular phylogeny of Haplosclerida using *cox1* gene sequence analysis. Maximum likelihood topology generated from partial sequences of *cox1* of the Haplosclerida in this study (bold) and from sequences downloaded from GenBank. Bootstrap values less than 50% were omitted from the tree. Clades A–B refer to Redmond *et al.* (2011) Fig. 3. Coding following the

species names refers to the museum catalogue number or collection location (PA–Panama, PR- Puerto Rico, BH-Bahamas) followed by lifestyle (AS-associated, FL-free-living). Associated samples from Puerto Rico involve *Plakortis symbiotica* and associated samples from the Bahamas and Panama involve *Plakortis deweerdtaephila*. Species highlighted in bold represented sequences provided by this study.

Despite the many examples of sponge epizoism, none represent specialized, obligate interactions, which makes the symbiosis in this study the first time that an association status with another sponge is a key taxonomic character for *Plakortis deweerdtaephila* sp. nov. and *Plakortis symbiotica* sp. nov. The phylogenetic analysis of partial fragments from the cytochrome oxidase gene confirmed that both *P. deweerdtaephila* sp. nov. and *P. symbiotica* sp. nov. are closely related to each other but distantly related to other *Plakortis* spp. No other homoscleromorph sponges have been found in association with haploscleromorph sponges, making the association status of *P. deweerdtaephila* sp. nov. and *P. symbiotica* sp. nov. a synapomorphic character of this clade.

Several morphological features of *P. deweerdtaephila* sp. nov. distinguish it from *P. symbiotica* sp. nov. Diods are straighter in *P. deweerdtaephila* sp. nov. and circular meshes of the ectosome are significantly larger. Small diods observed in *P. deweerdtaephila* sp. nov. (24.2 μm long) were not found in *P. symbiotica* sp. nov. but are similar in lengths to diods observed in *P. edwardsi*. However, *P. edwardsi* is genetically more similar to *P. halichondrioides*, which

further supports the opinion by Ereskovsky *et al.* (2013) that spicules in *Plakortis* are an ambiguous character, not supported by molecular phylogeny. A recent publication by Rützler *et al.* (2014) reports that *P. angulospiculatus* is overgrown by *X. deweerdtae*. However, this finding is only supported by spicule composition and not by molecular evidence. Considering the ambiguous character of spicule morphology, this could very well mean that the basibiont sponge overgrown by *X. deweerdtae* in Belize is one of the two new *Plakortis* spp. nov. described here.

This study also highlights four different conspecific morphotypes of *X. deweerdtae* that are characterized by lifestyle and environmental factors. Previous studies on phenotypic plasticity for Caribbean sponges have confirmed that sponge morphology can be influenced by predation (Loh & Pawlik 2009; Loh *et al.* 2012), high wave energy environments (Hill & Hill 2002) and by associated lifestyles with other sponges (Wilcox *et al.* 2002). This study shows similar results to those found by Wilcox *et al.* (2002), where associated individuals of *Geodia vosmaeri* had a thinner cortex. Like *G. vosmaeri*, associated *X. deweerdtae* individuals have smaller spicules and are more fragile than free-living sponges, which supports the hypothesis that associated sponges invest less energy in building a stronger skeleton than free-living sponges (Vicente *et al.* 2014). An alternate hypothesis is that nutrients are limiting for both sponges and one species might be depriving the other of silica. In Bocas del Toro, Panama free-living *X. deweerdtae* had strikingly different strongyles. As expected, strongyles were significantly larger than any other free-living form of *X. deweerdtae*. This did not come as a surprise as other sponge species from this region (DeBiasse &

Hellberg 2015) and other sponges in high silica environments have significantly larger spicules than in silica limited environments (Zea 1987). However, the S-bent and circular bracket shaped strongyles (Fig. 2.8I) were unexpected and have never been observed for this species. We confirmed conspecificity of the different morphotypes by determining partial sequences of *cox1,* 18S and 28S rRNA of the holotype specimen originally collected in Jamaica. Despite belonging to a highly polymorphic group of sponges (Redmond *et al.*, 2011), all *X. deweerdtae* morphotypes group under the same clade and are supported by high bootstrap values for these three genes (Fig. 2.9).

H. (*H.*) *plakophila* sp. nov. has very simple morphological features but differ enough from previously known chalinid sponges to consider it a new species. This is the ninth *Halichoclona* species reported for the TWA region and the third for Puerto Rico. Despite extensive survey efforts, I am are unaware of *H.* (*H.*) *plakophila* sp. nov. having a free-living lifestyle other than associating with *P. symbiotica* sp. nov. Phylogenetic analysis of the 18S rRNA and *cox1* genes (91% and 94% sequence homology to the closest relative respectively) placed *H.* (*H.*) *plakophila* sp. nov. distantly from any *Haliclona* spp. or any monophyletic clade reported by Redmond *et al.* (2011, 2013). Nevertheless, 18S rRNA and *cox1* genes are considered polyphyletic in haplosceromorph sponges and other sequence products should be considered for an accurate diagnosis of its phylogeny within Chalinidae.

Cryptic habitats of the Caribbean continue to reveal not only a large number of new species and genera but new symbiotic adaptations between

Homoscleromopha and Haplosclerida. In this study, novel sponge interactions add two more species of *Plakortis* spp., and one new *Haliclona* sp. to the TWA. Species diversity of these two classes from these unusual habitats in the TWA remains highly underestimated (Domingos *et al.* 2015; Muricy *et al.* 2015; Muricy *et al.* 2013; Ereskovsky *et al.* 2013; Rützler *et al.* 2014; Van Soest *et al.* 2014). Parasitic and mutualistic hypotheses are being evaluated to determine the nature of these interesting sponge pair interactions.

Chapter 3: Microbial community and stable isotope analysis of epibiont and basibiont sponges in specialized sponge symbioses

3.1. Abstract

The sponge microbiome influences a number of physiological processes that can be crucial to the survival of the sponge host. These processes often depend on microbial abundance and diversity. Sponges can either have a complex microbiome with high diversity or a very simple microbiome with low diversity of microbes carrying out important ecological roles for its host. These lifestyle disparities have been discovered to form symbiotic pairs in three recently discovered cases of sponge—sponge symbiosis between heterospecific species. Bacterial and sponge cell counts showed that both epibiont *Xestospongia deweerdtae* and *Haliclona plakophila* sponges are low microbial abundance sponges that overgrow high microbial abundance basibiont *Plakortis symbiotica* and *Plakortis deweerdtaephila* sponges. Next-generation sequencing of the 16S rRNA gene showed higher diversity indices of microbial symbionts in basibiont sponges than epibiont sponges. Free-living individuals of *X. deweerdtae* were also analyzed and the microbial community in free-living individuals showed less diversity than found in associated individuals. Relative abundance comparisons between free-living and associated *X. deweerdtae* showed OTUs belonging to microbial phyla found in *Plakortis* spp. basibionts to be present in associated *X. deweerdtae* suggesting that epibionts could be acquiring symbionts from the basibiont sponge through horizontal transmission. $\delta^{13}C$ and $\delta^{15}N$ isotope analysis of bulk tissue showed a variety of isotopic niches for each species in the pair in three different location of the Caribbean. In Panama both epibiont and basibiont had similar $\delta^{13}C$ and $\delta^{15}N$ values while significant differences were

observed in sponges from Puerto Rico and the Bahamas. These results suggest that each sponge in the pair has a different $\delta^{13}C$ and $\delta^{15}N$ isotopic niche space that is dependent on the available food source of the surrounding environment. Based on the difference in microbial communities and isotope niches of epibiont and basibiont sponges, it is unlikely that nutrients are a limiting factor for both sponges to cohere mutualistically.

3.2. Introduction

My recent discovery of sponge-sponge symbioses between sponges of the genera *Plakortis* and epibionts *Xestospongia deweerdtae* and *Haliclona plakophila* has motivated me to evaluate how the microbial community associated with each species in the sponge pairs might explain the nature of these associations. Morphological features of each species (discussed in Chapter 2) fit the description of the dichotomy between high microbial abundance (HMA) and low microbial abundance (LMA) sponges, enough leading me to hypothesize that sponges may be associating to help compensate for the physiological demands of these free-living lifestyles. For example, *Plakortis* spp. consists of a dense skeleton of diods and triods with a dense aquiferous system while *X. deweerdtae* and *H. plakophila* have a brittle skeleton with a more channel-enriched aquiferous system. These morphological features are generally consistent with those of HMA and LMA sponges respectively (Vacelet & Donadey 1977). In HMA sponges, the dense tissue is thought to increase the abundance of small water channels, requiring more energy to pump water than LMA sponges (Vogel 1978; Weisz *et al.* 2008; Schläppy *et al.* 2010). Interestingly, transversal sections of *Plakortis deweerdtaephila* and *X. deweerdtae* from the Bahamas show that the *X. deweerdtae* epibiont grows into the *P. deweerdtaephila* mesohyl forming wide (0.1-1 cm) inner channels (Fig. 2.7F) and that the LMA epibiont might be enriching the aquiferous system of the HMA basibiont.

Previous studies using bacterial and sponge cell quantification methods including 4,6-Diamidine-2-phenylindole dihydrochloride (DAPI) staining, and scanning electron microscopy have shown a clear distinction in bacteria/sponge cell ratios between the HMA and LMA sponge types (Gloeckner *et al.* 2014). These ratios show HMA sponges having significantly higher bacteria/sponge cell ratios than LMA sponges (Gloeckner *et al.* 2014). Among the sponges surveyed in Gloeckner *et al.* (2014), only one *Plakortis* sp. species was classified as a HMA sponge. Sponges belonging to the marine Haplosclerida have been shown to fall into both HMA and LMA lifestyles, which implies that the HMA/LMA dichotomy is not necessarily consistent with phylogeny.

Studies have also found that microbial abundance may sometimes correlate with microbial diversity (Giles *et al.* 2013; Poppell *et al.* 2014; Easson & Thacker 2015). However, next-generation sequencing of the 16S rRNA gene of both HMA and LMA sponges in the Caribbean have shown that not all HMA and LMA sponges conform to the definition that HMA sponges have higher microbial diversity than LMA sponges (Easson & Thacker 2015). For example, sponges that harbor high densities of photosynthetic cyanobacteria, considered HMA sponges, showed a very low number of operational taxonomic units (OTUs). Consequently, these sponges may show moderate OTU richness but a low Inverse Simpson's index (*D*), which indicates that these communities are dominated by only a few OTUs (Easson & Thacker 2015). Nevertheless, this hypothesis of HMA sponges having higher microbial abundance and vice versa appears to be consistent with findings in the epibiont and basibiont sponges in

this study as some *Xestospongia* spp. and *Haliclona* spp. have a lower *D* than *P. halichondrioides* (Thomas *et al*. 2016). The presence of an enriched microbial community with higher microbial diversity might allow sponges to have access to unique capabilities for chemical transformations of nitrogen, carbon, phosphate and sulfur (Hoffmann 2003; Mohamed *et al.* 2008; Freeman & Thacker 2011; Zhang *et al.* 2015).

The use of stable isotopes ($\delta^{13}C$ and $\delta^{15}N$) has helped decipher how sponges might be using metabolic products from microbial pathways. A study that used $\delta^{13}C$ and $\delta^{15}N$ isotope analysis on sponge and bacterial cells showed that nitrogen and carbon fixation are important biological processes that are carried out by the microbial community and products used by the sponge host as an important food source (Mohamed *et al.* 2008; Mohamed *et al.* 2010; Freeman *et al.* 2013; Zhang *et al.* 2015). Other studies that used isotope analysis on bulk sponge tissue of HMA and LMA sponges showed that HMA sponges span a wider isotopic niche spaces than LMA sponges (Weisz *et al.* 2007; Freeman *et al.* 2014). The presence of unique microbial taxa correlates with the ability to expand their $\delta^{13}C$ and $\delta^{15}N$ isotopic niche space. We therefore hypothesize that *Plakortis* spp. basibionts have a different microbial community from their epibionts and occupy a different $\delta^{13}C$ and $\delta^{15}N$ niche space than their epibionts and are therefore not competing for nutrients.

In order to test these hypotheses we: 1. Quantified DAPI-stained sponge and microbial cells of the sponge pairs using serial dilutions and direct quantification of stained sponge tissue sections, 2. Used next-generation

sequencing approach to describe the microbial communities associated with both sponge pairs, 3. Determined $\delta^{13}C$ and $\delta^{15}N$ values of each species in the sponge pair as well as free-living *X. deweerdtae* to test whether sponges are competing for similar isotopic niche spaces or if the different microbial communities span different spaces for each sponge to cohere mutualistically.

3.3. Methods

3.3.1. Sponge and seawater collection

Sponge individuals were collected from four geographic locations: Bahamas in July 2011, Mexico in July 2012, Puerto Rico in August 2012, and Panama in May 2015. A list of collected sponge samples and their locations are given in Table A1.1. Sponges in Panama were collected and analyzed in two locations because sponge pairs were found only in Dolphin Rock and free-living sponges were found only in Punta Caracol. Individuals of *P. halichondrioides* were collected from both of these sites to check for differences in microbial communities in sponges growing at different sites. Whole sponge pair individuals were collected in15-L O_2/CO_2 permeable plastic bags (Ken's Fish; Taunton, MA) and placed in flow-through holding tanks. Careful dissections were performed to remove epibiont sponges from their basibionts, making sure that we retrieved clean samples for cell quantification, DNA extraction and stable isotope analysis from each member of the pair. Sponge samples that included ectosome and choanosome were cut into ~1 cm^3 pieces and frozen or fixed using different methods depending on the objective (see below).

Seawater samples were collected in 20-L carboys that were filled with sterile DI water and brought to the sponge collection depth. Carboys were opened at depth and held until incoming salt water displaced all of the sterile DI water. Samples were immediately filtered through a 0.2 μm sterivex filter using a Millipore peristaltic pump. Triplicate samples (8-10 L of seawater filter^{-1}) were collected per site. Sterivex filters were drained and immediately frozen until later DNA extraction.

3.3.2. Sponge and bacterial cell quantification

We used two quantification methods to determine the abundance of sponge and bacterial cells for each sponge species. The first method was adapted from Gloeckner *et al.* (2014) and used on sponges collected in Panama. A piece of sponge tissue (1.1 ± 0.01 g) from each species with both ectosome and choanosome was removed and rinsed with 0.2 μm-filtered sterilized seawater. The sponge piece was added to 9 ml of 0.2 μm filtered seawater with a final concentration of 4.0 % paraformaldehyde (PFA). The tissue was homogenized with a sterile mortar and pestle. The homogenate was poured through Nitex (100-μm pore size) and stored at 4 °C until samples were quantified. A dilution series of the homogenate ranging from 10^{-1} to 10^{-4} as prepared for each sample. A volume of 1 ml was added to 9 ml of filter-sterilized seawater and filtered onto a black, 0.2 μm polycarbonate membrane 25 mm in diameter (Millipore, Germany) supported with a 0.45 μm cellulose nitrate filter. A filter tower (20 mL) was placed over the membrane and filter. The sample was

added and a slow vacuum was applied to pass the sample through. The filters were rinsed with sterile seawater and stained with 30 µl of 50 µg ml^{-1} (140 µM) of DAPI for 10 min. Filters were rinsed again with sterile seawater and let to dry for 5 min. Filters were mounted on microscope slides with immersion oil type FF for fluorescence. Sponge and bacterial cell counts were performed by epifluorescence microscopy using 100 × magnification (Axioplan microscope, Zeiss, Germany). Four replicates of each species were processed. For each replicate the average number of sponge (> 5 µm) and bacterial (< 5 µm) cells were counted in 10 different viewing areas each measuring 1,452 μm^2. Cyanobacteria were not detected under the red or green fluorescent filter sets for any sponge species in this study.

The second quantification method was adapted from Freeman *et al.* (2011) and used on sponges collected in Panama, Puerto Rico and the Bahamas. A small piece (1 cm^3) of sponge tissue from each species with both ectosome and choanosome was removed and rinsed with 0.2 µm filtered sterilized seawater. The sponge tissue was fixed in 9 ml of 4.0% PFA that was prepared with filtered seawater for 24 h and later transferred to 70% ethanol. A small subsample was cut from the fixed sponge tissue and stained with DAPI (140 µM) for 20 minutes. Samples were embedded in Cyromold (Sakura) with Tissue-Tek O.C.T medium (Sakura) and solidified on dry ice. Sections (1–5 µm thick) were cut on a cryostat microtome (Sakra Tissue-Tek Cryo 3) under -30°C and mounted on Superfrost Plus slides (Electron Microscopy Science). Sections were made perpendicular to the surface of the sponge through the ectosome and

choanosome. Sections were immediately covered with a cover slip. Sponge and bacterial cells were observed in 10 viewing areas (1,452 μm^2) selected at random and the average was calculated.

3.3.3. DNA extraction and next-generation sequencing

Dissected sponge samples for DNA extraction were preserved in RNAlater and frozen at -80°C. DNA was extracted using the AllPrep DNA/RNA Mini Kit (Qiagen) with a TissueLyser System (Qiagen). RNAse-free DNAse treatment steps from the Qiagen manufacturer's protocol were followed to retrieve RNA from sponges collected in Puerto Rico. The qScript cDNA Synthesis Kit (Quanta BioSciences, Inc) was used to make cDNA from RNA. DNA from seawater samples was extracted using a Power Water Sterivex DNA isolation kit (Mo Bio, Carlsbad, CA, USA) following the manufacturer's protocol. Quality of DNA and cDNA extracts were monitored by using extracts as PCR templates to amplify the 16S rRNA gene with universal primers prior to sequencing. RNA samples without the RT step were included as PCR templates to check for residual genomic DNA in the RNA samples. Aliquots of DNA and cDNA extracts that yielded a 16S rRNA product from sponges collected in Puerto Rico, Bahamas and Mexico were kept in the Hill laboratory and one aliquot was shipped to the University of Colorado, Boulder, USA for sequencing of the 16S rRNA gene following standard procedures of the Earth Microbiome Project (http://www.earthmicrobiome.org/emp-standard-protocols/16S). The V4 region of the 16S rRNA gene for sponge samples collected in the Puerto Rico, Bahamas

and Mexico was amplified using bacterial/archaeal primer pair 515F – 806rB following methods by Caporaso *et al.* (2012) and were sequenced using the HiSeq2500 platform (Illumina). Samples collected in Panama were sequenced using the primer pair 341F – 805R and were sequenced using a MiSeq platform.

3.3.4. Processing of sequencing data

Forward and reverse demultiplexed Illumina reads from the MiSeq platform were assembled (~450 BP product) and quality filtered using QIIME 1.3.0. The fastq file generated from QIIME was further processed using mothur v.1.37.4 (Schloss *et al.* 2009). Sequences were trimmed using the *trim.seqs* command (qwindowaverage=25, qwindowsize=5, maxambig=0, maxhomop=8, minlength=100, processors=16). Quality-filtered and demultiplexed sequences from the HiSeq platform were also quality trimmed (*trim.seqs*) but with the addition of the “keep.first =100” parameter. The trimmed files from both sequencing platforms were concatenated. Files were reduced to non-redundant sequences (*unique.seqs*) and aligned to a trimmed V4 region reference SILVA 123 bacteria database (6428-26103) (Quast *et al.* 2013). Sequences that did not align correctly were removed. The *screen.seqs* command was used to keep sequences at positions between (7434-9879). Since sequences from the MiSeq platform overlapped and were longer than sequences from the HiSeq platform we decided to chop these at 7434 and 9879 using a python script. Only sequences that were chopped at this position were kept (*filter.seqs*). The *unique.seqs* command was used again on the aligned reads to reduce sequence

redundancy. Aligned sequences were classified (*classify.seqs*) based on the trimmed SILVA database (Wang *et al.* 2007). Chimeras were identified using UChime (*chimera.uchime*) (Edgar *et al.* 2011) and removed from the alignment (*remove.seqs*). Classified sequences were clustered (*cluster.split*) using a 97% similiarity cutoff and pairwise distances between aligned sequences were also calculated (*dist.seqs*) using a 97% cutoff. Sequences were converted to a .shared file format (*make.shared*). Representative sequences of each OTU from the sequence clustering step were retrieved (*get.oturep*) and further classified based on the SILVA database. A database file with classified OTUs was created and combined with the .shared file to make a .RData file that was imported into R v. 3.3.0 (Team 2014); http://www.R-project.org).

3.3.5. Microbial community diversity analysis

A minimum threshold of 10,250 reads was used to calculate three different univariate measures of microbial community diversity (OTU richness (*S*), Shannon-Weaver index (*H'*), and inverse Simpson's index *D*), using the R package vegan (Oksanen *et al.* 2013). We also calculated Bray-Curtis microbial community distances for each sponge species and tested significance using the adonis command. Mean relative abundances of microbial phyla were calculated and compared between each species. We compared the different diversity indices between basibiont, epibiont, free-living and associated lifestyles of *X. deweerdtae* using analysis of variance (ANOVA). ANOVAs for samples collected in Panama were analyzed separate from samples collected in Puerto Rico,

Bahamas and Mexico as these were sequenced with a different set of primers. Tukey's honestly significant difference (HSD) tests were used to determine significant differences between means of all measured parameters.

3.3.6. $\delta^{13}C$ and $\delta^{15}N$ stable isotope analysis

Lyophilized sponge tissue was ground to a fine powder and homogenized using a ceramic mortal and pestle. Approximately 0.5 ± 0.001 mg of tissue were weighed into tin capsules (Costech). Each sample was then flash-combusted on a Costech ECS4010 elemental analyzer and analyzed for carbon ($\delta^{13}C$) and nitrogen ($\delta^{15}N$) isotopes through an interfaced Thermo Scientific Delta V Plus Stable Isotope Ratio Mass Spectrometer (IRMS) at the UNC Wilmington Center for Marine Science. Raw δ values were normalized on a two-point scale using glutamic acid reference materials with low and high values (USGS-40: $\delta^{13}C$ = −26.4‰, $\delta^{15}N$ = −4.5‰; USGS-41: $\delta^{13}C$ = 37.6‰, $\delta^{15}N$ = 47.6‰). Sample precision, based on repeated sampling of reference materials, was 0.1‰ and 0.2‰ for $\delta^{13}C$ and $\delta^{15}N$, respectively. Stable isotope ratios are expressed in δ notation in per mil units (‰), according to the following equation: $\delta X = [(R_{sample} / R_{base}) - 1] \times 1000$, where X is ^{13}C or ^{15}N and R_{sample} is the corresponding ratio $^{13}C/^{12}C$ or $^{15}N/^{14}N$. The R_{base} values were based on the Vienna PeeDee Belemnite (VPDB) for $\delta^{13}C$ and atmospheric N_2 for $\delta^{15}N$.

3.4. Results

3.4.1. Sponge and microbial cell quantification

Quantification of sponge and microbial cells from series dilutions of 1 g of wet sponge tissue from sponges collected in Panama showed that *P. symbiotica* had 1.3 × and 1.9 × the number of bacterial cells than epibiont and free-living cases of *X. deweerdtae* respectively (Table 1). The epibiont and free-living cases of *X. deweerdtae* had 49.3 × and 43.8 × the number of sponge cells than the *P. symbiotica* basibiont respectively. The resulting bacteria/sponge cell ratio was 89.23 for *P. symbiotica*, 7.06 for associated *X. deweerdtae* and 5.45 for free-living individuals (Table 3.1).

Sponge and microbial cell quantifications performed on DAPI-stained sponge tissue sections revealed that the average number of sponge cells (μm^{-1}) in free-living *X. deweerdtae* and epibiont sponges (*X. deweerdtae* and *H. plakophila*) had 2.8 × more the average number of sponge cells in basibiont sponges (*Plakortis* spp.) including *P. halichondrioides* (Fig. 3.1A). Conversely, the average number of bacterial cells (μm^{-1}) was 6.1 × higher in basibiont *Plakortis* spp. than free-living *X. deweerdtae* and epibiont (*X. deweerdtae*, *H. plakophila*) sponges (Fig. 3.1B). The sponge/bacterial cell ratios were 31× higher in basibiont *Plakortis* spp. sponges than in the *X. deweerdtae* and *H. plakophila* epibiont sponges (Fig. 3.1C).

Table 3.1 A compilation of microbial and sponge cell counts by DAPI staining (ml^{-1} of sponge homogenate) reported in Gloeckner *et al.* (2014) and in this study. Counts were performed on free-living and associated sponges of the genera *Plakortis* and *Xestospongia deweerdtae* collected in Panama. Cyanobacteria were not detected for any of the sponges in this study.

HMA/ LMA	Sponge species	Bacterial total Mean ± SE	Sponge nuclei Mean ± SE	Ratio (b/c)*	Reference
HMA	*Plakortis* sp.	$4.3 \times 10^9 \pm 8.0 \times 10^8$	$3.8 \times 10^8 \pm 2.6 \times 10^7$	89.23	Gloeckner *et al.* 2014
	Plakortis halichondrioides	$2.4 \times 10^9 \pm 1.14 \times 10^7$	$2.9 \times 10^7 \pm 1.1 \times 10^7$	80.03	This study
	Plakortis deweerdtaephila (AS)[1]	$7.11 \times 10^8 \pm 4.19 \times 10^6$	$1.66 \times 10^7 \pm 4.2 \times 10^6$	42.91	This study
	Xestospongia muta	$8.2 \times 10^9 \pm 7.7 \times 10^8$	$4.8 \times 10^8 \pm 4.1 \times 10^{7`}$	16.96	Gloeckner *et al.* 2014
LMA	*Xestospongia deweerdtae* (AS)	$5.56 \times 10^8 \pm 5.46 \times 10^7$	$7.9 \times 10^7 \pm 5.46 \times 10^7$	7.06	This study
	Xestospongia deweerdtae (FL)[2]	$3.8 \times 10^8 \pm 5.6 \times 10^7$	$7.0 \times 10^7 \pm 5.6 \times 10^7$	5.45	This study
	Iotrochota birotulata	$2.4 \times 10^9 \pm 2.8 \times 10^8$	$5.2 \times 10^8 \pm 4.3 \times 10^7$	4.67	Gloeckner *et al.* 2014
	Callyspongia vaginalis	$4.0 \times 10^6 \pm 2.0 \times 10^6$	$5.5 \times 10^8 \pm 1.1 \times 10^7$	0.01	Gloeckner *et al.* 2014
	Niphates digitalis	n.d.	$1.4 \times 10^8 \pm 2.3 \times 10^7$	0.00	Gloeckner *et al.* 2014

n.d. not detected according to Gloeckner *et al.* (2014).
(b/c)* bacteria/sponge nuclei ratio
(AS)[1] associated lifestyle
(FL)[2] free-living lifestyle

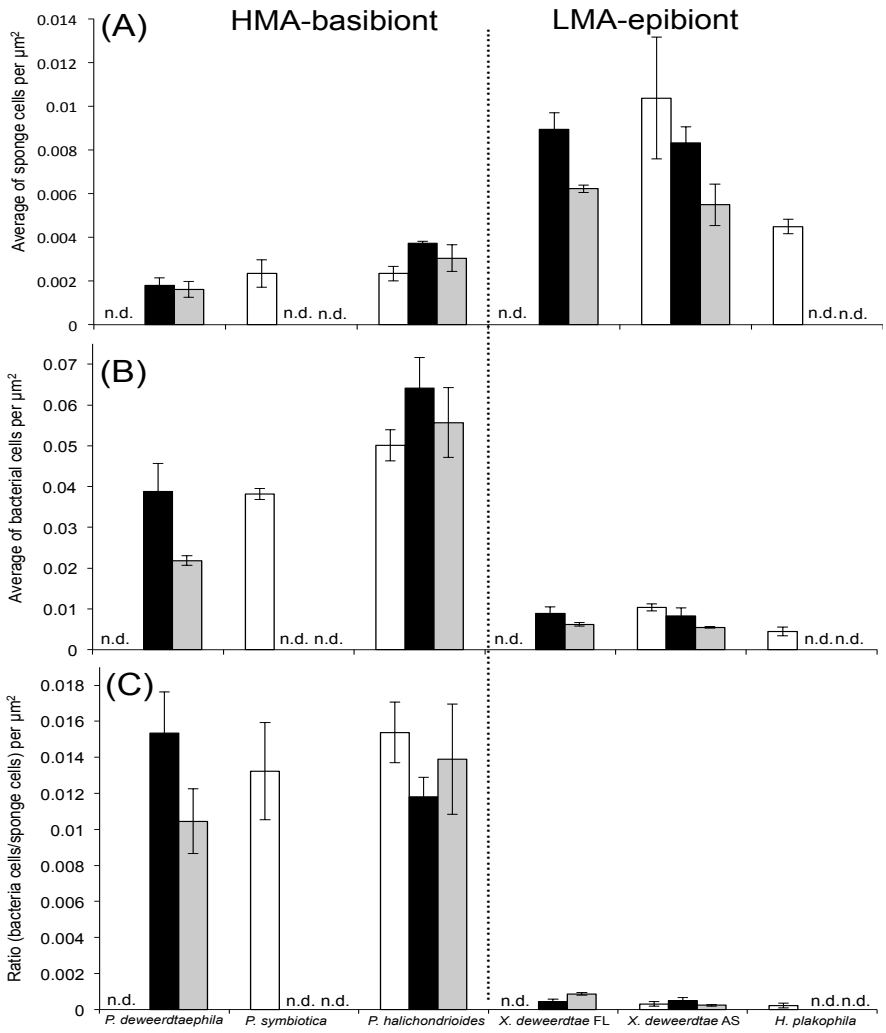

Figure 3.1 Sponge and microbial cell counts of basibiont and epibiont sponge species in each sponge pair, free-living Xestospongia deweerdtae and Plakortis halichondrioides. ***Average and standard error of DAPI-stained (A) sponge cell counts, (B) bacterial cell counts and (C) sponge/bacterial cell ratios for species in each sponge pair per µm^2 of sponge tissue. Collection sites of each species are indicated by bar colors (Puerto Rico-white, Panama-grey, Bahamas-black). n.d. (not determined) indicates that these sponges were not collected.***

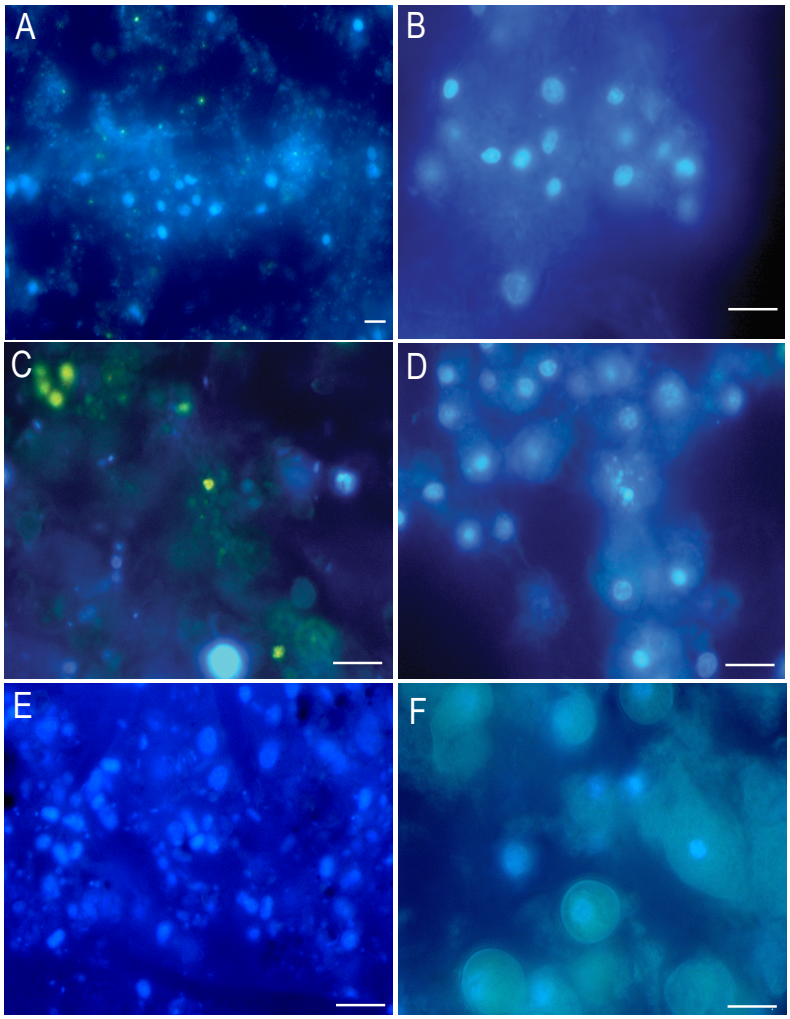

Figure 3.2 Sponge and microbial cells stained by DAPI of samples from sponge species in each sponge pair, free-living *Xestospongia deweerdtae* and *Plakortis halichondrioides*. Sponge (> 5 µm) and bacterial cells (< 5 µm) from DAPI-stained sponge samples of high microbial abundant sponges (A) *Plakortis halichondrioides*, (C) *Plakortis deweerdtaephila*, (E) *Plakortis symbiotica* and low microbial abundant sponges (B) *Xestospongia deweerdtae* free-living, (D) *X. deweerdtae* associated and (F) *Haliclona plakophila*. Polyphosphate granules (yellow granules) were observed in *P. halichondrioides* (A) and *P. deweerdtaephila* (C). Scale bar for all images = 5 µm.

Both quantification methods confirmed that *Plakortis* spp. basibionts are high microbial abundance sponges and that epibionts are low microbial abundance sponges. The high number of microbial cells in basibionts and the high number of nucleated cells of epibionts are clearly visible in Figure 3.2. Epifluorescent microscopy on DAPI-stained sections also showed the presence of polyphosphate granules in *P. halichondrioides* and *P. symbiotica* (Fig. 3.2A, C) but not in the epibionts.

3.4.2. Microbial community diversity

A summary of the different univariate measures of microbial diversity indices is given in Table 3.2. The ANOVA performed on OTU richness (*S*), inverse Simpson's index (*D*), and Shannon Weaver index (*H'*) between epibiont and basibiont sponge species from Puerto Rico, Bahamas and Mexico showed significant differences between species and lifestyle ($F_{5,29}$=29.91, p<0.0001; $F_{5,29}$=69.04, p<0.0001; $F_{5,29}$=37.4, p<0.0001 respectively) (TableA1.2-A1.4). Pairwise comparison of Tukey's post-hoc analyses showed that basibiont *Plakortis* spp. had a significantly higher *S* than the *H. plakophila* epibiont (p<0.0001) but not the *X. deweerdtae* epibiont. Both *Plakortis* spp. had significantly higher *S* than free-living *X. deweerdtae* (p =0.0004). Pairwise comparisons between associated and free-living lifestyles of *X. deweerdtae* were borderline non-significant (p=0.0548). Pairwise results of mean *D* and *H'* calculated from each sponge species showed that *D* for basibiont *Plakortis* spp. epibionts were significantly greater than either *H. plakophila* or *X. deweerdtae*

epibiont (p<0.0001). Mean differences in *D* and *H'* showed that associated *X. deweerdtae* had higher diversity indices than the free-living lifestyle. A scatter plot between *S* vs. *D* shows how epibionts and basibionts clearly group separately from each other for each location sampled (Fig. 3.3 A, B, C).

Similar results were obtained for samples collected from Panama where significant ANOVA results were obtained for *S*, *D*, and *H'* ($F_{4,15}$=8, p=0.0012; $F_{4,15}$=74.7, p<0.0001; $F_{5,29}$=35.6, p<0.0001 respectively) (Table A1.5; Fig. 3.3B). The *X. deweerdtae* epibiont had significantly higher *S* values than the basibiont *P. deweerdtaephila* but significantly lower *D* and *H'* indices than the basibiont (p<0.0001). *X. deweerdtae* epibionts also showed significantly higher *D* and *H'* than the free-living lifestyle (p<0.0001). These results show similar results regardless of the primers that were used to sequence the 16S rRNA gene of epibiont and basibiont sponges.

Multidimensional scaling of Bray-Curtis distances showed that each sponge species had host specific microbiomes that were significantly different from one another and from the surrounding seawater in the four geographic locations ($F_{26,140}$=4.9, p=0.001) (Fig.3.4). Samples from *X. deweerdtae* grouped closer to seawater samples than did those from any other species. Microbial community differences were also observed between associated and free-living *X. deweerdtae,* where samples from the associated lifestyle grouped closer to the *Plakortis* spp. basibiont rather than grouping with the free-living lifestyle. Similar groupings were also observed for samples collected in Panama, which were sequenced with different primer sets (Fig. 3.4B).

Table 3.2 Mean and standard error of microbial diversity indices for each sponge pair, free-living *Xestospongia deweerdtae* and *Plakortis halichondrioides* in four locations of the Caribbean. Analysis was performed with a minimum threshold of 10,250 reads and OTUs defined by 97% sequence similarity. Samples from Panama were sequenced with primers 341F – 805R, which yielded lower diversity indices for each species and seawater sample than samples sequenced with the 515F – 806rB primer pair.

Location	Species or seawater	gDNA/cDNA	*S*	*D*	*H'*	n
Puerto Rico	*P. symbiotica*	cDNA	1672.1 ± 64	42.9 ± 6.0	5.2 ± 0.1	8
	P. symbiotica	gDNA	1580.2 ± 33	35.1 ± 2.8	4.9 ± 0.1	11
	P. halichondrioides	cDNA	1796.3 ± 46	98.9 ± 8.0	5.7 ± 0.0	3
	P. halichondrioides	gDNA	1910.3 ± 40	70.1 ± 4.7	4.9 ± 0.0	4
	X. deweerdtae AS	cDNA	1589.3 ± 116	7.6 ± 0.7	4.3 ± 0.1	3
	X. deweerdtae AS	gDNA	1562.3 ± 99	9.7 ± 3.6	4.4 ± 0.4	3
	X. deweerdtae FL	gDNA	1339	7	3	1
	H. plakophila	cDNA	1402.25 ± 128	8.7 ± 1.2	4.1 ± 0.2	4
	H. plakophila	gDNA	929.4 ± 71	4.7 ± 0.5	3.1 ± 0.1	5
	Seawater	gDNA	2693.0 ± 339	102.4 ± 1	6.2 ±0.2	3
Panama	*P. deweerdtaephila***	gDNA	852.0 ± 78	39.8 ± 3.28	4.6 ± 0.1	4
	P. halichondrioides **	gDNA	855.0 ± 24	56.7 ± 3.1	4.8 ± 0.1	4
	P. halichondrioides *	gDNA	969.4 ± 41	61.9 ± 3.9	4.9 ± 0.0	4
	X. deweerdtae AS**	gDNA	1222.0 ± 45	16.3 ± 2.3	4.5 ± 0.1	4
	X. deweerdtae FL*	cDNA	511	4.8	3	1
	X. deweerdtae FL*	gDNA	898.3 ± 68	5.6 ± 0.7	3.2 ± 0.2	4
	Seawater*	gDNA	1510.0 ± 35	52.1 ± 3.5	5.2± 0.0	3
Bahamas	*P. deweerdtaephila*	gDNA	1770.8 ± 25	61.7 ± 1.8	5.4 ± 0.0	4
	X. deweerdtae AS	gDNA	1517.3 ± 84	11.1 ± 3.9	4.4 ± 0.2	3
	X. deweerdtae FL	gDNA	1327	10.6	4.2	1
	Seawater San Salvador	gDNA	1919.7 ± 44	5.2 ± 0.0	22.2 ± 0.5	3
	Seawater Plana Key	gDNA	1506.0 ± 54	4.2 ± 0.1	7.3 ± 0.7	3
Mexico	*X. deweerdtae* FL	gDNA	1255.7 ± 174	7.0 ± 1.7	3.9 ± 0.3	3
	Seawater	gDNA	1626.7 ± 242	17.5 ± 6.3	4.6 ± 0.5	3

S OTU richness, *D* inverse Simpson's index, *H'* Shannon index, n number of individuals
*Samples collected from Punta Caracol.
**Samples collected from Dolphin Rock
AS-associated
FL-free-living

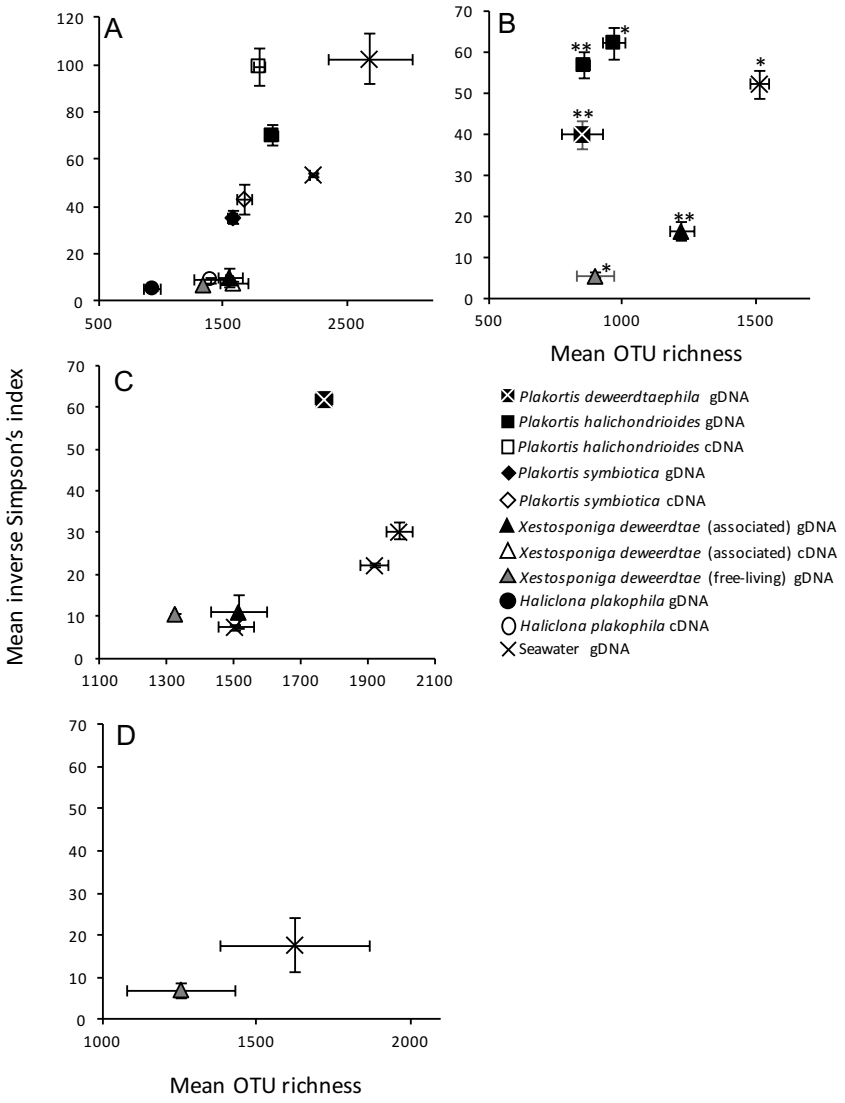

Figure 3.3 Scatter plot of mean and standard error of OTU richness (S) and inverse Simpson's index (*D*) in samples from each sponge pair species, free-living *Xestospongia deweerdtae*, *Plakortis halichondrioides* and seawater samples. Samples were collected in (A) Puerto Rico, (B) Panama, (C) Bahamas and (D) Mexico. Only free-living individuals of *Xestosopngia deweerdtae* were found in Mexico. Sponge species and seawater samples are

indicated by the legend. *Sponges collected from Punta Caracol. **Sponges collected from Dolphin Rock.

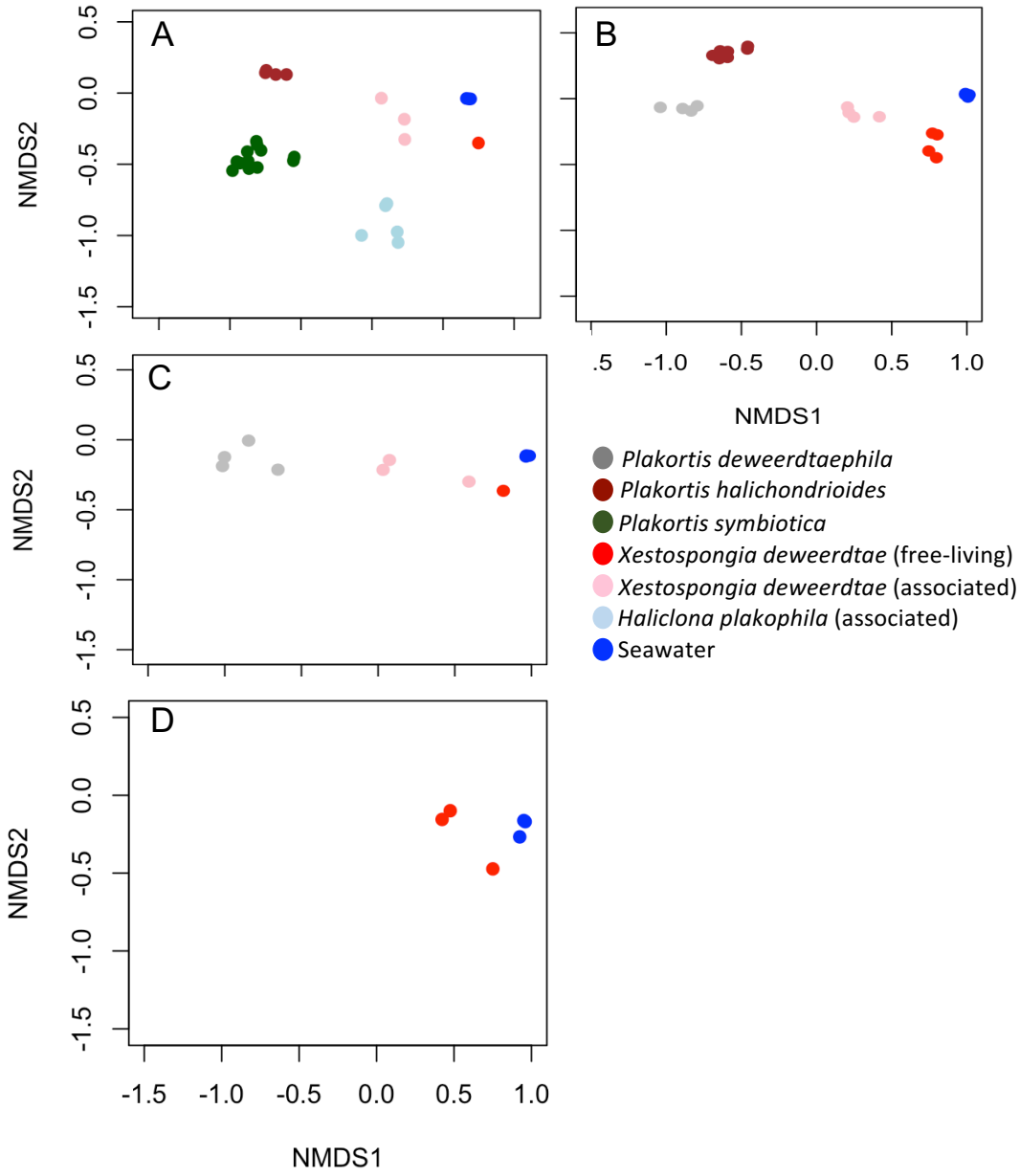

Figure 3.4 Microbial community similarity of host sponge species in each sponge pair species, free-living *Xestospongia deweerdtae*, *Plakortis halichondrioides* and seawater samples. Samples were collected from (A)

Puerto Rico, (B) Panama, (C) Bahamas and (D) Mexico. Clustering was performed using Multidimensional scaling of Bray-Curtis distances. Sponge species and seawater samples are indicated by the legend.

OTU classification defined at 97% sequence similarity showed the presence of 23 phyla in sponge and seawater samples. Further investigation of host specific microbial communities revealed that the most common microbial phyla in *P. halichondrioides* and *Plakortis* spp. basibiont sponges were Chloroflexi and Proteobacteria which accounted for 64% of all unique OTUs (Fig. 3.5). Actinobacteria and Acidobacteria were also present in *Plakortis* spp. and accounted for 10% of unique OTUs. Approximately 10% of unique OTUs of *Plakortis* ssp. were unclassified. The Archaea phylum Thaumarchaeota also accounted for a small percentage (7%) of unique OTUs. The microbial community of epibiont sponges showed a much simpler distribution of phyla as a consequence of the large dominance of the Proteobacteria which made up to 96% of unique OTUs associated with *H. plakophila* and 50% of unique OTUs associated with *X. deweerdtae*. Interestingly, the phylum Thaumarchaeota represented the second largest number of OTUs (27%) in free-living *X. deweerdtae* and 18% in the associated lifestyle. The primer pair (341F – 805R) did not amplify the Thaumarchaeota in either epibiont or basibiont sponges from Panama. Cyanobacteria were present (5-10%) in *X. deweerdtae* but absent in *Plakortis* spp.

The distribution of samples from associated *X. deweerdtae* that grouped closer to the basibiont *Plakortis* spp. based on Bray-Curtis distance (Fig. 3.4) motivated me to perform an ANOVA on the relative abundance of OTUs belonging to microbial phyla that changed relative abundances between lifestyles (Thaumarchaeota, unclassified Proteobacteria, Deltaproteobacteria) or that were only found in basibiont *Plakortis* spp. (Acidobacteria, Chloroflexi).

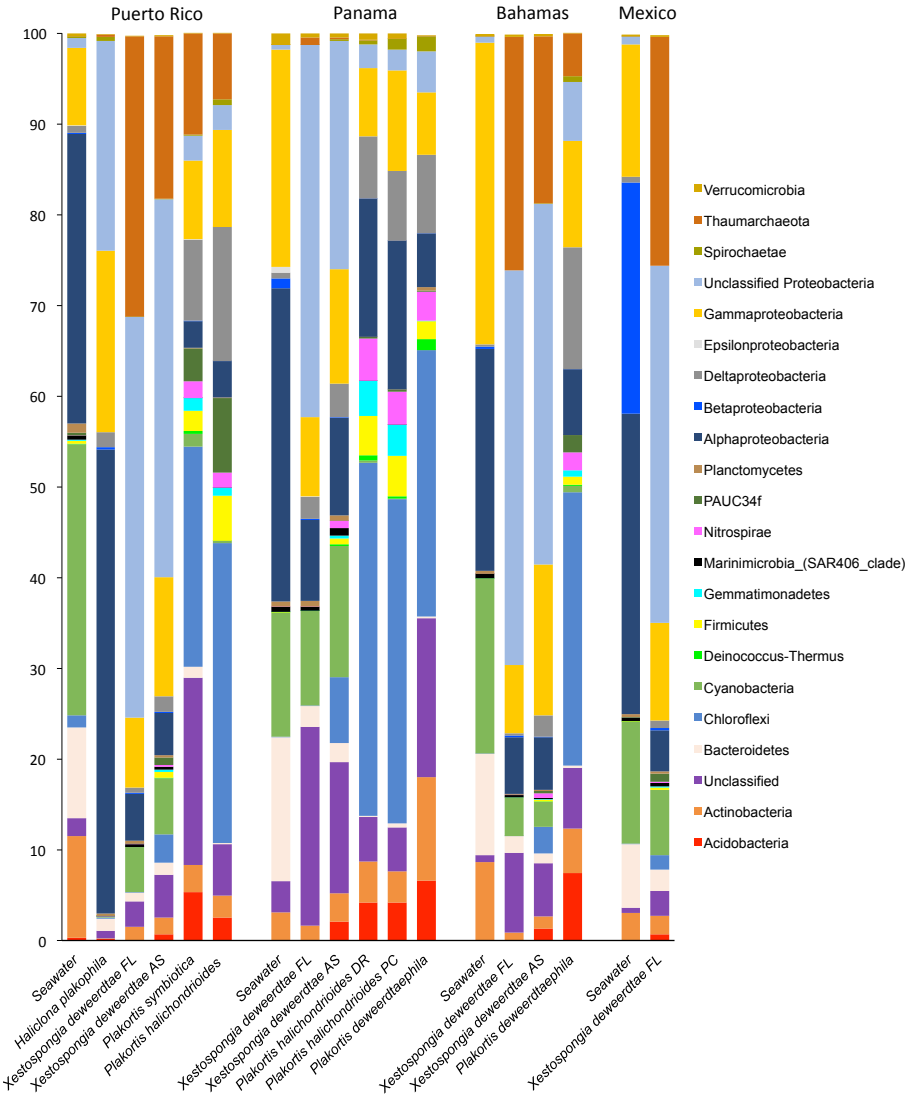

Figure 3.5 Mean relative abundance of each microbial phylum within host sponge species of each sponge pair, free-living (FL) *Xestospongia*

***deweerdtae*, *Plakortis halichondrioides*, and seawater samples from Puerto Rico, Panama, Bahamas and Mexico.** Only free-living individuals of *Xestospongia deweerdtae* were found in Mexico.

Prior to running the ANOVA, microbial phyla from free-living *X. deweerdtae* individuals from Puerto Rico (n=1), Bahamas (n=1) and Mexico (n=3) were averaged, as were microbial phyla from associated lifestyles from Puerto Rico (n=3) and Bahamas (n=3) since these were all sequenced with the same primers. The only microbial phyla that significantly changed their relative abundance between free-living and associated lifestyles of *X. deweerdtae* from PR, BH or MX were the Deltaproteobacteria which increased 1.4% in associated individuals of *X. deweerdtae* ($F_{1,9}$=5.4, p=0.0451) (Fig.3.6). The ANOVA performed on samples collected in Panama showed that associated samples also had a 1.5% higher abundance of Deltaproteobacteria ($F_{1,6}$=29.4, p=0.0016). In addition, the higher relative abundance of Chloroflexi (8%) and Acidobacteria (3%) in associated individuals of *X. deweerdtae* were also significant ($F_{1,6}$=479.1, p<0.0001 and $F_{1,6}$=199.3, p<0.0001 respectively) (Fig. 3.6).

ANOVA results on mean relative abundance comparisons between the gDNA (16S rRNA gene) and the cDNA (16S rRNA gene) extracted from samples in Puerto Rico showed that the Chloroflexi abundance derived from cDNA samples of *H. plakophila*, and *P. symbiotica* were significantly greater than that from gDNA samples (p<0.0001 and p=0.0003 respectively) but significantly lower in cDNA samples of *P. halichondrioides* (p=0.0369) (Table A1.6; Figure 3.7A).

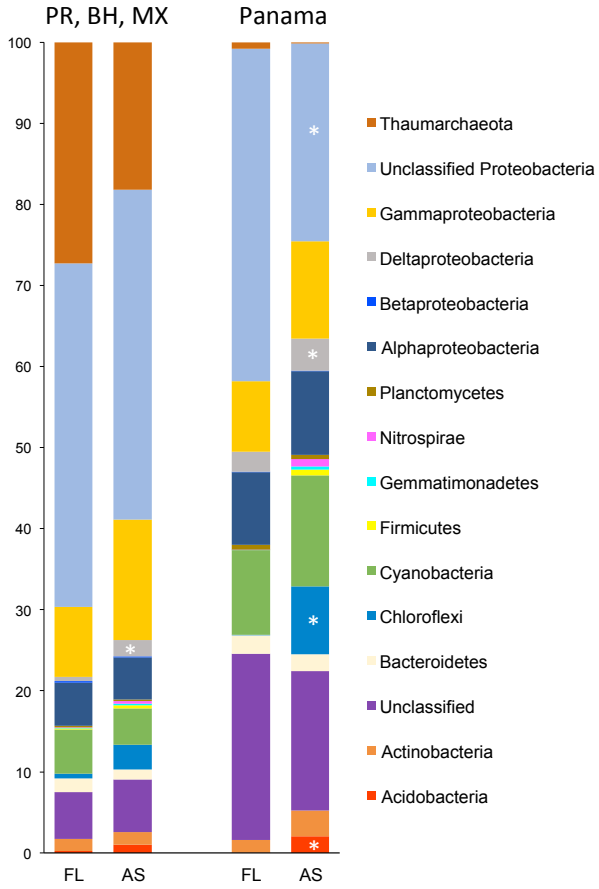

Figure 3.6 Mean relative abundance of each microbial phylum within associated (AS) and free-living (FL) *Xestospongia deweerdtae* from Puerto Rico (PR), Bahamas (BH), Mexico (MX) and Panama. Samples from PR, MX and BH were averaged separately from Panama samples as these were sequenced with different primer pairs. ANOVA results from samples collected in Panama revealed that Chloroflexi and Acidobacteria have a higher relative abundance in the associated lifestyle compared to the free-living lifestyle and that unclassified Proteobacteria was less abundant in the associated lifestyle (p<0.0001). Significant ANOVA outcomes on mean relative abundance differences from microbial phyla are indicated by a white asterisk.

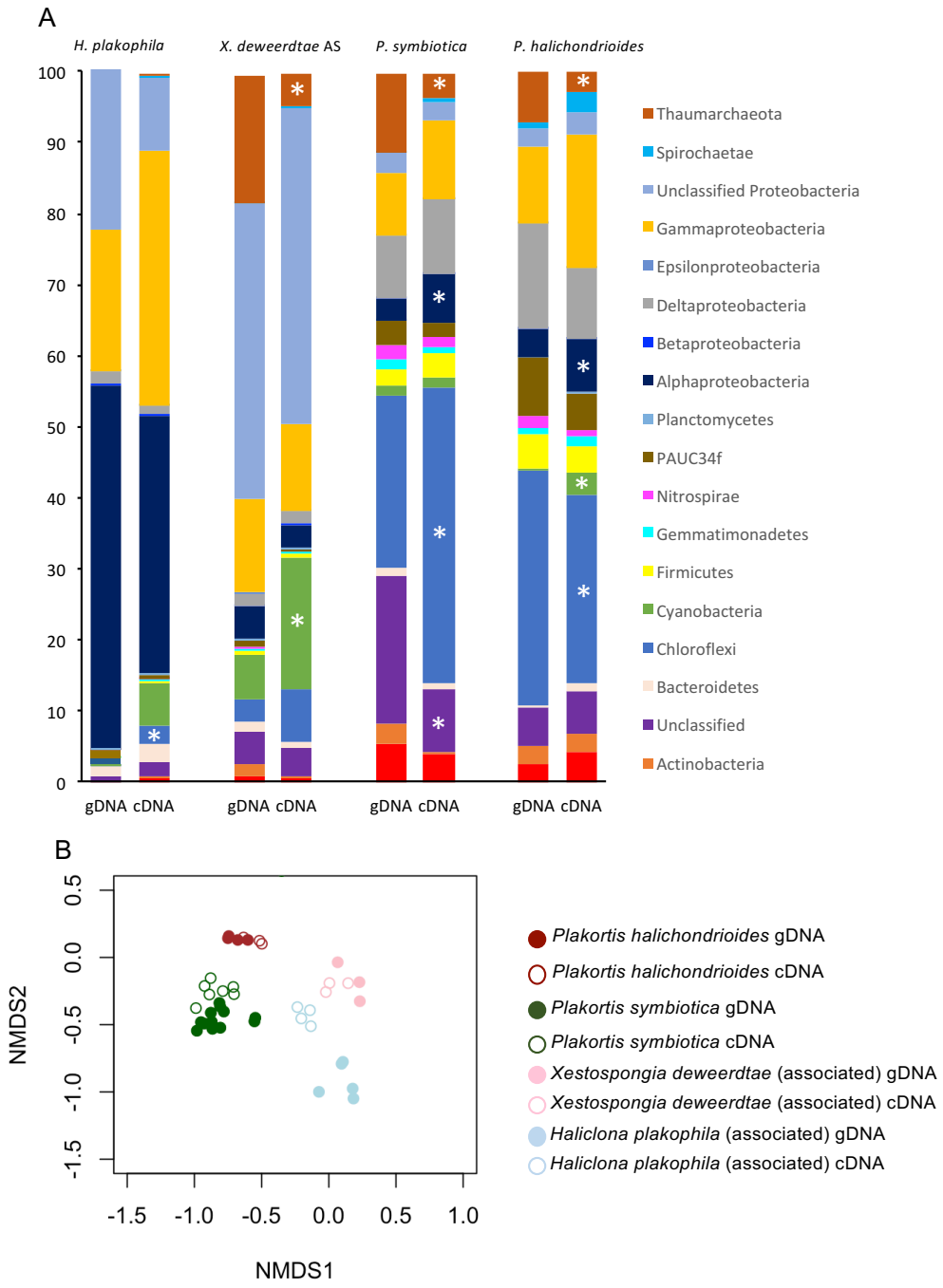

Figure 3.7 Mean relative abundance and multidimensional scaling based on Bray-Curtis distances of microbial phyla from gDNA and cDNA samples extracted from sponge species in sponge pairs from Puerto Rico and

***Plakortis halichondrioides*.** (A) Mean relative abundance of present (gDNA) and active (cDNA) microbial phyla associated with epibionts (*Haliclona plakophila* and *Xestospongia deweerdtae*), basibiont *Plakortis symbiotica* and free-living *Plakortis halichondrioides* from Puerto Rico. Significant ANOVA outcomes on mean relative abundance differences from microbial phyla are indicated by an asterisk. (B) Microbial community similarity of gDNA and cDNA of epibionts (*X. deweerdtae*, *H. plakophila*) and basibiont (*P. symbiotica*) and *P. halichondrioides*. Closed circles refer to gDNA samples and closed circles refer to cDNA samples as indicated by the legend.

Cyanobacteria had a 12% higher relative abundance in cDNA samples of associated *X. deweerdtae* (p=0.0342) as well as a 3% higher relative abundance in *P. halichondrioides* cDNA (p=0.0232) than gDNA samples. Relative abundance of Thaumarchaeota in the cDNA of all sponges except for *H. plakophila* were also lower than gDNA samples (13% less in *X. deweerdtae* AS, p=0.0035; 8% less in *P. symbiotica*, p=0.0186; and 5% less in *P. halichondrioides*, p=0.0043). Alphaproteobacteria were 4% higher in cDNA samples of *P. halichondrioides* and *P. symbiotica* than gDNA samples (p=0.0120 and p=0.0028 respectively). Shifts in the relative abundance of microbial phyla between gDNA and cDNA samples were significant enough to affect Bray-Curtis distances in *H. plakophila* and *P. symbiotica* (Fig. 3.7B).

3.4.3. $\delta^{13}C$ and $\delta^{15}N$ stable isotope analysis

Significant ANOVA outcomes from mean $\delta^{13}C$ and $\delta^{15}N$ values were obtained from sponge species comparisons in Puerto Rico ($\delta^{13}C$ $F_{2,6}$=10.06, p=0.0121; $\delta^{15}N$ $F_{2,6}$=6.73, p=0.0293) and Panama ($\delta^{13}C$ $F_{4,10}$=12.07, p=0.0008; $\delta^{15}N$ $F_{4,10}$=6.66, p=0.0070) (Fig. 3.8; Table A1.7). Only sponge species collected in the Bahamas showed significant differences in $\delta^{15}N$ values ($F_{4,8}$=23.10, p=0.0003). In Puerto Rico, *P. symbiotica* averaged -19.8% ± 0.5 for $\delta^{13}C$ and 2.5‰ ± 0.5 for $\delta^{15}N$. The $\delta^{13}C$ values of *P. symbiotica* were significantly different from both the *H. plakophila* (p=0.0149) and *X. deweerdtae* (p=0.0258) epibionts, which averaged -15.8‰ ± 0.5 and -16.2‰ ± 1.0 respectively (Fig. 3.8A).

Sponges in Panama were collected in Punta Caracol and Dolphin Rock. *P. halichondrioides* collected at both sites had significantly different $\delta^{13}C$ values (p=0.0305; Fig. 3.8B). Samples collected in Punta Caracol averaged -19.6‰ ± 0.1 and samples collected in Dolphin Rock averaged -20.3‰ ± 0.1. However, free-living *X. deweerdtae* collected at Punta Caracol and associated individuals collected at Dolphin Rock shared similar, non-significant $\delta^{13}C$ (-20.6‰ ± 0.2) and $\delta^{15}N$ (6.2‰ ± 0.2) values, suggesting that assimilation of $\delta^{13}C$ and $\delta^{15}N$ is not influenced by the association with *P. deweerdtaephila* or collection site. The basibiont *P. deweerdtaephila* also shared similar $\delta^{13}C$ and $\delta^{15}N$ values as free-living and associated *X. deweerdtae*. In the Bahamas $\delta^{15}N$ values were significantly higher in associated individuals of *X. deweerdtae* (4.8‰ ± 0.1) than free-living individuals (3.7‰ ± 0.3) and the basibiont *P. dewe*erdtaephila (3.7‰ ± 0.3) (p=0.0328). *Plakortis halichondrioides* had consistent, significantly lower

δ^{15}N values than any of the *X. deweerdtae*/*P. deweerdtaephila* sponge pair species from Panama and Bahamas (p=0.0289) (Fig. 3.8B, C).

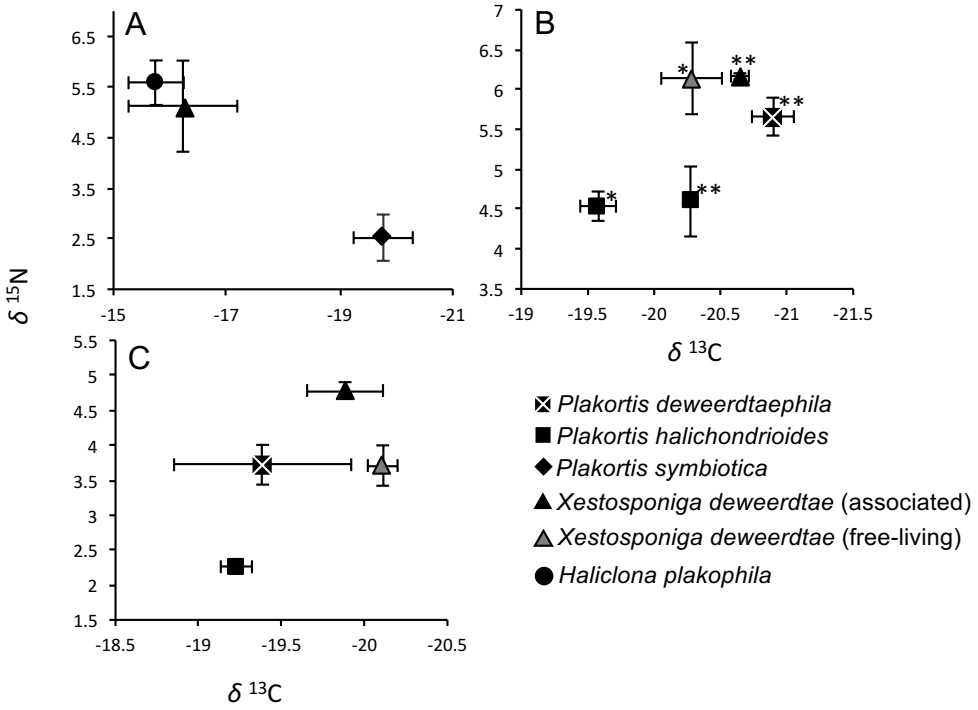

Figure 3.8 δ^{13}C and δ^{15}N values for the sponge tissue of sponge pair species, free-living *Xestospongia deweerdtae* and *Plakortis halichondrioides*. Samples were collected in (A) Puerto Rico, (B) Panama and (C) Bahamas. * Sample collected in Punta Caracol. **Samples collected in Dolphin Rock.

3.5. Discussion

My hypothesis that the three sponge pairs in this study consist of a low microbial abundance sponge epibiont growing on a high microbial abundance sponge basibiont was confirmed. Bacteria and sponge cell counts using two quantification methods showed that *X. deweerdtae* and *H. plakophila* epibionts

are low microbial abundance sponges and *P. symbiotica* and *P. deweerdtaephila* basibionts are high microbial abundance sponges. Different diversity metrics showed that both epibionts and basibionts had a similar total number of microbial species (*S*), but that the microbial community in epibionts was dominated by a significantly fewer number of microbial species (low *D*). These results idicate that basibiont *Plakortis* spp. have a more abundant and diverse microbial community than their *Xestospongia* sp. or *Haliclona* sp. epibionts. Relative abundance of *H. plakophila* epibionts showed that these were mainly dominated by Proteobacteria (96%). The *X. deweerdtae* epibiont showed slightly higher diversity indices than *H. plakophila* because of the presence of Proteobacteria, Cyanobacteria and the archaeal Thaumarchaeota while *Plakortis* spp. were dominated by Proteobacteria, Chloroflexi, Actinobacteria, and Acidobacteria. These observations are in agreement with previous studies that have observed higher microbial abundances and higher microbial diversity in HMA than LMA sponges (Weisz *et al.* 2007; Kamke *et al.* 2010; Schmitt *et al.* 2012; Giles *et al.* 2013; Moitinho‐Silva *et al.* 2014; Poppell *et al.* 2014).

Diversity metrics also showed that associated individuals of *X. deweerdtae* in Panama have higher diversity indices (*S, D, H'*) than free-living individuals which support the hypothesis that bacterial diversity is influenced by lifestyle and that symbionts from *Plakortis* spp. could potentially be translocating into the *X. deweerdtae* epibiont. Samples averaged from Puerto Rico, Bahamas and Mexico showed borderline non-significance between associated and free-living individuals possibly due to increased error from the incorporation of free-living

samples from Mexico where associated lifestyles were absent. Further support for this hypothesis was observed by multidimensional scaling of Bray-Curtis distances which grouped the microbial community of the associated *X. deweerdtae* lifestyle away from the free-living individuals in Panama and closer to the *P. deweerdtaephila* basibiont. Relative abundance comparisons between associated and free-living lifestyles also showed the presence of *Plakortis* spp. symbionts like Chloroflexi and Acidobacteria in associated individuals that were not present in free-living individuals.

Previous examples of symbiont acquisition in sponges include vertical transmission from adult to larvae (Usher *et al.* 2001; Ereskovsky *et al.* 2005; Schönberg & Loh 2005; Enticknap *et al.* 2006; Sharp *et al.* 2007; Collin *et al.* 2010), horizontal acquisition from the surrounding (Maldonado & Riesgo 2009; Webster *et al.* 2010) or leaky transmission where a combination of both horizontal and vertical transmission are used to acquire symbionts (Enticknap *et al.* 2006; Schmitt *et al.* 2007; Schmitt *et al.* 2008), all discussed by (Thacker & Freeman 2012). This study adds a novel mechanism of horizontal transmission of symbionts from an HMA sponge that enriches the microbial community of an LMA sponge. It is uncertain whether this translocation might be happening from the microbial community of the epibiont to the basibiont as only associated forms of both *Plakortis* spp. and *H. plakophila* have been found and baseline data on the microbial communities of free-living individuals from these species are unavailable. It is also unclear whether the translocated microbial phyla are metabolized by the sponge or symbiotically incorporated by the epibiont.

Comparisons of the gDNA and cDNA data did show that microbial members of the Chloroflexi phylum were present in the *X. deweeerdtae* epibiont and had significantly increased copy numbers in the cDNA from sponges *H. plakophila* and *P. symbiotica* from Puerto Rico. These results suggest that these are active members in the community (DeLong *et al.* 1989; Poulsen *et al.* 1993; Kamke *e*t *al.* 2010). There was also a significant increase in copy numbers of the Cyanobacteria in cDNA samples of epibiont *X. deweerdtae* and free-living *P. halichondrioides*, even though phototrophic bacteria were not detected with the red or green epifluorescent filter sets. Not observing any Cyanobacteria through neither of the epifluorescent filter sets suggests that Cyanobacteria are likely present in very low numbers throughout the sponge tissue. We also observed that Cyanobacteria were present in similar abundances within seawater samples for the three collection sites of the Caribbean, which suggests that sponges are likely feeding on Cyanobacteria filtered from the surrounding seawater. Further analyses on the distribution of specific OTUs belonging to the shared microbial phyla between epibiont and basibiont sponges also needs to be addressed. The design of probes for each of the shared microbial phyla would also help identify how horizontally transmitted symbionts are distributed throughout the sponge pair (Sharp *et al.* 2007; Webster & Thomas 2016).

Stable isotope analysis of $\delta^{13}C$ and $\delta^{15}N$ of bulk sponge tissue from epibiont and basibiont sponges showed that both sponge species in each pair had different isotopic signatures that varied according to different collection sites. For example, in Puerto Rico, *P. symbiotica* had a significantly different $\delta^{13}C$

isotopic niche than both *H. plakophila* and *X. deweerdtae* epibionts but only a significantly different $\delta^{15}N$ niche to *H. plakophila*. In Panama, all basibiont and epibiont sponges shared similar $\delta^{13}C$ and $\delta^{15}N$ isotopic niches showing no significant differences between epibiont or basibiont species. In the Bahamas, the epibiont shared a different $\delta^{15}N$ isotopic niche space than the epibiont and the free-living form. One possible interpretation is that selection of a particular food source is dependent on the environment in which the sponge pairs live.

Both epibiont sponges in this study are found in light-limited, cryptic habitats, lacking photosymbionts, thus are unable to receive their nitrogen and carbon source from primary producers as observed in other Caribbean sponge species (Mohamed *et al.* 2008; Freeman & Thacker 2011; Freeman *et al.* 2013). The absence of photosynthetic symbionts makes this analysis more problematic to interpret as primary producers are known to be good predictors of $\delta^{13}C$ and $\delta^{15}N$ values in sponges (Wilkinson 1983; Freeman *et al.* 2014) while other sources of $\delta^{13}C$ and $\delta^{15}N$ have overlapping values (Layman *et al.* 2007). Consequently, sponge pairs may either rely more on heterotrophic feeding (López-Legentil & Pawlik 2009) and could assimilate DOM (De Goeij *et al.* 2013) or could rely on chemoautotrophy. Intriguingly, some microbial members of the archaeal phylum Thaumarchaeota which are present in epibiont and basibiont sponges couple ammonia oxidation to fix carbon through a chemolithotrophic pathway (Könneke *et al.* 2014). The Thaumarchaeota are also one of three abundant phyla in the LMA sponge *Ianthella basta* (Luter *et al.* 2010).

The Thaumarchaeota averaged between 25-30% in free-living *X. deweerdtae* and decreased to 20% in associated individuals. Despite not being detected by primers 341F-805R for samples collected in Panama, the "unclassified" phyla ratios between free-living and associated *X. deweerdtae* matches this decrease in relative abundance (Fig. 3.5). These results suggest that the Thaumarchaeota might be less abundant in associated lifestyles due to a shift in ammonia or carbon nutrient sources.

One interesting anecdotal observation during the DAPI stained bacterial and sponge cell quantification method was the presence of polyphosphate granules observed in *P. halichondrioides* and in *P. deweerdtaephila* but not in epibiont sponges (Fig. 3C, E). Zhang and colleagues (2015) first documented the presence of polyphosphate granules in symbionts, including *Leptolyngbia* (Cyanobacteria) associated with the sponge *Ircinia strobilina*. It is unlikely that Cyanobacteria are forming polyphosphate granules in either *Plakortis* spp. but it is possible that other bacterial groups in basibiont sponges might be responsible. These sources of phosphate transformations might be an advantage to access phosphate by epibiont sponges associating with *Plakortis* spp. This requires further investigation.

Tracer enrichment experiments would also be required in order to understand how carbon and nitrogen sources are metabolized in each sponge species of the pair. Expression of functional genes such as nitrogenase (*nifH*), nitrification ammonia monoxygenase (*amoA*), or polyphosphate kinase (*ppk*) would also help to determine whether key nutrients are being produced by the

bacterial communities in either sponge (Mohamed *et al.* 2008, 2010; Zhang *et al.* 2015). Due to the disparities of microbial communities in each sponge pair and difference in isotopic niches, it is likely that each species has the ability to assimilate nutrients in a variety of ways that would not impact on their sponge partner.

Chapter 4: Sponge symbiosis between *Xestospongia deweerdtae* and *Plakortis* spp. does not involve shared chemical defenses against predators

4.1. Abstract

Sponges engage in a diversity of interactions with other benthic organisms, including sponge-sponge epizoism. The recently described epizoic sponge-sponge symbioses between *Xestospongia deweerdtae*, *Plakortis deweerdtaephila* and *Plakortis symbiotica* presents an unusual case of sponge interactions. The objective of this study was to evaluate the hypothesis that *X. deweerdtae* grows epizoic to these two species of *Plakortis* due to a shared chemical defense against predators. Free-living individuals of *X. deweerdtae* and symbiotic colonies were collected from a wide geographical range to generate crude organic extracts and a series of polarity fractions from sponge extract. We tested the deterrency of these extracts against three common coral reef predators: the bluehead wrasse, *Thalassoma bifasciatum*, the Caribbean sharpnose puffer, *Canthigaster rostrata*, and the white spotwrist hermit crab, *Pagurus criniticornis*. While the chemical defenses of *P. deweerdtaephila* and *P. symbiotica* appear more potent than those of *X. deweerdtae*, all of the sponge species tested deterred feeding significantly by all three generalist predators. The free-living form of *X. deweerdtae* is mostly defended across the region, with a few exceptions. The associated form of *X. deweerdtae* is always defended, and both species of *Plakortis* are very strongly defended, with puffers refusing to consume extract-treated pellets until the extract was diluted to 1/256× concentration. Using diode-array high performance liquid chromatography (HPLC) coupled with mass spectrometry (LC-MS) we found certain secondary metabolites, probably derivatives of known plakinic acids, in high concentration in

P. deweerdtaephila, but also in low concentration in the associated, but not the free-living, form of *X. deweerdtae*, suggesting a possible translocation of defensive chemicals from the basibiont to the epibiont. The higher deterrency of of *Plakortis* spp. extracts compared to the *X. deweerdtae* extracts suggests that that there may be some sharing of chemical defenses: one partner in the symbiosis is clearly more defended than the other and perhaps sharing a small amount of its defensive chemistry. However, the multiple lines of evidence we gathered provide no convincing support for the hypothesis that this symbiosis is driven by shared chemical defenses. Given the diversity of other potential food resources on coral reefs it is improbable that the evolution of this sponge-sponge symbiosis has been driven by predation pressure.

4.2. Introduction

Sponges interact with neighboring benthic organisms in a wide diversity of ways, ranging from mutually beneficial to mutually antagonistic (reviewed by Wulff, 2006). Many studies have explored these interactions, documenting cases of allelopathic competition (Porter & Targett 1988; Engel & Pawlik 2000; Pawlik *et al.* 2008b), collaborative mutualism (Wulff 1997, 2008b), and varying degrees of proximal association including epizoism (Rützler 1970; Sarà 1970; Wooster *et al.* 2016). These sorts of associations may enhance sponge survivorship through increased structural support or protection from predators (Wulff 1997, 2008a; Loh & Pawlik 2009; Ramsby *et al.* 2012; Wooster *et al.* 2016), although sponges sometimes harm the associated organism (Porter & Targett 1988; Engel & Pawlik 2000; Pawlik *et al.* 2007; Loh *et al.* 2015). The first formal description of sponge-sponge epizoism was from temperate marine caves, where Rützler observed communities of marine sponges so dense that they were growing on top of one another (Rützler 1970). There are now many reports of epizoic sponge associations, although the causes and consequences of the associations are not always explored [e.g. (Cedra-García-Rojas *et al.* 1994; Jung *et al.* 1995; Ávila *et al.* 2007; Cárdenas 2016)].

One sponge-sponge interaction that has been particularly well explored is the case of *Amphimedon erina* growing epizoic to *Geodia vosmaeri.* First reported by Engel & Pawlik (2000), these sponge genera represent different approaches to chemical defenses: *Geodia* spp. are consistently palatable and preferentially preyed upon, while predators refuse to consume *Amphimedon* spp.

(Pawlik *et al.* 1995; Waddell & Pawlik 2000a, 2000b; Wulff 2008b; Loh & Pawlik 2014). Given the different chemical defenses of each participant in the symbiosis, Engel & Pawlik (2000) proposed that *A. erina* may protect *G. vosmaeri* by providing a layer of chemically defended tissue. Wilcox *et al.* (2002) went on to survey the distribution and abundance of the interaction, and also collected morphological data about each sponge participant. Using gel-screen feeding assays in the field and choice experiments in the laboratory with whole tissue offered to sea stars, Ramsby *et al.* (2012) confirmed that *A. erina* is chemically defended against predators and *G. vosmaeri* is not. These results support the hypothesis that one sponge shares its chemical defenses with another through the symbiosis. In addition, growth experiments suggested that *G. vosmaeri* provides vertical habitat for *A. erina* to grow, protecting it from sedimentation and the energetic expense of mucous production removal (Ramsby *et al.* 2012). In this case, the interaction provides clear benefits to each participant.

A more peculiar example of sponge-sponge epizoism is the symbiosis between *Xestospongia deweerdtae* and one of two possible basibionts: *Plakortis deweerdtaephila* or *Plakortis symbiotica* (Vicente *et al*. 2014; Vicente *et al.* 2016). Sponges in the genus *Plakortis* are rich in cytotoxic secondary metabolites (del Sol Jiménez *et al.* 2003; Kossuga *et al.* 2008; Zhang *et al.* 2013; Hoye *et al.* 2015; Santos *et al.* 2015) and have been shown to swiftly kill neighboring organisms [e.g. Porter & Targett (1988)]. It is therefore unusual that any organism would make contact with any species of *Plakortis*, let alone form a long-term partnership. *X. deweerdtae* was first described as a free-living deep

reef sponge from the north shore of Jamaica (Lehnert & Van Soest 1999) but the discovery of this symbiosis (Vicente *et al.* 2014) prompted a new description of polymorphism to account for its association to *P. deweerdtaephila* and *P. symbiotica* (Vicente *et al.* 2016). Since the *X. deweerdtae* can survive on its own and the two species of potential basibionts—*P. deweerdtaephila* and *P. symbiotica*—are likely toxic to proximal organisms, this symbiosis provides a unique scenario to explore sponge-sponge interactions. Vicente *et al.* (2014) suggest that this symbiosis represents a mutualism on the basis of five lines of evidence:

(1) These sponges appear to preferentially live together: biogeographic surveys found *X. deweerdtae* to be 4-23 times more abundant in association than in free-living form at sites where symbiotic partners *P. deweerdtaephila* and/or *P. symbiotica* were present (Vicente *et al.* 2014). At sites where *Plakortis* spp. are absent, *X. deweerdtae* does grow in its free-living form but it is much less abundant. Furthermore, *P. deweerdtaephila* and *P. symbiotica* have never been found in a free-living form despite considerable survey efforts across the Caribbean.

(2) Both *X. deweerdtae* and *Plakortis* spp. exhibit smaller spicules in their associated forms compared to free-living forms (Vicente *et al.* 2014). Although no free-living individuals of *P. deweerdtaephila* and *P. symbiotica* have been documented, Vicente *et al.* (2014) compare these basibionts to the closely-related *Plakortis halichondrioides*, which exhibits similar tissue density but presents significantly longer spicules. The association may allow the sponges to

share responsibility for structural support and expend less energy on skeleton synthesis.

(3) Vicente *et al.* (2014) argue that the symbiosis is life-long and does not cause mortality through smothering (Fig. 2.4). Biogeographic surveys have identified young recruits of *P. deweerdtaephila* and *P. symbiotica* (≤5cm colony diameter) (Fig. 1.3A, D), and at this early life stage the basibiont already has epizoic *X. deweerdtae* (Vicente *et al.* 2014). Even large adult individuals exhibit healthy tissue despite a layer of *X. deweerdtae* on top. Perhaps the best indication that smothering does not occur is that free-living individuals of *X. deweerdtae* show no indication of having smothered a basibiont at some point in the past.

(4) Recently, sponge pairs were discovered to host different microbial communities with different microbial abundances (Chapter 3). In addition, sponges share different $\delta^{13}C$ and $\delta^{15}N$ isotopic niche space in different locations of the Caribbean. By having different microbial communities, each sponge is able to expand a unique isotopic niche space and not compete for similar nutrients.

(5) As a final line of evidence to suggest that this symbiosis is mutualistic, sponge pairs are more interlaced than in other sponge-sponge associations. Dissections of symbiotic colonies revealed that *X. deweerdtae* not only grows across the surface of its *Plakortis* basibiont, but also grows within the mesohyl and even forms deep oscular channels that may increase the pumping capacity of the basibiont (Vicente *et al.* 2014). A possible benefit for the *X. deweerdtae* epibiont may be that it is able to access microbial phyla from the *Plakortis* spp.

basibiont. In exchange the *Plakortis* spp. basibiont uses the *X. deweerdtae* tissue to “irrigate” (Gloeckner *et al.* 2014) its dense mesohyl tissue and reduce the energy demands of water pumping.

In the original description of the symbiosis, Vicente *et al.* (2014) proposed a shared chemical defense hypothesis that one sponge might benefit by receiving a chemical defense against predators from its symbiotic partner. Clear trade-offs between basic life functions and chemical defenses have been established for the Caribbean sponge fauna (Walters & Pawlik 2005; Pawlik *et al.* 2008; Leong & Pawlik 2010), most species of which can be organized into one of two categories: palatable sponges, which lack defenses but grow or reproduce fast enough to persist on reefs, and defended sponges, which grow and reproduce slowly but are not attacked by predators (Pawlik 2011; Loh & Pawlik 2014). These studies provide a reasonable framework to examine a hypothesis of shared defense in a sponge symbiosis. In the case of *A. erina* and *G. vosmaeri*, knowledge of sponge chemical defenses was able to successfully predict (Engel & Pawlik 2000) the outcome of further studies (Ramsby *et al.* 2012). However the chemical defenses of *X. deweerdtae*, *P. deweerdtaephila*, and *P. symbiotica* have not been previously evaluated. We undertook this study to consider the hypothesis that *X. deweerdtae* grows in tight sponge-sponge symbioses with either *P. deweerdtaephila* or *P. symbiotica* due to a shared chemical defense against predators. *P. deweerdtaephila* and *P. symbiotica* are obvious candidates for the sponges that provide defensive chemistry; as discussed above, many species within the genus *Plakortis* are rich in bioactive

secondary metabolites. Pawlik *et al.* (1995) found the congeneric *P. angulospiculatus*, *P. halichondrioides*, and *P. lita* to significantly deter fish feeding in laboratory assays with bluehead wrasse, *Thalassoma bifasciatum*. However it is not unprecedented for a fish predator to tolerate *Plakortis* chemicals: Slattery *et al.* (2016) recently observed the Caribbean sharpnose puffer, *Canthigaster rostrata*, taking bites on *P. halichondroides* and used laboratory feeding assays to demonstrate that this predator was not deterred by some crude extracts generated from *P. halichondroides* tissue. Whether or not *P. deweerdtaephila* and *P. symbiotica* are chemically defended, it is also possible that *X. deweerdtae* may be defended. A related species, *Xestospongia muta*, has been shown to deter predators with chemical defenses in laboratory and field assays (Chanas & Pawlik 1997), although its chemical defenses are categorized as 'variably defended' because some individuals exhibit defense while others do not (Marty *et al.* 2016).

As in the symbiosis between *G. vosmaeri* and *A. erina*, it would make sense for the exposed sponge that grows on top to provide the chemical defenses, unless either the veneer of tissue is so thin that predators would bite both species at the same time or the basibiont species produces copious amounts of defensive metabolites that could be translocated to the epibiont. The first condition is not uncommon in this sponge pair; many specimens exhibit only a few millimeters of *X. deweerdtae* tissue. The second condition would represent an unusual situation, but requires attention due to the high levels of secondary metabolites in the tissues of other species form the genus *Plakortis*.

To ensure a comprehensive test of the hypothesis, the chemical defenses of *X. deweerdtae*, *P. deweerdtaephila*, and *P. symbiotica,* were examined. The study design includes samples from a broad biogeographic region in order to consider differences among populations. Both the free-living and the associated forms of *X. deweerdtae* were sampled along with an equal mixture of the two sponge tissues from each symbiotic colony, in equal parts, to approximate the response of a predator whose bite volume captures more than just the epibiont tissue. Finally, we looked for translocation of metabolites by testing fish responses to different polarity fractions of each sponge type and running diode-array high performance liquid chromatography (HPLC) coupled with mass spectrometry (LC-MS) to look for secondary metabolites that appear in the extracts of the basibiont and the epibiont.

I began this study with three criteria for the acceptance of the shared chemical defense hypothesis. (1) One of the partners in the symbiosis must be consistently palatable to predators. This condition could be met if the free-living form of *X. deweerdtae* is palatable even if the associated form is defended (a situation that could arise from translocation of deterrent metabolites). (2) The other partner in the symbiosis must be consistently defended against predators. (3) If the palatable sponge is the associated epibiont *X. deweerdtae*, the 1:1 mix of epibiont:basibiont tissue must be deterrent to predators.

4.3. Methods

4.3.1. Sponge collection:

Sponge tissue was collected from 13 coral reef sites across the Caribbean in the Bahamas, the Mexican Yucatan, Panama, and Puerto Rico (Table 4.1). A small piece of tissue (<20 mL) was taken from each sponge. For colonies of associated *X. deweerdtae* and *P. deweerdtaephila* or *P. symbiotica*, live tissue was dissected immediately after collection to separate the tissues of each sponge from one another. Extra tissue from each colony was also combined, in equal portions, to form a sample group in 1:1 mixture of tissue. Wet tissue for all sample types was frozen until extraction or placed immediately into solvents; volume of extracted tissue was measured by volumetric displacement.

4.3.2. Extraction for general feeding assays

The chemical extraction procedures for general feeding assays were conducted as described by Marty & Pawlik (2015). Briefly, the tissue was agitated vigorously in a 1:1 solvent mixture of dichloromethane (DCM) and methanol (MeOH) for a 6 h extraction period. The polar and nonpolar fractions of the DCM:MeOH extract were filtered, then dried separate from one another using rotary evaporation at low heat (<40°C) with a subsequent extraction in MeOH. All of the fractions were then combined into one crude organic extract and dried using vacuum concentration, again at low heat (<40°C). Dried extracts were stored under N_2 gas at -20°C until use in feeding assays.

Table 4.1 Collection locations for sponge material and assay predators employed in this study.

Location	Site	GPS Coordinates
Bahamas	Acklins Is.	22°10.617'N 74°17.367'W
	Great Inagua Is.	21°04.983'N 73°38.917'W
	Little Inagua Is.	21°27.048'N 73°03.404'W
	Mayaguana Is.	22°26.150'N 73°08.083'W
	Mira Por Vos	22°06.052'N 73°32.444'W
	Plana Cays Is.	22°36.270'N 73°32.792'W
	San Salvador Is.	24°02.433'N 74°31.882'W
Mexico	Banco Chinchorro	18°34.894'N 87°25.067'W
	Cozumel Is.	20°22.937'N 87°01.746'W
Panama	Dolphin Rock	9°21.207'N 82°11.132'W
	Hospital Point	9°20.020'N 82°13.140'W
	Punta Caracol	9°22.690'N 82°18.230'W
	STRI Point	9°20.576'N 82°15.489'W
Puerto Rico	Desecheo Is.	18°23.506'N 67°28.558'W
	La Parguera	17°53.297'N 66°59.887'W

4.4.3. Extraction for fractionation assays

Additional tissue samples of *X. deweerdtae* (both the free-living and associated forms) and *P. deweerdtaephila* collected in Bocas del Toro were

extracted using the following procedure in order to examine different polarity fractions of each extract. Centrifuge tubes (50-mL) containing 15-mL of tissue were agitated vigorously during a 4 h extraction period for each solvent. First, wet tissue was extracted in MeOH, resulting in a moderately polar solvent mixture of H_2O and MeOH. After removal of this moderately polar extract, the dehydrated tissue was extracted a second time in MeOH, representing a less polar fraction. A third extraction was achieved using chloroform, with the series of extracts representing a series of polarity fractions, progressing from moderately polar to non-polar. Fractions were filtered, then dried using rotary evaporation and vacuum concentration at low heat (<40°C) and stored dry under N_2 gas at -20°C until use in feeding assays.

4.4.4. Extraction for LC-MS analysis

Additional tissue samples of *X. deweerdtae* (both the free-living and associated forms) and *P. deweerdtaephila* collected in Bocas del Toro were extracted using the following procedure in order to examine ultraviolet mass spectra. Tissue samples were lyophilized, and 500 mg of each was extracted four times in a 1:1 solvent mixture of chloromethyl and MeOH. The four extracts were then combined, filtered, and concentrated using rotary evaporation under pressure and low heat (<40°C). Extractions were performed on three individuals of each species in the pair, including free-living *X. deweerdtae*.

4.4.5. Feeding assays

The core data in this study were generated using feeding assays that have been designed to isolate the taste of a potential prey item and evaluate the response of a model predator to that taste in a simulated predation event. We follow the principles for chemical defense feeding assays discussed by Marty & Pawlik (2015), using two fish species that have been employed previously in these sorts of assays as well as a novel assay with hermit crabs. All experimental protocols involving the use of live vertebrates were approved by the Institutional Animal Care and Use Committees (IACUCs) at the University of North Carolina Wilmington (UNCW) and the Smithsonian Tropical Research Institute (STRI). Yellow-phase bluehead wrasses (*Thalassoma bifasciatum*) were collected off Key Largo, Florida and immediately shipped air freight to UNCW by a licensed fish vendor in Florida. For feeding assays conducted at the STRI in Bocas del Toro, Panama, we collected the Caribbean sharpnose puffer, *Canthigaster rostrata*, at Hospital Point and the white spotwrist hermit crab, *Pagurus criniticornis*, at STRI Point (Table 4.1).

Experimental foods were prepared as described by Marty & Pawlik (2015). Extracts, suspended in a minimal volume of MeOH, were reconstituted in a nutritionally appropriate food matrix of sodium alginate and squid mantle at the *volumetric* concentration of the source sponge, then formed into hardened strands in calcium chloride and cut into 4 mm pellets. Control pellets were prepared in the same manner—including the addition of MeOH—but without sponge extract. Pellets from each extract were presented in laboratory feeding

assays to each of 10 independent groups of three wrasse. Feeding assays with puffers were run in the same fashion, except fish were held in isolation from one another. Extract-treated pellets were considered rejected if sampled by the fish three times or sampled once and subsequently ignored. We also conducted feeding assays with hermit crabs held individually in 300 mL glass bowls. These hermit crabs forage on coral reef sponges at night (Marty *et al.* 2016) so we conducted assays after sundown, although the experimental bowls were illuminated for the duration of experiments. Hermit crabs were offered pellets generated in the same manner as those that were fed to fishes. Since this species of hermit crab is very small (< 2 cm carapace) a pellet represented more than a single bite: in order for a pellet to be scored as accepted, the hermit crab had to pick up the pellet and feed for 60 seconds. If the hermit crab began feeding but discarded the pellet before 60 seconds were up, the pellet was scored as rejected. Also, if the hermit crab held the pellet for 60 seconds but constant spitting was observed as the crab attempted to feed, the pellet was scored it as rejected. For all three model predators, a rejection of any treated pellet was followed by the offering of a control pellet. If the criteria for accepting a pellet were met with the subsequent control pellet, the sample could be scored as rejected (Marty & Pawlik 2015).

4.4.6. Serial dilution and fractionation assays

To evaluate the magnitude of chemical defense, extract-treated pellets were first offered to puffers at 2× concentrations, and serially diluted to 1×, then

1/2× and so on until the extract was fully palatable. In the cases where no data are available for 2× concentration, this is because the extracts were mixed first at 1× before I decided to make dilution ladders. The samples that were extracted in different polarity fractions were first mixed into food at 4× concentration, then serially diluted to 2× and 1× concentrations for feeding assays with puffers. It is possible for metabolites to interact in a summative or synergistic way, and fractionation may remove this interaction effect, so it is important to test each fraction at higher concentrations (Pawlik 2012).

4.4.7. Statistical analysis of feeding assay data

Significance of differences in consumption of treated versus control pellets was evaluated using a modified version of Fisher's exact test in which the marginal totals for control and treated pellets were fixed, treating them both as random samples (Marty & Pawlik, 2015). Individual extracts were scored as deterrent if six or fewer pellets were consumed ($p<0.05$), and in the case of a group of extracts (e.g. all *P. deweerdtaephila* extracts from Mayaguana that were tested on puffers), the group was considered deterrent if the mean number of pellets eaten plus standard error was less than or equal to six (Marty *et al.* 2016).

4.4.8. LC-MS analysis of plakinic acids

Samples were suspended in 500 µl of MeOH and 5 µl were injected onto a C8 (LiChrosphere 125 mm x 4 mm, 5 µm bead size RP-8, Agilent) column at 30°C and subjected to a 0.8 ml / min. 10% to 95% acetonitrile:water gradient

over 25 min using a high performance liquid chromatography (HPLC, Agilent 1100). Metabolite peaks were detected using an Agilent Diode Array Detector (DAD, Model #G1315B) with a micro high-pressure flow cell (G1315B#020; 6 mm pathlength, 1.7 µl volume) over the wavelength range 190 to 950 nm. Based on the UV spectra the absorption at 235 ± 4 nm was used to detect plakinic acids. All of the UV spectra were saved for each UV detectable peak. The eluate from the DAD detector was fed to the electro-spray nozzle of the mass spectrometer (Agilent G1956A SL) for ionization with the following spray chamber conditions using nitrogen as the drying gas: flow rate 10 L/min, pressure 60 psi, temperature 350°C, fragmentor voltage 70 V, capillary voltage 4000 V. Isoproponal (0.01 ml/min) was added post detector to provide appropriate conditions for positive mode ionization. For plakinic acid analysis mass spectra (200 - 600 m/z) were obtained for all UV peaks.

4.5. Results

4.5.1. Assays with crude extracts at volumetric concentration

In feeding experiments with three model predators, the crude extracts from *X. deweerdtae* (free-living and associated), *P. deweerdtaephila*, and *P. symbiotica* yielded similar results; most extract-treated food pellets were consumed significantly less than controls (Figs 4.1 and 4.2). For free-living individuals of *X. deweerdtae*, the mean number of treated food pellets eaten by both fish species (puffers and wrasse) from each of the nine collection sites was significantly less than controls, with three exceptions: Acklins Island (µ = 6.67/10)

and Bocas del Toro (μ = 9.67/10) for puffers, and Desecheo (μ = 7/10) for wrasse (Fig. 4.1).

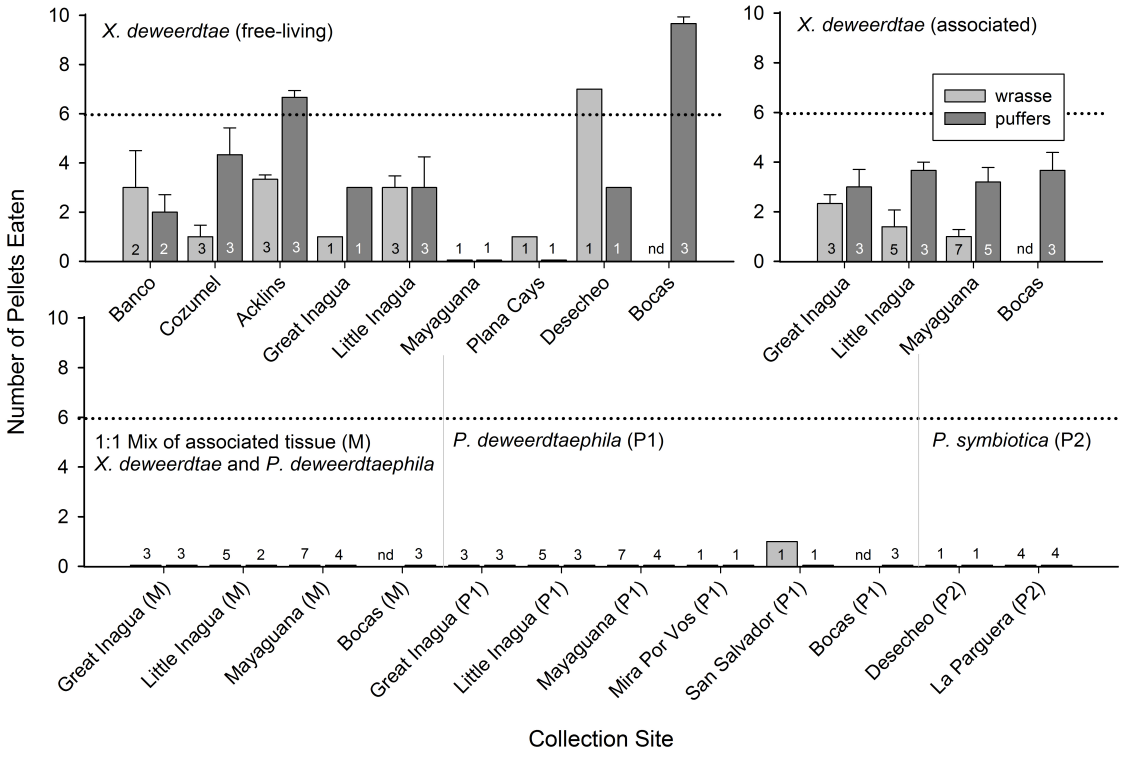

Figure 4.1 Results of feeding assays with bluehead wrasse (*Thalassoma bifasciatum*) and Caribbean sharpnose puffers (*Canthigaster rostrata*). Crude organic tissue extracts from sponges, incorporated at a 1× volumetric concentration into artificial food pellets, were offered to each species of fish. Bars indicate the mean number of pellets eaten (out of 10) for multiple extracts of the given sponge at the given site, and error bars show standard error. In every case, 10/10 control pellets were consumed. The dotted line indicates a threshold for statistical significance as determined by a modified Fisher's Exact Test; a sample is significantly deterrent (p <0.05) if six or fewer pellets are consumed (Marty & Pawlik 2015). The horizontal axis specifies the geographic location from

which the samples were collected, and the number of replicate sponges tested from each site is shown as a number overlaid or on top of the bar. nd = no data collected.

Pellets treated with extract of free-living *X. deweerdtae* from Bocas del Toro and Little Inagua were also offered to hermit crabs, and the mean number of pellets eaten was less than or equal to 6, although one individual extract from Bocas del Toro was eaten by 7/10 hermit crabs (Fig. 4.2). Extract-treated pellets generated from the associated form of *X. deweerdtae* were also consumed significantly less than controls by both fish predators (Fig. 4.1) and by hermit crabs (Fig. 4.2). The 1:1 mix of *X. deweerdtae* and *P. deweerdtaephila* was consistently and completely rejected by both fish species, with zero pellets eaten in 28 assays (Figure 4.1). The same pattern of complete rejection continued for *P. deweerdtaephila* extracts, where only one pellet was eaten in one assay (with an extract from San Salvador, eaten by a wrasse) out of 32 assays for the two fish species (Fig. 4.1). In assays with hermit crabs, *P. deweerdtaephila* was also significantly deterrent (Fig. 4.2). We also tested extracts from *P. symbiotica* collected in Puerto Rico, and consistent with the congener *P. deweerdtaephila*, all extracts were significantly deterrent, with no pellets eaten by either fish species (Fig. 4.1).

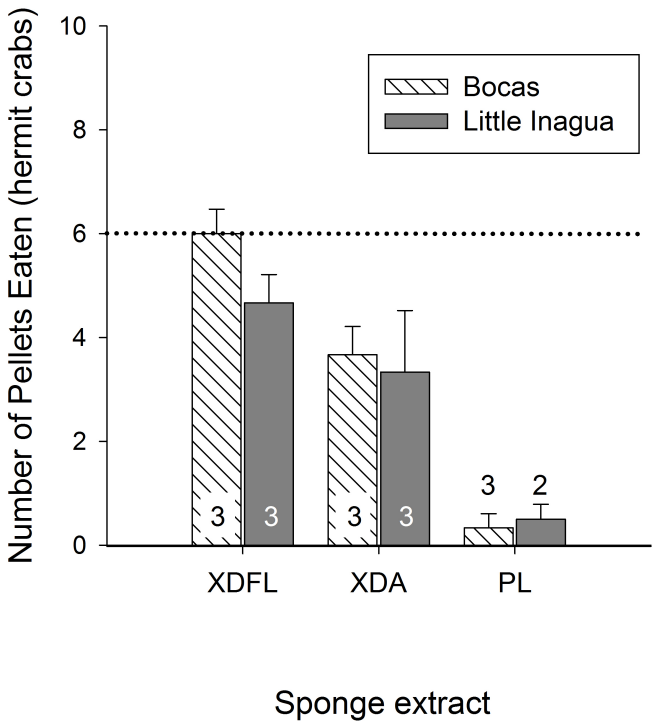

Figure 4.2 Results of feeding assays with white spotwrist hermit crabs (*Pagurus criniticornis*). Crude organic tissue extracts from sponges, incorporated at a 1× volumetric concentration into artificial food pellets, were offered to hermit crabs. Bars indicate the mean number of pellets eaten (out of 10) for multiple individuals of the given sponge at the given site, and error bars show standard error. In every case, 10/10 control pellets were consumed. The dotted line indicates a threshold for statistical significance as determined by a modified Fisher's Exact Test; a sample is significantly deterrent (p <0.05) if six or fewer pellets are consumed (Marty and Pawlik, 2015). The horizontal axis specifies species and growth form used to generate each extract: XDFL = *Xestospongia deweerdtae* free-living; XDA = *X. deweerdtae* associated; PL =

Plakortis deweerdtaephila. The number of replicate sponges tested from each site is shown as a number overlaid on the bar.

4.5.2. Serial dilution assays

A subset of the sponge extracts was tested at higher and lower concentrations with sharpnose puffers as a model predator. Food pellets containing the 1× volumetric concentration of crude extract from the free-living form of *X. deweerdtae* collected at Little Inagua and Cozumel were consumed significantly less than controls, but extracts from Bocas del Toro at the same concentration were not different from controls (Fig. 4.3). A more concentrated version of the free-living *X. deweerdtae* extract from Bocas del Toro at 2× was also not significantly different from controls, while the extracts from Little Inagua and Cozumel remained significantly different from controls at 1/2×; pellets from these sites had to be diluted to 1/4× concentration before they were accepted by more than 6/10 puffers on average (Fig. 4.3). For the associated form of *X. deweerdtae* from all sites, food pellets treated with extract at a 1× volumetric concentration were consumed significantly less than controls by both fish species (Fig. 4.1). However, when extracts from Bocas del Toro and Little Inagua were diluted to 1/2× concentration and fed to puffers, pellets were consumed at threshold levels that were not significantly different from controls (Fig. 4.4). The 1:1 mix of *X. deweerdtae* and *P. deweerdtaephila* tissue was significantly deterrent to both fish predators at 1× concentration (Fig. 4.1) and the extracts from Bocas del Toro required a dilution to 1/32× before puffers would consume

more than 6/10 pellets on average (Fig. 4.4). *P. deweerdtaephila* from Bocas del Toro and *P. symbiotica* from La Parguera were also significantly deterrent at 1× for both fish predators (Fig. 1) and required a dilution to 1/256× before puffers would consume more than 6/10 pellets on average (Fig. 4.4)

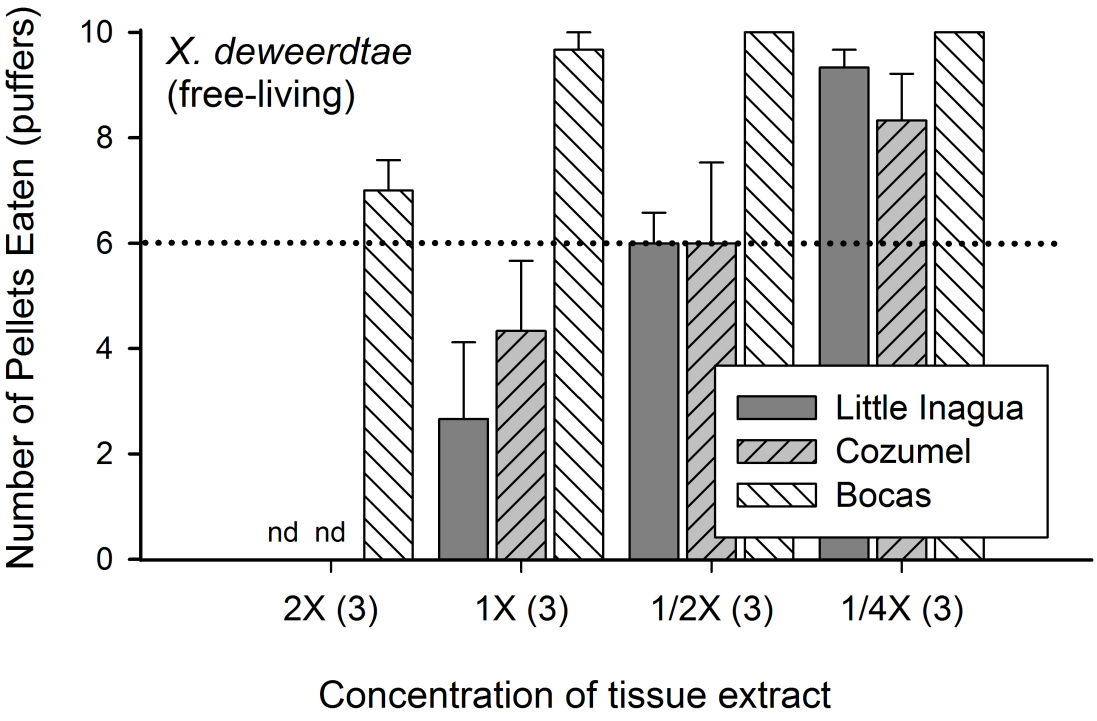

Figure 4.3 Results from serial dilution feeding assays with Caribbean sharpnose puffers (*Canthigaster rostrata*), using tissue extract from the free-living form of *Xestospongia deweerdtae* from three geographic locations. Horizontal axis shows a progression from concentrated (2×) to dilute (1/4×). Vertical axis and other details as described for Fig. 4.1.

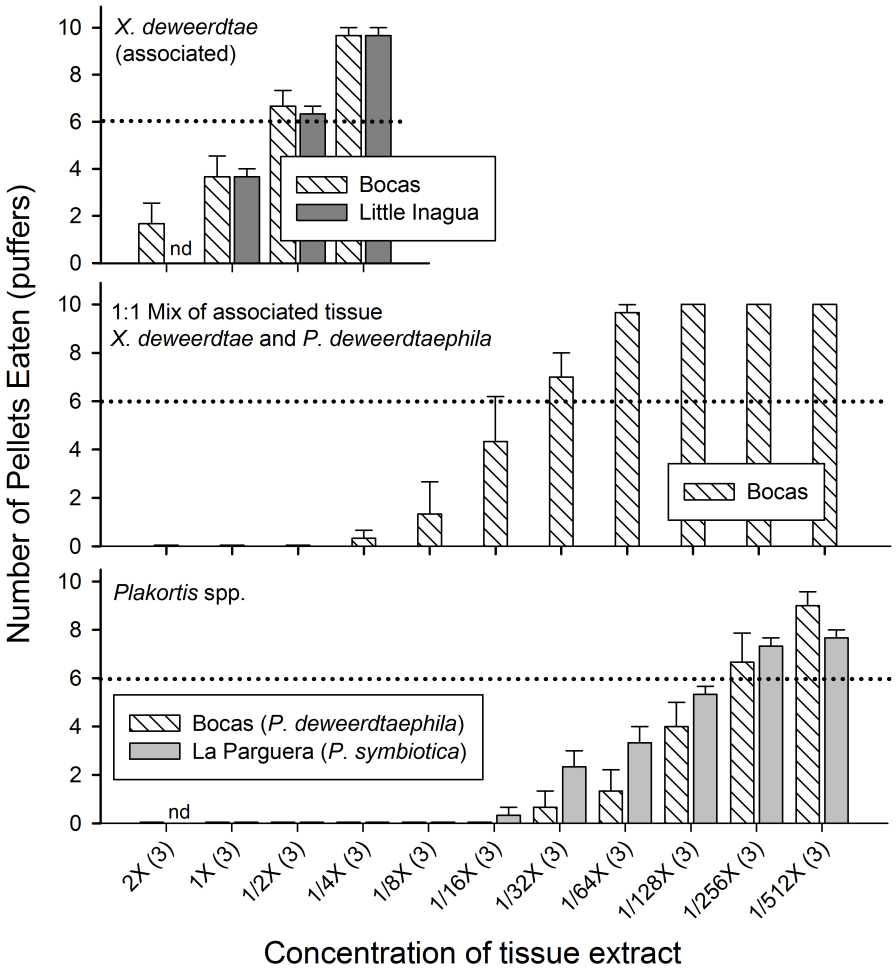

Figure 4.4 Results from serial dilution feeding assays with Caribbean sharpnose puffers (*Canthigaster rostrata*) on associated *Xestospongia deweerdtae*, 1:1 mix of *X. deweerdtae* and *Plakortis deweerdtaephila* tissue and on dissected *Plakortis* spp. Results of tissue extract from the associated form of *Xestospongia deweerdtae* (top panel), a 1:1 Mix of tissue from both sponge genera (middle panel), and *Plakortis* spp. (bottom panel). Horizontal axis shows a progression from concentrated (2×) to dilute (1/512×). Vertical axis and other details as described for Fig. 4.1.

4.5.3. Fractionation Assays

Sponge tissue samples from *X. deweerdtae* (both the free-living and associated forms) and *P. deweerdtaephila* collected in Bocas del Toro were each extracted into three polarity fractions: moderately polar, less polar, and non-polar. Each extract was tested at 4×, 2×, and 1× concentrations in feeding assays with puffers. None of the fractions of free-living *X. deweerdtae* were consumed significantly less than controls except for the 4× concentration of the moderately polar fraction (Fig. 4.5). In contrast, most fractions of associated *X. deweerdtae* were consumed significantly less than controls, with the exceptions of 2× and 1× concentrations of the less polar fraction (Fig. 4.5). For *P. deweerdtaephila*, all concentrations of all fractions were completely rejected by puffers, with zero pellets eaten (Fig. 4.5).

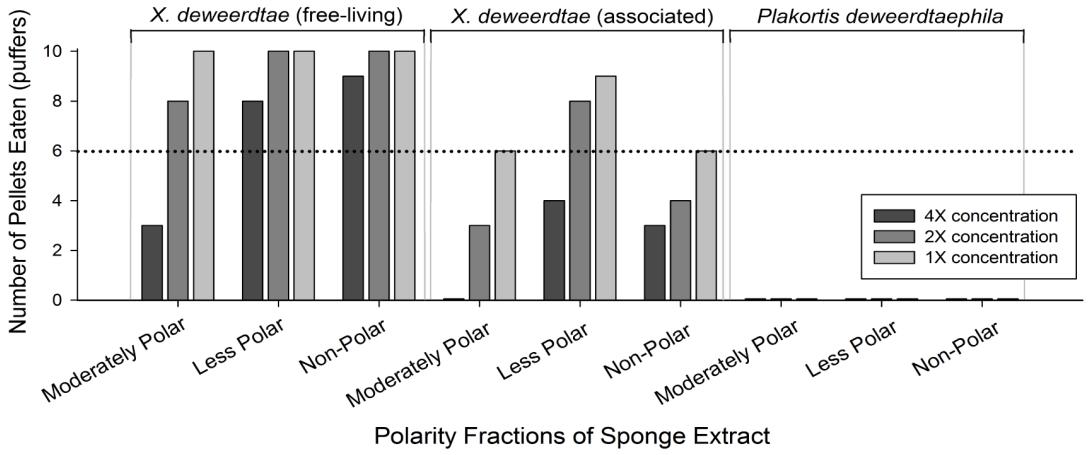

Figure 4.5 Results from feeding assays in which pellets containing different polarity fractions of sponge extract were offered in serial dilutions to Caribbean sharpnose puffers (*Canthigaster rostrata*). The horizontal axis indicates polarity fractions, and different shades on bars represent different

concentrations of the extract fraction. Vertical axis and other details as described for Fig. 4.1.

4.5.4. Identification of plakinic acids using diode-array high performance liquid chromatography (HPLC) coupled with mass spectrometry (LC-MS)

Two peaks at λ max 235 nm were observed to be consistent between extracts from *X. deweerdtae* and *P. deweerdtaephila*: one peak had a retention time (*Rt*) of 15.3 min (*m/z* 402.2 $[M + H]^+$), hereafter Main Compound 1 and another peak with *Rt* 16.2 min (*m/z* 416.3 $[M + H]^+$), hereafter Main Compound 2 (Fig. 4.6). On average, Main Compound 1 represented 11.52% of the crude extract in *P. deweerdtaephila* and 0.06% of the crude extract in *X. deweerdtae*, while Main Compound 2 represented 2.09% of the crude extract in *P. deweerdtaephila* and 0.02% of the crude extract in *X. deweerdtae* (Table 4.2). Neither peak from the two Main Compounds was observed in the chromatogram for the free-living form of *X. deweerdtae* (Fig. 4.6A).

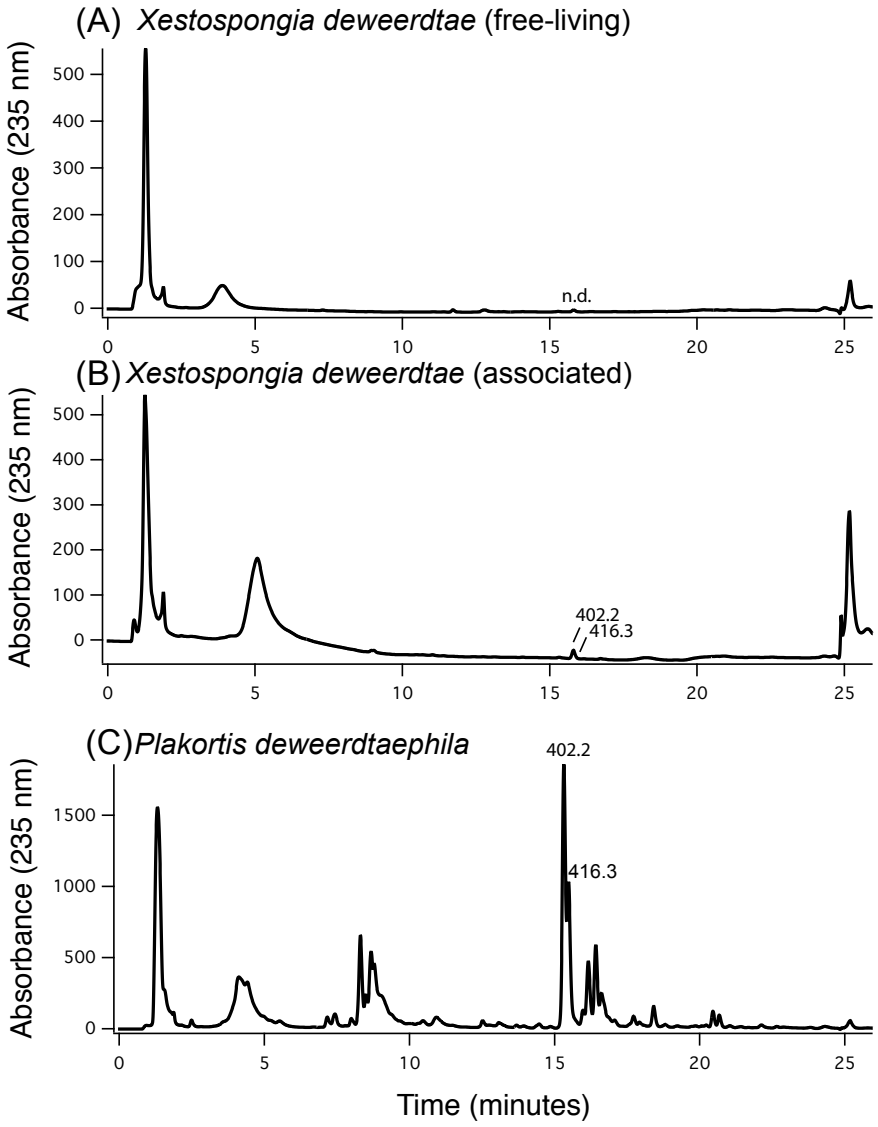

Figure 4.6 Chromatograms of UV absorbance at 235 nm indicating the m/z value of Main Compounds 1 and 2 from crude extracts dissolved in MeOH from free-living and associated *Xestospongia deweerdtae* and *Plakortis deweerdtaephila* tissue samples. Neither main compounds were detected in crude extracts of (A) free-living *X. deweerdtae*. Main Compounds 1 and 2 were detected in crude extracts of (B) associated *X. deweerdtae* and these were major components of the (C) *P. deweerdtaephila* crude extract.

Table 4.2. Yield and percent of Main Compounds 1 and 2 in crude extracts of *Plakortis deweerdtaephila*, free-living and associated *Xestospongia deweerdtae*, λ max. 235, using LC-MS.

Sponge species	Crude Extract (mg)	Main Compound 1* (mg)	Main Compound 1* % of crude	Main Compound 2** (mg)	Main Compound 2** % of crude
P. deweerdtaephila	100	2.592	**2.592**	0.685	**0.685**
	68.4	9.570	**13.992**	1.717	**2.510**
	40.4	7.262	**17.976**	1.245	**3.081**
X. deweerdtae (associated)	52.2	0.015	**0.029**	0.002	**0.004**
	33.6	0.018	**0.054**	0.007	**0.020**
	29.8	0.028	**0.095**	0.006	**0.020**
X. deweerdtae (free-living)	48.0	NO PEAK		PEAK	
	40.1				
	57.6				

*Main Compound 1 eluted from the column at *Rt* 15.319 (*m/z* 402.2 $[M + H]^+$).

**Main Compound 2 eluted from the column at *Rt* 16.158 (*m/z* 416.3 $[M + H]^+$).

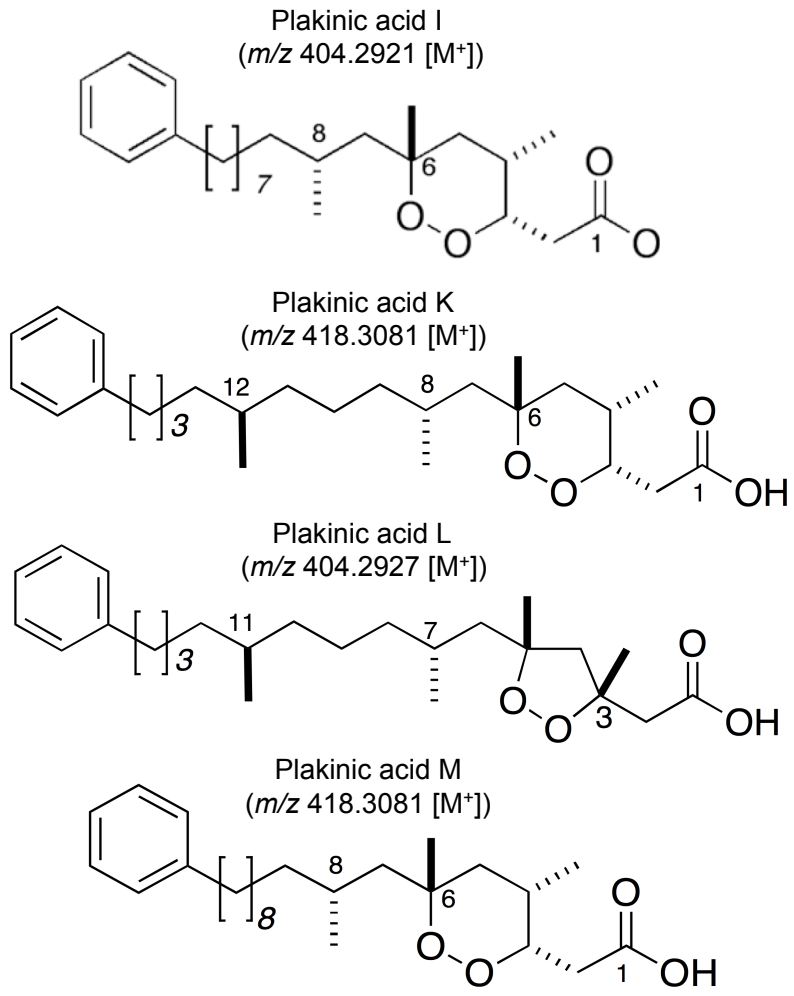

Figure 4.7 Chemical structures of four previously isolated plakinic acids derivatives with similar ion mass [*m/z*] to Main Compounds 1 and 2. Plakinic Acid I (*m/z* 404.2921 $[M]^+$) was previously isolated from *Plakortis halichondrioides* (Dalisay *et al.* 2009), plakinic acid L (*m/z* 404.32927 $[M]^+$), plakinic acid K (*m/z* 418.3081 $[M]^+$), and plakinic acid M (*m/z* 418.3081 $[M]^+$) were all isolated from the *Plakortis deweerdtaephila* / *Xestospongia deweerdtae* pair previously reported as *P. halichondrioides* / *X. deweerdtae* sponge pair (Dalisay *et al.* 2011).

4.6. Discussion

In this study, I evaluate the hypothesis that *X. deweerdtae* grows in a specialized sponge-sponge symbiosis with either *P. deweerdtaephila* or *P. symbiotica* due to a shared chemical defense against predators. I collected free-living individuals of *X. deweerdtae* and symbiotic colonies from a wide geographical range and tested the chemical defenses of these sponges against three common coral reef predators in feeding assays with crude extracts, serial dilutions of extracts, and a series of polarity fractions from sponge extract. The multiple lines of evidence we gathered provide no support for the hypothesis that this symbiosis is driven by shared chemical defenses. To attribute the symbiosis to a shared defense would require at least one of the partners in symbiosis be consistently palatable to predators. While the chemical defenses of *P. deweerdtaephila* and *P. symbiotica* are more potent than those of *X. deweerdtae*, all of the sponge species we tested significantly deterred feeding by all three generalist predators. The free-living form of *X. deweerdtae* is mostly defended across the region, with a few exceptions. The associated form of *X. deweerdtae* is always defended, and both species of *Plakortis* are very strongly defended, with puffers refusing to consume extract-treated pellets until the extract was diluted to 1/256× concentration. We even found metabolites from *P. deweerdtaephila* at very low concentrations in associated *X. deweerdtae* tissue. Comparing the immense deterrency of *Plakortis* spp. extracts to the *X. deweerdtae* extracts gives the impression that there may be some sharing of chemical defenses: one partner in the symbiosis is clearly more defended than

the other and perhaps sharing a small amount of its defensive chemistry. However, the chemical defenses in both sponges deter feeding in fish and arthropod predators, and given the diversity of other potential food resources on coral reefs it is improbable that the evolution of this specialized sponge-sponge symbiosis has been driven by predation pressure.

The free-living form of *X. deweerdtae* presents a peculiar pattern of variable deterrency across its geographic range, with assay fishes rejecting pellets treated with the crude extract of some individuals while consuming pellets treated with the crude extracts of other individuals. This variability can be seen clearly in the serial dilution assays with puffers, where samples from Bocas remain palatable even when concentrated to 2×, but samples from Little Inagua and Cozumel require a 1/4× dilution before they are palatable (Fig. 4.3). Some common Caribbean sponges, such as the chicken liver sponge *Chondrilla caribensis*, the giant barrel sponge *Xestospongia muta*, and the pink vase sponge *Niphates digitalis*, exhibit an exaggerated form of this pattern, where even within the same population, individuals will vary dramatically in their levels of chemical defense (Chanas & Pawlik 1997; Swearingen III & Pawlik 1998; Marty *et al.* 2016). It is possible that variation in the trait of chemical defense allows the species to avoid predation because predators incur a handling cost when rejecting defended individuals and ultimately decide to forage on other resources (Marty *et al.* 2016). In any case, the free-living form of *X. deweerdtae* is defended at so many of the sites throughout the region that it fails to meet the criteria of a ‘variably defended’ sponge for the region (*sensu* Loh & Pawlik, 2014)

and as a morphotype of the species, it is properly categorized as defended. Fractionation assays with tissue from Bocas suggest that any deterrent compounds are in the moderately polar fraction; however, the Bocas tissue was not defended as a crude extract and may not indicate the defenses that cause fish to reject this species from the sites where it is defended. The associated form of *X. deweerdtae* is consistently defended across its range, although a dilution to 1/2× puts it just above threshold palatability. As with the free-living form, the moderately polar fraction of associated *X. deweerdtae* was deterrent in fractionation assays with puffers. Distinct from the free-living form however, the non-polar fraction was also deterrent. The divergence in defenses between the free-living and the associated forms of *X. deweerdtae* also appears in hermit crab assays (Fig. 4.2), however these assays were conducted with tissue from two sites where the crude extracts of each growth form were also different. Overall, extracts from *X. deweerdtae*, in both the free-living and associated forms, deter feeding by fishes and hermit crabs, and this species should be classified as a chemically defended sponge.

The two basibiont *Plakortis* spp. showed remarkable deterrency. Crude extracts of both species significantly deterred feeding in puffers and wrasse, and extract-treated pellets of *P. deweerdtaephila* were also rejected by hermit crabs. Serial dilutions provided striking results: puffers were significantly deterred from feeding by all treated pellets until dilution reached 1/256× (Fig. 3.4). While there may be multiple defensive roles for secondary metabolites, both species of *Plakortis* examined in this study clearly have more chemical defense than

necessary to deter predators. Fractionation assays were not informative because the extracts were not adequately diluted. I also tested a mixture of equal parts tissue from each sponge in a given sponge pair. This was designed to approximate the taste of a casual bite by a fish predator on a sponge pair. The bite volume of most spongivorous fishes is large enough to capture not just tissue from the epibiont *X. deweerdtae*, but also the *Plakortis* spp. basibionts. It is clear that a combination of the two sponges is adequate to deter predators, which makes it theoretically possible for the chemical defense of the basibiont to deter fish predators with substantial bite volume from attacking the epizoic *X. deweerdtae*.

Another hypothesis I set out to explore was that excess secondary metabolites produced in *P. deweerdtaephila* might translocate into the tissue of *X. deweerdtae*. The fact that *X. deweerdtae* occurs in a free-living form allowed us to make a preliminary evaluation of this idea. We used tissue from Bocas del Toro, Panama, where the crude extracts of free-living *X. deweerdtae* were palatable while extracts of the associated form were not. The two LC-MS peaks that were shared between the associated form of *X. deweerdtae* and *P. deweerdtaephila* probably represent slight modifications of known plakinic acids.

For example, the Main Compound 1 differs by having a mass loss of 2 *m/z* compared to plakinic acids I and L that were previously isolated from *Plakortis halichondrioides* and the *P. deweerdtaephila/X. deweerdtae* sponge pair previously thought to be P. *halichondrioides/X.deweerdtae* (Dalisay *et al.* 2009; 2011). The 2 *m/z* loss suggests an additional double bond formation to either

plakinic acid I or L (Fig. 4.7). Two other plakinic acids, K and M, isolated by Dalisay *et al.* (2011), also exceeds the mass of Main Compound 2 by 2 *m/z* as well, indicating a potential double bond modification in Main Compound 2 derivative (Fig. 4.7). It is not surprising that we were unable to detect any of the plakinic acid previously isolated by Dalisay *et al.* (2009, 2010) in *P. deweerdtaephila* collected in Panama, as the production of secondary metabolites by the same sponge species could vary according to different collection sites (Nuñez *et al.* 2008). Although purified plakinic acids have not been tested for deterrency in feeding assays, it is probable that these compounds deter feeding given their substantial contribution to the crude extract in *P. deweerdtaephila* and the immense deterrency of the crude extract. Also, plakinic acids are endoperoxide-containing metabolites like plakortide F that protects *Plakortis angulospiculatus* from predation by *C. rostrata* (Slattery et al. 2016).

While both bluehead wrasses and puffers have been used to study the chemical defenses of sponges in the past (e.g., Pawlik 2011; Slattery *et al*. 2016), this is the first time that a direct comparison has been made between the chemical defense feeding assay results of these fish species from two distinct orders. The responses of these two fishes rarely produced statistically different outcomes in these assays, and the minor differences that are observed are not consistent across samples (Fig. 4.1). For the free-living form of *X. deweerdtae*, there were three sites where puffers consumed more treated pellets than wrasse, and only one of them resulted in a different assay outcome (Acklins Is.).

Conversely, there were three sites where wrasse consumed more treated pellets than puffers, again with only one of the sites resulting in a different assay outcome (Desecheo Is.). Puffers were consistently more willing to consume pellets containing extracts from the associated form of *X. deweerdtae* than wrasse were, but they still strongly rejected with extract-treated pellets compared to controls. The comparison of these two model predators merits further investigation using a broader suite of prey organisms with diverse chemical defenses in order to examine differences in fish response.

I also employed a novel feeding assay with hermit crabs that generated similar results to those obtained with the fish-feeding experiments. Although previous studies have compared the feeding of fishes and crabs, my assay designs allow for a direct comparison of results. Pennings *et al.* (1994) tested the deterrency of sponge metabolites against *Canthigaster solandri* (closely related to *C. rostrata*) and intertidal xanthid crabs from the genus *Leptodius*, and found different predator responses; however, the design of their assays left ambiguity as to whether the different results were actually caused by differences in gustatory perception by the predator or whether the differences were caused by the design of the assay. Waddell & Pawlik (2000a) evaluated the response of the hermit crab *Paguristes punticeps* to crude extracts generated from a suite of Caribbean sponges that had previously been tested against bluehead wrasse, *T. bifasciatum* (Pawlik *et al.* 1995). Although the assay design between the two studies was slightly different, the results were similar, and Waddell & Pawlik (2000a) conclude that chemical defenses in sponges are broadly effective

against a diversity of predators. The hermit crab assays shared the same design as the fish-feeding assays, and a direct comparison of the results suggests that the chemical defenses of *X. deweerdtae* and *Plakortis* spp. are broadly effective against fish and arthropod predators.

While our use of these three model predators is substantial, it does not exhaustively evaluate the potential predators of this sponge pair, and there may be predators who are not deterred in their feeding by the defensive chemistry of these sponges. An alternative scenario is that chemical defenses in the epizoic *X. deweerdtae* protect *P. deweerdtaephila* and *P. symbiotica* from some surface-feeding predator (like a gastropod or an asteroid). While this scenario is improbable, it fits with the observation that neither species of *Plakortis* can be found in a free-living form. Sponges in the genus *Aplysina*, for example, are exceptionally well-defended against vertebrate and invertebrate predators (Pawlik *et al.* 1995; Waddell & Pawlik, 2000a, 2000b) using brominated tyrosine derivatives as a chemical defense [e.g. (Puyana *et al.* 2003)]. However, cowries in Belize (Pawlik & Deignan 2015) and limpets in Panama (Vicente, *unpublished data*) have recently been observed to feed voraciously on *Aplysina* spp. despite the substantial chemical defenses. In an effort to consider alternative predators of *X. deweerdtae* and *Plakortis* spp., we attempted gel-screen feeding assays with a limpet and a dorid nudibranch, but these gastropod predators refused to cooperate under the control conditions.

In summary a broad biogeographic survey of the chemical defenses in this epizoic sponge symbiosis did not yield results to support the shared chemical

defense hypothesis. Although the LC-MS analysis provided evidence for the translocation of secondary metabolites from *P. deweerdtaephila* to *X. deweerdtae*, this probably does not provide a necessary chemical defense to *X. deweerdtae.* This study is an important contribution to understanding sponge-sponge symbioses and the nature of this particular interaction.

Chapter 5: Mutualism between *Xestospongia deweerdtae* and *Plakortis deweerdtaephila* in the face of climate change

5.1. Abstract

Ocean acidification and increasing sea surface temperatures pose imminent threats and disruption to a variety of biological systems, from individual organisms to the ecosystem level. In this study I explore how increasing acidity and thermal stress affect the recently discovered mutualistic interaction between *Plakortis deweerdtaephila* sp. nov. and *Xestospongia deweerdtae*. Equal numbers of individuals from both lifestyles were collected and placed in experimental tanks where pCO_2 and temperature were manipulated as individual and combined factors that simulated conditions to be expected by the end of the century (+3°C, 950 µatm) based on the CO_2 Representative Concentration Pathway (RCP6.0) for a duration of 34 days. A balanced experimental design using both free-living and associated individuals of *X. deweerdtae* allowed us to determine whether the individuals in associated lifestyles were at an advantage over free-living sponges. The results showed that under ambient conditions and experimental treatments all individuals of *X. deweerdtae* developed necrotic tissue and that the highest necrotic tissue rates were observed in the sponges maintained at High T & Ambient pCO_2 treatments. Associated individuals of *X. deweerdtae* developed less necrotic tissue than free-living individuals but also exhibited the highest necrotic tissue rates in treatments with elevated temperatures. These differences were higher in the associated *X. deweerdtae* than the free-living lifestyle. Acidification conditions caused *P. deweerdtaephila* to develop less disease than individuals exposed to higher temperatures and when factors were coupled, acidification significantly reduced the necrotic tissue progress rate caused by higher

temperatures. These results suggest that both *X. deweerdtae* and *P. deweerdtaephila* are sensitive to warmer temperatures but not to acidification or the coupled effects of temperature and acidification. Acidification also seems to help *X. deweerdtae* FL, *X. deweerdtae* AS and *P. symbiotica* resist necrosis caused from thermal stress. Overall, these results support the hypothesis that these associations are mutualistic in nature as sponge pairs overall were more resilient than free-living forms of *X. deweerdtae* and that these symbioses will likely survive predicted temperature and pCO_2 conditions for the end of the century.

5.2. Introduction

Climate change is predicted to have devastating impacts on foundational organisms and their ecosystems. Adaptive strategies to offset the physiological challenges posed by climate change are crucial for species survival. Migratory responses to increasing temperatures are already apparent in terrestrial and marine habitats, where organisms are moving to higher latitudes (Chen *et al.* 2011; Poloczanska *et al.* 2013). In addition, phenotypic plasticity in terrestrial habitats has been an important adaptation strategy on the coloration of some animals like the increasing number of the conspicuous brown morphed tawny owls in winters with less snow (Mills *et al.* 2013). The rate at which these adaptations happen is important as it may determine the “winners” and “losers” in a changing climate (Karell *et al.* 2011).

In marine habitats, organisms not only need to adapt to an increase in sea surface temperatures, but also to ocean acidification that is a result of increasing atmospheric pCO_2. There are only a few examples of marine organisms using phenotypic plasticity to adapt to either acidification or thermal stress. For example, the coral *Oculina patagonica* may acquire an anemone-like lifestyle without a calcium carbonate skeleton under predicted acidification conditions and can rebuild its calcium carbonate skeleton when pCO_2 is brought to present conditions (Fine & Tchernov 2007). In response to thermal stress, corals may also acquire more resilient *Symbiodinium* clades in order to resist future bleaching events (Baker *et al.* 2004). The quickest adaptation strategy in some

coral species is to increase the production of heat shock and transport proteins that protect them from thermal stress (Palumbi *et al.* 2014).

Despite being considered the winners of climate change, sponges can be sensitive to acute temperature increases (Webster *et al.* 2008) and in some species these consequences could cause mass extinction events of a single species (Cebrian *et al.* 2011). However, there are no studies addressing how different adaptation strategies may help sponges become more resilient to climate change. My discovery of a Caribbean-wide two sponge symbiosis between *Xestospongia deweerdtae* / *Plakortis deweerdtaephila* enables comparison with the free-living form of *X. deweerdtae*, allowing me to evaluate whether the ability to associate with a heterospecific sponge could be used as an adaptation strategy to better withstand the consequences of climate change, in comparison to free-living morphotypes. In other words, is the association status of *X. deweerdtae* with P*. deweerdtaephila* more resilient to ocean acidification and thermal stress than free-living lifestyles? Based on previous studies that observed how pairing up with heterospecific species allowed sponges to grow faster and increase their survival (Wulff 1997), I hypothesized that sponge pairs would be more resilient than free-living forms.

In order to test this hypothesis, I compared the following parameters for free-living and associated lifestyles: 1. mass gain/loss, 2. spicule length differences to determine impact on skeleton synthesis, 3. necrotic tissue progress rate, and 4. the stability of the association by measuring healthy and necrotic sponge tissue ratios for *X. deweerdtae* / *P. deweerdtaephila* pairs. This

study allowed the evaluation of whether the phenotypic plasticity of *X. deweerdtae* is an advantageous strategy to cope with some of the stresses imposed by climate change as observed in other organisms.

5.3. Methods

5.3.1. Sponge collection

Pieces from sponge pairs *Plakortis deweerdtaephila/Xestospongia deweerdtae* (n=72) were collected on May 28, 2015 at Dolphin Rock off Isla Bastimentos, Panama (9.35076° N, -82.1863° W) at a depth of 15 m. Free-living (n=72) individuals of *X. deweerdtae* were collected on May 29, 2015 at Punta Caracol reef off Isla Colon (9.3777° N, 82.1265° W) at a depth of 5 m. Sponges were labeled and six pieces of each life-style were distributed to 12 individual 100-L tanks at the Smithsonian Tropical Research Institute's ocean acidification facility in Bocas del Toro. The room temperature of the mesocosm facility was 20°C and each tank was supplied with a submersible aquarium heater to control for water temperature. Tanks were also supplied with a gas line that received pre-mixed pCO_2 using mass flow controllers (C100L Sierra Instruments). The gas line was connected to a water pump that kept seawater well mixed. Sponges acclimated for 27 days with each tank receiving seawater from the bay side of Isla Colón. Parameters for acclimation conditions were set to the ambient conditions of Isla Colón at the time of the experiment (28°C and 450 µatm). Incoming seawater was set to a flow rate of 400 ml min^{-1} with a turnover every 4 h (Table 5.1, Figure A2.1).

Table 5.1 Experimental seawater chemical parameters. Mean and standard error for chemical parameters collected at depth for collection sites (Dolphin Rock and Airport Point on May 23, 2015), during a 27-day acclimation period and for all experimental tanks in the 35-day flow-through experiment.

Parameter	Collection sites		Acclimation	Treatments				Intake
	Dolphin Rock	Airport Point		Ambient T & Ambient pCO_2	Ambient T & High pCO_2	High T & Ambient pCO_2	High T & High pCO_2	
Temp (°C)	27.5 ± 0.12	28.5 ± 0.01	28.2 ± 0.12	28.0 ± 0.02	28.0 ± 0.07	31.0 ± 0.04	30.9 ± 0.03	27.6 ± 0.05
Salinity (ppt)	36.4 ± 0.05	34.2 ± 0.03	33.6 ± 0.12	32.0 ± 0.23	32.0 ± 0.22	32.3 ± 0.26	32.3 ± 0.26	31.8 ± 0.28
A_T(µmol kg $^{-1}$)	2215.9 ± 13.7	2227.6 ± 11.7	2237.2 ± 5.19	2154.0 ± 11.5	2158.5 ± 10.9	2149.5 ± 11.9	2153.4 ± 11.4	2147.8 ± 15.5
pH_T	8.008 ± 0.001	8.032 ± 0.001	8.019 ± 0.008	7.980 ± 0.003	7.702 ± 0.003	7.958 ± 0.002	7.688 ± 0.003	7.99 ± 0.009
pCO_2(µatm)	405 ± 2.6	385 ± 2.4	449 ± 10.2	447 ± 5.0	928 ± 5.8	462 ± 3.1	952 ± 7.1	408 ± 3.8
HCO_3^-(µmol kg $^{-1}$)	1683 ± 9.4	1670 ± 10.3	1746 ± 6.9	1686 ± 17.1	1888 ± 6.5	1667 ± 1.4	1861 ± 3.1	1672 ± 8.4
CO_3^-(µmol kg $^{-1}$)	214.6 ± 2.0	221.6 ± 1.7	199.9 ± 1.8	187.4 ± 2.1	110.4 ± 1.5	196.3 ± 2.5	119.2 ± 1.9	194.1 ± 3.3
Ω_{arag}	3.41 ± 0.03	3.6 ± 0.02	3.2 ± 0.03	3.1 ± 0.03	1.8 ± 0.02	3.3 ± 0.04	2.0 ± 0.05	3.2 ± 0.05
$Si(OH)_4$(µmol L^{-1})	3.25 ± 0.25	13.23 ± 0.06	14.23 ± 1.5	13.38 ± 0.2	13.35 ± 0.3	13.46 ± 0.1	13.28 ± 0.2	13.78 ± 0.54
O_2 (mg L-1)	5.77 ± 0.02	5.38 ± 0.04	5.86 ± 0.05	5.98 ± 0.05	5.97 ± 0.04	5.69 ± 0.05	5.66 ± 0.05	5.98 ± 0.05

5.3.2. Experimental design

Temperature and pCO_2 values were manipulated in randomly selected tanks after the acclimation period with values that corresponded closely to ambient and projected levels for 2100 (+3°C, 1100 ppm) (Riahi *et al.* 2011). Temperature and pCO_2 values were manipulated to obtain four experimental treatments: Ambient T & Ambient pCO_2, Ambient T & High pCO_2, High T & Ambient pCO_2 and High T & High pCO_2. Treatments with ambient conditions were kept at the same values as during the acclimation period. Treatments with high temperatures and high pCO_2 conditions were set at 31°C and 950 µatm respectively. There were three replicate tanks and 18 individuals of each sponge species and lifestyle per experimental treatment in a completely randomized design. Replication was considered as the number of tanks per treatment and not by the number of individuals in each tank. Temperature, pH_T, salinity, and dissolved oxygen of each tank were measured every 12 h and seawater flow was monitored and adjusted twice a day to ensure consistency for all tanks. A_T and silica concentrations were measured every 3 d (Table 5.1).

Sponges were weighed with an analytical scale before and after the experiment to determine percent mass gain or loss for each sponge throughout the experiment. Sponges were placed in a 500-ml beaker with seawater; sponges were briefly exposed to air during the transfer from the tank to the beaker (Pawlik *et al.* 2013). Thin sections from the surface of each sponge and small sponge pieces (1 cm^3) were collected before and after 35 days to measure

differences in spicule length. Spicule preparations were made following the methods in (Vicente *et al.* 2016)

Pictures were taken every 7 days to monitor progress of necrotic tissue and the stability of the *P. deweerdtaephila* + *X. deweerdtae* symbiosis. Pictures were analyzed with imageJ (Abràmoff *et al.* 2004; http://imagej.nih.gov/ij/) to measure the surface area of necrotic tissue in proportion to healthy tissue. Necrotic tissue progress rate was calculated every seven days [Rate = ($NA_{t2,i}$ - $NA_{t1,i}$) / (time)], where NA is the necrotic surface area in cm^2 from sponge *i*, t_1 first time point, t_2 the second time point, and time between seven days. We also calculated the total necrotic tissue progress rate by using the same formula but using 35 days for t_2. The stability of the *P. deweerdtaephila* and *X. deweerdtae* association was calculated by measuring the ratio between both species in the pair every 7 days [Ratio = (HA_{XDi} / HA_{PDi})], where HA is the healthy sponge surface in cm^2 from either *X. deweerdtae* (*XD*) or *P. deweerdtaephila* (*PD*) of individual *i*.

5.3.3. Measuring seawater chemistry

Samples (250 mL) for A_T analysis were collected and processed within 7 h using open cell potentiometric titrations on a Mettler Toledo DL15 titrator (Dickson *et al.* 2007). A certified reference material (CRM- Reference Material for Oceanic CO_2 Measurements, A. Dickson, Scripps Institution of Oceanography) was run at the beginning of each sample set. Titrator accuracy was within ± 0.8% from the CRM standard and A_T measurements were corrected for this error. The

precision was 4.16 µEq (measured as the standard deviation of the duplicate water samples).

Seawater pH was measured on the total scale using a Tris calibrated Mettler Toledo DG 115-SC pH probe with an Orion 3star pH portable meter. Calibrations for the pH probe were performed each week following the SOP 6a protocol from Dickson et al. (2007). Other carbon parameters (pCO_2, HCO^-_3, CO_3^-, Ω_{arag}) were calculated using the CO_2SYS_V2.1 (Lewis et al. 1998) with known pH_T, A_T, temperature and salinity values. The K1K2 equilibrium constants were taken from Mehrbach *et al.* (1973) and refitted by Dickson & Millero (1987). The HSO_4^- dissociation constants were used from Uppström (1974) and Dickson *et al.* (2007). Salinity and dissolved oxygen measurements (mg/L) were taken using a dissolved oxygen and conductivity meter YSI Pro2030 sonde calibrated using one-point saturated water for the oxygen probe and using a 50 mS/cm conductivity standard (YSI Catalog# 3169) for the salinity probe following calibration protocols.

Duplicate samples to measure DSi concentrations were taken with 15 mL sterile falcon tubes. A Hach low range silica test kit was used for closed system experiments which follows a molybdate-reactive standard colorimetric method for measuring silicate (Grasshoff *et al.* 2009). Standard curves were generated prior to each run using a wavelength of 820 nm. Only dilutions that generated a standard curve with an R^2>0.99 were used to calculate DSi concentrations. Chemical reagents were added following the Hach protocol guidelines at 24°C.

Precision for silica samples was greater than 0.1 μM L^{-1} (measured as the standard deviation of the triplicate water samples).

5.3.4. Statistical analysis

All data were analyzed using *R* (Team *et al*. 2014; http://www.R-project.org/). Water chemistry parameters (Temperature and pCO_2), sponge weight loss, differences in spicule length, taken from the tissues of *X. deweerdtae* FL, *X. deweerdtae* AS and *P. deweerdtaephila* were log transformed to meet assumptions of normality. A two-way ANOVA using treatment, time and the treatment × time interaction, on pCO_2 and temperature values was conducted to confirm that carbonate and temperature conditions were well maintained for each treatment during the 35-day experiment. We used a factorial three-way ANOVA using pCO_2 (high, low), temperature (high, low) and lifestyle (free-living, associated) as factors to assess differences in sponge mass loss between free-living sponges and sponge pairs. A factorial three-way ANOVA using pCO_2, temperature and species (*X. deweerdtae* AS, *X. deweerdtae* FL, *P. deweerdtaephila* and sponge pair) that separated both lifestyles of *X. deweerdtae* was used to analyze differences in spicule length. Tukey's honestly significant difference (HSD) tests were used to determine significant differences between treatment means of all measured parameters.

Necrotic tissue rate data was negatively skewed and was ranked-transformed using the ARTool package in *R*. We used a repeated measures three-way ANOVA using (treatment × time × species) to monitor difference in

necrotic tissue rates between species every 7 days. We calculated the total necrotic tissue progress rate and were able to perform a factorial three-way (pCO_2 × Temperature × Species) ANOVA to determine whether mean differences in necrotic tissue rates were affected by pCO_2, temperature or the interaction of both. In addition, a two way ANOVA using treatment × species was performed to determine treatment differences on the total necrotic progress tissue rate. Post hoc pairwise comparisons of levels within individual factors were conducted using the lsmeans package and the "testInteractions" function from the phia package to measure significant interaction effects. To determine significant ratio differences between healthy tissue ratios of *X. deweerdtae* AS / *P. deweerdtaephila* across treatments we ran a two-way ANOVA using treatment × time as factors.

5.4. Results

5.4.1. Seawater parameters of treatment conditions

The mesocosm setup successfully produced significantly different temperature ($F_{10,88}$=6.38, p<0.0001) and pCO_2 ($F_{10,88}$=25.2, p<0.0001) conditions for the four treatments (Table 5.1 and Table A2.1). Tukey's HSD revealed that temperature for treatments held at 28°C were significantly lower than treatments held at 31°C p<0.0001. Likewise, pCO_2 levels for treatments held at 450 µatm were significantly lower than treatments held at 940 µatm p<0.0001. Ambient average pH_T, A_T, salinity, HCO_3^-, CO_3^-, Ω_{arag}, $Si(OH)_4$, O_2, values closely simulated conditions at the collection site of each sponge species, samples taken

during the acclimation period and samples taken at the intake of the flow-through system (Table 5.1). All parameters were successfully maintained in experimental tanks throughout the 35-day duration of the experiment (Fig. A2.2 and A2.3).

5.4.2. Mass loss

All sponges survived the 35-day experiment but a net % mass loss of 9.0 ± 0.33 (mean ± SEM) was observed for free-living individuals of *X. deweerdtae* and a loss of 6.1 ± 0.33 observed for sponge pairs in all treatments (Fig. 5.1). Results from the ANOVA for % mass loss showed no significant pCO_2, temperature or pCO_2 × temperature × lifestyle effects. However, there was a significant difference of the lifestyle main effect ($F_{1,15}$=18.4, p=0.0007) on the average % mass loss between free-living and associated sponges (Table A2.2).

5.4.3 Spicule length

Spicule lengths exhibited minor changes in the three sponge species (Figure 5.2). Results from the three-way ANOVA on average differences of spicule length showed no significant pCO_2, temperature or pCO_2 × temperature × species effects (Table A2.3). There was significance in the species main effect ($F_{2,24}$=4.5, p=0.0215). Tukey's HSD showed that the overall average spicule length of diods (-2.9 ± 1.1 µm) from *P. deweerdtaephila* in all treatments decreased. This decrease was significantly greater than the average decrease in strongyle spicule lengths from associated *X. deweerdtae* (-0.2 ± 0.5 µm) and the

average increase in strongly spicule lengths from free-living *X. deweerdtae* (0.8 ± 0.5 µm).

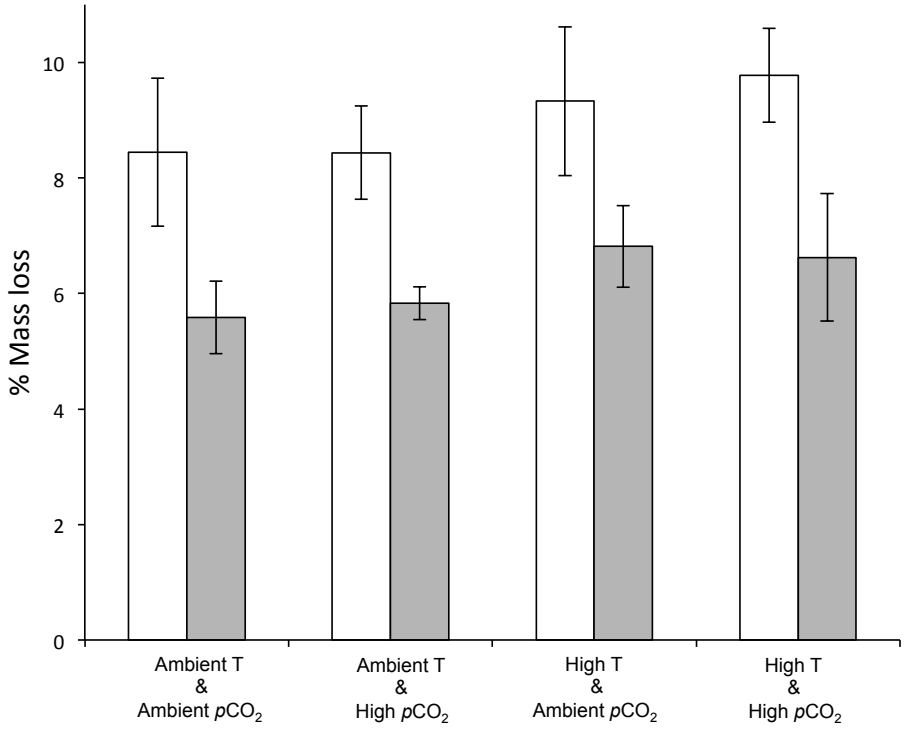

Figure 5.1 Differences in % mass loss between free-living *Xestospongia deweerdtae* and the *X. deweerdtae* + *Plakorits deweerdtaephila* pairs Mean and standard error of % mass loss of free-living individuals of *Xestospongia deweerdtae* (white bars) and the *X. deweerdtae* + *Plakorits deweerdtaephila* pairs (grey bars) in each treatment. A significant main effect of lifestyle on % mass loss was observed regardless of pCO_2 or temperature manipulations in each treatment.

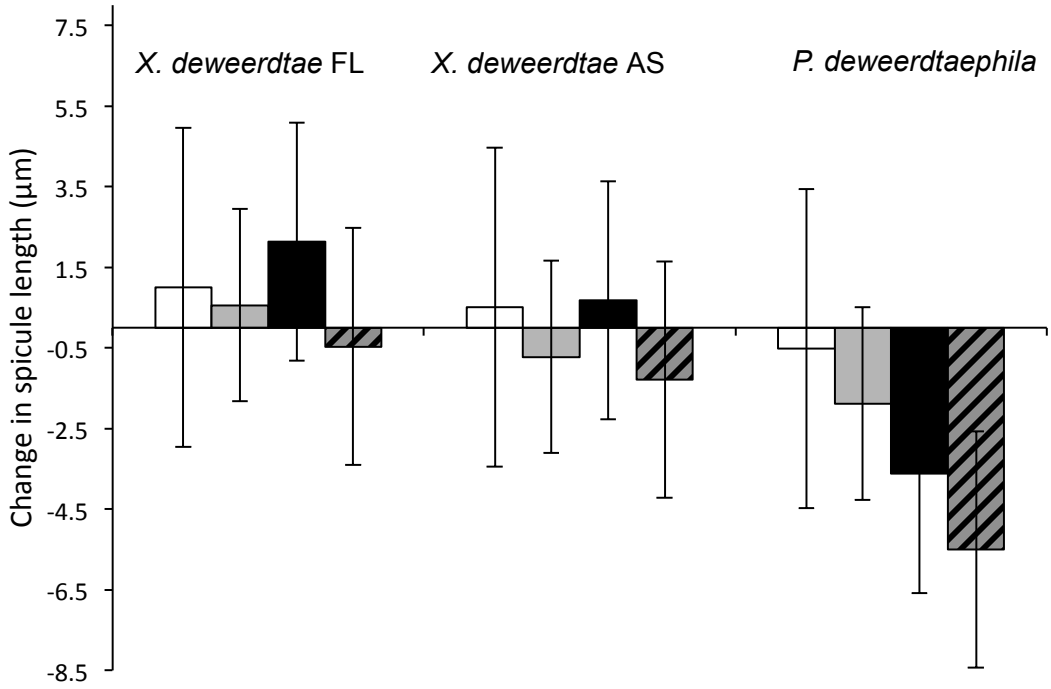

Figure 5.2 Spicule length differences of free-living *Xestospongia deweerdtae*, associated *X. deweerdtae,* and *Plakortis deweerdtaephila* exposed to different experimental treatments. Mean and standard error of spicule length differences of strongyles from *Xestospongia deweerdtae* free-living (FL), associated *X. deweerdtae* (AS) lifestyles, and diods from *Plakortis deweerdtaephila* after a 35-day exposure to exposed to Ambient T & Ambient pCO_2 (white bars), Ambient T & High pCO_2 (gray bars), High T & Ambient pCO_2 (black bars), and High T & High pCO_2 (black and gray striped bars). The ANOVA did not reveal a significant interactive effect of factors or the pCO_2, or temperature main effect. However the species main effect showed that that the overall net decrease of diod spicule lengths of *P. deweerdtaephila* was significant

when compared to strongyle lengths of free-living and associated *X. deweerdtae* ($F_{2,24}$=4.5, p=0.0215).

5.4.4. Necrotic tissue progress rate

All sponges responded well to the flow through conditions in experimental tanks except for *X. deweerdtae* FL. These individuals in ambient temperature and pCO_2 conditions had a necrotic tissue rate of 0.32 $cm^2\ day^{-1}$ by the end of the experiment (Fig. 5.3A). The two-way (treatment × time) ANOVA ran on individual species, showed that the treatment main effect had a significant impact on the progress of necrotic tissue in *P. deweerdtaephila* that caused a significant increase of necrotic tissue on the sponge pair as a whole ($F_{3,8}$=8.84, p=0.0064 and $F_{3,8}$=5.50, p=0.0240 respectively) (Table A2.4). This increase was a result of treatments with high temperature but ambient pCO_2 conditions (p<0.0001). Time also had a significant main effect on the progress of necrotic tissue in all species except for *X. deweerdtae* AS. The treatment × time interaction showed a significant effect only in *X. deweerdtae* FL and *P. deweerdtaephila* ($F_{9,24}$=0.04, p=0.0433 and $F_{9,24}$=2.48, p=0.0380 respectively). The post hoc analysis using chisquare tests showed that the increase in necrotic tissue rate of *X. deweerdtae* FL from the treatment × time interaction was a result of the 0.44 $cm^2\ day^{-1}$ increase of necrotic tissue rate observed in the High T & High pCO_2 treatment between day 15 and 29 in comparison to the 0.2 $cm^2\ day^{-1}$ increase in the ambient conditions (p=0.0228) (Fig. 5.3A). The chisquare tests for the significant treatment × time interaction of the necrotic tissue increase of *P. deweerdtaephila*

was a result of the 0.25 $cm^2\ day^{-1}$ increase of necrotic tissue rate observed in the High T & Ambient pCO_2 treatment compared to the complete absence of necrotic tissue observed in the Ambient T & High pCO_2 treatment throughout the 29 days (p=0.0429) (Fig. 5.3B). Necrotic tissue from the High T & Ambient pCO_2 treatment also increased to 0.23 $cm^2\ day^{-1}$ through the 27 days in *X. deweerdtae* AS but these results were not significant in comparison to ambient T and pCO_2 conditions (Fig. 5.3C) Despite seeing a significant treatment × time interaction in the ANOVA results (p=0.0452) for the sponge pairs, this was not supported by post hoc chisquare tests (Table A2.4, Fig. 5.3D).

The three-way (treatment × time × species) ANOVA revealed significant differences from main effects and interactions (Table A2.5). The effect of the three-way interaction highlighted the significant impact the High T & Ambient pCO_2 treatment had on *X. deweerdtae* AS and the sponge pair in comparison to *X. deweerdtae* FL ($F_{27,120}$=2.02, p=0.0053). For example between days 15 and 29, necrotic tissue progress rate in *X. deweerdtae* AS increased by 0.21 $cm^2\ day^{-1}$ in the Temperature & Ambient pCO_2 treatment and this increase was significant in relation to the 0.01 $cm^2\ day^{-1}$ necrotic tissue rate increase observed in the High T & High pCO_2 treatment (Fig 5.4A). Overall these differences were significantly different from *X. deweerdtae* FL (p=0.0319). The difference of 0.14 $cm^2\ day^{-1}$ necrotic tissue rate increase observed in the sponge pair exposed to the High T & Ambient pCO_2 treatment compared to sponge pairs in the ambient T & ambient pCO_2 treatment was significantly higher than the 0.02 $cm^2\ day^{-1}$ observed in *X. deweerdtae FL* (p=0.0118) (Fig. 5.4B).

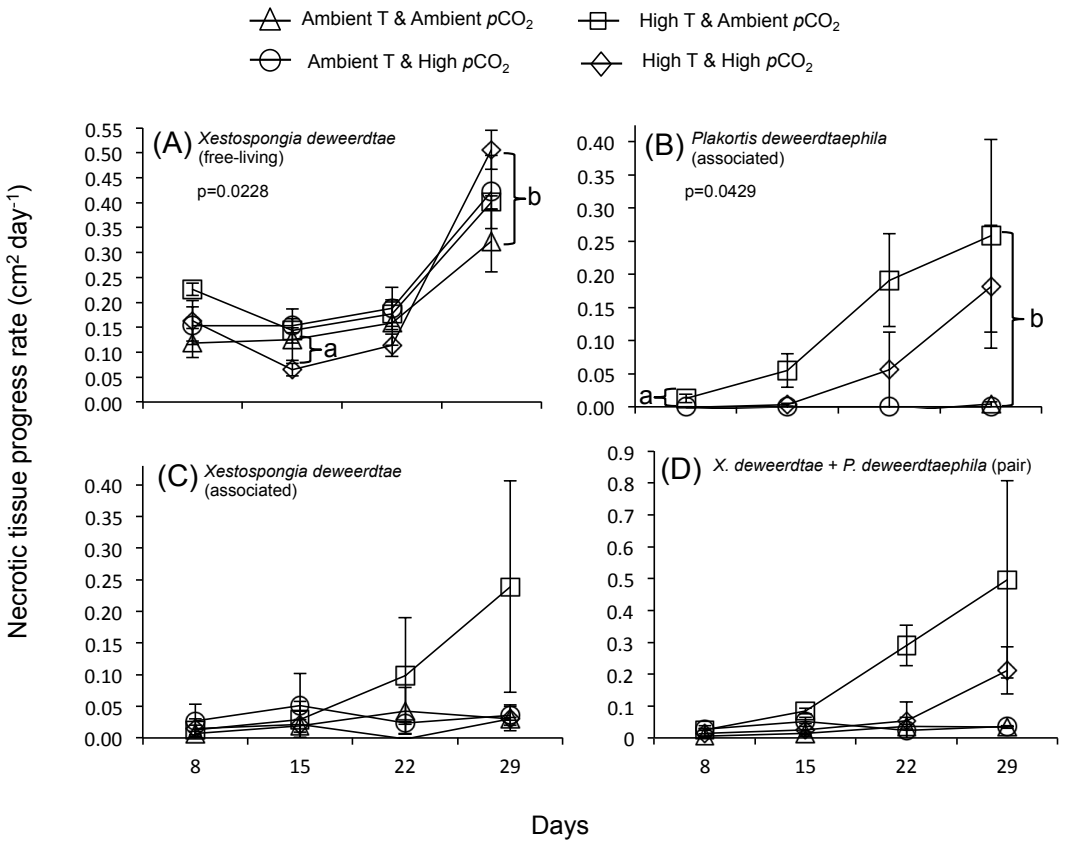

Figure 5.3. Necrotic tissue progress rate of free-living *Xestospongia deweerdtae*, associated *X. deweerdtae, Plakortis deweerdtaephila* and the sponge *X. deweerdtae* + P*. deweerdtaephila* (pair). Necrotic tissue progress rate (cm^2 day^{-1}) was monitored every seven days for sponges exposed to treatment conditions as indicated in the legend. Significant treatment × time ANOVA results were observed only in (A) *Xestospongia deweerdtae* FL (p=0.0228) and (B) *Plakortis deweerdtaephila* (p=0.0429). Mean differences indicated by brackets between treatments with the same letters in common were not significantly different as indicated by the post hoc chisquare test.

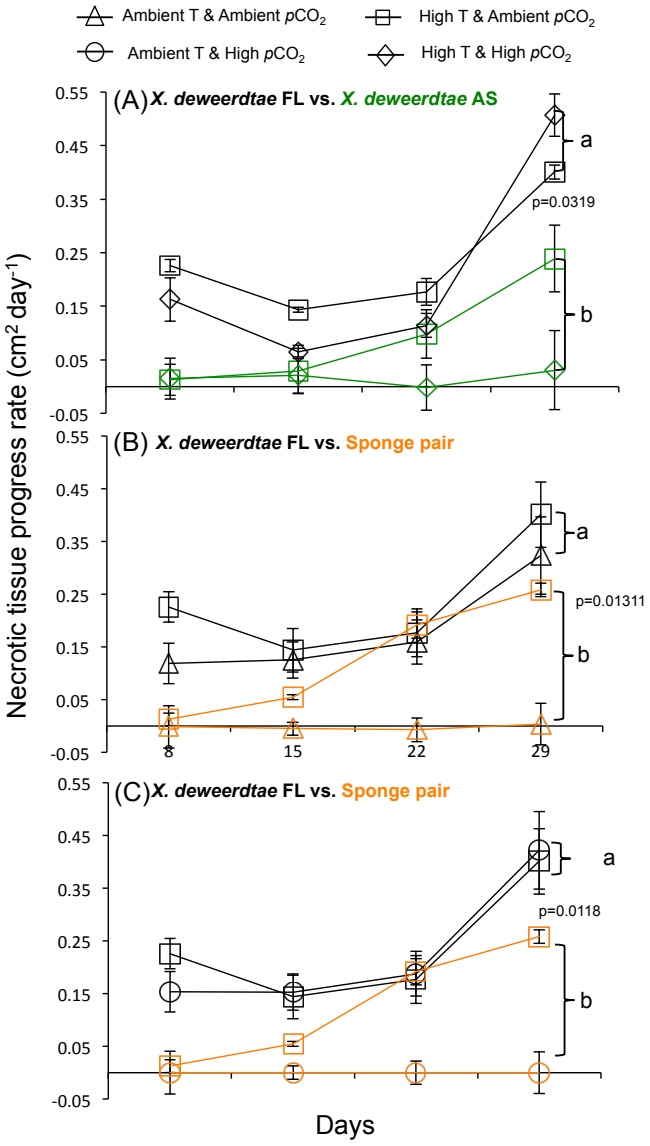

Figure 5.4. Significant post hoc chisquare results from the three-way ANOVA treatment × time × species interaction of free-living *Xestospongia deweerdtae*, associated *X. deweerdtae, Plakortis deweerdtaephila* and the *X. deweerdtae* + *P. deweerdtaephila* (pair). The increased necrotic tissue progress rate as a result of the Ambient pCO_2 & Temperature treatment was significant in *X. deweerdtae* and the sponge pair in relation to *X. deweerdtae* FL. Similar significant differences between sponge pairs and *X. deweerdtae* FL were

observed between necrotic tissue increases in the Ambient T & High pCO_2 treatment and the Ambient T & High pCO_2 treatment (p=0.0118) (Fig. 5.4C). These results suggest that the increase observed for necrotic tissue progress rates are caused by high temperatures and not pCO_2.

5.4.5 Total necrotic tissue progress rate

The three-way factorial ANOVA revealed that *X. deweerdtae* FL had the highest total necrotic tissue progress rate of all sponges regardless of the temperature or pCO_2 values with an average of 0.21 ± 0.01 cm^2 day^{-1} (Table A2.6, Fig. 5.5A, Fig 5.6A, D, G, J). This difference was a significant outcome of the species main effect ($F_{3,24}$=35.78, p<0.0001) that was further confirmed by post-hoc pairwise comparisons with all other species (p<0.0001) (Table A2.6). Temperature had a significant main effect on the average rate of all sponges in treatments with high temperatures (0.13 ± 0.01 cm^2 day^{-1}) compared to the average rate of all sponges in treatments with low temperatures (0.06 ± 0.03 cm^2 day^{-1}) ($F_{1,8}$=18.26, p=0.0027) (Table A2.6). The pCO_2 × temperature interaction also showed significance ($F_{1,8}$=18.26, p=0.0027) meaning that the average total necrotic tissue increase as a consequence of treatments with high temperatures in all species (0.13± 0.01 cm^2 day^{-1}) is dependent on pCO_2 enrichment (Fig. 5.5B). The significant temperature × species interaction ($F_{3,24}$=6.97, p=0.0017) revealed that the increase in necrotic tissue rate observed in treatments with high vs. ambient temperatures in associated individuals of *X. deweerdtae* (Fig. 5.6B, E, H, K), *P. deweerdtaephila* (Fig. 5.6C, F, I, L) and the sponge pair was

significantly higher than the increase in necrotic tissue rate observed in free-living individuals of *X. deweerdtae* (p<0.0001) (Table A2.6, Fig. 5.5C). Increase in necrotic tissue rates from treatments at high temperatures were higher in *P. deweerdtaephila* than its epibiont *X. deweerdtae* AS (p=0.0231) (Table A2.6, Fig. 5.5C).

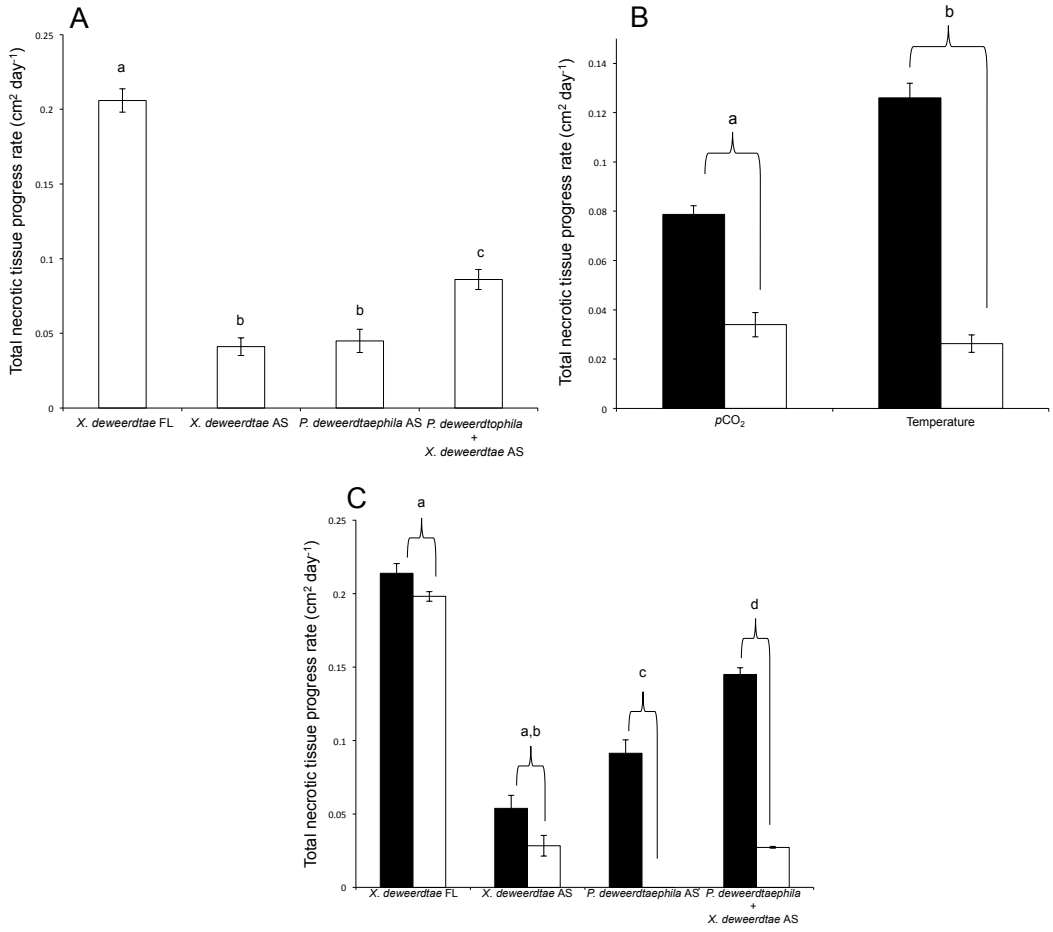

Figure 5.5 Results from the post-hoc analysis of significant ANOVA results of the species main effect, pCO$_2$ × temperature interaction, and temperature × species interaction of free-living *Xestospongia deweerdtae*, associated *X. deweerdtae, Plakortis deweerdtaephila* and the *X. deweerdtae + P. deweerdtaephila* (pair). Post-hoc analysis of the (A) species main effect, (B)

pCO_2 × temperature interaction and (C) temperature × species interaction. Black bars indicate high values for either pCO_2 or temperature and white bars indicate ambient values for either temperature or pCO_2. Within each subplot, means with the same letters in common note significantly different outcomes as indicated by Tukey's HSD analysis or chisquare.

The species × treatment two-way ANOVA, combining temperature and pCO_2 levels into the four treatment, was significant ($F_{9,24}$=3.05, p<0.0139) (Table A2.7). Pairwise comparisons from chisquare tests revealed that the 0.12 $cm^2\ day^{-1}$ increase of necrotic tissue progress rate in *P. deweerdtaephila* and the 0.19 $cm^2\ day^{-1}$ increase for the sponge pair exposed to the ambient pCO_2 & high temperature treatment in relation to the Ambient Temperature & High pCO_2 treatment was significantly higher than the increase observed in *X. deweerdtae* FL between these two treatments (p=0.0211 and p=0.0110 respectively) (Fig. 5.7). In addition, the 0.20 $cm^2\ day^{-1}$ increase between the Ambient Temperature & Ambient pCO_2 treatment and the Ambient pCO_2 & High Temperature treatment of the sponge pair was also significant in comparison to the increase observed in *X. deweerdtae* FL for these two treatments (p=0.0270) (Fig. 5.7).

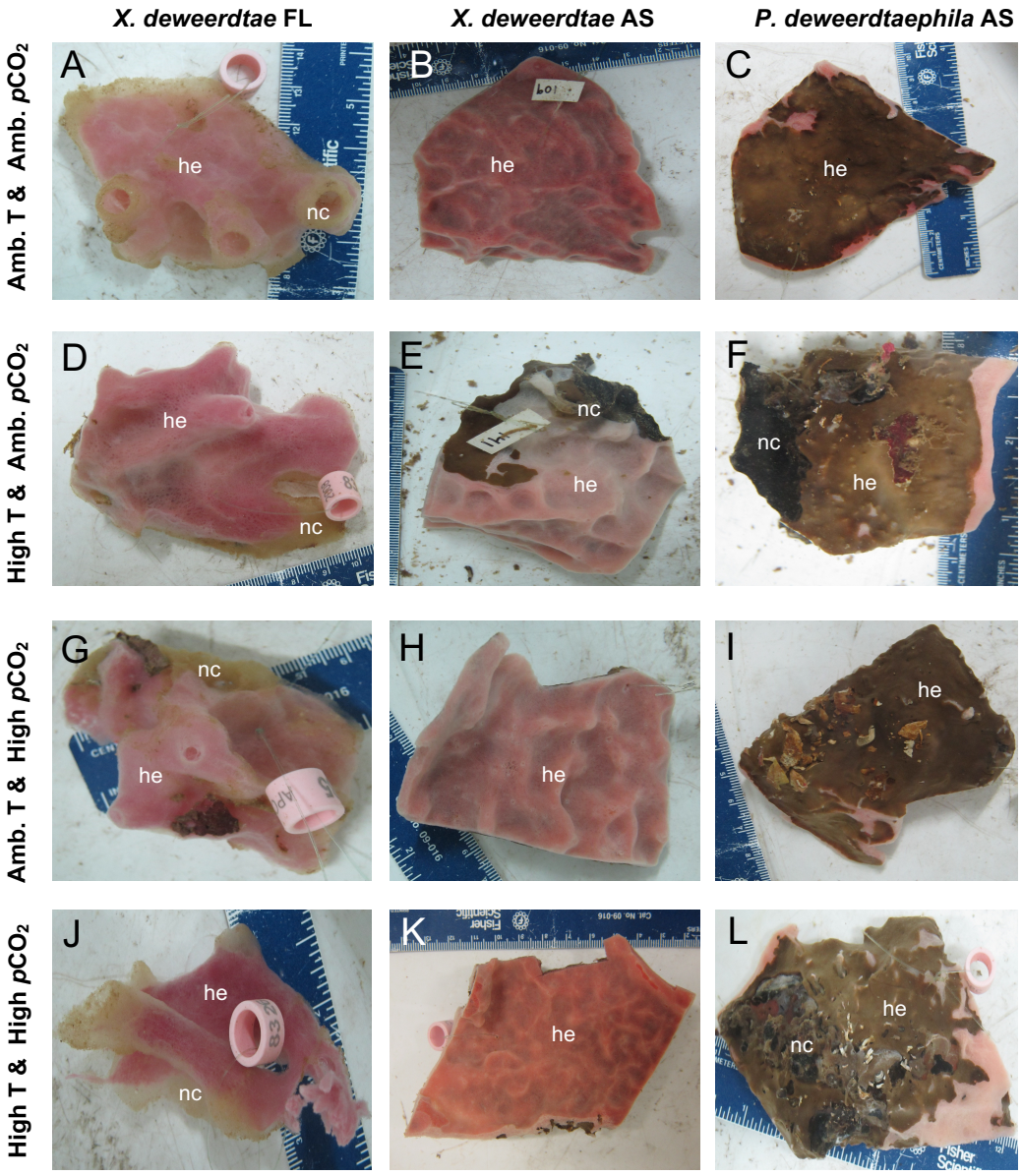

Figure 5.6 Images of *Xestospongia deweerdtae* FL, *X. deweerdtae* AS and *Plakortis deweerdtaephila* in each treatment after 29 days of the experiment. Pictures of *X. deweerdtae* AS and *P. deweerdtaephila* AS from the second and third column for each treatment are from the same sponge pair. In each image healthy he=healthy tissue and nc=necrotic tissue.

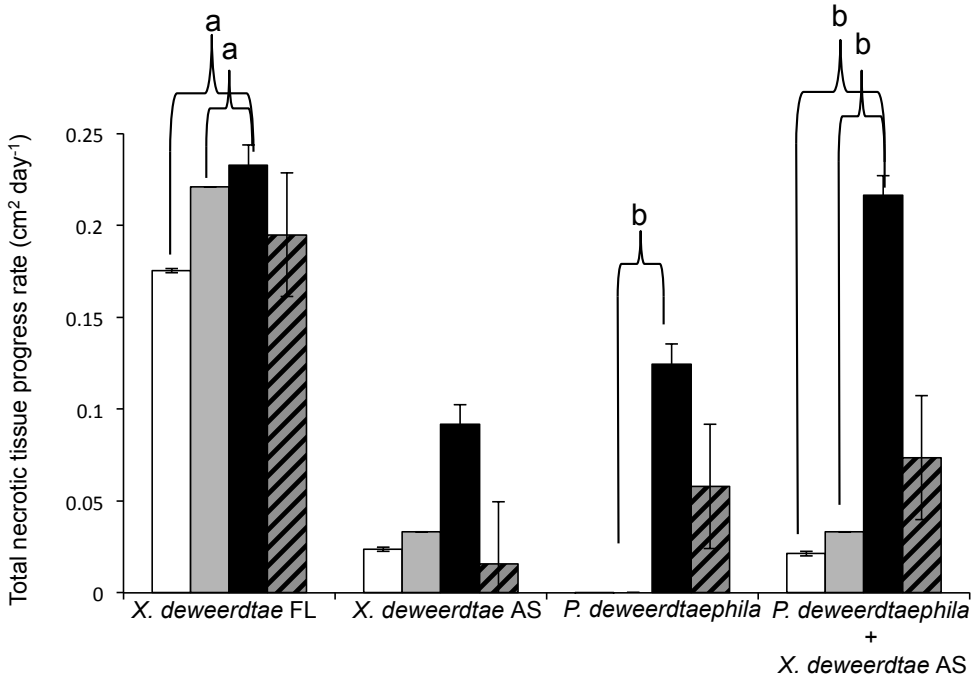

Figure 5.7 Mean and standard error of total necrotic tissue progress rate of free-living *Xestospongia deweerdtae*, associated *X. deweerdtae, Plakortis deweerdtaephila* and the *X. deweerdtae* + *P. deweerdtaephila* (pair). sponges exposed to different treatments. Treatment conditions are indicated as follows: Ambient T & Ambient pCO_2 (white bars), Ambient T & High pCO_2 (gray bars), High T & Ambient pCO_2 (black bars), and High T & High pCO_2 (black and gray striped bars). Mean differences indicated by brackets between treatments with the same letters in common are not significantly different as indicated by the posthoc chisquare test.

5.4.6 *Xestospongia deweerdtae* AS / *Plakortis deweerdtaephila* pair healthy tissue ratio

Treatments with ambient temperatures showed a net ratio decrease of 0.03 after 29 days and treatments with high temperatures showed an increase of

0.05 for the High T & ambient pCO_2 treatment and an increase of 0.03 for the High T & High pCO_2 treatment (Fig. 5.8). However, the treatment × time two-way ANOVA on *X. deweerdtae* / *P. deweerdtaephila* healthy tissue ratios showed that neither time nor the interaction of time × treatment as a significant effect on these ratio differences (Table 5.9). Significant ratio differences from the treatment main effect ($F_{3,52}$=13.26, p<0.0001) were considered as a random consequence of the sponge selection process for the different treatments. Ratio differences were already different for the different treatments before the beginning of the experiment.

5.5. Discussion

All associated and free-living sponges survived for the duration of the experiment with ambient and high temperature/pCO_2 treatment manipulations, showing that both *X. deweerdtae* lifestyles will probably continue existing under climate change scenarios for the end of the century. These results show no evidence of phenotypic plasticity being used as an adaptation strategy to withstand either ocean acidification or thermal stress. Treatment conditions also had no effect on spicule length differences suggesting that neither thermal stress nor warming will affect silica biomineralizing in either *X. deweerdtae* or *P. deweerdtaephila*.

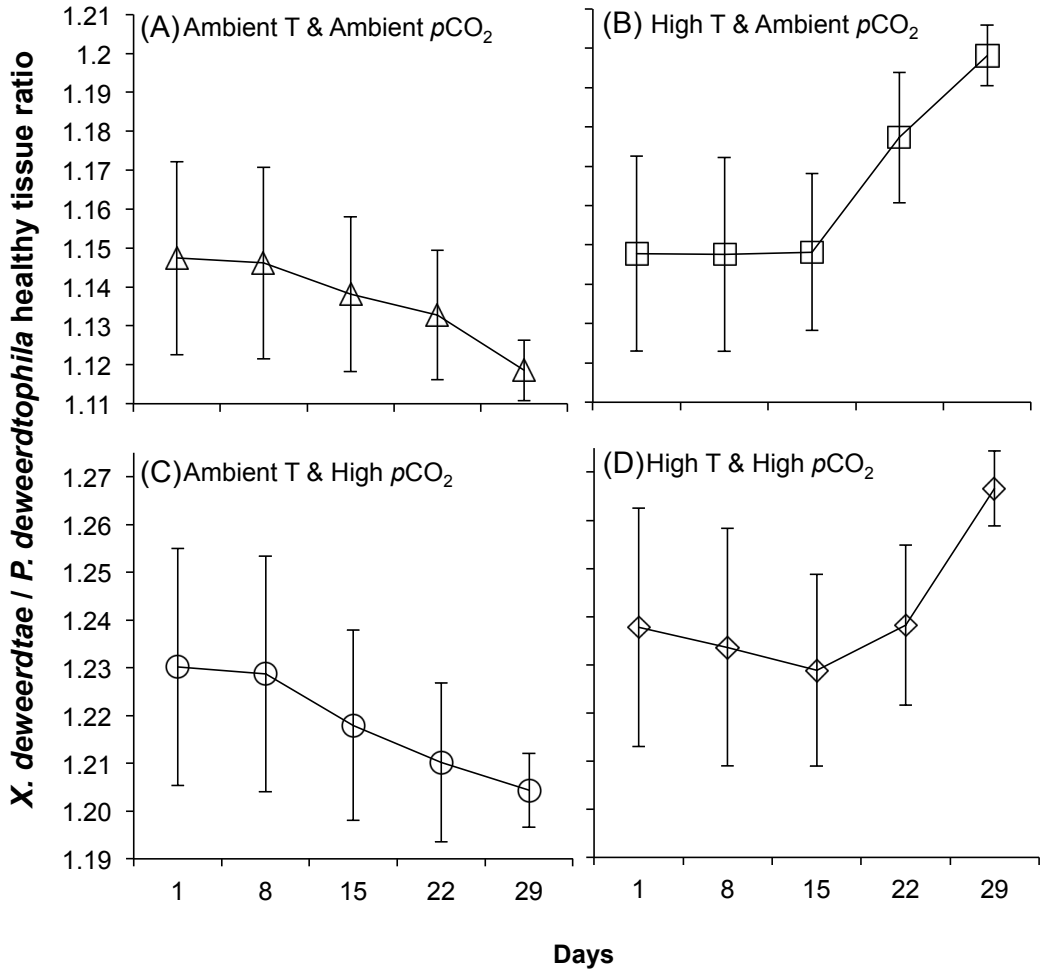

Figure 5.8*. Xestospongia deweerdtae* / *Plakortis deweerdtaephila* healthy sponge tissue ratio. Overall healthy tissue ratios for both species of the sponge pair remained stable throughout the duration of the experiment as indicated by the ANOVA results.

Free-living individuals of *X. deweerdtae* were more sensitive than sponge pairs to the flow-through conditions in each tank, as free-living individuals lost 3% more mass than sponge pairs, irrespective of either temperature or pCO_2 values. Despite such subtle differences in mass loss, these were a consequence of sponge tissues becoming more necrotic throughout the experiment. The effect of

necrotic tissue did reveal interesting potential immunological responses by both lifestyles under different temperature and pCO_2 conditions.

Necrotic tissue development became apparent in free-living *X. deweerdtae* from the onset of the experiment in all treatments and was a probable artifact of sponges not acclimating fully to the flow-through conditions in each tank. Necrotic tissue in free-living *X. deweerdtae* caused healthy sponge tissues to become translucent presumably as a result of cell death. In some cases the remaining tissue sloughed off and likely caused the 9.0% ± 0.49 mass loss (Fig. 5.6A, D, G, J). In free-living *X. deweerdtae*, necrotic tissue in sponge pairs developed only after eight days as a consequence of the High T & Ambient pCO_2 treatment. Necrosis was first observed in *P. deweerdtaephila* and appeared as black patches (Fig. 5.6F) that in some cases spread to the associated *X. deweerdtae* epibiont after 15 days (Fig. 5.6E). Necrotic tissue in *P. deweerdtaephila* also sloughed off in some individuals (Fig. 5.6L) and was probably responsible for the 6.2% ± 0.35 mass loss observed in sponge pairs. Similar to free-living *X. deweerdtae*, the highest necrotic tissue rate was observed in the High T & Ambient pCO_2 and progress rates became significantly higher after 8 days in *P. deweerdtaephila* and after 15 days in the *X. deweerdtae* epibiont. Morphological differences in necrosis and different acquisition times of necrosis in sponge pairs vs. free-living *X. deweerdtae* suggests that the cause of necrosis in both lifestyles is probably a consequence of different pathogenic infections or immune responses.

It is difficult to conclude which lifestyle of *X. deweerdtae* was more resilient in withstanding necrosis as a result of acidification and thermal stress, as free-living individuals were sensitive to experimental tank conditions regardless of temperature or pCO_2 values in this study. Observing early necrotic tissue development in *P. deweerdtaephila* and its eventual transfer to the *X. deweerdtae* epibiont suggests that associating to a sponge that is sensitive to either temperature or pCO_2 might act as a vector of infection and actually be a disadvantageous trait. Nevertheless, this response allowed us to observe how different morphotypes can have different immunological responses according to their lifestyle, which could be an overall advantage over sponge species that exhibit the immune response of one lifestyle.

In all sponge species and lifestyles total necrotic tissue progress rates depended on whether pCO_2 was high or low. For example, necrotic tissues were the highest for all three sponges exposed to High T & Ambient pCO_2 treatments but necrosis was significantly less in High T & high pCO_2. These results show that ocean acidification might actually be beneficial for sponges to withstand necrotic tissue development as a result of infection and adds support to the hypothesis that sponges will adjust efficiently to ocean acidification (Bell *et al.* 2013).

Examples of antagonistic effects between temperature and pCO_2 have been reported for life history stages of calcifying organisms (Byrne & Przeslawski 2013). Warmer temperatures have been shown to decrease the effect of acidification on larval growth of the hooded oyster (*Saccostrea glomerata*)

(Parker *et al.* 2010). In the sea urchin *Heliocidaris erythrogramma* warmer temperatures reduce the effect of acidification on calcification (Byrne *et al.* 2009). A comparative study between phototrophic and heterotrophic sponges showed that acidification had ameliorating effects only in phototrophic sponges exposed to increased temperature treatments (Bennett *et al.* 2016). This study highlights the first report of acidification reducing necrotic tissue rates in heterotrophic symbiotic sponges exposed to warmer temperatures.

Chapter 6: Impact of high pCO_2 and warmer temperatures on the process of silica biomineralization in the sponge *Mycale grandis*

6.1. Abstract

Siliceous sponges have survived pre-historic mass extinction events caused by ocean acidification and recent studies suggest that siliceous sponges will continue to resist predicted increases in ocean acidity. In this study, I monitored silica biomineralization in the Hawaiian sponge *Mycale grandis* under predicted pCO_2 and sea surface temperature scenarios for 2100. My goal was to determine if spicule biomineralization was enhanced or repressed by ocean acidification and thermal stress by monitoring silica uptake rates during short-term (48 h) experiments and comparing biomineralized tissue ratios before and after a long-term (26 days) experiment. In the short-term experiment, t silica uptake rates were not impacted by high pCO_2 (1050 µatm), warmer temperatures (27°C) or combined high pCO_2 with warmer temperature (1119 µatm; 27°C) treatments. The long-term exposure experiments revealed no effect on survival or growth rates of *M. grandis* to high pCO_2 (1198 µatm), warmer temperatures (25.6°C) or combined high pCO_2 with warmer temperature (1225 µatm, 25.7°C) treatments, indicating that *M. grandis* will continue to prosper under predicted increases in pCO_2 and sea surface temperature. However, ash dry weight to dry weight ratios, subtylostyle lengths, and silicified weight to dry weight ratios decreased under conditions of high pCO_2 and combined pCO_2 warmer temperature treatments. These results show that rising ocean acidity and temperature are likely to have only marginal negative effects on spicule biomineralization and will not affect sponge survival rates of *M. grandis*.

6.2. Introduction

Skeleton mineralogy plays an important role in the sensitivity of marine invertebrates to ocean acidification and warming. Calcifying organisms are particularly vulnerable to rising ocean acidity and temperatures (Hoegh-Guldberg *et al*. 2007; Fabry *et al.* 2008; Hofmann *et al.* 2010), but non-calcifying organisms such as siliceous sponges are thought to be less affected (Bell *et al.* 2013). Studies testing the physiological response of calcifying and non-calcifying organisms to ocean acidification have led to predictions about which invertebrates will dominate in tropical, benthic ecosystems in a more acidified ocean. For example, small-scale benthic community shifts have been reported in pH gradients caused by natural volcanic CO_2 seeps of Papua New Guinea (Morrow *et al.* 2014), where a transition from coral to sponge dominance was observed with closer proximity to the seep (higher pCO_2). Large-scale shifts of coral to sponge-dominated reefs are already being observed in coral reefs of the Caribbean (Diaz & Rützler 2001; Pawlik 2011; Loh *et al.* 2015; McMurray *et al.* 2015). Transitions from coral to sponge-dominated reefs may cause carbon release rates to increase (De Goeij *et al.* 2013) which could play an important role in structuring higher trophic levels of the ecosystem (Silveira *et al.* 2015). Because of results from these studies and others, predicting the impact of ocean acidification and warming on sponges is gaining considerable attention (Duckworth *et al.* 2012; Webster *et al.* 2013; Goodwin *et al.* 2014; Stubler *et al*. 2014).

Sponge skeletons can be composed of calcium carbonate, silica, or collagen fibers (Hooper & Van Soest 2002). Like corals, calcifying sponges are vulnerable to dissolution when exposed to lower pH levels (Smith *et al.* 2013), but siliceous and collagenous sponges are believed to resist dissolution in more acidified ocean conditions (Bell *et al.* 2013). For example, growth and survival rates in six Caribbean sponges with skeletons composed of silica and collagen fiber were not affected by a 24-day exposure period to increased ocean acidity and temperatures relative to ambient conditions (Duckworth *et al.* 2012). In fact, studies have shown that some sponges may even benefit from predicted ocean acidification conditions; bioerosion rates from clionid boring sponges increased in low pH treatments relative to controls (Wisshak *et al.* 2012; Wisshak *et al.* 2013; Stubler *et al.* 2014; Enochs *et al.* 2015). Despite the number of studies showing an increase of bioerosion by marine sponges and no detrimental impacts on sponges under high CO_2 scenarios, little is known about the response of sponge morphology or skeleton synthesis to warmer and more acidic conditions.

Like ocean acidification, thermal tolerance may vary across sponge species with different skeletal compositions. In the Caribbean and in the Mediterranean Sea, warmer seawater temperatures have caused local extinction events in keratose (aspiculated) sponges (Vicente 1989; Cebrian *et al.* 2011). In mesocosm studies, thermal stress caused necrosis and eliminated key bacterial symbionts from the keratose sponge *Rhopaloeides odorabile* at 33°C (Webster *et al.* 2008). While several species of keratose sponges are sensitive to warmer temperatures, spiculated sponges are able to tolerate these conditions and

actually accelerate their attachment rates to substrates (Duckworth *et al*. 2012). However, studies that measure thermal tolerance of sponges have not considered whether resistance to thermal stress by sponges correlates with a particular skeleton type. Looking at the process of siliceous skeleton synthesis under high pCO_2 and warmer temperatures will help us understand whether sponges with a siliceous skeleton could be at an advantage under different pCO_2 and temperature regimes.

Many studies support the hypothesis that siliceous sponges will adapt to ocean acidification (Duckworth & Peterson 2012; Duckworth *et al.* 2012; Wisshak *et al.* 2012; Stubler *et al.* 2014); however, it is not clear whether having a siliceous skeleton is actually an advantageous trait for sponges under these conditions. Silica uptake rates for sponges with a siliceous skeleton are believed to follow a Michaelis-Menten kinetic model and are also heavily dependent on silica concentrations—silica uptake rates increase exponentially when exposed to higher silica concentrations (Maldonado *et al.* 2012). Other environmental factors such as high nutrients in upwelling habitats influence the shape and size of spicules (Uriz *et al.* 2003). Although the process by which silica is taken up remains speculative, there is a preliminary model that suggests that silicate assimilated by the sponge *Suberites domuncula* for spicule synthesis is co-transported through sclerocyte cells with a Na^+-HCO_3^- symporter protein (Schröder *et al.* 2004). Polycondensation of silica in *S. domuncula* primmorph cells occurs within vesicles by silicatein proteins in the intracellular space of sclerocytes where the axial filament of a spicule is formed (Wang *et al.* 2012).

Fibrils then associate with one end of the spicule and extrude it out of the cell where silicate continues to deposit in layers around the axial filament. *M. grandis* may have a similar mechanism of silica uptake to *S. domuncula* because these two sponges belong to the same class and both have densely spiculated skeletons. If all siliceous Demosponges use a Na^+-HCO_3^- symporter mechanism to take up $Si(OH)_4$ through the cell membrane, we speculate that siliceous sponges may benefit from high pCO_2 during spicule synthesis. In addition, the chemical equilibrium shift of dissolved silica (DSi) caused by high pCO_2 will favor the speciation of $Si(OH)_4$ and HCO_3^- which could make $Si(OH)_4$ and HCO_3^- substrates more available for the Na^+-HCO_3^- symporter protein to transport and facilitate uptake of silica through the cell membrane (Zeebe & Wolf-Gladrow 2001).

In this study we used end of the century pCO_2 (1100 ppm) and temperature (+3°C) values from the Representative Concentration Pathway (RCP) 8.5 climate scenario (Riahi *et al.* 2011) to test the impact of rising ocean acidity and temperature on spicule biomineralization in the Hawaiian invasive sponge *Mycale grandis* (Gray 1867). *M. grandis* was introduced in Kāne‘ohe Bay in the mid -1990s and was found aggressively overgrowing the hermatypic coral species *Montipora capitata* and *Porites compressa* by 2005 (Coles & Bolick 2007). Studies have shown that *M. grandis* percent cover doubled in some reefs of Kāne‘ohe Bay between 2005-2006 (Coles *et al.* 2006). *M. grandis* is a fast growing sponge with a densely spiculated siliceous skeleton, making it a fitting

model organism to measure silica uptake and spicule biomineralization in short time periods.

We measured DSi uptake rates using closed system 48-hour incubation experiments, exposing individuals of *M. grandis* to increased temperature (+3°C), increased pCO_2 (1100 µatm), combined increased pCO_2 and temperature (+3°C; 1100 µatm), and ambient temperature and pCO_2 from Kāneʻohe Bay (24°C, 580 µatm). Sponges were also exposed to similar conditions during a 26-day flow-through system experiment to test the impact of high pCO_2 and temperature on spicule synthesis.

Based on the silica uptake models proposed for other siliceous sponges, like *S. domuncula*, we hypothesize that: 1) treatments with pCO_2 enrichment will accelerate silica uptake rates of *M. grandis* resulting in enhanced spicule production and denser skeletons (more silicification) and 2) temperature increments of 3°C will increase silica uptake rates through increased metabolism (Nwewll & Northcroft 1967) although there are currently no published studies on the impacts of temperature on sponge spicule production and morphology. This is the first study that addresses the impact of high pCO_2 and thermal stress on the process of spicule biomineralization in marine sponges.

6.3. Methods

6.3.1. Silica uptake closed system experiment

6.3.1.1. Sponge collection

One sponge piece from each of 72 individuals of *M. grandis* (wet weight: 4-56 g) was collected with a sterile scalpel around Moku Loʻe (Coconut Island) in Kāneʻohe Bay at a depth of 3-9 m. Confirmation of species identity was determined by comparing partial sequences of the 18S and 28S rRNA genes to those in GenBank. For a full description of the phylogenetic analysis see (Fig. A3.1).

M. grandis grows as thickly encrusting cushions in between coral colonies making it difficult to collect without causing a large area of injury (injury area size: 1-35 cm^2). Brittle stars found living on the surface of the sponge tissue were removed to avoid interference with Ash dry weight/ Dry Weight (ADW/DW) ratio calculations. Brittle stars that were embedded deep inside the sponge tissue were left and removed after the experiment to avoid further injury to the sponge. To stabilize the sponges in incubation chambers, we gently tied fishing weights (85 g) with small (6 cm) tie wraps around each sponge. Sponge individuals were acclimated to their intended pH and temperature treatment conditions in flow-through tanks and were allowed to heal for 36 h at background silica concentrations (6-7 µM).

6.3.1.2. Silica uptake rates

To test the impact of high pCO_2 and temperature on silica uptake in sponges, we used a closed-system experimental set-up at the Hawaii Institute of Marine Biology (HIMB) mesocosm facility. This facility was well suited for the experimental conditions (Putnam 2012; Silbiger & Donahue 2015). All experiments were performed between March and May 2014.

Incubation chambers (plastic buckets) were prepared with 4 L of filtered seawater (3 µm pore size Pentair bag filter) and a water pump to ensure a well-mixed system. Chambers were sealed with Saran® wrap with clips to prevent evaporation and off-gassing. In each incubation chamber, pCO_2 was maintained by bubbling in CO_2 or CO_2-free air with airlines equipped with air-stones. A gas blending system was used to manipulate pCO_2 by mixing pure CO_2 -free atmospheric air with pure CO_2 using mass flow controllers (C100L Sierra Instruments). pCO_2 conditions were controlled using a calibrated CO_2 analyzer (A151, Qubit System) that measured the output pCO_2 going into each chamber. pCO_2 conditions were monitored and adjusted every 8 h. Temperature was controlled with dual-stage temperature controllers (Aqualogic TR115DN) and aquarium heaters. An LED system (AI Sol, 72W 100 to 240 VAC/50-60Hz, C2 Development Inc., Ames, Iowa) was used to control lighting. Lights were set over each tank and were switched on at sunrise (06:15), and ramped up for 4 h until 600 µmol photons m^{-2} s^{-1} irradiance was reached which resembled similar conditions to the reefs in Kāneʻohe Bay. Irradiance was held at maximum for 4 h before ramping down to zero by sunset (18:15) (Gibbin *et al.* 2015). All buckets,

air stones, air lines, and water pumps were pre-cleaned with 5% hydrochloric acid (HCl) and rinsed with DI water before every experiment.

We had four experimental treatments: control (C; 24°C, 593 µatm), high temperature (T; +3°C), high pCO_2 (pCO_2; 1050 µatm), and high temperature and pCO_2 (pCO_2T; +3°C, 1119 µatm) (Table 6.1, Table A2.1 and Fig. A2.2). The conditions closely simulated ambient Kāneʻohe Bay conditions (Silbiger & Donahue 2015) and future temperature and pCO_2 values predicted by 2100 (+3°C, 1100 ppm) (Riahi *et al.* 2011). A +3°C temperature increase also closely resembles sea surface temperature values for the summer in Kāneʻohe Bay. Treatments were randomly assigned to incubation chambers. Incubation chambers were pre-conditioned for 12 h without sponges until the desired pCO_2 and temperature conditions were achieved: experiments began only when parameters were consistent across all incubation chambers. Sponges were rinsed with filtered seawater to remove any diatom contamination and transferred from their flow-through acclimation tank to the incubation chamber. Sponges were acclimated to incubation chamber conditions for 12 h prior to each experimental run. Background silica concentrations (6-7 µM) were calculated for each bucket before the start of each experiment. After incubation chambers were at the desired pCO_2 and temperature conditions, they were enriched with 45-50 mg of sodium hexafluorosilicate (SHF) in order to bring the DSi concentration to 60-70 µM in each bucket.

Table 6.1 Seawater parameter setup of treatments for the silica uptake rate experiment. Experimental setup of treatments with mean and standard error of parameters from all buckets for each treatment during 48 h incubations.

Treatment	Hr	Temp (°C)	Salinity (ppt)	A_T (µmol kg $^{-1}$)	pH (*t*)	pCO_2 (µatm)	HCO_3^- (µmol kg $^{-1}$)	CO_3^- (µmol kg $^{-1}$)	Ω_{arag}
Control	**0**	24.1± 0.04	34.82 ± 0.1	2174 ± 3.0	7.82 ± 0.01	672 ± 7.3	1849 ± 3.1	131.3 ± 1.2	2.08 ± 0.02
Ambient	**8**	24.2 ± 0.06	34.92 ± 0.08	-	7.83 ± 0.02	-	-	-	-
N_{bucket}= 17	**16**	24.1 ± 0.04	35.06 ± 0.09	-	7.85 ± 0.02	-	-	-	-
	24	24.1 ± 0.04	35.12 ± 0.09	-	7.88 ± 0.02	-	-	-	-
	32	24.3 ± 0.06	35.12 ± 0.1	-	7.84 ± 0.02	-	-	-	-
	40	24.0 ± 0.04	35.22 ± 0.1	-	7.88 ± 0.02	-	-	-	-
	48	24.0 ± 0.04	35.23 ± 0.1	1942 ± 18.2	7.89 ± 0.09	515 ± 34.0	1595 ± 23.8	136.1 ± 5.5	2.15 ± 0.09
T	**0**	27.3 ± 0.10	35.04 ± 0.1	2173.5 ± 3.3	7.85 ± 0.03	630 ± 10.7	1794 ± 7.9	153.6 ± 3.1	2.47 ± 0.03
2100 T	**8**	27.2 ± 0.08	35.1 ± 0.08	-	7.81 ± 0.04	-	-	-	-
prediction	**16**	27.1 ± 0.09	35.24 ± 0.08	-	7.84 ± 0.04	-	-	-	-
N_{bucket}=14	**24**	27.1 ± 0.08	35.31 ± 0.09	-	7.86 ± 0.05	-	-	-	-
	32	27.1 ± 0.09	35.34 ± 0.09	-	7.82 ± 0.04	-	-	-	-
	40	27.2 ± 0.08	35.44 ± 0.1	-	7.85 ± 0.04	-	-	-	-
	48	27.1 ± 0.07	35.47 ± 0.1	1953.2 ± 17.7	7.87 ± 0.05	570 ± 50.9	1594 ± 25.2	145.9± 6.2	2.33 ± 0.15
***p*CO$_2$**	**0**	23.8 ± 0.07	34.97 ± 0.1	2175± 3.7	7.61 ± 0.01	1121 ± 18.4	1962 ± 3.3	85.2 ± 1.3	1.34 ± 0.02
2100 *p*CO_2	**8**	24.0 ± 0.05	35.02 ± 0.1	-	7.62 ± 0.01	-	-	-	-
N_{bucket}=13	**16**	23.9 ± 0.06	35.21 ± 0.09	-	7.61 ± 0.02	-	-	-	-
	24	23.9 ± 0.05	35.26 ± 0.09	-	7.62 ± 0.02	-	-	-	-
	32	23.9 ± 0.05	35.33 ± 0.1	-	7.62 ± 0.02	-	-	-	-
	40	23.9 ± 0.06	35.42 ± 0.1	-	7.61 ± 0.02	-	-	-	-
	48	24.0 ± 0.07	35.44 ± 0.1	1964 ± 15.8	7.63 ± 0.02	978± 50.8	1745 ± 1676	82.1 ± 4.0	1.29 ± 0.06
***p*CO$_2$ T**	**0**	27.0 ± 0.08	35.12 ± 0.07	2175.8 ± 2.8	7.60 ± 0.01	1190 ± 18.1	1945 ± 3.9	93.3 ± 1.2	1.49 ± 0.02
2100 *p*CO_2 and T	**8**	27.1 ± 0.10	35.18 ± 0.07	-	7.62 ± 0.01	-	-	-	-
prediction	**16**	27.0 ± 0.07	35.36 ± 0.07	-	7.62 ± 0.02	-	-	-	-
N_{bucket}=14	**24**	27.1 ± 0.05	35.45 ± 0.08	-	7.61 ± 0.02	-	-	-	-
	32	27.2 ± 0.07	35.42 ± 0.07	-	7.62 ± 0.01	-	-	-	-
	40	27.0 ± 0.09	35.46 ± 0.07	-	7.61 ± 0.01	-	-	-	-
	48	26.8 ± 0.08	35.47 ± 0.07	1978.8 ± 12.8	7.61 ± 0.01	1048 ± 35.2	1762 ± 11.2	85.9 ± 2.8	1.37 ± 0.04
6 µM DSi	**0**	24.0 ± 0.07	34.14 ± 0.08	2158.5	7.86 ± 0.02	618 ± 19.1	1819 ± 7.6	137.0 ± 3.0	2.18 ± 0.05
N_{bucket}=8	**8**	24.0 ± 0.08	34.29 ± 0.06	-	7.86 ± 0.01	-	-	-	-
	16	23.8 ± 0.09	34.69 ± 0.06	-	7.90 ± 0.02	-	-	-	-
	24	24.0 ± 0.05	34.68 ± 0.06	-	7.87 ± 0.01	-	-	-	-
	32	24.1 ± 0.04	34.76 ± 0.03	-	7.86 ± 0.01	-	-	-	-
	40	23.9 ± 0.04	34.63 ± 0.07	-	7.86 ± 0.01	-	-	-	-
	48	23.8 ± 0.04	34.84 ± 0.06	2189.7 ± 9.9	7.87 ± 0.01	605 ±13.6	1836 ± 9.5	142.7 ± 2.0	2.25 ± 0.03

I chose to increase the silica concentration rather than using background concentrations to increase the likelihood of finding detectable differences in silica uptake over the short time period of the experiment. The experiment was run four times. On the first run we used three incubation chambers (replicates) per treatment. On runs two, three and four we used four incubation chambers (replicates) per treatment in each run resulting in a total of 15 replicates per treatment. A 48-h period was chosen to assure that the absorbed silica was biomineralized into spicules and that sponges did not starve (Weissenfels 1981; Maldonado *et al.* 2011). An additional no-sponge control was added to test for silica uptake from diatoms in the filtered seawater (Fig. A3.3). Silica concentration in empty incubation chambers was analyzed for each treatment (three per treatment) during each experimental run. To examine silica uptake rates of *M. grandis* at normal silica concentrations (6 µM DSi), we ran eight uptake experiments with sponges held at control temperature and pCO_2 concentrations. Salinity, temperature, pH_T, and DSi were monitored every 8 h for 48 h. Total alkalinity (A_T) samples (250 mL) were collected from the pre-filtered seawater prior to the start of each experiment and subsequent samples were taken from individual incubation chamber after the 48-hour period.

After each experiment, we recorded the sponge wet weight on an analytical scale and sponge volume via volume displacement. To calculate size of injury (cm^2) per individual, I took photographs of each individual and analyzed them in ImageJ® (Abràmoff *et al.* 2004) (http://imagej.nih.gov/ij/). Samples were combusted (500°C) for 12 h to determine the ash dry weight (ADW).

Silica uptake rates were normalized to sponge volume (ml), ADW (g) and injury area (cm^2) caused by the incision produced at the time of collection. Size of injury was considered an additional variable as sponge silica uptake rates are shown to increase when sponges are injured (Ayling 1983; Maldonado *et al.* 2011). Sponges that showed signs of necrosis or incubation chambers that showed signs of diatoms (dramatic DSi uptake) at the end of the experiment were discarded and were not used in the statistical analysis. Uptake rates were calculated at each 8 h interval [Uptake = $(DSi_{t2,i} - DSi_{t1,i})/(time \times V_i)$], where DSi is the concentration of dissolved Si in µmol from sponge *i*, t_1 is the first time point, t_2 is the second time point, *time* is the time between collections in hours and V is volume of water in the bucket for sponge i. Total uptake rates across 48 h were also calculated for sponges exposed to each treatment by calculating the difference in silica concentrations between 0 and 48 h.

6.3.2. Flow-through system experiment

6.3.2.1. Sponge collection

Sponge pieces from individuals (n=72) of *M. grandis* (wet weight: 29-263 g) were collected around Moku Loʻe (Coconut Island) in Kāneʻohe Bay at a depth of 3-9 m. Sponge samples were acclimated to aquaria facilities with ambient Kāneʻohe Bay seawater for 3 weeks prior to the experiment. Sponges were tagged with pigeon tags using a small tie wrap. The morphological characteristics used to determine spicule biomineralization were spicule size dimensions (L × W), ash dry weight to dry weight (ADW/DW) ratios and silicified weight to dry

weight (SIW/DW) ratios. One thick section (~500 µm) from the surface of each sponge were cut by hand and collected to compare spicule sizes, and six, smaller, 1 cm^3 (1-2 g) sections were cut from each individual to calculate ADW/DW and SIW/DW ratios in triplicate. To determine SIW/DW, we exposed sponge tissues to 5% hydrofluoric acid (HF). All incisions were performed adjacent to one another to reduce potential variance of spicule types or silica densities in the irregular sponge body.

All samples for spicule measurements, ADW/DW and SIW/DW ratio analyses were collected again using the same methods at the end of the experiment (day 26) to compare morphological differences before and after exposure to treatments. Thin sections for spicule analysis were made on healed tissue from the first sampling incision to ensure that the spicules collected were biomineralized during the time of the experiment.

6.3.2.2. Morphological response of *M. grandis*

To measure morphological differences in silica biomineralization, we used a 26-day, flow-through experimental set-up with similar pCO_2 and temperature conditions to the silica uptake experiment. The control conditions were changed to mimic ambient Kāneʻohe seawater temperature which cooled by 1°C at the time of the experiment (NOAA.NOS.CO-OPS Moku o Loʻe station 1612480). The four treatments were: control (C; 23°C, 692 µatm), high temperature (T; +3°C), high pCO_2 (pCO_2; 1100 µatm), and a combination of high temperature and pCO_2 (pCO_2T; +3°C, 1100 µatm) (Table 2, Table S1 and Figure S4). Ambient water

from Kāne‘ohe Bay passed through a water chiller (Aqualogic Multi Temp MT-1 model no. 2TTB3024A1000AA) and was fed into one of two 150 L header tanks. pCO_2 was manipulated in each header with gas-lines pumping in pre-mixed pCO_2 and then water from each header tank was fed into six 50 L experimental tanks (a total of six high CO_2 and six control CO_2 tanks). Temperature was controlled in each tank with aquarium heaters and dual-stage temperature controllers (Aqualogic TR115DN) similarly to the silica uptake experiment. There were three tank replicates per treatment in a completely randomized design; six sponges were placed in each tank for a total of 18 individuals per experimental treatment. The flow rate in each tank was maintained at 200 mL min^{-1} with a turnover every 4.2 h. Each incubation chamber was equipped with a submersible power head pump (Sedra KSP-7000 power head) to keep seawater well mixed. The same light parameters described in the silica uptake experiment were used. Temperature, pH_T, salinity and dissolved oxygen of each tank were measured daily in each aquarium and seawater flow was monitored and adjusted twice a day to ensure consistency for all tanks. A_T and silica concentrations were measured every three days (Table 6.

Table 6.2 Seawater parameter setup of treatments for flow-through experiment. Mean and standard error for chemical parameters in all tanks for each treatment during the flow-through system experiment.

Parameter	Control	T	pCO_2	pCO_2T	Header T*	Header T3*
Temp (°C)	23.1 ± 0.03	25.6 ± 0.03	23.0 ± 0.03	25.7 ± 0.04	24.09 ± 0.14	24.04 ± 0.14
Salinity (ppt)	33.82 ± 0.07	33.99 ± 0.07	33.79 ± 0.07	33.87 ± 0.08	34.31 ± 0.09	34.16 ± 0.10
A_T (µmol kg $^{-1}$)	2167.9 ± 3.1	2165.4 ± 3.2	2168.4 ± 3.3	2171.2 ± 2.8	2177.2 ± 9.2	2170.0 ± 5.3
pH_T	7.82 ± 0.004	7.82 ± 0.004	7.60 ± 0.004	7.60 ± 0.004	7.54 ± 0.006	7.90 ± 0.006
pCO_2(µatm)	693 ± 13.9	692 ± 11.3	1198 ± 22.5	1225 ± 21.4	1442 ± 37.6	569 ± 24.1
HCO_3^-(µmol kg $^{-1}$)	1863 ± 4.9	1836 ± 4.7	1972 ± 4.1	1960 ± 3.5	2000 ± 26.9	1807 ± 14.1
CO_3^-(µmol kg $^{-1}$)	122.9 ± 1.6	132.9 ± 1.5	79.3 ± 1.3	85.7 ± 1.2	71.6 ± 1.5	147.9 ± 1.9
Ω_{arag}	1.94 ± .03	2.13 ± .02	1.26 ± .02	1.37 ± 0.02	1.14 ±0.02	2.35 ± 0.03
$Si(OH)_4$ (µmol L^{-1})	4.16 ± 0.28	3.98 ± 0.27	3.91 ± 0.23	4.49 ± 0.22	6.1 ± 0.41	6.04 ± 0.43
O_2 (mg/L)	6.11± 0.35	6.02 ± 0.41	5.97 ± 0.36	5.86 ± 0.37	5.94 ± 0.07	5.99 ± 0.04

* Header T2 supplies seawater for buckets with treatments pCO_2, pCO_2T and Header T3 supplies seawater for buckets with treatments Control, T.

Sponges were weighed on an analytical scale (g) before and after the experiment by placing them in a 500-ml beaker with seawater; sponges were briefly exposed to air during the transfer from a tank to a beaker (Pawlik *et al*. 2013). To determine differences in spicule size across treatments, mean spicule dimensions (L × W) were compared before and after exposure to treatments. To measure spicule sizes, sponge sections (n=18 per treatment, 1 section per sponge) were submerged in 1 ml of 65% nitric acid using a 2 mL Eppendorf tube. Tubes were hand shaken and incubated at room temperature for 24 hours. Samples were then centrifuged (110 × g) and supernatant discarded. Pellets were rinsed with distilled water and a few drops of liquid containing spicules were mounted on a microscope slide. Photographic images of 20 subtylostyle spicules per sponge (a total of 360 spicules per treatment) were photographed and measured (L × W) using ImageJ. Subtylostyles were chosen as the response variable because they made up >90% of spicule content.

Triplicate samples collected for ADW measurements were dried (60°C) and weighed until a consistent weight was reached. Dry weights of samples were recorded and samples were then combusted (500°C) for 8-12 h, following the protocol of (Maldonado *et al.* 2012). To measure desilicification of sponge samples, triplicates of each individual were dried at 60°C until a consistent weight was reached. Samples were then submerged in HFA (5%) in 15-ml Falcon tubes and incubated at room temperature for 48 h. Samples were centrifuged (2,700 × g) and the supernatant discarded. The pellets were rinsed with distilled water and centrifuged again. The supernatant was discarded and pellets were dried (60°C)

for three days or until a consistent weight was reached. To obtain silicified weight, we subtracted the desilicified weight (DSI) and divided by DW to obtain the DSI/DW ratio. To determine treatment differences between ADW/DW and SIW/DW ratios, the average of each triplicate sample for each individual was taken. All averages showed a precision within ± 0.02 SE (standard error). Differences in ADW/DW and SIW/DW ratios were used to examine biomineralized silica in proportion to the whole mass of the sponge.

6.3.3. Measuring seawater chemistry parameters

All sample vials and stoppers were prewashed with 10% HCl for 24 h and rinsed three times with MilliQ water. Containers for all water samples collected to measure chemical parameters were rinsed three times with sampled water before a final sample was taken.

Samples (250 ml) for A_T analysis were collected and processed within 4 hours using open cell potentiometric titrations on a Mettler T50 autotitrator (Dickson *et al.* 2007). A certified reference material (CRM- Reference Material for Oceanic CO_2 Measurements, A. Dickson, Scripps Institution of Oceanography) was run at the beginning of each sample set. Titrator accuracy was within ±0.8% from the CRM standard and A_T measurements were corrected for this error. The precision was 4.75 μEq (measured as the standard deviation of the duplicate water samples).

Seawater pH was measured on the total scale. For the open-system experiment, borosilicate glass vials (20 ml) were used to take duplicate pH_T

samples. Samples were immediately processed and brought to a constant temperature of 25°C in a water bath. An m-cresol dye was added to each sample and analyzed using a spectrophotometric technique (Dickson *et al.* 2007). The precision for pH_T measurements was 0.003 pH_T units (measured as the standard deviation of the duplicate water samples). During the closed system experiments, pH_T was measured using a Tris calibrated Mettler Toledo DG 115-SC pH probe with an Orion 3star pH portable meter. Calibrations for the pH probe were performed each week following the SOP 6a protocol from Dickson *et al.* (2007). Other carbon parameters (pCO_2, HCO^-_3, CO_3^-, Ω_{arag}) were calculated using the CO_2SYS_V2.1 (Lewis *et al.* 1998) with known pH_T, A_T, temperature, and salinity values. The K1K2 equilibrium constants were taken from Mehrbach *et al.* (1973) and refitted according to Dickson & Millero (1987). The HSO_4^- dissociation constants from Uppström (1973) and Dickson (1990) were used. Dissolved oxygen measurements in open system experiments were taken using a ROX™ Optical Dissolved Oxygen mg L^{-1} 6150 Sensor integrated in a YSI 6920 V2 sonde that was calibrated using the one-point saturated water following standard calibration protocols. Salinity measurements were taken with a YSI conductivity, salinity, temperature meter (model # 30-50) and calibrated using a 50 mS cm^{-1} conductivity standard (YSI Catalog# 3169) following standard calibration protocols.

Triplicate samples were taken with 15 mL sterile falcon tubes to measure DSi concentrations. A Hach ultra low range (0-6 µM) silica reagent set was used to measure DSi for flow-through experiments and a Hach low range (20-120 µM)

silica test kit was used for closed system experiments. These two silica test kits with different detection limits were used because the open and closed-system experiments had different silica concentrations. Both of these methods follow a molybdate-reactive standard colorimetric method for measuring silicate (Grasshoff *et al.* 2009). Standard curves were generated prior to each run using a wavelength of 820 nm. Only dilutions that generated a standard curve with an R^2>0.99 were used to calculate DSi concentrations. Chemical reagents were added at 24°C following the Hach protocol guidelines. Precision for silica samples was greater than 0.4 μM L^{-1} (measured as the standard deviation of the triplicate water samples).

6.3.4. Statistical analysis

We used two-way repeated measures ANOVA to test for differences in silica uptake rates normalized to three different variables (ADW, sponge volume, and injury size) across the treatments. Time (each 8-h interval over the 48 hour experiment), treatment, and the interaction between time and treatment were included in the analysis. ANOVAs were also done by time period for all variables with partitioning of the treatment effect into the pCO_2 and temperature main effects and the interaction between these two factors. Because we had an unbalanced design (i.e. there were missing data points), we used a general linear model procedure (Proc GLM). pH_T, temperature, pCO_2, and A_T for each 8-h time period was also analyzed with a two-way repeated measures ANOVA to ensure that treatments were kept at the intended pH and temperature values. F-tests

were performed to test the homogeneity of the error variances obtained in the ANOVAs for the six time periods for both analyses. We removed twelve sponges (Control=1, pCO_2= 4, T=3, pCO_2T=1, 6 µMDSi=3) from the analysis that showed signs of necrosis, which caused silica concentrations to increase inside the incubation chamber. A total of 54 sponge individuals (Control=14, pCO_2= 11, T=10, pCO_2T=11, 6 µMDSi=8) remained healthy throughout the 48-h incubations and were used in the analysis.

In the flow-through experiment sponge weight loss, spicule sizes, ADW/DW and SIW/DW ratio differences were log transformed to meet assumptions of normality. We used an ANOVA to assess differences in spicule size, ADW/DW, SIW/DW ratios, pH, temperature, pCO_2 and A_T across treatments (Control, T, pCO_2, and pCO_2T) during the 26-day flow-through experiment. A two-way ANOVA was run for carbonate chemistry and temperature variables (pH, temperature, pCO_2 and A_T) using factors treatment, time, and treatment by time. Time refers to the number of days of the experiment. ANOVAs were also done by time period for all variables with partitioning of the treatment effect into the pCO_2 and temperature main effects and the interaction between these two factors. All data were analyzed using Statistical Analysis Systems (SAS) (Statistical Analysis Systems Institute, 2001). Duncan's multiple range tests was used to test for significant differences between treatment means. All statistical test interpretations were made at the 5% confidence interval level of significance.

6.4. Results

6.4.1. Silica uptake experiments

6.4.1.1. Silica uptake experiment seawater control

In general, pH_T values for Control and T treatments were higher than pH_T values from pCO_2 and pCO_2T (Table 6.1 and Fig. S2). The average pH_T values for the Control and T treatments were 7.86 ± 0.02 (mean ± SE) and 7.84 ± 0.04 respectively. The average pH_T values for both pCO_2 and pCO_2T treatments was 7.62 ± 0.01. pH_T increased with time in all treatments (p=0.0011, Table 6.3), but the mean increase was minimal with a range of 0.04 from across the 48 hours. We maintained a 0.24 difference in pH_T across treatments. The pCO_2 values calculated with CO_2SYS_V2.1 were also consistent across time points: average values were 593.9 ± 78.9 for Control, 600.4 ± 29.9 for T, 1050.2 ± 71.8 for pCO_2 and 1119.3 ± 70.9 for the pCO_2T treatment. For pH and pCO_2, treatment and time were significant sources of variation, while for temperature only treatment was a significant source of variation for temperature. Temperatures were significantly lower in Control and pCO_2 treatments than the T and pCO_2T treatments (p<0.0001). Average temperatures were 24.1 ± 0.04°C for Control, 23.9 ± 0.06 for pCO2, 27.2 ± 0.07°C for T, and 27.0 ± 0.08 for the pCO_2T treatment, which closely approximates the goal of a 3.0°C difference between the two treatment sets (Table 6.1 and A3.2). An average A_T decrease of 215.1µmol kg $^{-1}$ was observed in all treatments throughout the 48 h, possibly due to calcification from brittle stars that we were unable to remove from the sponges

without injury. Measurements of other chemical parameters are listed in Table 6.1.

6.4.1.2. Uptake rates

Results from the ANOVA for silica uptake rate showed no significant treatment or treatment × time interaction effects when normalized to any of the variables (ADW, injury area, sponge volume) (Fig. 6.1, Table 6.4). The factorial ANOVAs conducted by time of sampling showed no significant pCO_2 and temperature main effects nor a pCO_2 × temperature interaction. However, there was a significant difference by time ($p<0.001$ for ADW and Volume, $p=0.0011$ for Injury; Table 6.4) and coefficients of variation for the ANOVAs ranged from 0.6-52.9 %.

Table 6.3 Two-way ANOVA results for experimental seawater parameters. P-values from a two-way ANOVA for water parameters collected during the silica uptake and flow-through experiment.

		Source of variation			
Experiment	**Variable**	**Treatment (TMT)**	**Time (T)**	**TMT × T**	**CV,%***
Silica uptake	pH_T	**0.0001**	**0.0011**	0.1807	0.04
	Temperature	**<0.0001**	0.1298	0.4077	0.6
	pCO_2	**<0.0001**	**<0.0001**	0.0009	15.7
	TA	0.4193	**<0.0001**	0.4827	2.2
Flow-through	pH_T	**<0.0001**	**<0.0001**	**0.0031**	0.3
	Temperature	**<0.0001**	**0.0049**	0.7065	1.1
	pCO_2	**<0.0001**	**<0.0001**	**0.0009**	7.0
	TA	0.3225	**<0.0001**	0.2926	0.51

*Time= hours for the silica uptake experiment and number of days for the flow-through experiment.
**CV=coefficient of variation.

In general, each silica uptake rate across all treatments followed a curvilinear pattern. Rates for all three variables were lowest during the 0-8 h period while maximum uptake rate was at the 16-24 h period with 0.20 μmol Si g^{-1} ADW sponge h^{-1}, 0.06 μmol Si cm^{-2} injury area of sponge h^{-1}, and 0.04 μmol Si mL^{-1} of sponge h^{-1} (Fig. 6.2). A decrease in uptake rate was observed for all three variables from the 24 to the 40-hour period, a slight increase between 32 to 40 hour period and a slight decrease between the 40 to 48 h period. There was no detectable DSi uptake in incubation chambers without sponges with values remaining between 60-65 μM of DSi throughout 48 hours, indicating that filtered seawater was free of diatoms (Fig. A3.2).

Total silica uptake rates showed no significant differences across treatments. However, the total silica uptake rate of the enrichment condition applied to all treatments and was substantially higher than the background silica (6 μM DSi) treatment. The 6 μM DSi was run only one time with six replicates as a control and therefore could not be included in the ANOVA. Average uptake rates across the 48 h of *M. grandis* for background levels of silica (6 μM DSi) were 0.016 ± 0.003 (mean ± SE) μmol Si g^{-1} ADW h^{-1} (Table 6.5). Total silica uptake rates in the Control with enriched DSi (70 μM) conditions accelerated to 0.155 ± 0.029 μmol Si g^{-1} ADW h^{-1}, an almost ten-fold increase in uptake rates compared to background DSi levels (Table 6.5).

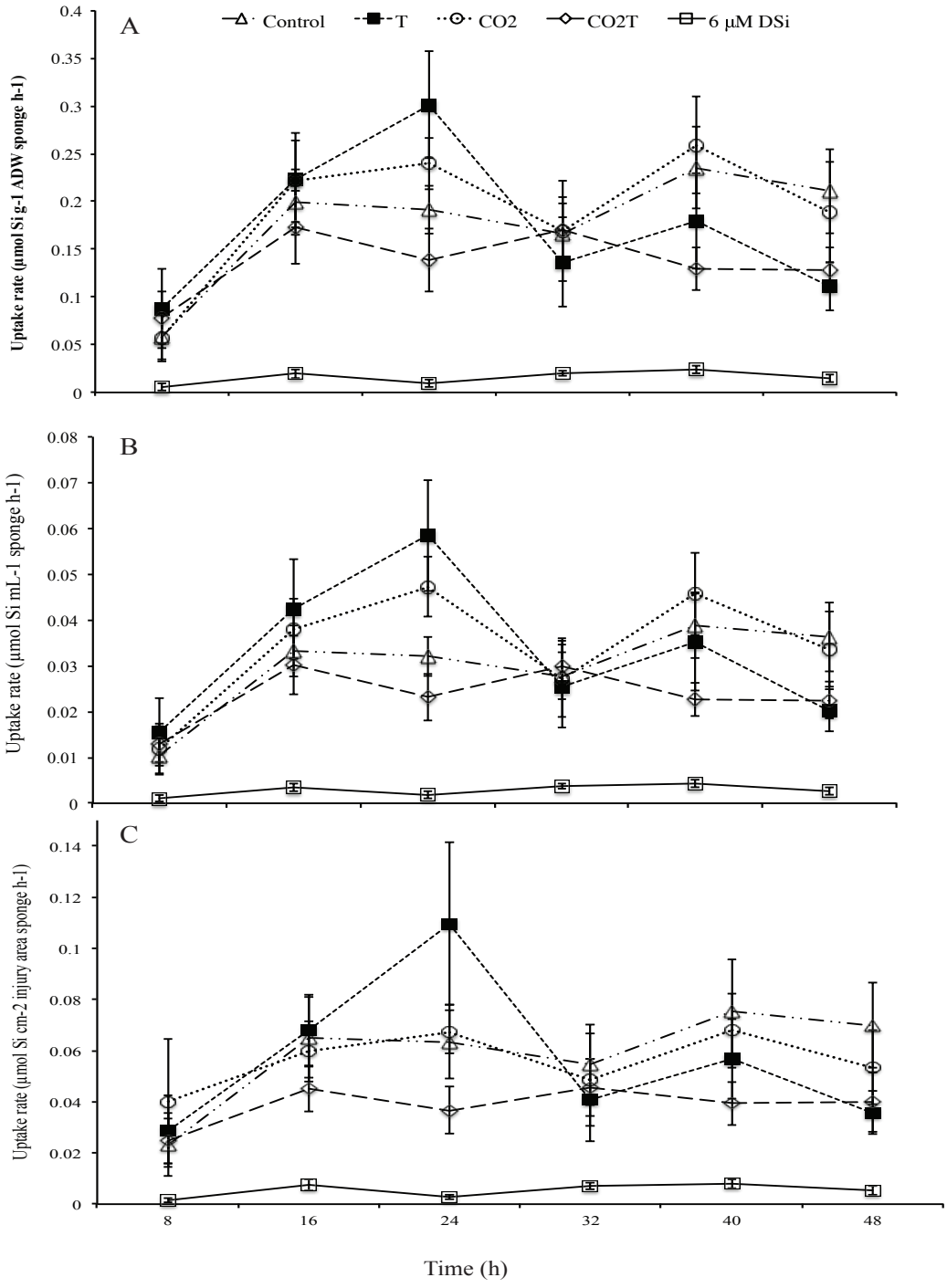

Figure 6.1 Mean and standard error of dissolved silica uptake rates by the sponge *Mycale grandis.* Uptake rates were determined by (A) Ash dry weight (g), (B) sponge volume (mL), and (C) area of injury (cm^2).

Table 6.4 ANOVA results of silica uptake and flow-through experiments. P-values from a two-way ANOVA for *M. grandis* silica uptake rates normalized by ADW, volume, and injury size. P-values from an ANOVA for the changes in *M. grandis* weight loss, spicule size, ADW/DW and SIW/DW ratios across treatments during the flow-through experiment. Bold values are significant. Significant differences were only observed in changes of ADW/DW ratios.

		Source of variation			
Experiment	**Variable**	**Treatment (TMT)**	**Time (T)***	**TMT × T**	**CV,%****
Silica uptake	ADW	0.7339	**<0.0001**	0.2898	46.0
	Volume	0.4843	**<0.0001**	0.2017	50.8
	Injury	0.3976	**0.0011**	0.3195	52.9
-	-	-	-	-	-
Flow-through	Weight loss	0.7020	-	-	21.1
	Spicule length	0.4324	-	-	238.9
	Spicule width	0.7696	-	-	309.1
	ADW/DW ratio	**0.0001**	-	-	21.3
	SIW/DW ratio	0.0673	-	-	596.0

*Time for silica uptake experiment was for every 8 hours and for the flow through and days for the flow-through experiment.

**CV=coefficient of variation.

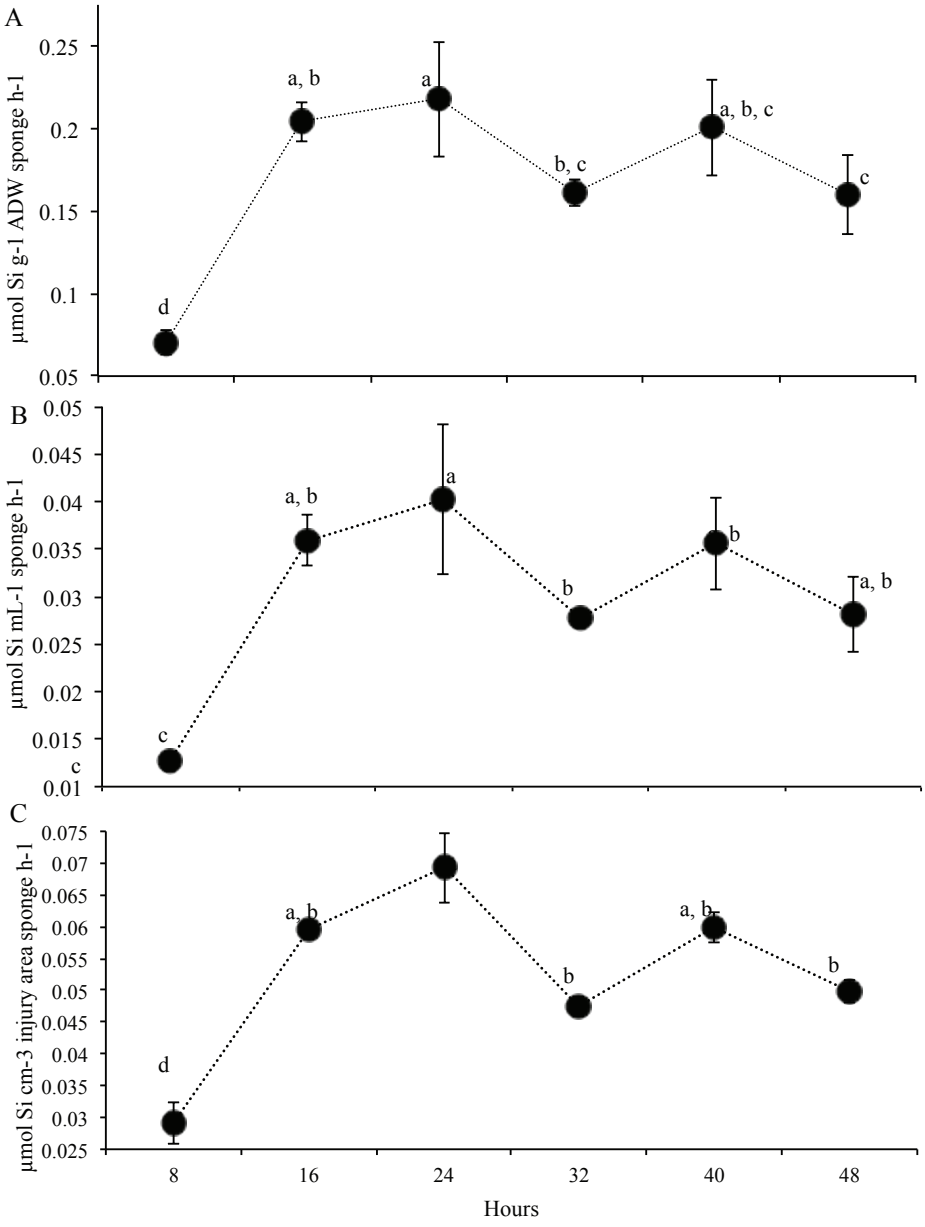

Figure 6.2: Silica uptake rates with time averaged (N=46) across treatments determined by (A) ash dry weight, (B) Sponge volume (mL), and (C) area of injury (cm^2). Within each subplot, means with the same letters in common are not significantly different as indicated by Duncan's Multiple Range Test.

Table 6.5 Total silica uptake rate of *M. grandis* through 48 h. Mean and standard error of DSi uptake rate with standard error of *M. grandis* silica concentrations taken at time 0 and at 48 hours.

Treatment	µmol Si mL^{-1} sponge h^{-1}	µmol Si g^{-1} ADW h^{-1}	µmol Si cm^{-3} injury h^{-1}
Control	0.025 ± 0.004	0.155 ± 0.029	0.051 ± 0.015
pCO_2	0.028 ± 0.006	0.164 ± 0.033	0.045 ± 0.011
T	0.030 ± 0.005	0.158 ± 0.031	0.051 ± 0.010
pCO_2T	0.021 ± 0.003	0.123 ± 0.023	0.035 ± 0.006
6 µM DSi*	0.003 ± 0.001	0.016 ± 0.003	0.006 ± 0.001

6 µM DSi* treatment was only ran once using six replicates

6.4.2. Flow-through system experiment

6.4.2.1. Seawater controls for flow-through system experiment

All chemical parameters were well kept throughout the duration of the experiment. Coefficients of variation for the ANOVAs ranged from 0.3 to 7.0% for the chemical parameters (Table 6.3). pH was consistently higher in the Control and T treatments relative to the pCO_2 and pCO_2T treatments (Table 6.2). The average pH difference across the treatment groups was 0.22 which met the experimental goal (average pH of 7.82 ± 0.003 for the Control, 7.81 ± 0.02 for the T, 7.61 ± 0.03 for the pCO_2 and 7.60 ± 0.03 for the pCO_2T treatment) (Figure A3.4). However, a slightly lower pH for pCO_2T than the pCO_2 treatment on days 5 and 7 caused a significant interaction between treatment × time (p=0.0001, Table 6.2). The average pCO_2 value for the Control was 693 ± 19 and 693.0 ± 26 for the T treatment. These values were higher than Control pCO_2 values for the silica uptake experiment, but still within the range of ambient Kāneʻohe Bay conditions (Silbiger & Donahue 2015). The average pCO_2 values for the pCO_2 and pCO_2T treatments were 1198 ± 40 and 1225 ± 45 respectively. The average

A_T was 2168.3 ± 4 µmol kg^{-}1; consistent across treatments. Measurements of salinity, HCO_3-, CO_3- and Ω_{arag} are listed in Table 6.2.

Temperature was significantly higher for the T and pCO_2T treatments compared to the Control and pCO_2 treatments ($p<0.0001$; Table 6.3). The significant time main effect was a result of slight fluctuations of temperature within the two treatment groups probably due to a slow response from the chillers in keeping temperatures consistent. Overall the average temperature was 23.1 ± 0.13°C in the Control, 23.0 ± 0 in the pCO_2, 25.6 ± 0.1°C for the T and 25.7 ± 0.2 for the pCO_2T treatments. This resulted in a difference of 2.6°C which approximated the goal of 3°C.

6.4.2.2. Morphological response of *Mycale grandis*

All sponge individuals used for the flow-through system experiments survived the 26-day experiment. A weight loss of 28.4% was observed for all treatments but no significant differences were observed between treatments. The coefficient of variation for weight loss was 21.1% (Table 6.4; Figure 6.3A). There were no significant differences across treatments for spicule length, width or SIW/DW (Table 6.4; Figure 6.3B,C). The factorial ANOVA with partitioning of the treatment effect into main effects (pCO_2 and temperature) and interaction (pCO_2 × temperature) showed no significant differences.

There was a significant difference across treatments for ADW/DW ratios (p=0.0001, Table 6.4; Figure 6.3D). The factorial ANOVA showed a non-significant pCO_2 × T interaction (p=0.99) and a non-significant temperature main

effect (p=0.12). The pCO_2 main effect was significant (p=0.0013). In general increasing pCO_2 from background levels to 1100 μatm decreased ADW/DW ratio by 0.03 mg units regardless of the temperature level. The coefficient of variations for ADW/DW and SIW/DW ratios were 21.3 and 596.0%, respectively (Table 6.4).

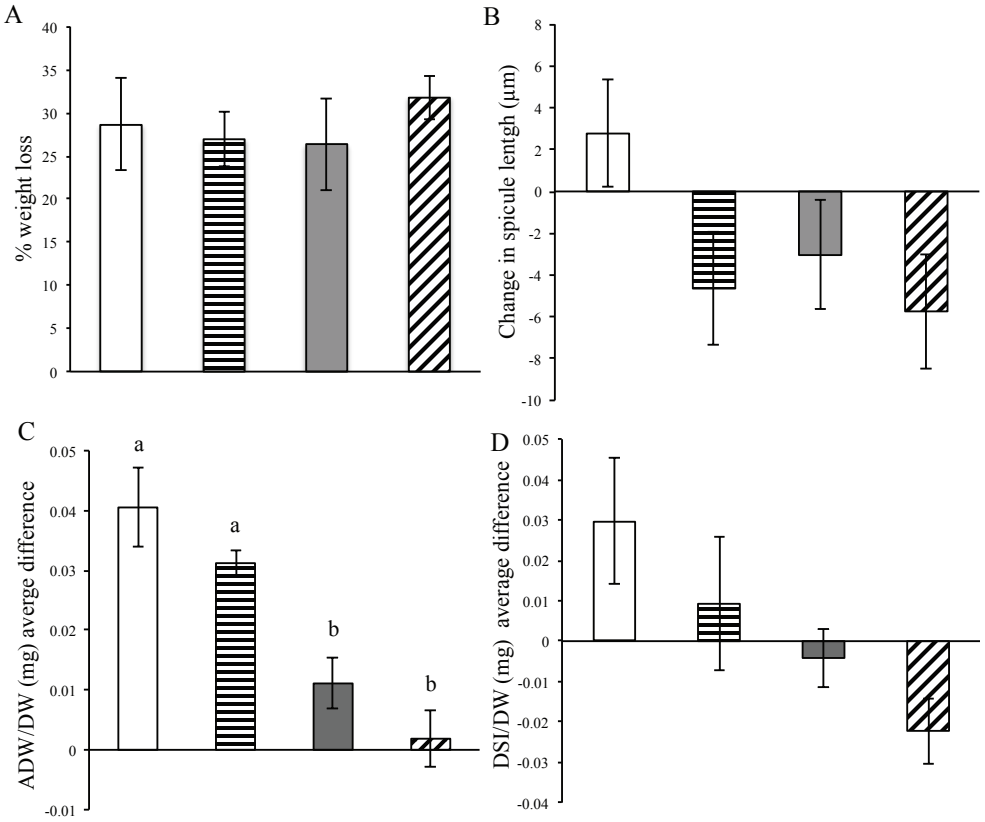

Figure 6.3 Morphological response of *Mycale grandis* to experimental treatments. Mean and standard error of (A) % biomass loss for sponges in each treatment. Morphological differences between (B) subtylostyle length, (C) AFW/DW ratio and (D) DSI/DW ratio of sponges in the 26-day flow-through experiment. Within each subplot, means with the same letters in common are not

significantly different as indicated by Duncan's Multiple Range Test. The factorial ANOVA for ADW/DW ratio showed a non-significant pCO_2 × T interaction (p=0.99) and a non-significant temperature main effect (p=0.12). The pCO_2 main effect was significant (p=0.0013). Treatments are indicated as follows: control (white bars), T (bars with horizontal lines), pCO_2 (gray bars), pCO_2T (bars with diagonal lines).

Average differences between spicule lengths ranged between 2 - 6 ± 2.0 µm and widths ranged between 0.1 - 0.6 ± 0.2 µm for all treatments. Although no differences between treatments were found for spicule length, the control treatment means increased slightly while all other treatments showed a net decrease (Figure 6.3B). An average decrease of 0.21 ± 0.1 µm spicule width was observed for all four treatments. The coefficient of variations for spicule length and width were 93.3% and 309.1% respectively (Table 6.4).

The average ADW/DW ratio differences of sponge samples ranged from 0.67 to 0.81 and averaged 0.74 ± 0.006 before exposure. Differences in ADW/DW ratios throughout the 26 days resulted in net ratios that were significantly lower in treatments pCO_2 and pCO_2T than Control and T treatments (p=0.0001, Table 6.4). ADW/DW ratios had the highest increase in the Control treatment (0.04 ± 0.01) followed by T (0.03 ± 0.002), pCO_2 (0.01 ± 0.004) and pCO_2T (0.002 ± 0.004) (Figure 6.3C).

SIW/DW ratio differences of sponge samples ranged from 0.71 to 0.99 and averaged 0.88 ± 0.006 before exposure. There were no significant differences in SIW/DW ratios throughout the 26 days (Table 6.3). However,

similar to ADW/DW ratios, net average SIW/DW ratio differences followed a similar trend with the highest net increase observed in the Control (0.03 ± 0.02) followed by T (0.01 ± 0.02). A net decrease was observed for pCO_2 (-0.004 ± 0.01) and a greater decrease in pCO_2T (-0.02 ± 0.01) (Figure 6.3D).

6.5. Discussion

Neither higher pCO_2 nor warmer temperature treatments affected silica uptake rates in the sponge *M. grandis* over 48 h (Figure 6.1). The availability of HCO_3^- and $Si(OH)_4$ did not facilitate up-regulation of silica uptake. It is possible that sponges are using the membrane symporter mechanism described for *S. domuncula* by Schröder and colleagues (2004), but that neither pCO_2 nor termperature affect the rate of silica transport by this process. The 26-day exposure to end-of-century pCO_2 (1198 µatm) revealed a decrease in the proportion of mineralized tissue (ADW/DW) that appears to be aggravated when combined with a temperature increase (pCO_2T) (1225 µatm, +3°C *µ*atm); Figure 6.3C). However, the factorial analysis revealed that the negative effect of pCO_2 on ADW/DW ratio happened regardless of the temperature value, indicating that temperature had no effect. A decreasing trend was also observed in SIW/DW ratios and spicule lengths (Figure 6.3D).

These results show that although no differences in silica uptake nor growth rates were detected as a result of high pCO_2 or warmer temperatures, these factors did have a marginal effect on the process of silica biomineralization in *M. grandis.* Previous studies have found that sponge growth rates of six

Caribbean species were not affected by pH or warmer temperatures (Duckworth *et al*., 2012), although other morphological characteristics such as spicule composition or biomineralization were not assessed. Other studies that have monitored sponge biodiversity and spicule composition along a natural pH gradient found that acidification caused a decrease in sponge cover but no differences in spicule morphology (Goodwin *et al*. 2014). Particular interest has been paid to understanding how ocean acidification will affect sponge boring rates, where some species are found to accelerate their boring rates when exposed to acidification (Duckworth and Peterson, 2012; Wisshak *et al*., 2013; Stubler *et al.* 2014). Future ocean acidification studies on sponge boring rates should observe the morphological response of the sponge to see if faster boring rates correlate with a decrease in silica biomineralization. Under acidification scenarios, sponges might allocate their metabolic requirements less towards skeleton synthesis and more towards other processes that help fulfill the biochemical requirement for acid-base regulation (Pörtner 2008).

Silica uptake rates for *M. grandis* increased proportionally with silica concentrations. A ten-fold increase was observed when concentrations were spiked from 6-7 µM to 60-70 µM during closed system experiments (Table 6.5). These results suggest that *M. grandis* is potentially limited by silica and follows a similar uptake rate pattern to *Halichondria panicea* (Reincke & Barthel 1997), *Axinella* sp. and *Hymeniacidon perlevis* (Maldonado *et al.* 2011; Maldonado *et al.* 2012). However, uptake rates for *M. grandis* (0.003 ± 0.001 µmol Si mL^{-1} sponge h^{-1}) at background silica concentrations were the lowest when compared to *H.*

panicea (0.06 ± 0.02 μmol Si mL^{-1} sponge h^{-1}) and *Axinella* sp. (0.016 μmol Si mL^{-1} sponge h^{-1}) suggesting that silica biomineralization is a slow process in *M. grandis*. These observations agree with the hypothesis stated by Maldonado and colleagues (2012) that uptake rates might be species dependent based on the proportion of their biomineralized silica to dry weight ratios. For example, the proportion of biomineralized silica in *M. grandis* averaged up to 74% (ADW/DW), and 88% (SIW/DW) of biomineralized tissue in proportion to dry weight, which is the highest of any sponge previously studied for silica uptake kinetics.

Although silica uptake rates were not impacted by temperature or high pCO_2, there was a significant effect of time on average silica uptake rates across all treatments. Uptake rates for *M. grandis* (at 60-70 μM) resulted in a non-circadian oscillation with time reaching a maximum after 24 h (0800) and a second maximum at 40 h (0000) after incubation. Similar oscillations have been observed by Maldonado and colleagues (2012) where *H. perlevis* had a maximum uptake rate between 0-6 h and a second maximum between 12-18 hours under silica enrichments of 70 μM. These results support the hypothesis by Maldonado and colleagues (2012) that silica transport is likely an active mechanism.

Sponge biomass decreased (25-35%) for all individuals in the 26-day experiment, an overall response probably due to my inability to fully simulate natural conditions of the reef environment. One possible explanation is that silica concentrations in experimental tanks were difficult to keep at natural incoming silica concentrations likely due to the presence of diatoms inside the tanks. For

example, silica concentrations of incoming water from Kāne‘ohe Bay into two of the header tanks averaged between 5-6 μM, but dropped to 3-4 μM in the experimental tanks (Table 6.2). A lack of food availability resulting from the slow flow rate might have also caused sponges to lose biomass. Despite observing an overall decrease in sponge biomass during the experiments, this effect did not prevent sponges from increasing biomineralization in the control treatment. It is also unlikely that spicules deposited in tanks from necrotic sponge tissue would affect spicule biomineralization as spicule dissolution happens at a very slow rate (Maldonado *et al.* 2005).

Addressing the molecular response of genes involved in spicule synthesis of *M. grandis* would allow us to understand if the decrease in silica biomineralization caused by high pCO_2 in this study is inhibiting gene expression of proteins involved in spicule synthesis. Specifically, monitoring silicatein gene expression would provide us with helpful information as silicatein proteins are known to be directly linked with spicule synthesis (Cha *et al.* 1999; Müller *et al.* 2003). A transcriptomic assessment of genes involved in spicule synthesis would allow us to gain a comprehensive understanding of how ocean acidification and thermal stress might affect *M. grandis*.

Predicting how *M. grandis* will respond to warmer and high pCO_2 conditions is important because this sponge has already been known to aggressively spread through coral reefs of Kāne‘ohe since its introduction (Coles *et al.* 2006). Despite showing resilience under acute warmer temperatures and high pCO_2, it is very difficult to assess whether these short experimental windows

are suggestive of a potential phase shift from coral to sponge by the end of the century, as suggested by (Bell *et al.* 2013). These findings highlight the exceptional ability of *M. grandis* to withstand pCO_2 and temperature conditions that are stressful to many organisms, suggesting that this invasive species will continue to be a competitor in the reefs of Kāneʻohe Bay in a warmer and more acidic oceans.

Chapter 7: Conclusions and future directions

7.1. Comprehensive summary of the evolutionary relationship between *Plakortis* spp. and their epibionts.

Mutualistic epizoic interactions have long been documented as a facilitation strategy by sponges to deal with competition in highly diverse and densely packed sponge communities of reef cave habitats (Rützler 1970). In this study I have discovered three new mutualistic cases of sponge-sponge symbioses living in light-limited, cryptic habitats. Extensive reef surveys throughout the Caribbean revealed a widespread distribution of sponge pairs exhibiting different morphologies in different life stages. For example, *Xestospongia deweerdtae* has a remarkable ability to acquire a range of polymorphic characters that vary according to its free-living or associated lifestyle with either *Plakortis* spp., or is a response to conditions in the surrounding environment. *X. deweerdtae* starts growing as small translucent patches (observed in recruits). In sponge pairs observed in the Bahamas, the *X. deweerdtae* penetrate the *Plakortis* spp. body whereas in Panama the association leads to the formation of thick tissues completely covering *Plakortis* individuals.

It is interesting to speculate on possibilities of how these associations might have originated. Based on biomass proportions of each associated sponge species, it seems as though at one point *X. deweerdtae* likely settled on the *Plakortis* spp. body either by larvae settlement or overgrowth. *X. deweerdtae* could have been resistant to antifouling allelochemcials produced by the *Plakortis* epibiont and overtime managed to grow from the *Plakortis* pinacoderm through

the mesohyl. Persistence of these associations presumably allowed for reproductive synchronization between species. A reef cave habitat rather than the bedrock of the upper mesophotic reef is likely to have been the setting in which these associations first occurred. In reef caves, larval dispersal from different sponge species is confined increasing the likelihood of sponges interacting with each other (Harmelin *et al.* 1985). Similar to the genetic isolation observed in the Mediterranean caves that allowed for speciation of four different cryptic species of *Plakina trilopha* (Muricy *et al.* 1996), a similar process may have resulted in speciation of *P. symbiotica* and *P. deweerdtaephila*.

At first glance these observations seem to suggest that *X. deweerdtae* is a parasitic symbiont of *Plakortis* spp. However, sponges from the genus *Plakortis* generally avoid epizoic interactions with other sponges (Hooper & Van Soest 2002), cause bleaching in neighboring coral species (Porter & Targett 1988) and are chemically defended in coral reef habitats (Pawlik et al. 1995). I also noticed that associated sponge pairs were commonly colonized by zoanthids. Intriguingly, zoanthids only colonized the *X. deweerdtae* tissue and not the *Plakortis* spp. tissue. A previous study that surveyed fouling of zoanthids on Caribbean sponges showed that it is also uncommon for Homoscleromorphs to host zoanthids (Swain & Wulff 2007). It is possible that *Plakortis* spp. produce antifouling compounds that prevent zoanthids from settling on them. Knowing how antagonistic *Plakortis* spp. sponges are to other organisms, including other sponge species, it seems unlikely that *Plakortis* would interact with other sponges on the reef, unless there is a substantial benefit that could be gained

over time by modulating its defensive mechanisms and associating with another sponge that supersedes the rejection response.

In this study we propose that sponge pair species likely have a mutualistic relationship. Sponge pairs are found 5-23 × more frequently than free-living individuals when both lifestyles are present, indicating that perhaps sponge pairs are reproducing more efficiently or have a higher survival than free-living forms. Sponge pair species have remarkably different morphological features, associated microbial communities and varying degrees of chemical deterrence against predators that might be influencing physiological processes with different energy demands. For example, it might be more energy demanding for *Plakortis* spp. to pump water through their bacteria rich, dense skeletons while *X. deweerdtae* and *H. plakophila* efficiently pump water through their hollow tissues depauperate of bacteria. Nevertheless, the less dense tissues of the epibionts might not have access to important microbial symbionts or microbial metabolic products (i.e. presence of polyphosphate granules in Fig. 3.2C, E) offered by a more microbial-rich sponge such as *Plakortis* spp. We propose that sponges might offset the limitations in energy demands of the free-living HMA or LMA lifestyle by living in symbiosis. The concept of outweighing the costs of energy investment in pumping water and sponge tissue nutrient enrichment by living in symbiosis, fits the definition of cooperation proposed by Sachs *et al.* (2004).

By living together, sponge pairs also expand their arsenal of chemicals and their ability to deter a larger suite of predators. We found that plakinic acids produced by *P. deweerdtaephila* are translocated to the tissue of the epibionts

and may result in a more chemically defended sponge pair in ecosystems with persisting high predation pressures. However, the data indicated translocation of only trace amounts of plakinic acids and did not show that epibionts were significantly more chemically defended than the free-living forms of *X. deweerdtae*. Living in symbiosis to offset these important chemical and physiological demands could be the driving force of why these sponges live in cooperation and help explain some of the polymorphic features observed in both sponge species.

Despite the multiple lines of evidence suggesting a mutualistic relationship between sponge pair species, it is important to discuss the possibility that these epibiont sponges are parasitic to *Plakortis* spp. or vice versa. Consistently, in sponges collected in Bahamas (silica limited) and Panama (silica rich), spicule lengths observed in associated individuals of *X. deweerdtae* are significantly smaller than free-living individuals. We attribute these results to be a consequence of the *Plakortis* spp. providing structure and offsetting the demands of *X. deweerdtae* to synthesize longer spicules required by a free-living lifestyle. We cannot exclude the possibility that nutrient availability requirements by each sponge is limited and that *Plakortis* spp. are actually parasitic to *X. deweerdtae*, depriving *X. deweerdtae* of nutrients needed to synthesize longer spicules. One other parasitic scenario that might be harmful for the *Plakortis* spp. basibiont is the presence of zoanthids that only grow on free-living and associated individuals of *X. deweerdtae*. Zoanthids are known to reduce pumping rates of host sponges (Lewis 1982) and their presence in the epibionts could be a disadvantageous trait

for *Plakortis* spp. hosts. Without the *X. deweerdtae* epibiont *Plakortis* spp. basibionts would probably avoid being colonized by zoanthids by chemical defense as discussed above.

Symbiotic associations can also be very dynamic and actually shift from mutualism, to cheating (i.e. one partner receives more benefits by associating than the other), or to parasitism (Ferriere *et al.* 2002; Douglas 2008). For example, mycorrhizal fungi provide multiple benefits (i.e. antifungal metabolites, enhancement of plant growth, and drought tolerance) to their plant host, but may also acquire a virulent lifestyle that is parasitic to the plant host (Modjo & Hendrix 1986; Redman *et al.* 2001). The different levels of polymorphism in *X. deweerdtae* in different locations of the Caribbean suggest the possibility that epibionts are “cheaters” acquiring different degrees of benefits from *Plakortis* spp. that vary according to the surrounding environmental conditions.

It is not yet clear how different environmental conditions might affect the dynamics of the symbiosis. For example, under different climate change scenarios (Chapter 5) we noticed that it might actually be disadvantageous for the *X. deweerdtae* epibiont to associate with a sponge that is more susceptible to diseases when exposed to higher temperatures. Nevertheless, necrotic tissue development was significantly repressed by high pCO_2 conditions in *P. deweerdtaephila*, free-living and associated lifestyles of *X. deweerdtae*. A similar response was observed by Bennet et al. (2016), where acidification had an ameliorating effect on necrosis, bleaching and larvae settlement in phototrophic sponges but not on heterotrophic sponges. These results can be explained

mechanistically since higher pCO_2 conditions allow symbiotic Cyanobacteria to have more CO_2 substrate to photosynthesize into glucose that is assimilated by the sponge. In the current study, sponges lack photosymbionts and are likely heterotrophic sponges. The results also show that ameliorating effects of higher pCO_2 conditions on necrosis from higher temperature treatments seem to be independent of bacterial abundance as well. These results suggest that the ameliorating effect of acidification on sponge necrosis could also be a consequence of other physiological or immunological enhancements in the sponge. Since warmer temperatures and higher pCO_2 conditions are predicted to occur simultaneously necrosis will probably not be detrimental to either associated or free-living lifestyles by the end of the century. Associating with *P. deweerdtaephila* might require a longer adaptation period to climate change but might not be an overall disadvantage for associated *X. deweerdtae*.

Resilience of sponges to climate change has important ecosystem based management implications, particularly in coral reef habitats of the Caribbean. Sponges are rivaling corals in reef environments and are now considered the most dominant habitat forming organisms (Pawlik 2011). Sponges that contribute to the three dimensional framework of the reef like the giant barrel sponge (*Xestospongia muta*) is important as these might provide future refuge habitats for important fisheries of the Caribbean. Management plans to foster and protect sponges should be implemented as corals are predicted to continue declining.

There are many possibilities that might explain the basis of these sponge associations. Nevertheless, much still needs to be learnt about all the factors

involved in the associations that might help keep the balance between the physiological demands of both species. It is important to determine how these different energy demands from different physiological processes (i.e. secondary metabolite production, water pumping) interact in order to comprehensively understand why sponges are developing specialized associations with one another.

7.2. Future work to better understand tradeoffs in the *Plakortis* spp. symbioses with *X. deweerdtae* and *H. plakophila* epibionts.

The findings of this study suggest that *Plakortis* spp. are living in cooperation with *X. deweerdtae* and *H. plakophila*. My work has indicated future research that is required to better understand these symbiotic systems. Throughout this study, my effort to identify potential benefits and disadvantages for *X. deweerdtae* to associate with *Plakortis* spp. was greatly facilitated because I found associated and free-living individuals of *X. deweerdtae*, enabling me to make direct comparisons. Nevertheless, we still know very little about what benefits and disadvantages might be gained by *Plakortis* spp. when associating with *X. deweerdtae*. This is difficult to do because free-living *Plakortis* spp. have never been found and therefore cannot be used as a reference to compare with associated lifestyles.

In order to fully assess what benefits may accrue to the *Plakortis* spp. basibiont it would be necessary to determine whether either *P. symbiotica* or *P. deweerdtaephila* are be able to live without being colonized by *X. deweerdtae*.

Numerous field surveys throughout the Caribbean revealed only associated individuals of *Plakortis* spp., and furthermore the sponges were found in association from an early recruiting stage. In addition, associated individuals are almost impossible to fully separate from each another, as they can be intertwined throughout the mesohyl, preventing a complete separation of both sponge pairs without excessively damaging individuals. The ideal experimental setup would consist of completely separating *Plakortis* spp. from their epibionts and comparing growth and survival of free-living *Plakortis* spp. for a prolonged period of time to *Plakortis* spp. in sponge pairs to determine if in fact these symbioses are truly obligate. Taking histological sections to target oogenesis or spermatogenesis (Ereskovsky 2010) from both species in the pair throughout a long-term monitoring period would help determine if reproduction of both species is synchronous as suggested by the presence of only sponge pair recruits in field surveys.

An important topic of future study is to determine the allorecognition mechanism by which individuals of *X. deweerdtae* and *Plakortis* spp. associate and what factors determine an associated vs. free-living lifestyle in *X. deweerdtae* during development (Müller 2007). It is difficult to perform experiments using early developmental stages (i.e. larvae settlement assays) as neither sponge species broods larvae (viviparous) as observed for in other *Xestospongia* spp. (Collin *et al.* 2010). However, parabiosis experiments pairing adult *X. deweerdtae* with *Plakortis* spp. would reveal if the ability to associate is acquired only by sponges that already have associated lifestyles or if free-living

sponges can learn to associate with *Plakortis* spp. Characterization of the aggregation factors involved in cellular adhesion of both heterospecifics could also aid in understanding self- to non-self-recognition mechanisms of these sponges (Haseley *et al.* 2001). Determining the allorecognition mechanism whereby heterospecific sponges associate is an exciting topic of investigation as this process can be very precise where even conspecifics have the ability to reject one another (Saito 2013).

Parabiosis experiments using free-living *X. deweerdtae* with *Plakortis* spp. would also allow us to confirm horizontal transmission of microbial symbionts or translocation of plakinic acids between sponges. Fluorescent in situ hybridization (FISH) microscopy using specific microbial phyla probes on sponge tissues free of either heterospecific sponge before and after exposure would help confirm horizontal transfer of microbial symbionts. Epifluorescent imaging could also be overlaid with MALDI-MS images that highlight plakinic acids using different ionization methods (Simmons *et al.* 2008) to localize and detect translocation of these metabolites from *Plakortis* spp. to the *X. deweerdtae* tissue.

Recent advances and the low costs of next-generation sequencing (NGS) technology (Mardis 2008) have provided an invaluable tool for gaining a precise understanding of sponge phylogeny and physiological processes in different life stages (Srivastava *et al.* 2010; Pérez‐Porro *et al.* 2013; Riesgo, Farrar*, et al.* 2014; Guzman & Conaco 2016). It would be useful to add a genomic and transcriptomic component to these experiments when comparing free-living and associated lifestyles. Further work is needed to fully resolve the phylogeny of

associated and free-living individuals of *X. deweerdtae*. My results showed that free-living and associated lifestyles of *X. deweerdtae* are homologous based on 18S rRNA, 28S rRNA and COI gene sequences, but note that the marine Haplosclerida have been shown to be polymorphic when using these genes as biomarkers (Redmond et al. 2011). It could be that these sponges are closely related but represent distinct genetic populations between lifestyles. Developing microsatellite markers that would pickup sequence dissimilarities at finer scales between lifestyles would help resolve the genetic structure of both lifestyles (Wörheide *et al.* 2005). Reduced genome sequencing using ezRAD, a novel strategy for restriction site-associated DNA (RAD), is a recent approach developed to efficiently identify single nucleotide polymorphisms in a diversity of taxonomic phyla that also could be used to resolve the genetic structure of *X. deweerdtae* (Toonen *et al.* 2013). Comparison of full genomes between associated and free-living sponge species would also allow us to determine if these symbiotic relationships have existed for long enough periods of time to cause a genome reduction in either sponge as observed in other symbiotic systems (Charles *et al.* 2011).

A transcriptomic approach would allow the determination of what genes are expressed in both lifestyles and provide insights into which genes involved in key physiological processes might be suppressed or enhanced by the association. A transcriptional approach could also be used as a proxy to determine which biological processes are more energy demanding, as discussed above. For example, monitoring silicatein gene expression in sponges from both

lifestyles would be important to determine whether smaller spicule production in associated sponges correlates with less copy numbers of silicatein genes than free-living *X. deweerdtae*. Silicatein gene expression might also help explain why *X. deweerdtae* is polymorphic in different geographic locations and whether silicatein gene expression correlates with higher levels of silicate in the environment (Krasko *et al.* 2000). Gene expression of heterospecifics in the pair will also help decipher whether these sponges are working independently, relying on each other, or cheating by using the other sponge's transcriptome to offset the demands of basic physiological functions. Similar approaches have been used to study how sponge transcriptomes change once they acquire important symbionts, such as *Symbiodinium* in Caribbean boring sponges (Riesgo *et al.* 2014).

Transcriptome analyses have also been used to study the impact of thermal stress on the physiology of sponges for different life stages (Webster et al. 2013) and on the expression of genes involved in nitrogen cycling (Lopez-Legentil *et al.* 2010). Using this approach in experiments with different treatment levels allows for a more sensitive approach to monitor the physiological response of sponges, especially since they are generally slow growers and can be difficult to study at a physiological level. Targeting the expression of heat shock protein 70 (HSP70) in *X. muta* and *R. odorabile* revealed that increasing temperatures correlated with increased expression of HSP70 indicating a stress response by the sponge. A transcriptomic analysis using HSP70 in both experiments simulating different climate change scenarios (Chapters 5 and 6) would help

reveal if sponges were stressed while exposed to different pCO_2 and temperature combinations. It would be particularly interesting to look at the different expression levels of HSP70 for the sponge pairs to determine whether one species was performing better (less stressed) than its pair when exposed to the different treatment levels. Monitoring the expression levels of silicatein genes in *M. grandis* when exposed to acidification and thermal stress may give us a more precise answer with a decreased coefficient of variation observed for the different morphological parameters evaluated in Chapter 6.

Identifying the two sponge species in the pair as HMA and LMA sponges inspires a series of hypotheses regarding food acquisition and pumping rates that require further experimentation to understand how these interactions influence the sponge symbioses. For example, HMA sponges in sponges from Florida have a higher density of choanocyte chambers than LMA sponges (Poppell *et al.* 2013). Popell and colleagues proposed that with a higher choanosome density, LMA sponges pump significantly more seawater than HMA sponges. Scanning electron microscopy in both sponge species in the pair would help reveal the number of choanosomes present in each sponge and if HMA sponges are using LMA sponges to offset the demands of pumping seawater.

Isotope analysis on bulk sponge tissue from both sponge pair species showed significant differences in $\delta^{13}C$ and $\delta^{15}N$ in some locations suggesting that these values are less influenced by the sponge microbiome and more by the surrounding environment. Using bulk sponge tissue combines both bacteria and sponge cells which limit our understanding of which partner in the sponge system

is producing or using compounds that would influence δ ^{13}C and δ ^{15}N niches (Thacker & Freeman 2012). Isotope analysis on separated sponge and bacterial cells would allow for a more accurate distinction of the isotopic niche spaces in both cell types in epibiont and basibiont sponges. This approach may also reveal whether the microbial community of one sponge is feeding the other sponge or if the metabolic waste products of one sponge are taken up by its partner.

In order to understand the microbial processes that are involved in each sponge species it is important to not only investigate the diversity of the microbial community using the 16S rRNA gene but also investigate diversity using functional genes. Of particular interest, is the investigation of genes involved in chemolithotrophic pathways as those observed in the recently classified Thaumarchaeota phyla (Brochier-Armanet *et al.* 2008), which had a high relative abundance in *X. deweerdtae*. All members of this phylum are chemolithotrophs that oxidize ammonia to nitrate while assimilating inorganic carbon (Vajrala *et al.* 2013). The microbial communities involved in ammonia oxidation in marine sponges has been well characterized by use of diversity and expression of the *amoA* gene (Webster *et al.* 2001; Bayer *et al.* 2008; Radax *et al.* 2012; Zhang *et al.* 2014) and even some members have even been known to be vertically transmitted from adult sponges to larvae (Steger *et al.* 2008). Monitoring biodiversity and expression of the *amoA* gene to compare between lifestyles of *X. deweerdtae* would provide insightful clues as to what the role of these symbionts in these sponge pairs are. Since Cyanobacteria were not detected in large numbers in sponge pairs it is unlikely that cyanobacterial nitrogen fixing

genes (i.e. *nifH*) or carbon fixation are contributing to nutrient production in these systems. Nitrogen fixation by other bacterial genera may be significant. Other genes involved in nitrogen metabolism like denitrification have also been detected in sponges (Siegl *et al.* 2011) and should be considered to help understand the cycling of nitrogen between sponge species in the pair. The anecdotal observations of polyphosphate granules in the tissues of *Plakortis* spp. motivates future work to screen sponges for the presence of polyphosphate kinase genes as well as quantification of these granules in proportion to the total phosphate present in both sponge tissues, following the Zhang *et al.* (2015) protocol.

I have discussed a number of hypotheses that should be tested in future studies in order to better understand the sponge pair interactions between *Plakortis* spp. basibionts and their *X. deweerdtae* and *H. plakophila* epibionts. This study provides novel findings of three new symbiotic adaptations between sponges. In this study I provide the foundational taxonomy of species, revealing three new sponge species for Porifera. I used bottom-up and top-down approaches to determine important factors that influence these associations. I also exposed sponge pairs to different climate change scenarios to better predict whether species that associate with other sponges are at an evolutionary advantage over free-living forms in a changing climate. The results support the conclusion that novel sponge symbioses are likely influenced by the restrictive physiological demands of either an HMA or LMA lifestyle that could likely apply to other well-known sponge pairs of the Caribbean.

Appendix 1: Supplementary material for Chapter 3.

Table A1.1 Sponge species and location of each sample collected for the sponge microbial community analysis

Species	Location	Latitude	Longitude	Country	DNA	n
P. symbiotica	La Parguera	17°53.297'N	66°59.887'W	Puerto Rico	cDNA	8
P. symbiotica	La Parguera	17°53.297'N	66°59.887'W		gDNA	11
P. halichondrioides	La Parguera	17°53.297'N	66°59.887'W		cDNA	3
P. halichondrioides	La Parguera	17°53.297'N	66°59.887'W		gDNA	4
X. deweerdtae AS	La Parguera	17°53.297'N	66°59.887'W		cDNA	3
X. deweerdtae AS	La Parguera	17°53.297'N	66°59.887'W		gDNA	3
X. deweerdtae FL	Desecheo	18°23.506'N	67°28.558'W		gDNA	1
H. plakophila	La Parguera	17°53.297'N	66°59.887'W		cDNA	4
H. plakophila	La Parguera	17°53.297'N	66°59.887'W		gDNA	5
Seawater	La Parguera	17°53.297'N	66°59.887'W		gDNA	3
*P. deweerdtaephila***	Dolphin Rock	9°21.207'N	82°11.132'W	Panama	gDNA	4
*P. halichondrioides***	Dolphin Rock	9°21.207'N	82°11.132'W		gDNA	4
P. halichondrioides *	Punta Caracol	9°22.690'N	82°18.230'W		gDNA	4
X. deweerdtae AS**	Dolphin Rock	9°21.207'N	82°11.132'W		gDNA	4
X. deweerdtae FL*	Punta Caracol	9°22.690'N	82°18.230'W		cDNA	1
X. deweerdtae FL*	Punta Caracol	9°22.690'N	82°18.230'W		gDNA	4
Seawater*	Punta Caracol	9°22.690'N	82°18.230'W		gDNA	3
P. deweerdtaephila	San Salvador	24°02.433'N	74°31.882'W	Bahamas	gDNA	4
X. deweerdtae AS	San Salvador	24°02.433'N	74°31.882'W		gDNA	3
X. deweerdtae FL	Plana Key	22°36.270'N	73°32.792'W		gDNA	1
Seawater	San Salvador	24°02.433'N	74°31.882'W		gDNA	3
Seawater	Plana Key	22°36.270'N	73°32.792'W		gDNA	3
X. deweerdtae FL	Cozumel	20°22.937'N	87°01.746'W	Mexico	gDNA	3
Seawater	Cozumel	20°22.937'N	87°01.746'W		gDNA	3

Table A1.2 ANOVA results of average OTU richness (*S*) compared between gDNA samples extracted from epibiont and basibiont sponge species collected in Puerto Rico, Bahamas and Mexico. Post-hoc Tukey pair-wise comparisons was performed for each species combination. For *X. deweerdtae*, AS-associated, FL-free-living. Significant *p*-values are in bold.

ANOVA	**df**	**SS**	**MS**	***F*-value**	***P***
Species	5	2890922	578184	29.91	**<0.0001**
Residuals	29	560666	19333	-	-
Tukey's HSD		**Diff**	**Lower 95 % conf. interval**	**Upper 95 % conf. interval**	**Adjusted *P* value**
Pdew-Hpla		841.4	557.0	1125.7	**0.0000**
Phal-Hpla		980.9	696.5	1265.2	**0.0000**
Psym-Hpla		644.4	415.8	873.0	**0.0000**
Xdew(FL)-Hpla		357.2	89.1	625.3	**0.0041**
Xdew(AS)-Hpla		610.4	353.8	867.1	**<0.0001**
Phal-Pdew		139.5	-160.2	439.2	0.7157
Psym-Pdew		-196.9	-444.4	50.6	0.1807
Xdew(FL)-Pdew		-484.2	-768.5	-199.8	**0.0002**
Xdew(AS)-Pdew		-230.9	-504.5	42.7	0.1366
Psym-Phal		-336.4	-583.9	-88.9	**0.0033**
Xdew(FL)-Phal		-623.7	-908.0	-339.3	**0.0000**
Xdew(AS)-Phal		-370.4	-644.0	-96.8	**0.0035**
Xdew(FL)-Psym		-287.2	-515.8	-58.6	**0.0076**
Xdew(AS)-Psym		-34.0	-249.1	181.1	0.9965
Xdew(AS)-Xdew(FL)		253.2	-3.4	509.9	0.0548

Table A1.3 ANOVA results of Inverse Simpson's Index (*D*) compared between gDNA samples extracted from epibiont and basibiont sponge species collected in Puerto Rico, Bahamas and Mexico. Post-hoc Tukey pair-wise comparisons was performed for each species combination. For *X. deweerdtae*, AS-associated, FL-free-living. Significant *p*-values are in bold.

ANOVA	**df**	**SS**	**MS**	***F*-value**	***P***
Species	5	18722	3744	69.04	**3.29E-15**
Residuals	29	1573	54		
Tukey's HSD		**Diff**	**Lower 95 % conf. interval**	**Upper 95 % conf. interval**	**Adjusted *P* value**
Pdew-Hpla		57.0	42.0	72.1	**0.0000**
Phal-Hpla		65.4	50.4	80.5	**0.0000**
Psym-Hpla		30.4	18.3	42.5	**0.0000**
Xdew(FL)-Hpla		3.1	-11.1	17.3	**0.9853**
Xdew(AS)-Hpla		5.7	-7.9	19.3	**0.7900**
Phal-Pdew		8.4	-7.5	24.3	0.5981
Psym-Pdew		-26.7	-39.8	-13.6	0.0000
Xdew(FL)-Pdew		-54.0	-69.0	-38.9	**0.0000**
Xdew(AS)-Pdew		-51.3	-65.8	-36.8	0.0000
Psym-Phal		-35.1	-48.2	-22.0	**0.0000**
Xdew(FL)-Phal		-62.4	-77.4	-47.3	**0.0000**
Xdew(AS)-Phal		-59.7	-74.2	-45.2	**0.0000**
Xdew(FL)-Psym		-27.3	-39.4	-15.2	**0.0000**
Xdew(AS)-Psym		-24.6	-36.0	-13.2	0.0000
Xdew(AS)-Xdew(FL)		2.7	-10.9	16.3	0.9902

Table A1.4 ANOVA results of Shannon indices (*H'*) compared between gDNA samples extracted from epibiont and basibiont sponge species collected in Puerto Rico, Bahamas and Mexico. Post-hoc Tukey pair-wise comparisons was performed for each species combination. For *X. deweerdtae*, AS-associated, FL-free-living. Significant *p*-values are in bold.

ANOVA	**df**	**SS**	**MS**	***F*-value**	***P***
Species	5	20	4	37.4	**8.70E-12**
Residuals	29	3	0		
Tukey's HSD		**Diff**	**Lower 95 % conf. interval**	**Upper 95 % conf. interval**	**Adjusted *P* value**
Pdew-Hpla		2.3	1.6	3.0	**0.0000**
Phal-Hpla		2.4	1.8	3.1	**0.0000**
Psym-Hpla		1.8	1.2	2.3	**0.0000**
Xdew(FL)-Hpla		0.9	0.2	1.5	**0.0029**
Xdew(AS)-Hpla		1.5	0.9	2.1	**0.0000**
Phal-Pdew		0.2	-0.6	0.9	0.9864
Psym-Pdew		-0.5	-1.1	0.1	0.1128
Xdew(FL)-Pdew		-1.4	-2.1	-0.8	**0.0000**
Xdew(AS)-Pdew		-0.8	-1.4	-0.1	**0.0094**
Psym-Phal		-0.7	-1.2	-0.1	**0.0195**
Xdew(FL)-Phal		-1.6	-2.2	-0.9	**0.0000**
Xdew(AS)-Phal		-0.9	-1.6	-0.3	**0.0015**
Xdew(FL)-Psym		-0.9	-1.5	-0.4	**0.0002**
Xdew(AS)-Psym		-0.3	-0.8	0.2	0.5486
Xdew(AS)-Xdew(FL)		0.6	0.0	1.2	**0.0386**

Table A1.5 ANOVA results of OTU richeness (*S*), inverse Simpson's index (*D*), and Shannon index (*H'*) compared between gDNA samples extracted from epibiont and basibiont sponge species collected in Panama. Post-hoc Tukey pair-wise comparisons was performed for each species combination. For *X. deweerdtae*, AS-associated, FL-free-living. Samples were collected in Dolphin Rock (DR) and Punta Caracol (PC). Significant *p*-values are in bold.

Diversity Index	ANOVA	df	SS	MS	*F*-value	*P*-value
S	Species	4	380897	95224	8	**0.0012**
	Residuals	15	178923	11928	-	-
	Tukey's HSD		**Diff**	**Lower 95 % conf. interval**	**Upper 95 % conf. interval**	**Adjusted *P* value**
	XdewASDR-PdewDR		370.0	131.5	608.5	**0.0019**
	XdewASDR-PhalDR		367.0	128.5	605.5	**0.0020**
	XdewASDR-PhalPC		253.0	14.5	491.5	**0.0351**
	XdewFLPC-XdewASDR		-323.8	-562.2	-85.3	**0.0060**
D	Species	4	9719	2430	74.7	**<0.0001**
	Residuals	15	488	33		
	Tukey's HSD		**Diff**	**Lower 95 % conf. interval**	**Upper 95 % conf. interval**	**Adjusted *P* value**
	PhalDR-PdewDR		16.9	4.5	29.4	**0.0059**
	PhalPC-PdewDR		22.2	9.7	34.6	**0.0005**
	XdewASDR-PdewDR		-23.4	-35.9	-11.0	**0.0003**
	XdewFLPC-PdewDR		-34.2	-46.7	-21.8	**0.0000**
	XdewASDR-PhalDR		-40.4	-52.8	-27.9	**0.0000**
	XdewFLPC-PhalDR		-51.1	-63.6	-38.7	**0.0000**
	XdewASDR-PhalPC		-45.6	-58.1	-33.2	**0.0000**
	XdewFLPC-PhalPC		-56.4	-68.8	-43.9	**0.0000**
H'	Species	4	7	2	35.6	**<0.0001**
	Residuals	15	1	0		
	Tukey's HSD		**Diff**	**Lower 95 % conf. interval**	**Upper 95 % conf. interval**	**Adjusted *P* value**
	XdewFLPC-PdewDR		-1.4	-1.9	-0.9	**0.0000**
	XdewFLPC-PhalDR		-1.6	-2.1	-1.1	**0.0000**
	XdewASDR-PhalPC		-0.4	-0.9	0.1	**0.1308**
	XdewFLPC-PhalPC		-1.7	-2.2	-1.2	**0.0000**
	XdewFLPC-XdewASDR		-1.3	-1.8	-0.8	**0.0000**

Table A1.6 ANOVA results of mean differences in relative abundance of microbial phyla between gDNA and cDNA samples extracted from sponges collected in Puerto Rico. Microbial phyla that shifted between gDNA and cDNA samples for each species were selected. Significant *p*-values are in bold.

Sponge	ANOVA	df	SS	MS	*F*-value	*P*-value
X. deweerdtae	Chloroflexi	1	31.07	31.07	1.81	0.2490
associated	Residual	4	68.56	17.14	-	-
	Cyanobacteria	1	223.36	223.36	9.98	**0.0342**
	Residual	4	89.57	22.39	-	-
	Thaumarchaeota	1	266.10	266.06	9.74	**0.0355**
	Residual	4	109.20	27.31	-	-
H. plakophila	Unid. Proteobacteria	1	367.90	367.90	2.98	0.1280
	Residual	7	864.60	123.50		
	Chloroflexi	1	13.36	13.36	183.60	**<0.0001**
	Residual	7	0.51	0.07	-	-
	Cyanobacteria	1	74.22	74.22	2.88	0.1340
	Residual	7	180.49	25.78	-	-
	Alphaproteobacteria	1	499.00	499.00	3.84	0.0909
	Residual	7	910.00	130.00	-	-
P. symbiotica	Chloroflexi	1	1413	1413.4	21.14	**0.0003**
	Residuals	17	1137	66.9	-	-
	Thaumarchaeota	1	264.7	264.74	6.766	**0.0186**
	Residual	17	665.2	39.13	-	-
	Alphaproteobacteria	1	67.34	67.34	12.15	**0.0028**
	Residuals	17	94.24	5.54	-	-
	Unid. bacteria	1	637.7	637.7	16.18	**0.0009**
	Residual	17	669.9	39.4	-	-
P. halichondrioides	Chloroflexi	1	76.2	76.2	7.984	**0.0369**
	Residuals	5	47.72	9.54	-	-
	Thaumarchaeota	1	35.39	35.39	24.49	**0.0043**
	Residual	5	7.23	1.45	-	-
	Alphaproteobacteria	1	21.019	21.019	14.86	**0.0120**
	Residuals	5	7.075	1.42	-	-
	Cyanobacteria	1	14.576	14.576	10.43	**0.0232**
	Residual	5	6.988	1.398	-	-

Table A1.7 ANOVA results of mean $\delta^{13}C$ and $\delta^{15}N$ value differences collected from tissue of sponge pair species, free-living *Xestospongia deweerdtae* and *Plakortis halichondrioides*. Each ANOVA was performed separately on each sampling location (Puerto Rico, Panama, and Bahamas). Significant *p*-values are in bold.

Site	ANOVA	df	SS	MS	*F*-value	*P*
Puerto Rico	$\delta^{13}C$	2	28.90	14.45	10.06	**0.0121**
	Residual	6	8.62	1.44	-	-
	$\delta^{15}N$	2	16.37	8.19	6.73	**0.0293**
	Residuals	6	7.30	1.22	-	-
Panama	$\delta^{13}C$	4	2.97	0.74	12.07	**0.0008**
	Residuals	10	0.61	0.06	-	-
	$\delta^{15}N$	4	7.78	1.94	6.66	**0.0070**
	Residuals	10	2.92	0.29	-	-
Bahamas	$\delta^{13}C$	3	1.54	0.51	1.93	0.2030
	Residual	8	2.12	0.27		
	$\delta^{15}N$	3	9.65	3.22	23.10	**0.0003**
	Residuals	8	1.11	0.14	-	-

Table A1.8 Significant Tukey's post-hoc HSD pairwise comparison of significant ANOVA outcomes on mean $\delta^{13}C$ and $\delta^{15}N$ value differences collected from sponge pair species, free-living *Xestospongia de*weerdtae and *Plakortis halichondrioides*. Each pair-wise comparison was performed separately on each sampling location (Puerto Rico, Panama, and Bahamas). For *Xestospongia deweerdtae* AS-associated and FL-free-living. Collection site DR-Dolphin Rock, PC-Punta Caracol. There were no significant differences between mean $\delta^{13}C$ from samples collected in Puerto Rico.

Location	Isotope	Species comparisons	Diff	Lower 95 % conf. interval	Upper 95 % conf. interval	Adjusted *P*-value
Puerto	$\delta^{13}C$	*Psym-Hpla*	-4.02	-7.02	-1.01	0.0149
Rico		*XdewAS-Psym*	3.54	0.54	6.54	0.0258
	$\delta^{15}N$	*Psym-Hpla*	-3.06	-5.83	-0.30	0.0333
Panama	$\delta^{13}C$	*PhalPC-PdewDR*	1.32	0.65	1.98	0.0005
		PhalPC-PhalDR	0.70	0.03	1.36	0.0395
		XdewASDR-PhalPC	-1.07	-1.73	-0.40	0.0026
		XdewFLPC-PhalPC	-0.70	-1.37	-0.04	0.0373
	$\delta^{15}N$	*XdewASDR-PhalDR*	1.57	0.12	3.02	0.0329
		XdewFLPC-PhalDR	1.54	0.09	3.00	0.0361
		XdewASDR-PhalPC	1.63	0.18	3.08	0.0267
		XdewFLPC-PhalPC	1.60	0.15	3.05	0.0293
Bahamas	$\delta^{15}N$	*Phal-Pdew*	-1.46	-2.44	-0.48	0.0060
		XdewAS-Pdew	1.06	0.09	2.04	0.0336
		XdewFL-Phal	1.45	0.47	2.42	0.0063
		XdewAS-Phal	2.52	1.55	3.50	0.0002
		XdewAS-XdewFL	1.07	0.10	2.05	0.0319

Appendix 2: Supplementary material for Chapter 5.

Figure A2.1. Seawater pH_T and temperature values for the acclimation period. Mean and standard error of daily seawater pH_T (a) and temperature (b) measurements of experimental tanks for each treatment (indicated by the legend) throughout the 27-day acclimation period. Measurements were taken at 8 AM. Measurements were not taken during days 2-8.

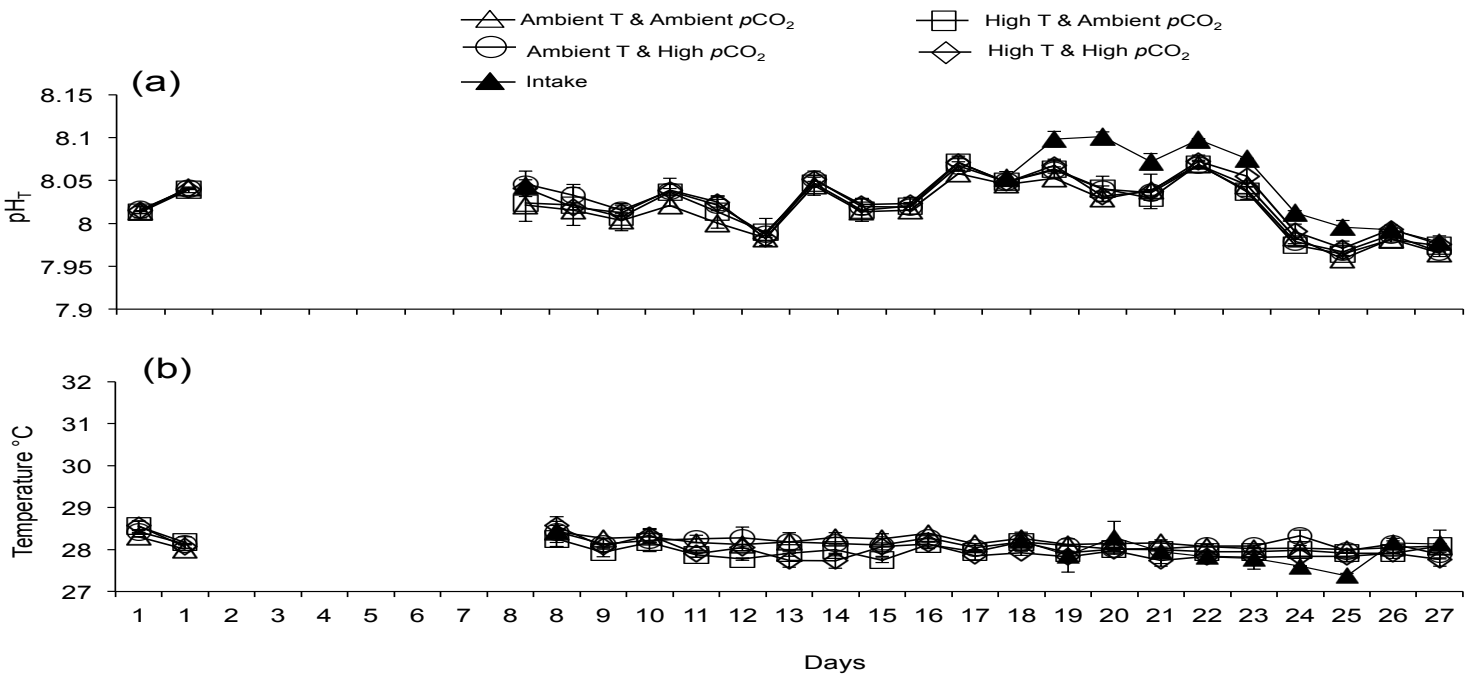

Figure A2.2 Experimental seawater pH_T and temperature values. Mean and standard error of daily seawater pH_T (a) and temperature (b) measurements of experimental tanks for each treatment (indicated by the legend) throughout the 35 day experimental period. Measurements were taken at 8:00 and 16:00 every day.

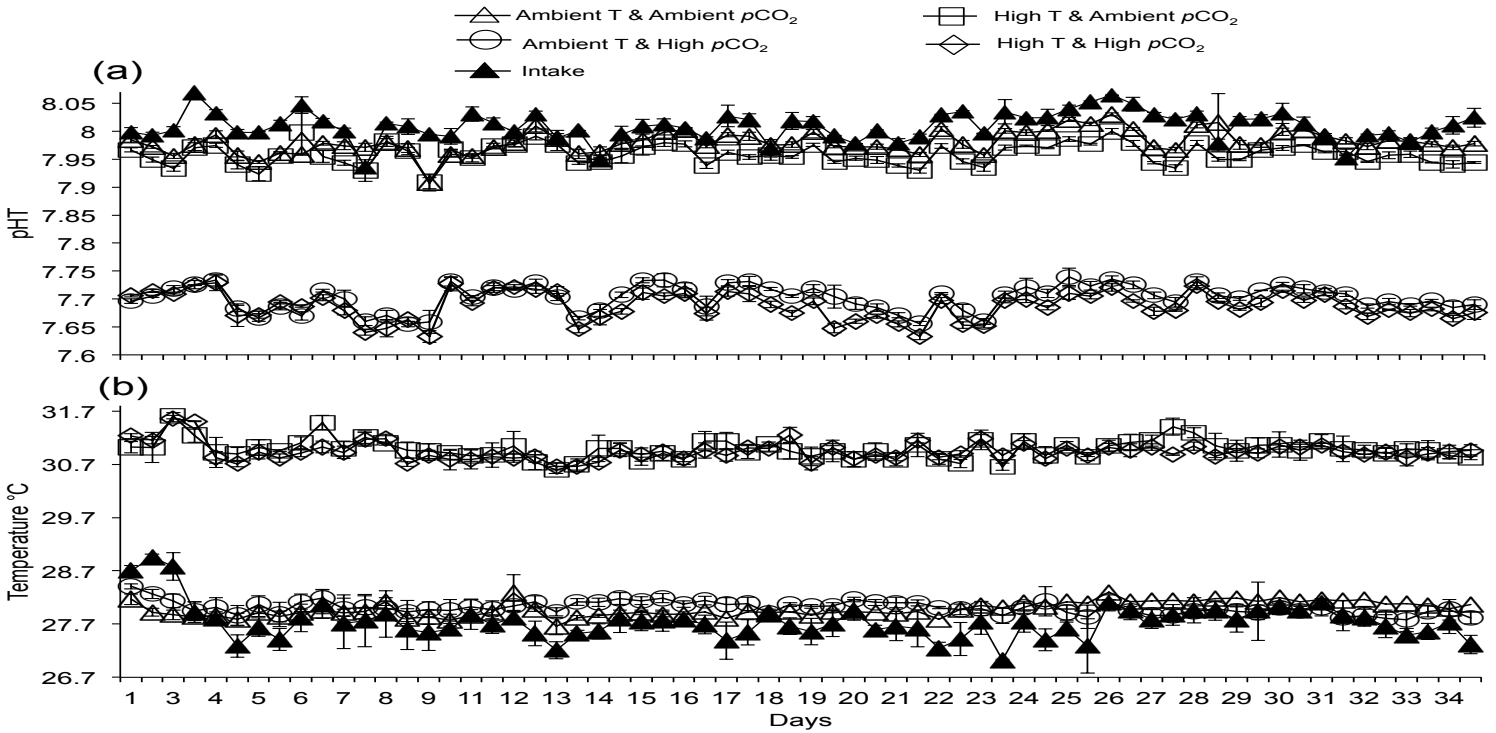

Figure A2.3 Experimental seawater pCO_2 and A_T values. Mean and standard error of seawater pCO_2 (a) and A_T (b) measurements of experimental tanks for each treatment (indicated by the legend) throughout the 35 day experimental period. Measurements were taken at 8:00 every 3 days. Measurements were not taken during days 31-35.

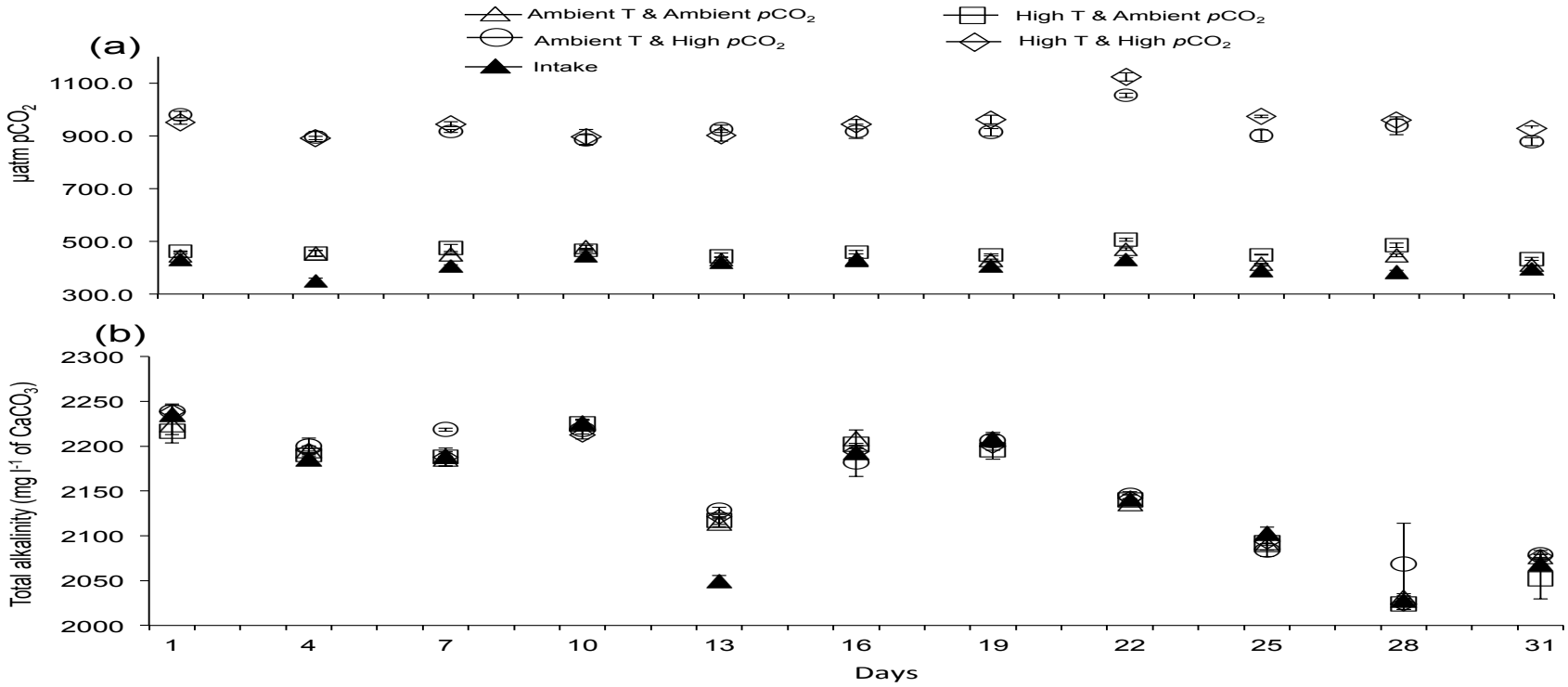

Table A2.1 Two-way ANOVA results for experimental seawater temperatures and pCO_2. Results of the analysis of variance (two-way ANOVA) of temperature and pCO_2 values from the four treatments, and time followed by the results of the post hoc Tukey's HSD pairwise comparison of the treatment main effect. Statistically significant results are indicated by the *p*-values in bold.

Response	ANOVA	df	SS	MS	*F*-value	*P*-value
Temperature	(Intercept)	3	1.01E-03	3.37E-04	2369.7	**<0.0001**
	Treatment	10	9.08E-06	9.10E-07	6.38	**<0.0001**
	Time	30	8.67E-06	2.90E-07	2.03	**<0.0001**
	Residuals	88	1.25E-05	1.40E-07		
pCO_2	(Intercept)	3	1.04E-02	3.47E-03	6810.8	**<0.0001**
	Treatment	10	1.28E-04	1.28E-05	25.2	**<0.0001**
	Time	30	6.07E-05	2.00E-06	3.97	**<0.0001**
	Residuals	88	4.48E-05	5.00E-07		
	Tukey's HSD		**Estimate**	**SE**	**t-value**	**Pr(>|t|)**
Temperature	Amb. T & High pCO_2 vs Amb. T & Amb. pCO_2		-4.73E-04	3.08E-04	-1.54	0.421
	High T & High pCO_2 vs Amb. T & Amb. pCO_2		-5.61E-03	3.08E-04	-18.22	**<0.0001**
	High T & Amb. pCO_2 vs Amb. T & Amb. pCO_2		-5.25E-03	3.08E-04	-17.06	**<0.0001**
	High T & High pCO_2 vs Amb. T & High pCO_2		-5.14E-03	3.08E-04	-16.69	**<0.0001**
	High T & Amb. pCO_2 vs Amb. T & High pCO_2		-4.78E-03	3.08E-04	-15.53	**<0.0001**
	High T & Amb. pCO_2 vs High T & High pCO_2		3.58E-04	3.08E-04	1.16	0.652
pCO_2	Amb. T & High pCO_2 vs Amb. T & Amb. pCO_2		-1.90E-02	5.83E-04	-32.66	**<0.0001**
	High T & High pCO_2 vs Amb. T & Amb. pCO_2		-1.83E-02	5.83E-04	-31.48	**<0.0001**
	High T & Amb. pCO_2 vs Amb. T & Amb. pCO_2		-8.88E-04	5.83E-04	-1.52	0.428
	High T & High pCO_2 vs Amb. T & High pCO_2		6.86E-04	5.83E-04	1.18	0.643
	High T & Amb. pCO_2 vs Amb. T & High pCO_2		1.81E-02	5.83E-04	31.13	**<0.0001**
	High T & Amb. pCO_2 vs High T & High pCO_2		1.75E-02	5.83E-04	29.96	**<0.0001**

Table A2.2. ANOVA results of the percent of mass loss between free-living *Xestospongia deweerdtae* and the *X. deweerdtae* + *Plakorits deweerdtaephila* pairs. Results of the analysis of variance (three-way ANOVA). of the percent of mass loss based on pCO_2, temperature and lifestyle.

ANOVA	df	SS	MS	*F*-value	*P*-value
Temperature	1	6.78	6.78	2.593	0.1281
pCO_2	1	0.06	0.06	0.023	0.8806
Lifestyle	1	48.02	48.02	18.379	**0.0007**
Temperature * pCO_2	1	0.09	0.09	0.035	0.8534
Temperature * Lifestyle	1	0.19	0.19	0.075	0.7885
pCO_2 * Lifestyle	1	0.01	0.01	0.003	0.9557
Temperature * pCO_2 * Lifestyle	1	0.05	0.05	0.019	0.8922
Residuals	15	39.19	2.61	-	-

Table A2.3 ANOVA results on average spicule length differences of free-living *Xestospongia deweerdtae*, associated *X. deweerdtae,* and *Plakortis deweerdtaephila*. Results of the analysis of variance (three-way ANOVA) of average spicule length differences of strongyles from *X. deweerdtae* FL (*XD*FL), *X. deweerdtae* AS (*XD*AS) and diods from *P. deweerdtaephila* (*PD*) based on pCO_2, temperature and species. A post-hoc Tukey's HSD pairwise comparisons were performed on the Species main effect.

ANOVA	**df**	**SS**	**MS**	***F*-value**	***P*-value**
Temperature	1	0.16	0.16	0.04	0.8401
pCO_2	1	0.04	0.04	0.01	0.9236
Species	2	34.08	17.04	4.52	**0.0215**
Temperature * pCO_2	1	0.31	0.31	0.08	0.7758
Temperature * Species	2	2.03	1.02	0.27	0.7659
pCO_2 * Species	2	1.58	0.79	0.21	0.8127
Temperature * pCO_2 * Species	2	0.28	0.14	0.04	0.9634
Residuals	24	90.40	3.77	-	-
Tukey's HSD		**Diff**	**Lower 95 % conf. interval**	**Upper 95 % conf. interval**	**Adjusted *P* value**
*XD*AS vs. *PD*		-2.17	-4.15	-0.19	**0.0294**
*XD*FL vs. *PD*		-1.93	-3.91	0.04	**0.0561**
*XD*FL vs. *XD*AS		0.24	-1.74	2.22	0.9517

Table A2.4 Results of the two-way ANOVA for the treatment × time on necrotic tissue progress rate of free-living *Xestospongia deweerdtae*, associated *X. deweerdtae, P. deweerdtaephila* and the *X.* deweerdtae + *P. deweerdtaephila* (pair). ANOVA results indicate that time had a significant main effect on all sponge species except for *X. deweerdtae* AS. The post hoc chisquare test on the treatment × time interaction was only significant for *X. deweerdtae* FL and *P. deweerdtaephila*. Significant ANOVA and post hoc pairwise comparisons are indicated by *p* values in bold.

ANOVA	**Factors and interactions**	**df**	**Df.res**	***F*-value**	***P*-value**
X. deweerdtae FL	Treatment	3	8	0.39	0.3932
	Time	3	24	0.00	**<0.0001**
	Treatment * Time	9	24	0.04	**0.0433**
X. deweerdtae AS	Treatment	3	8	1.10	0.4037
	Time	3	24	2.74	0.0655
	Treatment * Time	9	24	0.93	0.5172
P. deweerdtaephila	Treatment	3	8	8.84	**0.0064**
	Time	3	24	7.91	**0.0008**
	Treatment * Time	9	24	2.48	**0.0368**
Sponge pair	Treatment	3	8	5.50	**0.0240**
	Time	3	24	6.48	**0.0023**
	Treatment * Time	9	24	2.36	**0.0452**
Post-hoc (Chisquare test)		**df**	**Value**	**Chisq**	**P-value**
*XD*FL Treatment*Time	Amb. T & Amb. pCO_2 - High T & High pCO_2 : 15-29 days	1	46.33	11.67	**0.0228**
*PLAS*FL Treatment*Time	Amb. T & High pCO_2 - Hight T & Amb. pCO_2 : 8-29 days	1	46.67	10.50	**0.0429**
	Amb. T & Amb. pCO_2 - Hight T & Amb. pCO_2 : 8-29 days	1	43.67	9.20	0.0849

Table A2.5 Results of the three-way ANOVA for the treatment × time × species interaction on necrotic tissue progress rate of free-living *Xestospongia deweerdtae*, associated *X. deweerdtae, Plakortis deweerdtaephila* and the *X.* deweerdtae + *P. deweerdtaephila* (pair). ANOVA results indicate all factors and interactions had a significant effect on necrotic tissue progress rate. The post hoc chisquare test on the treatment × time × species interaction was only significant for high temperature treatment interactions between *X. deweerdtae* FL vs. *X. deweerdtae* AS and *X. deweerdtae* FL vs. Sponge pair. Significant ANOVA and post hoc pairwise comparisons are indicated by p values in bold.

ANOVA	**Factors and interactions**	**df**	**Df.res**	***F*-value**	***P*-value**
	Treatment	3	8	9.49	**0.0052**
	Time	3	120	27.41	**<0.0001**
	Species	3	120	55.46	**<0.0001**
	Treatment*time	9	120	6.46	**<0.0001**
	Treatment*species	9	120	3.68	**0.0004**
	Time*species	9	120	7.17	**<0.0001**
	Treatment*time*species	27	120	2.02	**0.0053**
Post-hoc (Chisquare test)		**df**	**Value**	**Chisq**	**P-value**
Treatment*Time*Species	High T & High pCO_2 - High T & Amb. pCO_2 : 15-29 days : *XD*AS-*XD*FL	1	327	14.38	**0.0319**
	Amb. T & High pCO_2 - High T & Amb. pCO_2 : 8-29 days : *PLXD*AS-*XD*FL	1	348.00	16.29	**0.0118**
	Hight T & High pCO_2 - High T & Amb. pCO_2 : 15-29 days : *PLXD*AS-*XD*FL	1	327.67	14.44	**0.0311**

Table A2.6: ANOVA results from the pCO_2 × temperature × species interaction on total necrotic tissue progress rate of free-living *Xestospongia deweerdtae*, associated *X. deweerdtae, Plakortis deweerdtaephila* and the *X.* deweerdtae + *P. deweerdtaephila* (pair). Results from the analysis of variance (three-way ANOVA) of total disease progress rate on *Xestospongia deweerdtae* FL (*XD*FL), *X. deweerdtae* AS (*XD*AS), *Plakortis deweerdtaephila* (*PD*) and the *X. deweerdtae* AS + *P. deweerdtaephila* sponge pair (*PDXD*AS) based on pCO_2, temperature and species. Post hoc pairwise comparisons were performed on significant main effects (Tukey's HSD) and interactions (Chisquare test).

ANOVA	**Factors and interactions**		**df**	**Df.res**	***F*-value**	***P*-value**
	Temperature		1	8	18.26	**0.0027**
	pCO_2		1	8	4.12	0.0768
	Species		3	24	35.78	**<0.0001**
	Temperature * pCO_2		1	8	10.12	**0.0130**
	Temperature * Species		3	24	6.87	**0.0017**
	pCO_2 * Species		3	24	2.28	0.1050
	Temperature * pCO_2 * Species		3	24	1.29	0.2993
Tukey's post hoc (main effect)		**Est.**	**df**	**SE**	**t ratio**	**P-value**
Temperature	Temp H-L	20.08	8	4.7	4.27	**0.0027**
Species	*PD-PDXD*AS	-11.75	24	3.14	-3.75	**0.0051**
	*PD-XD*AS	1.33	24	3.14	0.43	0.9736
	*PD-XD*FL	-27.25	24	3.14	-8.69	**<.0001**
	*PDXD*AS-*XD*AS	13.08	24	3.14	4.17	**0.0018**
	*PDXD*AS-*XDFL*	-15.50	24	3.14	-4.94	**0.0003**
	*XD*AS-*XD*FL	-28.58	24	3.14	-9.12	**<.0001**
Chisquare test Post hoc (interaction)			**df**	**Value**	**Chisq**	**P-value**
Temperature*pCO_2	Temp H-L: pCO_2 H-L		1	-34.00	10.12	**0.0014**
Temperature * Species	Temp H-L: *PD-PLXD*AS		1	-7.50	0.59	0.8840
	Temp H-L: *PD-XD*AS		1	26.00	7.10	**0.0231**
	Temp H-L: *PD-XD*FL		1	28.17	8.34	**0.0155**
	Temp H-L: *PDXD*AS-*XD*AS		1	33.50	11.79	**0.0030**
	Temp H-L: *PDXD*AS-*XDFL*		1	35.67	13.37	**0.0015**
	Temp H-L: *XD*AS-*XDFL*		1	2.17	0.05	0.8840

Table A2.7: ANOVA results from the treatment × species effect on total necrotic tissue progress rate of free-living *Xestospongia deweerdtae*, associated *X. deweerdtae, Plakortis deweerdtaephila* and the X. deweerdtae + *P. deweerdtaephila* (pair). Significant differences from the treatment × species interaction on the mean of the total necrotic tissue progress rate is indicated by p values in bold.

ANOVA	**Factors and interactions**	**df**	**Df.res**	***F*-value**	**P-value**
	Treatment	3	8	8.02	**0.0085**
	Species	3	24	35.78	**<0.0001**
	Treatment * Species	9	24	3.05	**0.0139**
Post-hoc (Chisquare Test)		**df**	**Value**	**Chisq**	**P-value**
Treatment * Species	Amb. T & High pCO_2 - High T & Amb. pCO_2 : *PD-XD*FL	1	-45.67	11.77	**0.0211**
	Amb. pCO_2 & Amb.. T-Amb. pCO_2 & High T:*PDXD*AS-*XD*FL	1	-44.67	11.26	**0.0270**
	High pCO_2 & Amb. T-Amb. pCO_2 & High T:*PDXD*AS-*XD*FL	1	-55.67	17.49	**0.0010**

Table A2.8: ANOVA results from the treatment × time effect on *Xestospongia deweerdtae* AS / *Plakortis deweerdtaephila* healthy tissue ratio differences. There were no significant differences Significant differences from the treatment × time interaction on the mean of the total necrotic tissue progress rate is indicated by p values in bold.

ANOVA	df	SS	MS	*F*-value	*P*
Treatment	3	0.0926	0.0309	13.26	**<0.0001**
Time	1	0.0002	0.0002	0.09	0.7710
Treatment * time	3	0.0091	0.0030	1.30	0.2850
Residuals	52	0.1210	0.0023	-	-

Appendix 3: Supplemental material for Chapter 6

Supplementary methods

DNA extraction and sequencing for phylogenetic analysis

Sponge samples (30 mg) of *M. grandis* were fixed with RNAlater and frozen at -80°C. DNA was extracted using Qiagen's AllPrep DNA/RNA Mini Kit. Primers (18SMycale) used by (Loh et al. 2012) were used to amplify a partial fragment of the 18S rRNA. There was coamplification of multiple genes and internal primers (18SMGRF 5'-AATAGCGTATATTAAAGTTGTTGC-3'/ 18SMGRR 5'-ACGGCCTGCCTTGAACACTCT-3') were designed to get the partial fragment (454 bp) of interest to compare to the 18S rRNA sequences of other *M. grandis* voucher samples. To amplify a partial (385 bp) fragment of the 28S rRNA, primer 28sCallyF 5'-TGCGACCGAAAGATGGTGAACTA-3' and reverse primer 28sCallyR 5'-ACCAACACCTTTCCTGGTATCTGC-3' were used (López-Legentil et al. 2010). Polymerase chain reactions (PCR) were carried out using a total volume of 50 µl and included 39.3 µl of H_2O, 1 µl of each primer (10 mM), 1 µl of dNTPs (10 mM), 5 µl of 10X Buffer, 1.5 µl of $MgCl_2$ (50 mM), 0.2 µl of Platinum Taq polymerase, 1 µl of template DNA (30 µM). An initial denaturation was ran at 94°C for 2 min followed by 35 cycles of 94°C for 30 s and annealing at 48°C. A final extension for 72°C followed. Final PCR products were ran in a 1% agarose gel and purified using the Qiaquick Gel Extraction Kit (Qiagen). Sequencing reactions were performed using the BigDye TM terminator v. 3.1 with species specific PCR primers and sequenced using an ABI Prism 2100 automated sequencer.

Phylogenetic analysis of *Mycale grandis*

Sequences were edited using Sequencher where the “trim ends” option was used to remove sequences in the priming region. Forward and reverse sequences were assembled in contigs and edited. Contigs were exported as fasta files and used in MEGA 5 (Tamura et al. 2011) to align sequences using the ClustalW function with default parameters. The top five closest relatives to these sequences were found by searching in GenBank using the BLAST function. The references sequences were used to generate the alignment for each gene. Fragments of each aligned gene were joined and concatenated trees were generated using neighbor-joining (NJ), maximum likelihood (ML) and maximum parsimony (MP) analyses. The NJ analysis was ran using a maximum composite likelihood model of nucleotide substitution to include Transitions + Transversions with a 1,000 bootstrap replicates resampled. The MP analysis was conducted using a heuristic search with a subtree pruning re-grafting method using 10 random addition replicates. A Close-Neighbor-Interchange branch – swapping algorithm was used, and data resampled using 1,000 bootstrap replicates. The Tamura Nei model with uniform rates among sites was used to run the ML analysis (Tamura & Nei 1993). The nearest-neighbor interchange ML heuristic method with data resampled using 1,000 bootstrap replicates was used. Sequences were deposited in GenBank under accession numbers (KR349620.1-KR349622.1).

Supplemental Results

Molecular phylogeny of *Mycale grandis*

The concatenated phylogenetic tree using partial sequences of 18S (454 bp) and 28S rRNA (384 bp) is shown in Fig. A2.1. We found that the closest concatenated sequences to the 18S/28S rRNA genes of *Mycale* sp. individuals used in our study were those of *M. grandis* (voucher Mgra) GenBank accession no. GU208840.1 for 18S rRNA and GU324506.1 for 28S rRNA. Our samples showed (99% identity, 100% coverage) for 18S rRNA and (100% identity, 100% coverage) for 28S rRNA to *M.* grandis. The second closest concatenated sequences were those of *Mycale* sp.1 (voucher 20110805-80) GenBank accession no. KC505235.1 for 18S rRNA and 100% identity, 100% coverage for 18S rRNA and 99% identity, 100% coverage for 28S rRNA. When comparing 421 bp of the 28S rRNA of these sequences to those of *Mycale* sp. 1, 99% identity was observed but with 4 bp (417/421) mismatches. The phylogenetic tree showed bootstrap values (88/93/82) supporting a split between *Mycale* sp. 1 to the *M. grandis* clade. We therefore confirmed that the sponge under investigation is *M. grandis*.

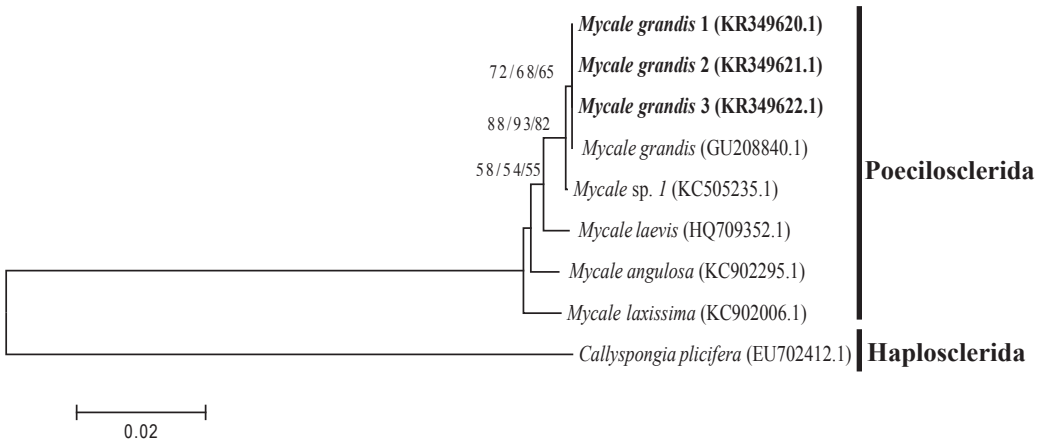

Figure A3.1 Concatenated phylogenetic tree generated from an alignment of 454 bp of the 18S rRNA gene and 385 bp of the 28S rRNA gene of three of *Mycale grandis* (bold) sequenced in this study. Reference sequences downloaded from GenBank are indicated by species name (italics) and 18SrRNA accession numbers. The tree topology was obtained from neighbor-joining (NJ) analysis. Well supported clades (bootstrap values >50) are labeled from NJ, maximum likelihood (ML) and maximum parsimony (MP).

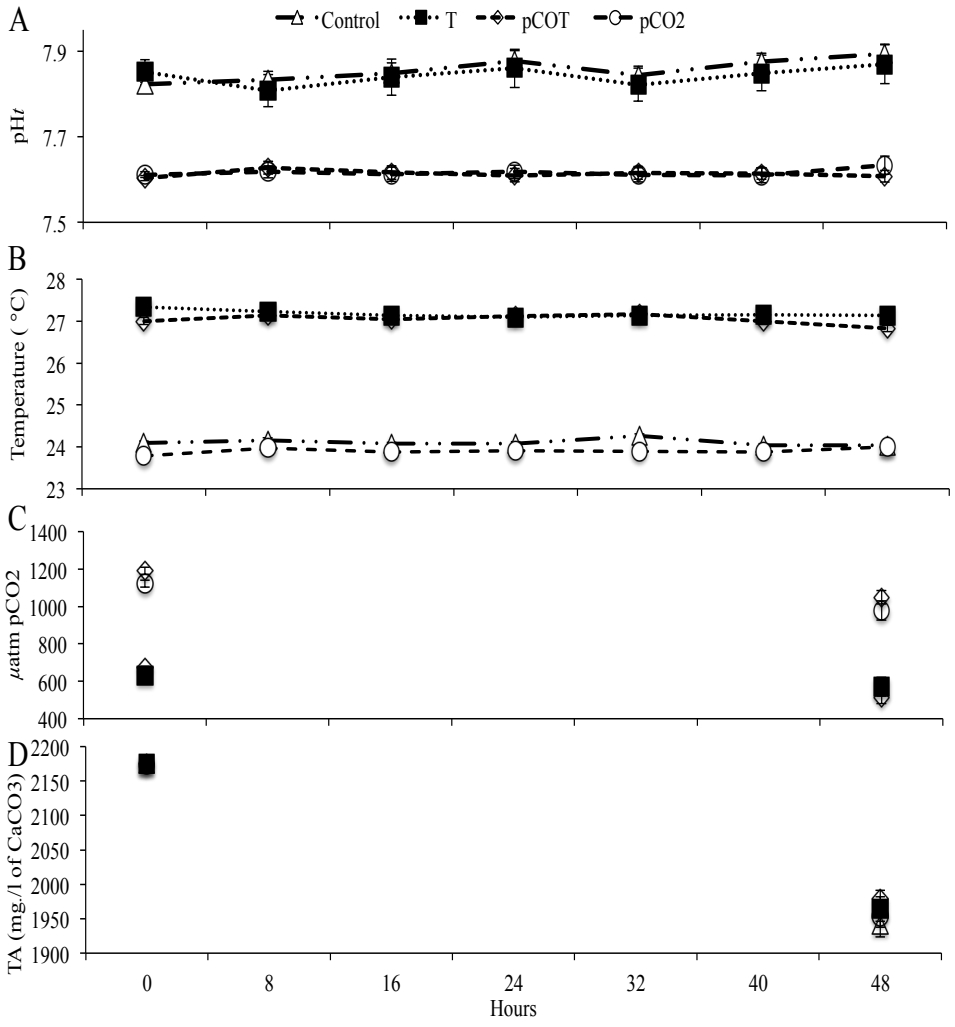

Figure A3.2 Seawater pH (A), temperature (B), pCO_2 and total alkalinity (D) measurements throughout the 48 hour experimental period. For each time period Duncan's multiple range test (DMRT) (p=0.05) indicated that treatments Control and T had higher pH values (lower pCO_2 values) than pCO_2 and pCO_2T treatments while total alkalinity remained constant.

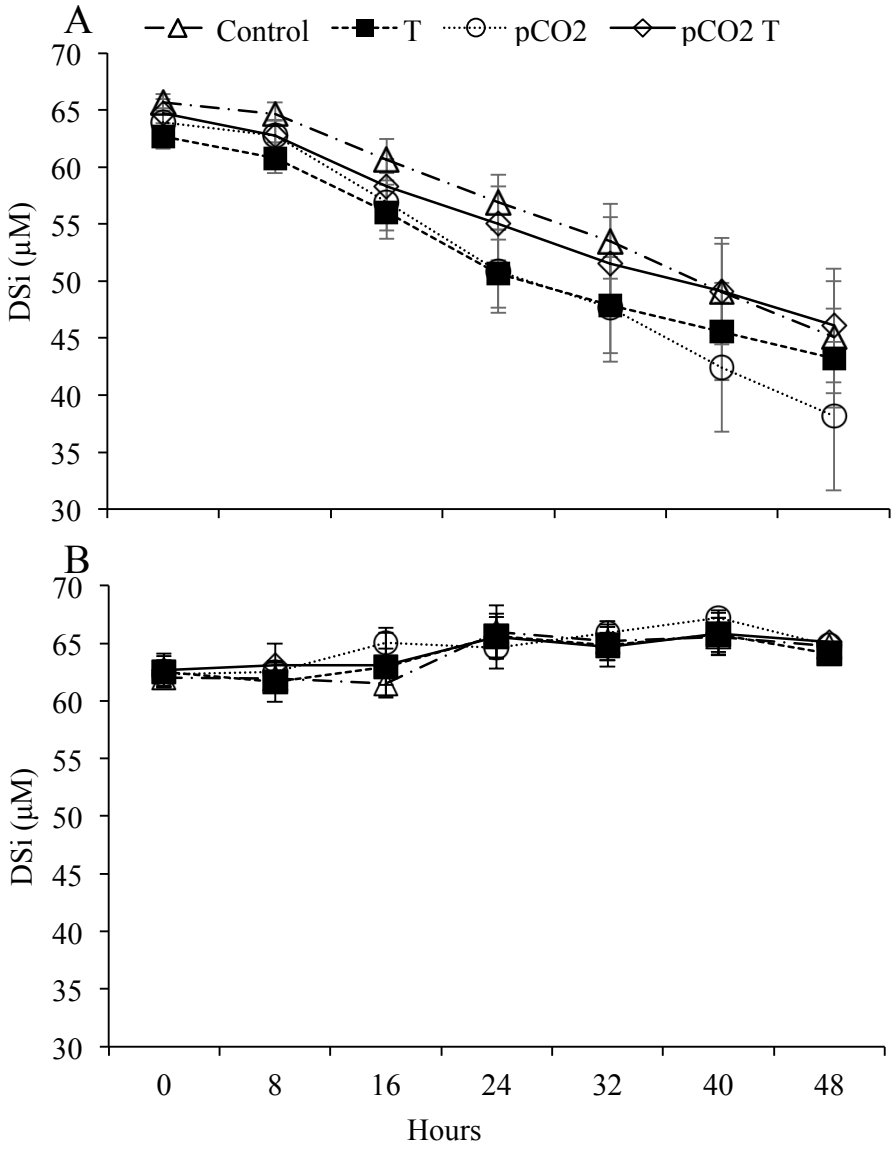

Figure A3.3 DSi negative control experiment to make sure that filtered seawater was free of diatoms. DSi uptake experiments were performed on incubation chambers (A) with sponges (normalized to AFDW) and (B**)** empty incubation chamber.

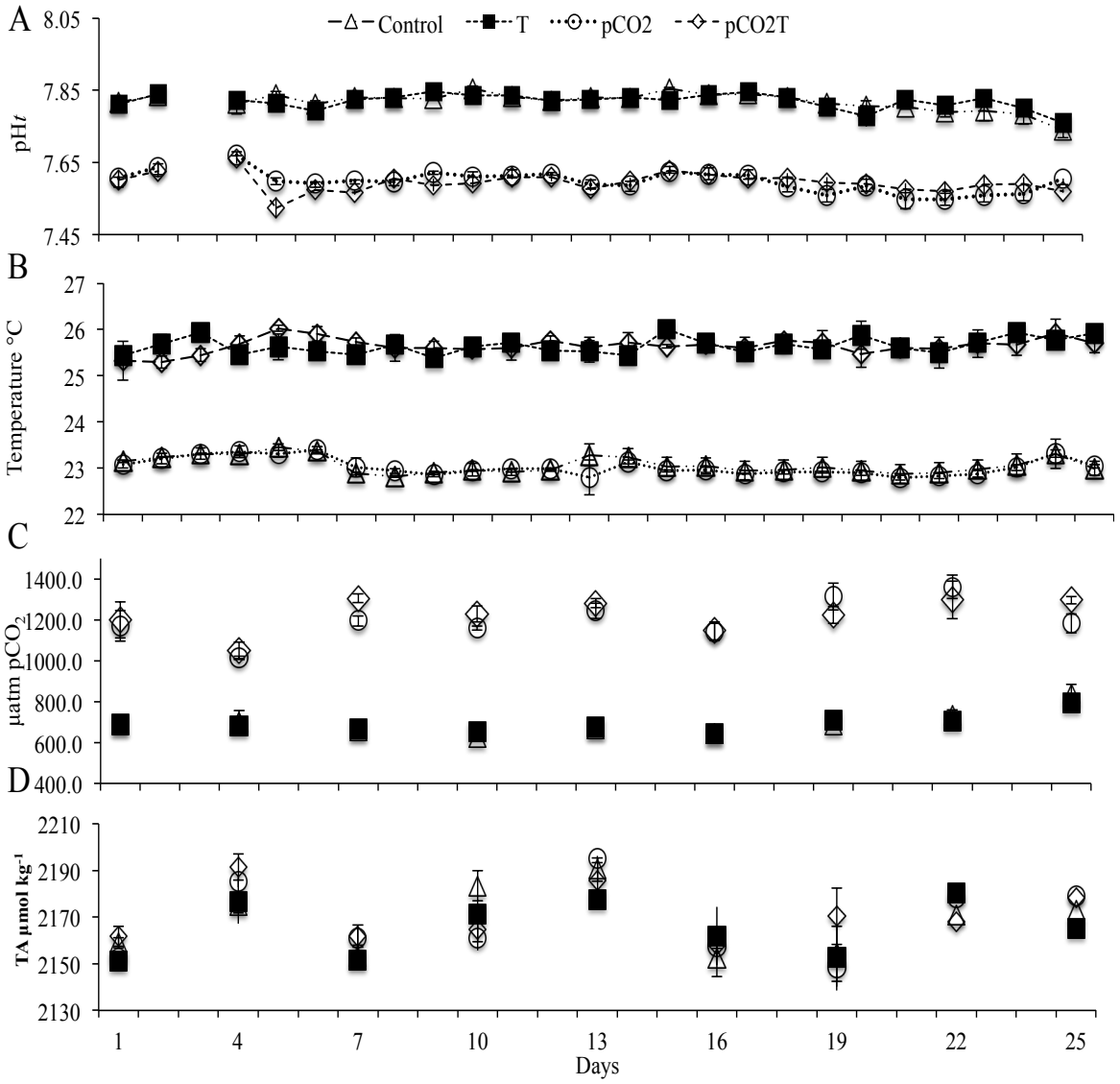

Figure A3.4 Seawater pH_T (A), temperature (B), pCO_2 (C), and A_T (D) measurements throughout the 26 day experimental period. For each time period Duncan's multiple range test (DMRT) (p=0.05) indicated that treatments Control and T had higher pH values (lower pCO_2) than pCO_2 and pCO_2T treatments while total alkalinity remained constant. For days 5 and 7 DMRT showed that pCO_2 treatment had a significantly higher pH than the pCO_2T treatment.

References

Abràmoff, M. D., Magalhães, P. J. & Ram, S. J. (2004) Image processing with ImageJ. *Biophotonics International, 11*, 36-42.

Angermeier, H., Glöckner, V., Pawlik, J. R., Lindquist, N. L. & Hentschel, U. (2012) Sponge white patch disease affecting the Caribbean sponge Amphimedon compressa. *Diseases of Aquatic Organisms, 99*, 95-102.

Ávila, E., Carballo, J. L. & Cruz-Barraza, J. A. (2007) Symbiotic relationships between sponges and other organisms from the Sea of Cortes (Mexican Pacific coast): same problems, same solutions. Porifera Research: Biodiversity. *Innovation and Sustainability*, 147-156.

Ayling, A. L. (1983) Growth and regeneration rates in thinly encrusting demospongiae from temperate waters. *The Biological Bulletin, 165*, 343-352.

Baker, A. C., Starger, C. J., McClanahan, T. R. & Glynn, P. W. (2004) Coral reefs: corals' adaptive response to climate change. *Nature, 430*, 741-741.

Bayer, K., Schmitt, S. & Hentschel, U. (2008) Physiology, phylogeny and in situ evidence for bacterial and archaeal nitrifiers in the marine sponge Aplysina aerophoba. *Environmental Microbiology, 10*, 2942-2955.

Bell, J. J., Davy, S. K., Jones, T., Taylor, M. W. & Webster, N. S. (2013) Could some coral reefs become sponge reefs as our climate changes? *Global Change Biology, 19*, 2613-2624.

Bennett, H. M., Altenrath, C., Woods, L., Davy, S. K., Webster, N. S. & Bell, J. J. (2016) Interactive effects of temperature and pCO_2 on sponges: from the cradle to the grave. *Global Change Biology*. doi: 10.1111/gcb.13474.

Bergquist, P. R. (1978) *Sponges*: University of California Press, Berkeley.

Berrué, F., Thomas, O. P., Funel-Le Bon, C., Reyes, F. & Amade, P. (2005) New bioactive cyclic peroxides from the Caribbean marine sponge *Plakortis zyggompha*. *Tetrahedron, 61*, 11843-11849.

Bewley, C., Holland, N. & Faulkner, D. (1996) Two classes of metabolites fromTheonella swinhoei are localized in distinct populations of bacterial symbionts. *Experientia, 52*, 716-722.

Bispo, A., Correia, M. D. & Hajdu, E. (2014) Two new shallow-water species of *Haliclona* from north-eastern Brazil (Demospongiae: Haplosclerida: Chalinidae). *Journal of the Marine Biological Association of the United Kingdom*, 1-13.

Blanquer, A., Uriz, M. J. & Agell, G. (2008) Hidden diversity in sympatric sponges: adjusting life-history dynamics to share substrate. *Marine Ecology Progress Series, 371*, 109-115.

Boury-Esnault, N., Muricy, G., Gallissian, M.-F. & Vacelet, J. (1995) Sponges without skeleton: a new Mediterranean genus of Homoscleromorpha (Porifera, Demospongiae). *Ophelia, 43*, 25-43.

Brochier-Armanet, C., Boussau, B., Gribaldo, S. & Forterre, P. (2008) Mesophilic Crenarchaeota: proposal for a third archaeal phylum, the Thaumarchaeota. *Nature Reviews Microbiology, 6*, 245-252.

Brown, B. (1997) Coral bleaching: causes and consequences. *Coral Reefs, 16*, S129-S138.

Byrne, M., Ho, M., Selvakumaraswamy, P., Nguyen, H. D., Dworjanyn, S. A. & Davis, A. R. (2009) Temperature, but not pH, compromises sea urchin fertilization and early development under near-future climate change scenarios. *Proceedings of the Royal Society of London B: Biological Sciences, 276*, 1883-1888.

Byrne, M. & Przeslawski, R. (2013) Multistressor impacts of warming and acidification of the ocean on marine invertebrates' life histories. *Integrative and Comparative Biology, 53*, 582-596.

Campos, M., Mothes, B., Eckert, R. & Van Soest, R. (2005) Haplosclerida (Porifera: Demospongiae) from the coast of Maranhao State, Brazil, Southwestern Atlantic. *Zootaxa, 963*, 1-22.

Caporaso, J. G., Lauber, C. L., Walters, W. A., Berg-Lyons, D., Huntley, J., Fierer, N., et al. (2012) Ultra-high-throughput microbial community analysis on the Illumina HiSeq and MiSeq platforms. *The International Society Microbial Ecology Journal, 6*, 1621-1624.

Cárdenas, P. (2016) Who Produces Ianthelline? The Arctic sponge *Stryphnus fortis* or its sponge epibiont *Hexadella dedritifera*: a probable case of sponge-sponge contamination. *Journal of Chemical Ecology, 42*, 339-347.

Carter, H. (1883) Contributions to our knowledge of the Spongida. *Journal of Natural History, 50*, 284-304, 343-360.

Cebrian, E., Uriz, M. J., Garrabou, J. & Ballesteros, E. (2011) Sponge mass mortalities in a warming Mediterranean Sea: are cyanobacteria-harboring species worse off? *PLoS One, 6*, e20211.

Cedra-García-Rojas, C. M., Harper, M. K. & Faulkner, D. J. (1994) Unstable enol sulfates from a two-sponge association. *Journal of Natural Products, 57*, 1758-1761.

Cha, J. N., Shimizu, K., Zhou, Y., Christiansen, S. C., Chmelka, B. F., Stucky, G. D., et al. (1999) Silicatein filaments and subunits from a marine sponge direct the polymerization of silica and silicones in vitro. *Proceedings of the National Academy of Sciences USA, 96*, 361-365.

Chanas, B. & Pawlik, J. (1997) Variability in the chemical defense of the Caribbean reef sponge *Xestospongia muta*. In: Lessios H.A., Macintyre, I.G. (Eds.) *Proceedings of the 8th international coral reef symposium, vol 2*. Smithsonian Tropical Research Institute, Balboa, pp. 1363–1368.

Charles, H., Balmand, S., Lamelas, A., Cottret, L., Pérez-Brocal, V., Burdin, B., et al. (2011) A genomic reappraisal of symbiotic function in the aphid/Buchnera

symbiosis: reduced transporter sets and variable membrane organisations. *PLoS One, 6*, e29096.

Chen, I.-C., Hill, J. K., Ohlemüller, R., Roy, D. B. & Thomas, C. D. (2011) Rapid range shifts of species associated with high levels of climate warming. *Science, 333*, 1024-1026.

Coles, S. & Bolick, H. (2007) Invasive introduced sponge *Mycale grandis* overgrows reef corals in Kāne ʻohe Bay, O ʻahu, Hawai ʻi. *Coral Reefs, 26*, 911-911.

Coles, S. L., Bolick, H. & Longenecker, K. (2006) Assessment of Invasiveness of the Orange Keyhole Sponge *Mycale armata* in Kāne ʻohe Bay, O ʻahu, Hawai ʻi. *Final Report Year, 1*, 2006-2002.

Collin, R., Mobley, A. S., Lopez, L. B., Leys, S. P., Diaz, M. C. & Thacker, R. W. (2010) Phototactic responses of larvae from the marine sponges *Neopetrosia proxima* and *Xestospongia bocatorensis* (Haplosclerida: Petrosiidae). *Invertebrate Biology, 129*, 121-128.

Corredor, J. E., Wilkinson, C. R., Vicente, V. P., Morell, J. M. & Otero, E. (1988) Nitrate release by Caribbean reef sponges. *Limnology and Oceanography, 33*, 114-120.

Cruz‐Barraza, J. A., Vega, C. & Carballo, J. L. (2014) Taxonomy of family Plakinidae (Porifera: Homoscleromorpha) from eastern Pacific coral reefs,

through morphology and *cox1* and *cob* mtDNA data. *Zoological Journal of the Linnean Society, 171*, 254-276.

D'Croz, L., Del Rosario, J. B. & Gondola, P. (2005) The effect of fresh water runoff on the distribution of dissolved inorganic nutrients and plankton in the Bocas del Toro Archipelago, Caribbean Panama. *Caribbean Journal of Science, 41*, 414-429.

Dalisay, D. S., Quach, T. & Molinski, T. F. (2011) Liposomal circular dichroism. Assignment of remote stereocenters in plakinic acids K and L from a *Plakortis*–*Xestospongia* sponge association. *Organic letters, 13*, 4152-4152.

De Goeij, J. M., Van Oevelen, D., Vermeij, M. J., Osinga, R., Middelburg, J. J., de Goeij, A. F., et al. (2013) Surviving in a marine desert: the sponge loop retains resources within coral reefs. *Science, 342*, 108-110.

De Laubenfels, M. W. (1934) *New sponges from the Puerto Rican deep*: Smithsonian Institution, *91*, 1-28.

De Weerdt, W. H., Kluijver, M. J. & Gomez, R. (1999) *Haliclona* (Halichoclona) *vansoesti* n. sp., a new chalinid sponge species (Porifera, Demospongiae, Haplosclerida) from the Caribbean. *Beaufortia, 49*, 47-54.

De Weerdt, W. H. (2000) A monograph of the shallow-water Chalinidae (Porifera, Haplosclerida) of the Caribbean. *Beaufortia, 50*, 1-67.

De Weerdt, W. H. (2002) Family Chalinidae Gray, 1867. In: Hooper, J.N.A. and Van Soest, R.W.M. (Eds.), *Systema Porifera*. Kluwer Academic/Plenum, New York, pp. 852-873.

De Weerdt, W. H., Rützler, K. & Smith, K. P. (1991) The chalinidae (Porifera) of Twin Cays, Belize, and adjacent waters. *Proceedings of the Biological Society of Washington*, *104*, 189-205.

DeBiasse, M. B. & Hellberg, M. E. (2015) Discordance between morphological and molecular species boundaries among Caribbean species of the reef sponge *Callyspongia*. *Ecology and Evolution, 5*, 663-675.

del Sol Jiménez, M., Garzón, S. P. & Rodríguez, A. D. (2003) Plakortides M and N, Bioactive Polyketide Endoperoxides from the Caribbean Marine Sponge *Plakortis halichondrioides*. *Journal of Natural Products, 66*, 655-661.

DeLong, E. F., Wickham, G. S. & Pace, N. R. (1989) Phylogenetic stains: Ribosomal RNA-based probes for the indentification of single cells. *Science, 243*, 1360.

Dendy, A. (1905) *Report on the sponges collected by Professor Herdman, at Ceylon in 1902*. London.

Desqeyroux-Faundez, R. & Van Soest, R. (1997) Shallow-water Demosponges of the Galapagos Islands. *Revue Suisse De Zoologie, 104*, 379-467.

Desqueyroux-Faúndez, R. & Valentine, C. (2002) Family Petrosiidae Van Soest, 1980. In: Hooper, J.N.A. and Van Soest, R.W.M. (Eds.), *Systema Porifera*. Kluwer Academic/Plenum, New York. pp. 906-917.

Diaz, M. & Ward, B. (1997) Sponge-mediated nitrification in tropical benthic communities. *Marine Ecology Progress Series, 156*, 97-107.

Diaz, M. C. & Rützler, K. (2001) Sponges: an essential component of Caribbean coral reefs. *Bulletin of Marine Science, 69*, 535-546.

Dickson, A. & Millero, F. J. (1987) A comparison of the equilibrium constants for the dissociation of carbonic acid in seawater media. *Deep Sea Research Part A. Oceanographic Research Papers, 34*, 1733-1743.

Dickson, A. G., Sabine, C. L. & Christian, J. R. (2007) Guide to best practices for ocean CO_2 measurements. *PICES Special Publication, 3*, 191.

Domingos, C., Lage, A. & Muricy, G. (2015) Overview of the biodiversity and distribution of the Class Homoscleromorpha in the Tropical Western Atlantic. *Journal of the Marine Biological Association of the United Kingdom*, 1-11.

Domingos, C., Moraes, F. & Muricy, G. (2013) Four new species of Plakinidae (Porifera: Homoscleromorpha) from Brazil. *Zootaxa, 3718*, 530-544.

Doney, S. C., Fabry, V. J., Feely, R. A. & Kleypas, J. A. (2009) Ocean acidification: the other CO_2 problem. *Washington journal of envrionmental law & policy , 6*, 213.

Doney, S. C., Ruckelshaus, M., Duffy, J. E., Barry, J. P., Chan, F., English, C. A., et al. (2012) Climate change impacts on marine ecosystems. *Marine Science, 4*, 11-37.

Douglas, A. E. (2008) Conflict, cheats and the persistence of symbioses. *New Phytologist, 177*, 849-858.

Duchassaing de Fonbressin, P. & Michelotti, G. (1864) Spongiaires de la mer Caraibe. *Natuurkundige verhandelingen van de Hollandsche maatschappij der wetenschappen te Haarlem, 2*, 1-24.

Duckworth, A. R. & Peterson, B. J. (2012) Effects of seawater temperature and pH on the boring rates of the sponge *Cliona celata* in scallop shells. *Marine Biology, 160*, 27-35.

Duckworth, A. R., West, L., Vansach, T., Stubler, A. & Hardt, M. (2012) Effects of water temperature and pH on growth and metabolite biosynthesis of coral reef sponges. *Marine Ecology Progress Series, 462*, 67-77.

Dunlap, M. & Pawlik, J. R. (1996) Video-monitored predation by Caribbean reef fishes on an array of mangrove and reef sponges. *Marine Biology, 126*, 117-123.

Easson, C. G. & Thacker, R. W. (2015) Phylogenetic signal in the community structure of host-specific microbiomes of tropical marine sponges. *Microbial Symbiosis of Marine Sessile Hosts-Diversity, Function and Applications*, *5*, 532.

Edgar, R. C., Haas, B. J., Clemente, J. C., Quince, C. & Knight, R. (2011) UCHIME improves sensitivity and speed of chimera detection. *Bioinformatics, 27*, 2194-2200.

Engel, S. & Pawlik, J. R. (2000) Allelopathic activities of sponge extracts. *Marine Ecology Progress Series, 207*, 273-281.

Enochs, I. C., Manzello, D. P., Carlton, R. D., Graham, D. M., Ruzicka, R. & Colella, M. A. (2015) Ocean acidification enhances the bioerosion of a common coral reef sponge: implications for the persistence of the Florida Reef Tract. *Bulletin of Marine Science, 91*, 271-290.

Enticknap, J. J., Kelly, M., Peraud, O. & Hill, R. T. (2006) Characterization of a culturable alphaproteobacterial symbiont common to many marine sponges and evidence for vertical transmission via sponge larvae. *Applied and Environmental Microbiology, 72*, 3724-3732.

Ereskovsky, A., Ivanisevic, J. & Pérez, T. (2009) Overview on the Homoscleromorpha sponges diversity in the Mediterranean. *In: Proc. of the First Mediterranean Symposium on the Coralligenous and other calcareous bio-concretions.* Okianos Tunisia, Tabarka, pp. 88-94.

Ereskovsky, A. V. (2010) *The comparative embryology of sponges*: Springer Science & Business Media, New York.

Ereskovsky, A. V., Gonobobleva, E. & Vishnyakov, A. (2005) Morphological evidence for vertical transmission of symbiotic bacteria in the viviparous sponge *Halisarca dujardini* Johnston (Porifera, Demospongiae, Halisarcida). *Marine Biology, 146*, 869-875.

Ereskovsky, A. V., Lavrov, D. V. & Willenz, P. (2014) Five new species of Homoscleromorpha (Porifera) from the Caribbean Sea and re-description of *Plakina jamaicensis*. *Journal of the Marine Biological Association of the United Kingdom, 94*, 285-307.

Erpenbeck, D., Duran, S., Rützler, K., Paul, V., Hooper, J. N. & Wörheide, G. (2007) Towards a DNA taxonomy of Caribbean demosponges: a gene tree reconstructed from partial mitochondrial CO1 gene sequences supports previous rDNA phylogenies and provides a new perspective on the systematics of Demospongiae. *Journal of the Marine Biological Association of the United Kingdom, 87*, 1563-1570.

Fabry, V. J., Seibel, B. A., Feely, R. A. & Orr, J. C. (2008) Impacts of ocean acidification on marine fauna and ecosystem processes. *ICES Journal of Marine Science: Journal du Conseil, 65*, 414-432.

Ferriere, R., Bronstein, J. L., Rinaldi, S., Law, R. & Gauduchon, M. (2002) Cheating and the evolutionary stability of mutualisms. *Proceedings of the Royal Society of London B: Biological Sciences, 269*, 773-780.

Fine, M. & Tchernov, D. (2007) Scleractinian coral species survive and recover from decalcification. *Science, 315*, 1811-1811.

Folmer, O., Black, M., Hoeh, W., Lutz, R. & Vrijenhoek, R. (1994) DNA primers for amplification of mitochondrial cytochrome c oxidase subunit I from diverse metazoan invertebrates. *Molecular Marine Biology and Biotechnology, 3*, 294-299.

Freeman, C. J., Easson, C. G. & Baker, D. M. (2014) Metabolic diversity and niche structure in sponges from the Miskito Cays, Honduras. *PeerJ, 2*, e695.

Freeman, C. J. & Thacker, R. W. (2011) Complex interactions between marine sponges and their symbiotic microbial communities. *Limnology and Oceanography, 56*, 1577-1586.

Freeman, C. J., Thacker, R. W., Baker, D. M. & Fogel, M. L. (2013) Quality or quantity: is nutrient transfer driven more by symbiont identity and productivity than by symbiont abundance. *International Society of Marine Ecology Journal, 7*, 1116-1125.

Gazave, E., Lapébie, P., Ereskovsky, A. V., Vacelet, J., Renard, E., Cárdenas, P., et al. (2012) No longer Demospongiae: Homoscleromorpha formal nomination as a fourth class of Porifera. *Hydrobiologia, 687*, 3-10.

George, W. C. & Wilson, H. V. (1919) Sponges of Beaufort (N.C.) Harbor and vicinity. *Bulletin of the Bureau of Fisheries, 36*, 130-179.

Gibbin, E. M., Putnam, H. M., Gates, R. D., Nitschke, M. R. & Davy, S. K. (2015) Species-specific differences in thermal tolerance may define susceptibility to intracellular acidosis in reef corals. *Marine Biology, 162*, 717-723.

Giles, E. C., Kamke, J., Moitinho-Silva, L., Taylor, M. W., Hentschel, U., Ravasi, T., et al. (2013) Bacterial community profiles in low microbial abundance sponges. *FEMS microbiology ecology, 83*, 232-241.

Gloeckner, V., Wehrl, M., Moitinho-Silva, L., Gernert, C., Schupp, P., Pawlik, J. R., et al. (2014) The HMA-LMA dichotomy revisited: an electron microscopical survey of 56 sponge species. *The Biological Bulletin, 227*, 78-88.

Gochfeld, D. J. & Hamann, M. T. (2001) Isolation and biological evaluation of filiformin, plakortide F, and plakortone G from the Caribbean sponge *Plakortis* sp. *Journal of Natural Products, 64*, 1477-1479.

Goodwin, C., Rodolfo-Metalpa, R., Picton, B. & Hall-Spencer, J. M. (2014) Effects of ocean acidification on sponge communities. *Marine Ecology, 35*, 41-49.

Grant, R. E. (1836) *Animal kingdom* (Vol. 1): Sherwood, Gilbert and Piper, London.

Grasshoff, K., Kremling, K. & Ehrhardt, M. (2009) *Methods of seawater analysis*: John Wiley & Sons, Federal Republic of Germany. New York.

Gray, J. (1867) Notes on the arrangement of sponges, with the descriptions of some new genera. *In: Proceedings of the Zoological Society of London*, pp. 492-558.

Griessinger, J.-M. (1971) *Étude des réniérides de Mediterranée (démosponges haplosclérides)*, *3*, 120-121.

Guzman, C. & Conaco, C. (2016) Comparative transcriptome analysis reveals insights into the streamlined genomes of haplosclerid demosponges. *Scientific Reports, 6*.

Harmelin, J.-G., Vacelet, J. & Vasseur, P. (1985) Les grottes sous-marines obscures: un milieu extrême et un remarquable biotope refuge. *Téthys, 1*, 214-229.

Haseley, S. R., Vermeer, H. J., Kamerling, J. P. & Vliegenthart, J. F. (2001) Carbohydrate self-recognition mediates marine sponge cellular adhesion. *Proceedings of the National Academy of Sciences USA, 98*, 9419-9424.

Hechtel, G. J. (1965) *A systematic study of the Demospongiae of Port Royal, Jamaica*: Peabody Museum of Natural History, Yale University.

Hentschel, U., Fieseler, L., Wehrl, M., Gernert, C., Steinert, M., Hacker, J., et al. (2003) Microbial diversity of marine sponges. *In:* Müller, W.E.G. (Eds.) *Molecular Marine Biology of Sponges*. Springer, Verlag Heidelberg, pp. 60-88.

Hentschel, U., Usher, K. M. & Taylor, M. W. (2006) Marine sponges as microbial fermenters. *FEMS microbiology ecology, 55*, 167-177.

Hill, M., Walter, C. & Bartels, E. (2016) A mass bleaching event involving clionaid sponges. *Coral Reefs, 35*, 153-153.

Hill, M. S. & Hill, A. L. (2002) Morphological plasticity in the tropical sponge *Anthosigmella varians*: responses to predators and wave energy. *The Biological Bulletin, 202*, 86-95.

Hoegh-Guldberg, O., Mumby, P. J., Hooten, A. J., Steneck, R. S., Greenfield, P., Gomez, E., et al. (2007) Coral reefs under rapid climate change and ocean acidification. *Science, 318*, 1737-1742.

Hoffmann, F. (2003) Microbial sulfate reduction in the tissue of the cold-water sponge *Geodia barretti* (Tetractinellida, Demospongiae). Ph.D. thesis, Department of Geosciences, Göttingen University.

Hoffmann, F., Larsen, O., Thiel, V., Rapp, H. T., Pape, T., Michaelis, W., et al. (2005) An anaerobic world in sponges. *Geomicrobiology Journal, 22*, 1-10.

Hofmann, G. E., Barry, J. P., Edmunds, P. J., Gates, R. D., Hutchins, D. A., Klinger, T., et al. (2010) The effect of ocean acidification on calcifying organisms

in marine ecosystems: an organism-to-ecosystem perspective. *Annual Review of Ecology, Evolution and Systematics, 41*, 127-147.

Hooper, J. N. A. & Van Soest, R. W. M. (2002) *Systema Porifera. A guide to the classification of Sponges*: Springer, NY.

Hoshino, T. (1981) Shallow-water demosponges of western Japan II. *Journal of Science of the Hiroshima University, 29*, 207-289.

Hoye, T. R., Alarif, W. M., Basaif, S. S., Abo-Elkarm, M., Hamann, M. T., Wahba, A. E., et al. (2015) New cytotoxic cyclic peroxide acids from *Plakortis* sp. marine sponge. *Current Medicinal Chemistry*, *23*, 383-405.

Huesemann, M. H., Skillman, A. D. & Crecelius, E. A. (2002) The inhibition of marine nitrification by ocean disposal of carbon dioxide. *Marine Pollution Bulletin, 44*, 142-148.

Jiménez-Romero, C., Ortiz, I., Vicente, J., Vera, B., Rodríguez, A. D., Nam, S., et al. (2010) Bioactive cycloperoxides isolated from the Puerto Rican sponge *Plakortis halichondrioides*. *Journal of Natural Products, 73*, 1694-1700.

Jung, J. H., Sim, C. J. & Lee, C.-O. (1995) Cytotoxic compounds from a two-sponge association. *Journal of Natural Products, 58*, 1722-1726.

Kamke, J., Taylor, M. W. & Schmitt, S. (2010) Activity profiles for marine sponge-associated bacteria obtained by 16S rRNA vs 16S rRNA gene comparisons. *International Society of Microbial Ecology Journal, 4*, 498-508.

Karell, P., Ahola, K., Karstinen, T., Valkama, J. & Brommer, J. E. (2011) Climate change drives microevolution in a wild bird. *Nature Communications, 2*, 208.

Könneke, M., Schubert, D. M., Brown, P. C., Hügler, M., Standfest, S., Schwander, T., et al. (2014) Ammonia-oxidizing archaea use the most energy-efficient aerobic pathway for CO_2 fixation. *Proceedings of the National Academy of Sciences, 111*, 8239-8244.

Kossuga, M. H., Nascimento, A. M., Reimão, J. Q., Tempone, A. G., Taniwaki, N. N., Veloso, K., et al. (2008) Antiparasitic, antineuroinflammatory, and cytotoxic polyketides from the marine sponge *Plakortis angulospiculatus* collected in Brazil. *Journal of Natural Products, 71*, 334-339.

Krasko, A., Lorenz, B., Batel, R., Schröder, H. C., Müller, I. M. & Müller, W. E. (2000) Expression of silicatein and collagen genes in the marine sponge *Suberites domuncula* is controlled by silicate and myotrophin. *European Journal of Biochemistry, 267*, 4878-4887.

Kubanek, J., Whalen, K. E., Engel, S., Kelly, S. R., Henkel, T. P., Fenical, W., et al. (2002) Multiple defensive roles for triterpene glycosides from two Caribbean sponges. *Oecologia, 131*, 125-136.

De Laubenfels, M. W. (1932) The marine and fresh-water sponges of California. *Proceedings of the United States National Museum*, *81*, 1-140.

Lavrov, D. V., Wang, X. & Kelly, M. (2008) Reconstructing ordinal relationships in the Demospongiae using mitochondrial genomic data. *Molecular Phylogenetics and Evolution, 49*, 111-124.

Layman, C. A., Quattrochi, J. P., Peyer, C. M. & Allgeier, J. E. (2007) Niche width collapse in a resilient top predator following ecosystem fragmentation. *Ecology Letters, 10*, 937-944.

Lehnert, H. & Van Soest, R. W. (1999) More North Jamaican deep fore-reef sponges. *Beaufortia, 49*, 141-169.

Lendenfeld, R. v. (1887) Die Chalineen des australischen Gebietes. *Zoologische Jahrbücher, 2*, 723-828.

Leong, W. & Pawlik, J. R. (2010a) Evidence of a resource trade-off between growth and chemical defenses among Caribbean coral reef sponges. *Marine Ecology Progress Series, 406*, 71-78.

Leong, W. & Pawlik, J. R. (2010b) Fragments or propagules? Reproductive tradeoffs among *Callyspongia* spp. from Florida coral reefs. *Oikos, 119*, 1417-1422.

Lesser, M. P. (2006) Benthic–pelagic coupling on coral reefs: feeding and growth of Caribbean sponges. *Journal of Experimental Marine Biology and Ecology, 328*, 277-288.

Lévi, C. (1953) Description de *Plakortis nigra* nov. sp. et remarques sur les Plakinidae (Démosponges). *Bulletin de Museum, 2e serie,, XXV, 3*.

Lévi, C. (1958) Spongiaires de mer rouge recuillis par la Calypso. *In: Annales de l'Institut Océanographique*, pp. 1-46.

Levi, C. & Porte, A. (1962) Electron microscopy study of the sponge *Oscarella lobularis* and its amphiblastula larvae. *Cahiers De Biologie Marine, 3*, 307-315.

Lewis, E., Wallace, D. & Allison, L. J. (1998) *Program developed for CO2 system calculations*: Carbon Dioxide Information Analysis Center, managed by Lockheed Martin Energy Research Corporation for the US Department of Energy Tennessee.

Lewis, S. (1982) Sponge-Zoanthid associations: Functional interactions: 465-474. *The Atlantic Barrier Reef ecosystem at Carrie Bow Cay, Belize, I structure and communities.* Smithsonian Institution Press, Washington.

Loh, T.-L., López-Legentil, S., Song, B. & Pawlik, J. R. (2012) Phenotypic variability in the Caribbean orange icing sponge *Mycale laevis* (Demospongiae: Poecilosclerida). *Hydrobiologia, 687*, 205-217.

Loh, T.-L., McMurray, S. E., Henkel, T. P., Vicente, J. & Pawlik, J. R. (2015) Indirect effects of overfishing on Caribbean reefs: sponges overgrow reef-building corals. *PeerJ, 3*, e901.

Loh, T.-L. & Pawlik, J. R. (2009) Bitten down to size: fish predation determines growth form of the Caribbean coral reef sponge *Mycale laevis*. *Journal of Experimental Marine Biology and Ecology, 374*, 45-50.

Loh, T.-L. & Pawlik, J. R. (2014) Chemical defenses and resource trade-offs structure sponge communities on Caribbean coral reefs. *Proceedings of the National Academy of Sciences, 111*, 4151-4156.

Lopez-Legentil, S., Erwin, P. M., Pawlik, J. R. & Song, B. (2010) Effects of sponge bleaching on ammonia-oxidizing Archaea: distribution and relative expression of ammonia monooxygenase genes associated with the barrel sponge *Xestospongia muta*. *Microbial Ecology, 60*, 561-571.

López-Legentil, S. & Pawlik, J. (2009) Genetic structure of the Caribbean giant barrel sponge *Xestospongia muta* using the I3-M11 partition of COI. *Coral Reefs, 28*, 157-165.

Luter, H. M., Whalan, S. & Webster, N. S. (2010) Exploring the role of microorganisms in the disease-like syndrome affecting the sponge *Ianthella basta*. *Applied and Environmental Microbiology, 76*, 5736-5744.

Luter, H. M., Widder, S., Botté, E. S., Wahab, M. A., Whalan, S., Moitinho-Silva, L., et al. (2015) Biogeographic variation in the microbiome of the ecologically important sponge, *Carteriospongia foliascens*. *PeerJ, 3*, e1435.

Maldonado, M. (2002) Family Pachastrellidae Carter, 1875. *In:* Hooper, J.N.A. and Van Soest, R.W.M. (Eds.), *Systema Porifera*. Kluwer Academic/Plenum, New York. pp. 141-162.

Maldonado, M., Cao, H., Cao, X., Song, Y., Qu, Y. & Zhang, W. (2012) Experimental silicon demand by the sponge *Hymeniacidon perlevis* reveals chronic limitation in field populations. *Hydrobiologia, 687*, 251-257.

Maldonado, M., Carmona, M. C., Velásquez, Z., Puig, A., Cruzado, A., López, A., et al. (2005) Siliceous sponges as a silicon sink: an overlooked aspect of benthopelagic coupling in the marine silicon cycle. *Limnology and Oceanography, 50*, 799-809.

Maldonado, M., Navarro, L., Grasa, A., Gonzalez, A. & Vaquerizo, I. (2011) Silicon uptake by sponges: a twist to understanding nutrient cycling on continental margins. *Scientific Reports, 1*, 30.

Maldonado, M., Ribes, M. & Van Duyl, F. C. (2012) 3 Nutrient Fluxes Through Sponges: Biology, Budgets, and Ecological Implications. *Advances in Marine Biology, 62*, 113.

Maldonado, M. & Riesgo, A. (2009) Gametogenesis, embryogenesis, and larval features of the oviparous sponge *Petrosia ficiformis* (Haplosclerida, Demospongiae). *Marine Biology, 156*, 2181-2197.

Mardis, E. R. (2008) The impact of next-generation sequencing technology on genetics. *Trends in Genetics, 24*, 133-141.

Marty, M. J., Blum, J. E. & Pawlik, J. R. (2016) No accounting for taste: Palatability of variably defended Caribbean sponge species is unrelated to predator abundance. *Journal of Experimental Marine Biology and Ecology, in press*.

Marty, M. J. & Pawlik, J. R. (2015) A fish-feeding laboratory bioassay to assess the antipredatory activity of secondary metabolites from the tissues of marine organisms. *JoVE (Journal of Visualized Experiments)*, e52429-e52429.

Marty, M. J., Vicente, J., Anker, A., Armstrong, F. A. & Hill, R. T. (2016) Coral reef sponges provide nocturnal foraging habitat for hermit crabs on a lagoonal reef in Panama. *PeerJ, in preparation*.

McClanahan, T. & Obura, D. (1996) Coral reefs and nearshore fisheries. *In:* McClanahan, T.T., Young, T.P. (Eds.), *East African Ecosystems and their Conservation*. Oxford University Press, NY, pp. 67-99.

McCormack, G., Erpenbeck, D. & Van Soest, R. (2002) Major discrepancy between phylogenetic hypotheses based on molecular and morphological criteria within the Order Haplosclerida (Phylum Porifera: Class Demospongiae). *Journal of Zoological Systematics and Evolutionary Research, 40*, 237-240.

McMurray, S. E., Finelli, C. M. & Pawlik, J. R. (2015) Population dynamics of giant barrel sponges on Florida coral reefs. *Journal of Experimental Marine Biology and Ecology, 473*, 73-80.

Mehbub, M. F., Lei, J., Franco, C. & Zhang, W. (2014) Marine sponge derived natural products between 2001 and 2010: Trends and opportunities for discovery of bioactives. *Marine Drugs, 12*, 4539-4577.

Mehrbach, C., Culberson, C., Hawley, J. & Pytkowicx, R. (1973) MeasuremeNT of the apparent dissociation constants of carbonic acid in seawater at atmospheric pressure *Limnology and Oceanography, 18*, 897-907.

Mills, L. S., Zimova, M., Oyler, J., Running, S., Abatzoglou, J. T. & Lukacs, P. M. (2013) Camouflage mismatch in seasonal coat color due to decreased snow duration. *Proceedings of the National Academy of Sciences USA, 110*, 7360-7365.

Modjo, H. & Hendrix, J. (1986) mycorrhizal fungus *Glomus macrocarpum* as a cause of tobacco stunt disease. *Phytopathology*, *76*, 688-691.

Mohamed, N. M., Colman, A. S., Tal, Y. & Hill, R. T. (2008) Diversity and expression of nitrogen fixation genes in bacterial symbionts of marine sponges. *Environmental Microbiology, 10*, 2910-2921.

Mohamed, N. M., Saito, K., Tal, Y. & Hill, R. T. (2010) Diversity of aerobic and anaerobic ammonia-oxidizing bacteria in marine sponges. *The International Society of Microbial Ecology Journal, 4*, 38-48.

Moitinho‐Silva, L., Bayer, K., Cannistraci, C. V., Giles, E. C., Ryu, T., Seridi, L., et al. (2014) Specificity and transcriptional activity of microbiota associated with

low and high microbial abundance sponges from the Red Sea. *Molecular Ecology, 23*, 1348-1363.

Moraes, F. C. & Muricy, G. (2003) Taxonomy of *Plakortis* and *Plakinastrella* (Demospongiae: Plakinidae) from oceanic islands off north-eastern Brazil, with description of three new species. *Journal of the Marine Biological Association of the UK, 83*, 385-397.

Morrow, K. M., Bourne, D. G., Humphrey, C., Botte, E. S., Laffy, P., Zaneveld, J., et al. (2014) Natural volcanic CO_2 seeps reveal future trajectories for host-microbial associations in corals and sponges. *International Society of Microbial Ecology Journal*, *9*, 894-908.

Müller, G. B. (2007) Evo–devo: extending the evolutionary synthesis. *Nature Reviews Genetics, 8*, 943-949.

Müller, W. E., Krasko, A., Le Pennec, G., Steffen, R., Wiens, M., Ammar, M. S. A., et al. (2003) Molecular mechanism of spicule formation in the demosponge *Suberites domuncula*: silicatein-collagen-myotrophin. *In:* Müller, W.E.G. (Eds.) *Silicon Biomineralization*. Springer, New York, pp. 195-221.

Muricy, G. (2011) Diversity of Indo-Australian *Plakortis* (Demospongiae: Plakinidae), with description of four new species. *Journal of the Marine Biological Association of the United Kingdom, 91*, 303-319.

Muricy, G., Boury-Esnault, N., Bézac, C. & Vacelet, J. (1998) Taxonomic revision of the Mediterranean *Plakina* Schulze (Porifera, Demospongiae, Homoscleromorpha). *Zoological Journal of the Linnean Society, 124*, 169-203.

Muricy, G., Esteves, E. L., Monteiro, L. C., Rodrigues, B. R. & Albano, R. M. (2015) A new species of *Haliclona* (Demospongiae: Haplosclerida: Chalinidae) from southeastern Brazil and the first record of *Haliclona vansoesti* from the Brazilian coast. *Zootaxa, 3925*, 536-550.

Muricy, G., Solé-Cava, A. M., Thorpe, J. P. & Boury-Esnault, N. (1996) Genetic evidence for extensive cryptic speciation in the subtidal sponge *Plakina trilopha* (Porifera: Demospongiae: Homoscleromorpha) from the Western Mediterranean. *Marine Ecology Progress Series, 138*, 181-187.

Nuñez, C. V., de Almeida, E. V., Granato, A. C., Marques, S. O., Santos, K. O., Pereira, F. R., et al. (2008) Chemical variability within the marine sponge *Aplysina fulva*. *Biochemical Systematics and Ecology, 36*, 283-296.

Nwewll, R. & Northcroft, H. (1967) A re‐interpretation of the effect of temperature on the metabolism of certain marine invertebrates. *Journal of Zoology, 151*, 277-298.

Oksanen, J., Blanchet, F. G., Kindt, R., Legendre, P., Minchin, P. R., O'Hara, R., et al. (2013) Package 'vegan'. *Community ecology package, version, 2*.

Pallas, P. S. (1766) *Elenchus zoophytorum sistens generum adumbrationes generaliores et specierum cognitarum succintas descriptiones, cum selectis auctorum synonymis*: Apud Petrum van Cleef, Varrentrapp.

Palumbi, S. R., Barshis, D. J., Traylor-Knowles, N. & Bay, R. A. (2014) Mechanisms of reef coral resistance to future climate change. *Science, 344*, 895-898.

Parker, L. M., Ross, P. M. & O'Connor, W. A. (2010) Comparing the effect of elevated pCO2 and temperature on the fertilization and early development of two species of oysters. *Marine Biology, 157*, 2435-2452.

Pawlik, J. (1997) Fish predation on Caribbean reef sponges: an emerging perspective of chemical defenses. *In:* Lessios, H.A., Macintyre, I.G. (Eds.) *Proceedings of the 8th international coral reef symposium*, vol 2. Smithsonian Tropical Research Institute, Balboa, pp. 1255-1258.

Pawlik, J. R. (2011) The chemical ecology of sponges on Caribbean reefs: natural products shape natural systems. *Bioscience, 61*, 888-898.

Pawlik, J. R. (2012) Antipredatory defensive roles of natural products from marine invertebrates. *In: Handbook of Marine Natural Products*. Springer, pp. 677-710.

Pawlik, J. R., Chanas, B., Toonen, R. & Fenical, W. (1995) Defenses of Caribbean sponges against predatory reef fish. I. Chemical deterrency. *Marine Ecology Progress Series, 127*, 183-194.

Pawlik, J. R. & Deignan, L. (2015) Cowries graze verongid sponges on Caribbean reefs. *Coral Reefs, 34*, 663.

Pawlik, J. R., Henkel, T. P., McMurray, S. E., López-Legentil, S., Loh, T.-L. & Rohde, S. (2008a) Patterns of sponge recruitment and growth on a shipwreck corroborate chemical defense resource trade-off. *Marine Ecology Progress Series, 368*, 137-143.

Pawlik, J. R., Henkel, T. P., McMurray, S. E., López-Legentil, S., Loh, T.-L. & Rohde, S. (2008b) Patterns of sponge recruitment and growth on a shipwreck corroborate chemical defense resource trade-off. *Marine Ecology Progress Series 368*, 137-143.

Pawlik, J. R., Loh, T.-L., McMurray, S. E. & Finelli, C. M. (2013) Sponge communities on Caribbean coral reefs are structured by factors that are top-down, not bottom-up. *PLoS One, 8*, e62573.

Pawlik, J. R., Steindler, L., Henkel, T. P., Beer, S. & Ilan, M. (2007) Chemical warfare on coral reefs: Sponge metabolites differentially affect coral symbiosis in situ. *Limnology and Oceanography, 52*, 907-911.

Pennings, S. C., Pablo, S. R., Paul, V. J. & Duffy, J. E. (1994) Effects of sponge secondary metabolites in different diets on feeding by three groups of consumers. *Journal of Experimental Marine Biology and Ecology, 180*, 137-149.

Pérez‐Porro, A. R., Navarro‐Gómez, D., Uriz, M. J. & Giribet, G. (2013) A NGS approach to the encrusting Mediterranean sponge *Crella elegans* (Porifera,

Demospongiae, Poecilosclerida): transcriptome sequencing, characterization and overview of the gene expression along three life cycle stages. *Molecular Ecology Resources, 13*, 494-509.

Poloczanska, E. S., Brown, C. J., Sydeman, W. J., Kiessling, W., Schoeman, D. S., Moore, P. J., et al. (2013) Global imprint of climate change on marine life. *Nature Climate Change, 3*, 919-925.

Pomponi, S. A. (1980) Cytological mechanisms of calcium carbonate excavation by boring sponges. *International Review of Cytology, 65*, 301-319.

Poppell, E., Weisz, J., Spicer, L., Massaro, A., Hill, A. & Hill, M. (2014) Sponge heterotrophic capacity and bacterial community structure in high‐and low‐microbial abundance sponges. *Marine Ecology, 35*, 414-424.

Porter, J. W. & Targett, N. M. (1988) Allelochemical interactions between sponges and corals. *The Biological Bulletin, 175*, 230-239.

Pörtner, H. (2008) Ecosystem effects of ocean acidification in times of ocean warming: a physiologist's view. *Marine Ecology Progress Series, 373*, 203-217.

Poulsen, L. K., Ballard, G. & Stahl, D. A. (1993) Use of rRNA fluorescence in situ hybridization for measuring the activity of single cells in young and established biofilms. *Applied and Environmental Microbiology, 59*, 1354-1360.

Pulitzer-Finali, G. (1986) A Collection of West Indian Demospongiae (Porifera): In appendix a List of the Demospongiae hitherto recorded from the West Indies: *Annali del Museo Civivo di Storia Naturale Giacomo Doria*, *86*: 65-216.

Pulitzer-Finali, G. (1993) A collection of marine sponges from East Africa: In In appendix a List of the Demospongiae hitherto recorded from the West Indies: *Annali del Museo Civivo di Storia Naturale Giacomo Doria, 89*, 247-350.

Putnam, H. M. (2012) Resilience and acclimatization potential of reef corals under predicted climate change stressors. *In*. University of Hawaii at Manoa.

Puyana, M., Fenical, W. & Pawlik, J. R. (2003) Are there activated chemical defenses in sponges of the genus *Aplysina* from the Caribbean? *Marine Ecology Progress Series, 246*, 127-135.

Quast, C., Pruesse, E., Yilmaz, P., Gerken, J., Schweer, T., Yarza, P., et al. (2013) The SILVA ribosomal RNA gene database project: improved data processing and web-based tools. *Nucleic Acids Research, 41*, D590-D596.

Radax, R., Hoffmann, F., Rapp, H. T., Leininger, S. & Schleper, C. (2012) Ammonia‐oxidizing archaea as main drivers of nitrification in cold‐water sponges. *Environmental Microbiology, 14*, 909-923.

Ramsby, B., Massaro, A., Marshall, E., Wilcox, T. & Hill, M. (2012) Epibiont–basibiont interactions: examination of ecological factors that influence specialization in a two-sponge association between *Geodia vosmaeri* (Sollas,

1886) and *Amphimedon erina* (de Laubenfels, 1936). *Hydrobiologia, 687*, 331-340.

Randall, J. E. & Hartman, W. (1968) Sponge-feeding fishes of the West Indies. *Marine Biology, 1*, 216-225.

Redman, R. S., Dunigan, D. D. & Rodriguez, R. J. (2001) Fungal symbiosis from mutualism to parasitism: who controls the outcome, host or invader? *New Phytologist, 151*, 705-716.

Redmond, N., Morrow, C., Thacker, R., Diaz, M., Boury-Esnault, N., Cárdenas, P., et al. (2013) Phylogeny and systematics of Demospongiae in light of new small-subunit ribosomal DNA (18S) sequences. *Integrative and Comparative Biology*, *53*, 388-415.

Redmond, N., Raleigh, J., van Soest, R. W., Kelly, M., Travers, S. A., Bradshaw, B., et al. (2011) Phylogenetic relationships of the marine Haplosclerida (Phylum Porifera) employing ribosomal (28S rRNA) and mitochondrial (cox1, nad1) gene sequence data. *PLoS One, 6*, e24344.

Redmond, N. E. & McCormack, G. P. (2009) Ribosomal internal transcribed spacer regions are not suitable for intra-or inter-specific phylogeny reconstruction in haplosclerid sponges (Porifera: Demospongiae). *Journal of the Marine Biological Association of the United Kingdom, 89*, 1251-1256.

Reincke, T. & Barthel, D. (1997) Silica uptake kinetics of *Halichondria panicea* in Kiel Bight. *Marine Biology, 129*, 591-593.

Reiswig, H. M. (1981) Partial carbon and energy budgets of the bacteriosponge *Verongia fistularis* (Porifera: Demospongiae) in Barbados. *Marine Ecology, 2*, 273-293.

Riahi, K., Rao, S., Krey, V., Cho, C., Chirkov, V., Fischer, G., et al. (2011) RCP 8.5—A scenario of comparatively high greenhouse gas emissions. *Climatic Change, 109*, 33-57.

Riesgo, A., Farrar, N., Windsor, P. J., Giribet, G. & Leys, S. P. (2014) The analysis of eight transcriptomes from all poriferan classes reveals surprising genetic complexity in sponges. *Molecular Biology and Evolution*, *31*, 1102.

Riesgo, A., Peterson, K., Richardson, C., Heist, T., Strehlow, B., McCauley, M., et al. (2014) Transcriptomic analysis of differential host gene expression upon uptake of symbionts: a case study with *Symbiodinium* and the major bioeroding sponge Cliona varians. *BMC Genomics, 15*, 1.

Rodríguez-Marconi, S., De la Iglesia, R., Díez, B., Fonseca, C. A., Hajdu, E. & Trefault, N. (2015) Characterization of bacterial, archaeal and eukaryote symbionts from Antarctic sponges reveals a high diversity at a three-domain level and a particular signature for this ecosystem. *PLoS One, 10*, e0138837.

Rudi, A., Afanii, R., Gravalos, L. G., Aknin, M., Gaydou, E., Vacelet, J., et al. (2003) Three new cyclic peroxides from the marine sponge *Plakortis* aff *simplex*. *Journal of Natural Products, 66*, 682-685.

Rützler, K. (1970) Spatial competition among Porifera: solution by epizoism. *Oecologia, 5*, 85-95.

Rützler, K., Piantoni, C., van Soest, R. W. & Diaz, M. C. (2014) Diversity of sponges (Porifera) from cryptic habitats on the Belize barrier reef near Carrie Bow Cay. *Zootaxa, 3805*, 1-129.

Sachs, J. L., Mueller, U. G., Wilcox, T. P. & Bull, J. J. (2004) The evolution of cooperation. *The Quarterly Review of Biology, 79*, 135-160.

Saito, Y. (2013) Self and nonself recognition in a marine sponge, *Halichondria japonica* (Demospongiae). *Zoological Science, 30*, 651-657.

Sandes, J., Bispo, A. & Pinheiro, U. (2014) Two new species of *Haliclona* Grant, 1836 (Haplosclerida: Chalinidae) from Sergipe State, Brazil. *Zootaxa, 3793*, 273-280.

Santos, E. A., Quintela, A. L., Ferreira, E. G., Sousa, T. S., Pinto, F. d. C. L., Hajdu, E., et al. (2015) Cytotoxic plakortides from the Brazilian marine sponge *Plakortis angulospiculatus*. *Journal of Natural Products, 78*, 996-1004.

Sarà, M. (1970) Competition and cooperation in sponge populations. *In: Symposium of the Zoological Society of London*, pp. 273-284.

Schläppy, M. L., Schöttner, S. I., Lavik, G., Kuypers, M. M., De Beer, D. & Hoffmann, F. (2010) Evidence of nitrification and denitrification in high and low microbial abundance sponges. *Marine Biology, 157*, 593-602.

Schloss, P. D., Westcott, S. L., Ryabin, T., Hall, J. R., Hartmann, M., Hollister, E. B., et al. (2009) Introducing mothur: open-source, platform-independent, community-supported software for describing and comparing microbial communities. *Applied and Environmental Microbiology, 75*, 7537-7541.

Schmidt, O. (1862) *Die Spongien des Adriatischen Meeres: I-VIII*. Engermann, Leipzig.

Schmitt, S., Angermeier, H., Schiller, R., Lindquist, N. & Hentschel, U. (2008) Molecular microbial diversity survey of sponge reproductive stages and mechanistic insights into vertical transmission of microbial symbionts. *Applied and Environmental Microbiology, 74*, 7694-7708.

Schmitt, S., Tsai, P., Bell, J., Fromont, J., Ilan, M., Lindquist, N., et al. (2012) Assessing the complex sponge microbiota: core, variable and species-specific bacterial communities in marine sponges. *International Society of Marine Ecology Journal, 6*, 564-576.

Schmitt, S., Weisz, J. B., Lindquist, N. & Hentschel, U. (2007) Vertical transmission of a phylogenetically complex microbial consortium in the viviparous sponge *Ircinia felix*. *Applied and Environmental Microbiology, 73*, 2067-2078.

Schönberg, C. H. & Loh, W. K. (2005) Molecular identity of the unique symbiotic dinoflagellates found in the bioeroding demosponge *Cliona orientalis*. *Marine Ecology Progress Series, 299*, 157-166.

Schöttner, S., Hoffmann, F., Cárdenas, P., Rapp, H. T., Boetius, A. & Ramette, A. (2013) Relationships between host phylogeny, host type and bacterial community diversity in cold-water coral reef sponges. *PLoS One, 8*, e55505.

Schröder, H.-C., Perović-Ottstadt, S., Rothenberger, M., Wiens, M., Schwertner, H., Batel, R., et al. (2004) Silica transport in the demosponge *Suberites domuncula*: fluorescence emission analysis using the PDMPO probe and cloning of a potential transporter. *Biochemical Journal, 381*, 665-673.

Schulze, F. E. (1877) Untersuchungen über den Bau und die Entwicklung der Spongien. *Zeitschrift für wissenschaftliche Zoologie, 30*, 379-420.

Schulze, F. E. (1880) Untersuchungen u¨ber den Bau und die Entwicklung der Spongien. Die Plakiniden. *Zeitschrift für Wissenchaftliche Zoologie, 34*, 407–451.

Sharp, K. H., Eam, B., Faulkner, D. J. & Haygood, M. G. (2007) Vertical transmission of diverse microbes in the tropical sponge *Corticium* sp. *Applied and Environmental Microbiology, 73*, 622-629.

Siegl, A., Kamke, J., Hochmuth, T., Piel, J., Richter, M., Liang, C., et al. (2011) Single-cell genomics reveals the lifestyle of Poribacteria, a candidate phylum symbiotically associated with marine sponges. *ISME J, 5*, 61-70.

Silbiger, N. & Donahue, M. (2015) Secondary calcification and dissolution respond differently to future ocean conditions. *Biogeosciences, 12*, 567-578.

Silveira, C. B., Silva‐Lima, A. W., Francini‐Filho, R. B., Marques, J. S., Almeida, M. G., Thompson, C. C., et al. (2015) Microbial and sponge loops modify fish production in phase‐shifting coral reefs. *Environmental Microbiology*.

Simmons, T. L., Coates, R. C., Clark, B. R., Engene, N., Gonzalez, D., Esquenazi, E., et al. (2008) Biosynthetic origin of natural products isolated from marine microorganism–invertebrate assemblages. *Proceedings of the National Academy of Sciences USA, 105*, 4587-4594.

Slattery, M., Gochfeld, D. J., Diaz, M. C., Thacker, R. W. & Lesser, M. P. (2016) Variability in chemical defense across a shallow to mesophotic depth gradient in the Caribbean sponge *Plakortis angulospiculatus*. *Coral Reefs, 35*, 11-22.

Smith, A. M., Berman, J., Key, M. M. & Winter, D. J. (2013) Not all sponges will thrive in a high-CO_2 ocean: Review of the mineralogy of calcifying sponges. *Palaeogeography, Palaeoclimatology, Palaeoecology, 392*, 463-472.

Sollas, P. (1885) A classification of the sponges. *Journal of Natural History: Series 5, 16*, 395-395.

Sollas, W. (1888a) Report on the Tetractinel-lida collected by HMS Challenger during the years 1873-1876: Rept. *Sci. Res. HMS Challenger, 25*.

Sollas, W. (1888b) Report on the Tetractinellida collected by HMS Challenger during the years 1873-1876: Rept. *Sci. Res. HMS Challenger, 25*.

Southwell, M. W., Weisz, J. B., Martens, C. S. & Lindquist, N. (2008) In situ fluxes of dissolved inorganic nitrogen from the sponge community on Conch Reef, Key Largo, Florida. *Limnology and Oceanography, 53*, 986.

Spalding, M. D., Fox, H. E., Allen, G. R., Davidson, N., Ferdaña, Z. A., Finlayson, M., et al. (2007) Marine ecoregions of the world: a bioregionalization of coastal and shelf areas. *Bioscience, 57*, 573-583.

Srivastava, M., Simakov, O., Chapman, J., Fahey, B., Gauthier, M. E., Mitros, T., et al. (2010) The *Amphimedon queenslandica* genome and the evolution of animal complexity. *Nature, 466*, 720-726.

Steger, D., Ettinger‐Epstein, P., Whalan, S., Hentschel, U., De Nys, R., Wagner, M., et al. (2008) Diversity and mode of transmission of ammonia‐oxidizing archaea in marine sponges. *Environmental Microbiology, 10*, 1087-1094.

Stubler, A. D., Furman, B. T. & Peterson, B. J. (2014) Effects of pCO2 on the interaction between an excavating sponge, Cliona varians, and a hermatypic coral, Porites furcata. *Marine Biology, 161*, 1851-1859.

Swain, T. D. & Wulff, J. L. (2007) Diversity and specificity of Caribbean sponge–zoanthid symbioses: a foundation for understanding the adaptive significance of symbioses and generating hypotheses about higher‐order systematics. *Biological Journal of the Linnean Society, 92*, 695-711.

Swearingen III, D. & Pawlik, J. R. (1998) Variability in the chemical defense of the sponge *Chondrilla nucula* against predatory reef fishes. *Marine Biology, 131*, 619-627.

Tamura, K. & Nei, M. (1993) Estimation of the number of nucleotide substitutions in the control region of mitochondrial DNA in humans and chimpanzees. *Molecular Biology and Evolution, 10*, 512-526.

Tamura, K., Peterson, D., Peterson, N., Stecher, G., Nei, M. & Kumar, S. (2011) MEGA5: molecular evolutionary genetics analysis using maximum likelihood, evolutionary distance, and maximum parsimony methods. *Molecular Biology and Evolution, 28*, 2731-2739.

Team, R. C. (2014) R: A language and environment for statistical computing. R Foundation for Statistical Computing, Vienna, Austria. 2013. *In*. ISBN 3-900051-07-0.

Thacker, R. W. & Freeman, C. J. (2012) 2 Sponge-microbe symbioses: Recent advances and new directions. *Advances in Marine Biology, 62*, 57-111.

Thomas, T., Moitinho-Silva, L., Lurgi, M., Björk, J. R., Easson, C., Astudillo-García, C., et al. (2016) Diversity, structure and convergent evolution of the global sponge microbiome. *Nature Communications, 7*.

Toonen, R. J., Puritz, J. B., Forsman, Z. H., Whitney, J. L., Fernandez-Silva, I., Andrews, K. R., et al. (2013) ezRAD: a simplified method for genomic genotyping in non-model organisms. *PeerJ, 1*, e203.

Topsent, E. (1928) Spongiaires de l'Atlantique et de la Méditerranée provenant des croisières du Prince Albert Ier de Monaco. Résultats des campagnes scientifiques accomplies par le Prince Albert I, Monaco 74, 1–376, pls. I–XI. *Imprimerie de Monaco, Monaco*.

Uppström, L. R. (1974) The boron/chlorinity ratio of deep-sea water from the Pacific Ocean. *Deep Sea Research and Oceanographic*, *21*, 161-162.

Uriz, M. J., Turon, X. & Becerro, M. A. (2003) Silica deposition in demosponges. *In:* Müller, W.E.G. (Eds.) *Silicon biomineralization*. Springer, Berlin, pp. 163-193.

Usher, K. M., Kuo, J., Fromont, J. & Sutton, D. C. (2001) Vertical transmission of cyanobacterial symbionts in the marine sponge *Chondrilla australiensis* (Demospongiae). *Hydrobiologia, 461*, 9-13.

Vacelet, J. & Donadey, C. (1977) Electron microscope study of the association between some sponges and bacteria. *Journal of Experimental Marine Biology and Ecology, 30*, 301-314.

Vajrala, N., Martens-Habbena, W., Sayavedra-Soto, L. A., Schauer, A., Bottomley, P. J., Stahl, D. A., et al. (2013) Hydroxylamine as an intermediate in ammonia oxidation by globally abundant marine archaea. *Proceedings of the National Academy of Sciences USA, 110*, 1006-1011.

Van Soest, R., Boury-Esnault, N., Hooper, J., Rützler, K. d., De Voogd, N., Alvarez de Glasby, B., et al. (2012) World porifera database. *The World Register*

of Marine Species (WoRMS). Available online: http://www*. marinespecies. org/porifera (accessed on 1 January 2016)*.

Van Soest, R. & De Weerdt, W. (2001) New records of *Xestospongia* species (Haplosclerida: Petrosiidae) from the Curacao reefs, with a description of a new species. *Beaufortia, 51*, 109-117.

Van Soest, R. W., Hummelinck, P. W. & Van der Steen, L. (1980) Marine sponges from Curacao and other Caribbean localities: Part II: Haplosclerida. *In: Studies on the Fauna of Curaçao and other Caribbean Islands*, 62, 1-173.

Van Soest, R. W., Meesters, E. H. & Becking, L. E. (2014) Deep-water sponges (Porifera) from Bonaire and Klein Curaçao, Southern Caribbean. *Zootaxa, 3878*, 401-443.

Vicente, J., Silbiger, N. J., Beckley, B. A., Raczkowski, C. W. & Hill, R. T. (2016) Impact of high pCO_2 and warmer temperatures on the process of silica biomineralization in the sponge *Mycale grandis*. *ICES Journal of Marine Science: Journal du Conseil, 73*, 704-714.

Vicente, J., Zea, S. & Hill, R. T. (2016) Sponge epizoism in the Caribbean and the discovery of new Plakortis and Haliclona species, and polymorphism of Xestospongia deweerdtae (Porifera). *Zootaxa, in press*.

Vicente, J., Zea, S., Powell, R. J., Pawlik, J. R. & Hill, R. T. (2014) New epizooic symbioses between sponges of the genera *Plakortis* and *Xestospongia* in cryptic habitats of the Caribbean. *Marine Biology, 161*, 2803-2818.

Vicente, V. P. (1989) Regional commercial sponge extinctions in the West Indies: are recent climatic changes responsible? *Marine Ecology, 10*, 179-191.

Vishnyakov, A. E. & Ereskovsky, A. V. (2009) Bacterial symbionts as an additional cytological marker for identification of sponges without a skeleton. *Marine Biology, 156*, 1625-1632.

Vogel, S. (1978) Evidence for one-way valves in the water-flow system of sponges. *The Journal of Experimental Biology, 76*, 137-148.

Waddell, B. & Pawlik, J. R. (2000a) Defenses of Caribbean sponges against invertebrate predators. I. Assays with hermit crabs. *Marine Ecology Progress Series, 195*, 125-132.

Waddell, B. & Pawlik, J. R. (2000b) Defenses of Caribbean sponges against invertebrate predators. II. Assays with sea stars. *Marine Ecology Progress Series, 195*, 133-144.

Walters, K. D. & Pawlik, J. R. (2005) Is there a trade-off between wound-healing and chemical defenses among Caribbean reef sponges? *Integrative and Comparative Biology, 45*, 352-358.

Wang, Q., Garrity, G. M., Tiedje, J. M. & Cole, J. R. (2007) Naive Bayesian classifier for rapid assignment of rRNA sequences into the new bacterial taxonomy. *Applied and Environmental Microbiology, 73*, 5261-5267.

Wang, X., Schröder, H. C., Wiens, M., Schloβmacher, U. & Müller, W. E. (2012) 5 Biosilica: Molecular biology, biochemistry and function in Demosponges as well as its applied aspects for tissue engineering. *Advances in Marine Biology, 62*, 231.

Webster, N., Pantile, R., Botte, E., Abdo, D., Andreakis, N. & Whalan, S. (2013) A complex life cycle in a warming planet: gene expression in thermally stressed sponges. *Molecular Ecology, 22*, 1854-1868.

Webster, N. S., Cobb, R. E. & Negri, A. P. (2008) Temperature thresholds for bacterial symbiosis with a sponge. *International Society of Marine Ecology Journal, 2*, 830-842.

Webster, N. S., Taylor, M. W., Behnam, F., Lücker, S., Rattei, T., Whalan, S., et al. (2010) Deep sequencing reveals exceptional diversity and modes of transmission for bacterial sponge symbionts. *Environmental Microbiology, 12*, 2070-2082.

Webster, N. S. & Thomas, T. (2016) The Sponge Hologenome. *mBio, 7*, e00135-00116.

Webster, N. S., Watts, J. E. & Hill, R. T. (2001) Detection and phylogenetic analysis of novel crenarchaeote and euryarchaeote 16S ribosomal RNA gene sequences from a Great Barrier Reef sponge. *Marine Biotechnology, 3*, 600-608.

Weissenfels, N. (1981) Bau und Funktion des Süßwasserschwamms *Ephydatia fluviatilis* L.(Porifera). *Zoomorphology, 98*, 35-45.

Weisz, J. B., Hentschel, U., Lindquist, N. & Martens, C. S. (2007) Linking abundance and diversity of sponge-associated microbial communities to metabolic differences in host sponges. *Marine Biology, 152*, 475-483.

Weisz, J. B., Lindquist, N. & Martens, C. S. (2008) Do associated microbial abundances impact marine demosponge pumping rates and tissue densities? *Oecologia, 155*, 367-376.

Wilcox, T., Hill, M. & DeMeo, K. (2002) Observations on a new two-sponge symbiosis from the Florida Keys. *Coral Reefs, 21*, 198-204.

Wilkinson, C. R. (1983) Net primary productivity in coral reef sponges. *Science, 219*, 410-412.

Wilson, H. (1902) The sponges collected in Porto Rico in 1899 by the US Fish Commission steamer Fish Hawk. *Bulletin of the United States Fish Commission, 2*, 375-411.

Wisshak, M., Schönberg, C. H., Form, A. & Freiwald, A. (2012) Ocean acidification accelerates reef bioerosion. *PLoS One, 7*, e45124.

Wisshak, M., Schönberg, C. H. L., Form, A. & Freiwald, A. (2013) Effects of ocean acidification and global warming on reef bioerosion—lessons from a clionaid sponge. *Aquatic Biology, 19*, 111-127.

Wood, H. L., Spicer, J. I. & Widdicombe, S. (2008) Ocean acidification may increase calcification rates, but at a cost. *Proceedings of the Royal Society of London B: Biological Sciences, 275*, 1767-1773.

Wooster, M. K., Marty, M. J. & Pawlik, J. R. (2016) Defense by association: Sponge-eating fishes alter the small-scale distribution of Caribbean reef sponges. *Marine Ecology, in review*.

Wörheide, G., Solé-Cava, A. M. & Hooper, J. N. (2005) Biodiversity, molecular ecology and phylogeography of marine sponges: patterns, implications and outlooks. *Integrative and Comparative Biology, 45*, 377-385.

Wulff, J. (2012) 4 Ecological Interactions and the Distribution, Abundance, and Diversity of Sponges. *Advances in Marine Biology, 61*, 273-344.

Wulff, J. L. (1994) Sponge feeding by Caribbean angelfishes, trunkfishes, and filefishes. In: Van Soest, R.W.M., Van Kempen, T.M.G., Braekman, J.C. (Eds.) *Sponges in time and space.* Balkema, Rotterdam, pp. 265-271.

Wulff, J. L. (1997) Mutualisms among species of coral reef sponges. *Ecology, 78*, 146-159.

Wulff, J. L. (2005) Trade‐offs in resistance to competitors and predators, and their effects on the diversity of tropical marine sponges. *Journal of Animal Ecology, 74*, 313-321.

Wulff, J. L. (2008a) Collaboration among sponge species increases sponge diversity and abundance in a seagrass meadow. *Marine Ecology, 29*, 193-204.

Wulff, J. L. (2008b) Life‐history differences among coral reef sponges promote mutualism or exploitation of mutualism by influencing partner fidelity feedback. *The American Naturalist, 171*, 597-609.

Zea, S. (1987) *Esponjas del Caribe colombiano*: Catálogo científico Bogotá.

Zea, S., Henkel, T. & Pawlik, J. (2009) The Sponge Guide: a picture guide to Caribbean sponges. *In*. NSF Biological Oceanography Program grants. Wilmington, NC, EE. UU.

Zea, S., Henkel, T. & Pawlik, J. (2014) The Sponge Guide: a picture guide to Caribbean sponges. *Available online at (http://www.thespongeguide.org)*.

Zeebe, R. & Wolf-Gladrow, D. (2001) CO2 in Seawater: Equilibrium, Kinetics, Isotopes. *Elsevier Oceanography Book Series, 65, 346 pp, Amsterdam*.

Zhang, F., Blasiak, L. C., Karolin, J. O., Powell, R. J., Geddes, C. D. & Hill, R. T. (2015) Phosphorus sequestration in the form of polyphosphate by microbial symbionts in marine sponges. *Proceedings of the National Academy of Sciences USA, 112*, 4381-4386.

Zhang, F., Pita, L., Erwin, P. M., Abaid, S., López-Legentil, S. & Hill, R. T. (2014) Symbiotic archaea in marine sponges show stability and host specificity in

community structure and ammonia oxidation functionality. *FEMS microbiology ecology, 90*, 699-707.

Zhang, F., Vicente, J. & Hill, R. T. (2015) Temporal changes in the diazotrophic bacterial communities associated with Caribbean sponges *Ircinia stroblina* and *Mycale laxissima*. *Frontiers in Microbiology*, *5,* 561.

Zhang, J., Tang, X., Li, J., Li, P., de Voogd, N. J., Ni, X., et al. (2013) Cytotoxic polyketide derivatives from the South China sea sponge *Plakortis simplex*. *Journal of Natural Products, 76*, 600-606.